Functionalization of PP for the enhancement of adhesion between polypropylene and polyamide multilayers

Von der Fakultät Energie-, Verfahrens- und Biotechnik der Universität Stuttgart
zur Erlangung der Würde eines Doktor-Ingenieurs (Dr.-Ing.)
genehmigte Abhandlung

Vorgelegt von

Claude Rustal

aus Fort-de-France (Martinique)

Hauptbericht:	Prof. Dr.-Ing. H.-G. Fritz
Mitberichter:	Prof. Dr.rer.nat. C.D. Eisenbach
Tag der mündlichen Prüfung:	14.10.2008

Institut für Kunststofftechnik der Universität Stuttgart

2009

ACKNOWLEDGEMENT

Claude Rustal,   Stuttgart, im Oktober 2008

CONTENT

SYMBOLS

List of abbreviations

AIBN	Azobisisobutyronitrile
ATR	Attenuated Total Reflectance
CTC	Charge Transfer Complex
CO_2	Carbon dioxide
DHBP	2,5-dimethyl-2,5-di(tert.butylperoxy) hexane
DSC	Differential Scanning Calorimetry
DSR	Dynamic Stress Rheometer
EPM	Ethylene-Propylenen Monomer
FTIR	Fourier Transform Infrared Spectroscopy
GMA	Glycidyl metahcrylate
HD	Polypropylene grade HD601CF
HB	Polypropylene grade HB205TF
IR	Infrared radiation
L/D	Length to diameter ratio of the screw
M	Monomer
MAH	Maleic anhydride
MMD	Molar mass distribution
N_2	Nitrogen
O_2	Oxygen
PA	Polyamide
PP	Polypropylene
PP-g-MAH	PP grafted with MAH
PP-g-GMA	PP grafted with GMA
P(St-alt-MAH)	Equimolar copolymer of alternating styrene and MAH
R	Radical
RD	Polypropylene grade RD20CF
RB	Polypropylene grade RB501BF
SEM	Scanning Electron Microscope
St	Styrene
TMCH	1,1-Bis(tert.butylperoxy)-3,3,5-trimethyl cyclohexane
ZME	Zahnmischelement
ZSK	Zweischneckenkneter, Twin-screw extruder

List of Latin symbols

a	[Pa.s]	Zero shear viscosity
A_0	[-]	Polymer constant
$A_{monomer}$	[-]	Surface or height of a specific absorption band of the monomer
A_{PP}	[-]	Surface or height of the absorption band of the PP
b	[s]	Material constant
b_p	[m]	Peeled distance
$b_p c_p$	[m²]	Interfacial area
c	[-]	Slope of the viscosity function at high shear rates
c_p	[m]	Peeled distance
C	[mol/l]	Peroxide concentration
C_{MAH}	[phr]	Quantity of MAH
C_{GMA}	[phr]	Quantity of GMA
D	[mm]	Diameter of the storage canal
E_A	[kJ/kmol]	Activation energy
E_0	[kJ/kmol]	Flow activation energy
d_p	[µm]	Depth of penetration
F	[N]	Peel force
F_Z	[N]	Normal force
G	[J/m²]	Fracture energy per unit interfacial area, joint strength or energy involved to separate materials
G_0	[J/m²]	Energy required to propagate a crack through a unit area of interface in the absence of viscoelastic energy losses
G'	[Pa]	Elastic modulus
G''	[Pa]	Loss modulus
H	[mm]	Slit height of die
ΔH_C	[J/mol]	Enthalpy of crystallisation
ΔH_m	[J/mol]	Enthalpy of mixing
ΔH_m	[J/mol]	Experimental melting enthalpy
ΔH^0_m	[J/mol]	Equilibrium enthalpy of fusion determined for a 100% crystalline polymer
ΔG_m	[J/mol]	Gibbs energy of mixing
K	[-]	Intrinsic rate constant
k_{max}	[-]	Maximal intrinsic rate constant
K	[-]	Polymer constant
L	[mm]	Slit width of a die
M	[Nm]	Torque amplitude
MFR	[g/10 min]	Melt Flow Rate
MVR	[cm³/10 min]	Melt Volume Rate
M	[g/mol]	Molecular weight
M_n	[g/mol]	Number average molecular weight
M_w	[g/mol]	Weight average molecular weight
N	[-]	Slope of the curve pressure drop against the flow rate
N_1	[-]	Refractive index of the ATR crystal
N_{21}	[-]	Ratio of the refractive index of the sample to that of

		the ATR crystal
P	[N/m]	Peel force per unit width
P	[bar]	Applied pressure
Δp	[bar]	Pressure drop
R	[kJ/kmol K]	Gas constant
R	[m]	Radius of the parallel plates in a rotational rheometer
S	[-]	Spreading coefficient of the liquid on a surface
S_a	[J/m^3]	Deformation energy per unit volume of the adhesive
S	[J/m^3]	Deformation energy per unit volume of the flexible adherend
ΔS_m	[J/l(mol.K)]	Entropy of mixing
T	[K]	Absolute temperature
T_0	[s]	Healing time
T	[s]	Reaction time
$T_{1/2}$	[s]	Half life time of the peroxide
$\dot{V}$	[kg/h]	Flow rate
W_{SL}	[J/m^2]	Work of adhesion
W	[J]	Work of peel
V	[J]	Deformation energy for peeling an interfacial area
V_{st}	[m/s]	Piston speed

List of Greek formulas

β	[-]	Material constant given by $-\frac{3}{2} \leq \beta \leq -\frac{1}{2}$
δ_1, δ_2	[J/m^3]$^{1/2}$	Parameter of solubility
δ	[rad]	Phase lag
$\eta(\dot{\gamma})$	[Pa.s]	Shear viscosity
H*	[Pa.s]	Complex viscosity
η_0	[Pa.s]	Zero shear viscosity
ε	[%]	Deformation
ε_B	[%]	Elongation at break
$\dot{\gamma}_w$	[s^{-1}]	Shear rate at the wall
$\dot{\gamma}_{korr}$	[s^{-1}]	Corrected shear rate
γ_{SV}	[N/m]	Surface tension of the solid-vapour interfaces
γ_{SV}	[N/m]	Surface tension of the solid-vapour interfaces
γ_{SL}	[N/m]	Surface tension of the solid-liquid interfaces
γ_{LV}	[N/m]	Surface tension of the liquid-vapour interfaces
γ_S	[N/m]	Surface free energy of the solid in vacuum
γ_{SV}	[N/m]	Surface free energy after equilibrium adsorption of vapour from the liquid
λ	[-]	Extension ratio
λ_0	[nm]	Wave length of the radiation in the air
Ω	[rad/s]	Angular velocity
ω	[rad/s]	Frequency
θ	[°]	Angle of incidence
θ	[°]	Peel angle
θ_W	[°]	Apparent advancing contact angle of a liquid on a rough surface
θ_S	[°]	Contact angle of a liquid on a smooth surface
Φ	[J]	Energy irreversibly dissipated in viscoelastic and

		plastic deformations
ϕ	[m^2]	Fractional interfacial contact area
π	[N/m]	Spreading pressure
σ_B	[MPa]	Tensile strength at break
Σ	[-]	Phase boundary
τ_C	[Pa]	Critical stress
τ_w	[Pa]	Shear stress at the wall
V	[m/s]	Bond separation speed
v_r	[cm^3/mol]	Molar volume of a repeat unit
Γ	[J]	Energy expended in separating an interfacial area
χ_{12}	[-]	Interaction parameter

KURZFASSUNG

Die Funktionalisierung von Polypropylen (PP) wurde durchgeführt um eine Verbesserung der Haftungseigenschaften von coextrudierten Schichten aus Polypropylen und Polyamid (PA) zu erreichen. Solche Mehrschichtfolien können beispielweise in der Verpackungs- oder Medizintechnikindustrie Verwendung finden. Im Gegensatz zu bereits praktizierten Herstellungsverfahren sollte auf die als Haftschichten dienende Zwischenschichten (Tielayers) verzichtet werden. Zwei Strategien wurden angewandt: Die Mischung der Polypropylen-Matrix mit Haftvermittlern und die direkte Pfropfung der Polypropylen-Matrix mit reaktiven Monomeren (Maleinsäureanhydrid, Glycidylmethacrylat).

In einem ersten Hauptteil wurde der Schwerpunkt auf die reaktive Extrusion von PP mittels eines gleichsinnig drehenden, dichtkämmenden Zweiwellenextruders gelegt. Dabei wurden die Pfropfrezepturen von Flachfolien variiert, um den Einfluss der Pfropfkomponenten und Prozessparameter auf die Kunststoffeigenschaften zu studieren. Die radikalisch initiierte MAH-Modifizierung des PP beeinflusst deutlich die physikalischen Eigenschaften des Materials. Durch die Ketteneinkürzung (β-Spaltung) nehmen die mechanischen Kennwerte, Dehnung und Zugfestigkeit, sowie auch die Viskosität mit steigendem Monomer- und Peroxid-Gehalt ab. Das Kristallisationsverhalten wurde ebenfalls mit einer erhöhten Kristallisationstemperatur modifiziert. Eine Polaritätssteigerung der Folienoberfläche konnte durch Kontaktwinkelmessungen belegt werden. Im Allgemeinen waren die Eigenschaften der gepfropften PP-Muster von der Molmasse sowie von dem PP-Typ stark abhängig.

Im zweiten Hauptteil wurden die Haftungseigenschaften der modifizierten PP- und PA-Folien untersucht. Zu diesem Zweck wurden PP/PA-Verbunde mittels einer hydraulischen Presse unter verschiedenen Prozessparametern (Zeit, Temperatur, Druck) hergestellt. Anschließend wurde deren Haftfestigkeit mechanisch mittels Trennversuchen charakterisiert. Das Haftungsverhalten unterschied sich zwischen den hochmolekularen und niedermolekularen gepfropften PP. Allerdings konnte man feststellen, dass die Molmasse eine entscheidende Rolle bei den Haftungseigenschaften spielt, was mit der mechanischen Kohäsion des modifizierten Materials korrelierbar ist. Der Einfluss der Prozessparameter Zeit und Temperatur zeigte sich am wichtigsten aufgrund der Beschleunigung von den Diffusions-, Fließ- sowie Reaktionsvorgängen an der Grenzfläche. Ein Vergleich zwischen PP/PA-Verbunden von der direkten Pfropfungs- und Konzentrat-Methode hat ergeben, dass die zweite Strategie zu den besseren Verbundhaftfestigkeiten geführt hat. Coextrudierte Dreischichtfolien wurden unter Variation

der Schichtrezepturen und Prozessparameter anschließend hergestellt. Der gerade erwähnte Trend wurde dabei verifiziert. Es wurde eine verstärkte Haftung zwischen den PP- und PA-Schichten durch die Konstruktion eines Coextrusionswerkzeugs mit verlängertem Düsenaustritt erzielt. Eine interessante verfahrenstechnische Herausforderung wäre im nächsten Schritt die Umwandlung dieses zweistufigen Prozesses (Pfropfung und Coextrusion) in einen einstufigen Prozess.

SUMMARY

The aim of the present work was the production of a polypropylene/polyamide three-layer film without using any tie-layers. These films could find an application, for instance, in the packaging or medical industries. To promote adhesion between the two immiscible polymers, two strategies were used: addition of compatibilizers in the polypropylene (PP) matrix and direct functionalization of the PP matrix with reactive monomers such as maleic anhydride and glycidyl methacrylate.

In the first part of the work, the main concern was the PP functionalization by reactive extrusion, using a corotating close intermeshing twin screw extruder. The grafting formulations were variied and cast films produced in order to study the influence of the functionalization components and process parameters on the materials' properties. In general, the material structure modifications due to monomer grafting induced clear impact on the physical properties. The PP degradation through β-scission during the radical initiated reaction caused a diminution of the mechanical characteristics (tensile strength and elongation) as well as the viscosity of the samples with increasing amounts of monomer and peroxide. The crystallisation behaviour was also influenced, showing an increasing crystallisation temperature. Moreover, the modified PP films showed a higher polarity than the pure resin's ones.

In the second part of the study, two-layer films were pressed in order to study the influence of the formulations as well as the process parameters (temperature, time, pressure) on the adhesion properties of the PP/PA bonds. T-peel tests were used for the adhesion characterization. Differences were found between the high molecular weight and low molecular weight grafted PP/PA bonds. Hence, it appeared that the molecular weight of the grafted PP played a predominant role on the adhesion performance of the joints. This could be correlated to the cohesiveness of the PP film. Time and temperature were found to be the most influencing factors among the process parameters because they accelerated the diffusion and flow processes as well as the chemical reactions at the

interface. A comparison of the two methods (direct grafting and addition of compatibilizers) in terms of adhesion showed that the second strategy led to better results. This trend was confirmed by the coextrusion trials. The variation of the layers formulations and the process parameters was performed. An improved layer adhesion was achieved by using a special coextrusion die exit system. A further challenging work should be done in order to integrate this two-step process, functionalization and coextrusion, into a one-step process.

1   Introduction

The continuous technological progress in the polymer field leads to growing requirements for the materials in use. Instead of creating brand new materials the trend in the industry is to modify them physically or chemically or associate them with other products in order to create targeted properties. Tailor-made products can thus be realized in a shorter time and with a better cost-effectiveness than required for a complete material development. This customer-driven research and development allows much more flexibility. These products are for instance blends of different polymers, composites of polymers and fillers (calcium carbonate, wood, silicates...), reinforced polymers of polymers and fibres, multilayer containers or films which show improvements in their functional and engineering properties in comparison to the raw materials [Utr95,Böl01,Kar95].

Among the packaging materials, multilayer films play an important role in the packaging industry. Apart from their decorative aspect, packaging films have mostly a protection role on the products to be packed. They prevent them from migrating or escaping from the enclosed packaging, entering the environment and also protect them against outside influences that could cause a deleterious effect on the products. Multilayer films are used for these reasons in numerous applications in the food and pharmaceutical industries as blood, plasma or solution bags for instance. They provide a better product protection, meet the need of flexibility created by the great product diversity and comply with federal requirements. Thanks to their excellent barrier properties they successfully replaced during the last two decades traditional metal and glass packaging. Lamination or coextrusion of different polymers, metallized films as well as specialized coatings was thus developed. The purpose of such products is to take advantage of the specific functions of each associated material in order to obtain improved or complementary characteristics for the final product. However, the combined materials are often immiscible polymers and adhesion between the species is a critical issue. Different strategies can be followed to achieve a good compatibilization of the laminates and prevent delaminating processes caused by a lack of interfacial adhesion. Moreover delamination is mostly responsible for the poor physical properties of the layered structures.

Among often used materials for multilayer films, polyolefins, which are non-polar by nature, are excellent economical moisture barriers. However, they possess poor oxygen blocking properties. On the one hand, polar materials such as polyamides and ethylene-vinyl alcohol are good gas barrier materials. On the other hand, they are not as good as polyolefins in the protection against moisture and are somewhat more expensive than polyolefins. Sandwich films made of polypropylene (PP) and polyamide (PA) are produced by coextrusion, which alternates the two material types. They form multilayer films which can protect from both moisture and gas. Between these thermodynamically incompatible monolayers thin adhesion promotor layers, tie layers, are inserted. Five-layer films with good barrier characteristics are usually manufactured in this way. However, the boundary surfaces between the adhesion promotors and the barrier layers can be delamination start points when the multilayer film undergoes stress or accumulation sites for gases or liquids, causing bubble formation and turbidity between the layers. Moreover, the polymers used for the intermediate layers are expensive and their presence requires additional equipment such as extruders and feed blocks. Elimination of the tie layers is on this account an interesting challenge.

A first method currently used to produce multilayer films without tie layers is blending the PP matrices with polyolefins which are grafted with reactive molecules such as maleic anhydride. The blend contains thus the necessary reactive groups which will afterwards react with the gas barrier material. A further method is the direct grafting of reactive molecules such as maleic anhydride or glycidyl methacrylate onto the polypropylene resins.

The main purpose of this work was to realize a three-layer coextruded film formed of a homopolymer as external layer, a copolymer as inner layer and a polyamide as central layer (Fig. 1.1). In order to achieve this goal, a development concept was elaborated (Fig. 1.2).

In a first step, reactive extrusion, a common method to produce functionalized polypropylenes, was used prior to the coextrusion experiments. After preliminary work on functionalization using a batch mixer, grafting trials using maleic anhydride and glycidyl methacrylate were carried out with a twin screw extruder. Grafting

formulations and process conditions were variied in order to study their influence on the materials' properties. Grafted polypropylene cast films were produced and their rheological, mechanical as well as thermal properties were investigated. The functionalized PP and the PA cast films were subsequently bonded using a hydraulic hot press. The influence of the bonding parameters and grafting formulations on adhesion between the chemically modified PP and the PA cast films were studied. The two above mentioned strategies, blending with compatibilizers as well as direct grafting, were realized. In a second step, the best formulations in terms of adhesion achieved with the press process were then used for coextrusion experiments. The multilayer systems were subsequently characterized in terms of adhesion and mechanical properties.
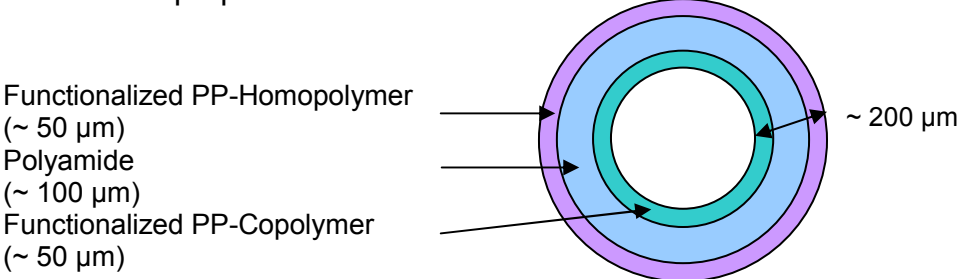

Functionalized PP-Homopolymer
(~ 50 μm)
Polyamide
(~ 100 μm)
Functionalized PP-Copolymer
(~ 50 μm)

~ 200 μm

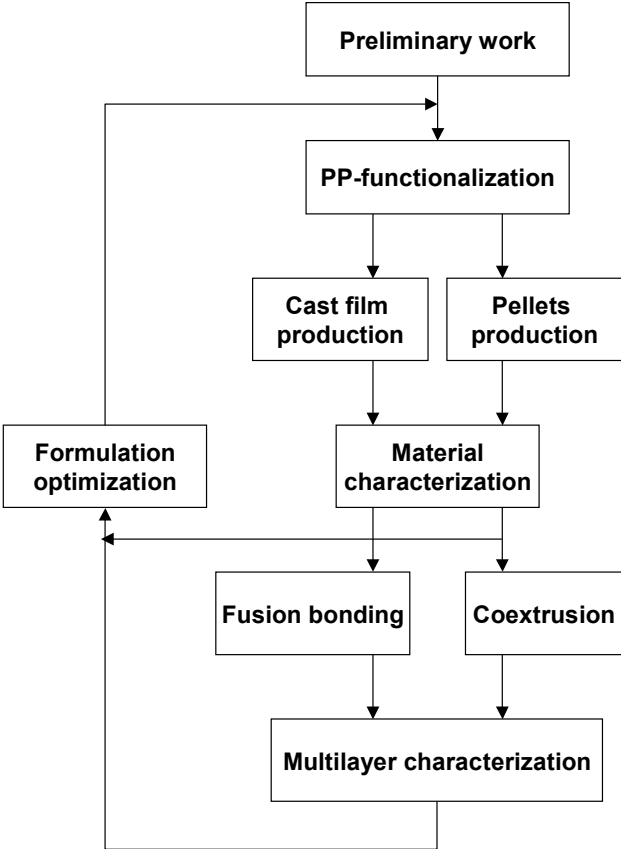**Fig. 1.1:** Scheme of the tubular three-layer film

Fig. 1.2: Concept of the study

2 Functionalization of polypropylene

Owing to its hydrocarbon nature and low polarity, polypropylene has poor chemical reactivity and can be physically or chemically modified to enhance its adhesive properties towards other polar materials. The modification can be achieved at the surface where reactive sites will be created or in the bulk for subsequent compatibilization processes. Among the commonest surface treatments, one can find the chemical plasma, the corona discharge and the flame plasma technologies. They are based on the ionization of a gas which alters the polymer surface chemistry as it impinges upon it. A combination of these methods with an ozone treatment is often used in the extrusion coating technology leading to good adhesion levels [Bez99].

The PP can be modified by using comonomers during or after its polymerization. However, the copolymerization of polypropylene and polar monomers is complex to realize due to the sensivity of the Ziegler-Natta catalysts [Fla91]. Thus, the functionalization of PP in a post-polymerization step is an attractive solution. Different techniques can be used to graft functional molecules on the polymer backbone such as: irradiation of the polymer/monomer mixture, polymerization of the monomer in presence of the polymer, peroxide initiated abstraction of a PP-hydrogen to form macroradicals in the solid state, solution or melt. One of the most important chemical modification methods is the free-radical grafting of reactive monomers onto polymers. This functionalization can be processed in the solid as well as in the molten state by means of batch mixers or extruders which are, in this case, employed as chemical reactors [Fla91,Xan92,Hu96,Moa99]. In the present work, the polar molecules are the commonly used maleic anhydride (MAH) and, as an alternative to the first one, glycidyl methacrylate (GMA).

2.1 Fundamentals of free-radical grafting of monomers onto polypropylene

2.1.1 General description of the grafting reaction

The free-radical grafting of a monomer onto polypropylene is usually carried out in a melt state process in presence of organic peroxides (Fig. 2.1.1). The reaction initiators are thermally activated and the radicals R abstract the PP hydrogen atoms resulting in new radicals onto the PP chains. The macroradicals formed on the PP backbones will undergo degradation (β-scission), monomer M grafting or crosslinking. The β-scission is predominant for polypropylenes and propene-rich Ethylene-Propylene-

Monomers (EPM) whereas polyethylenes and ethene-rich EPM are prone to crosslinking or branching [Xan92,Ro95,Hu96,Moa99,Dui03]. The β-scission is due to the presence of tertiary carbons on the PP backbone and the abstraction potential of their cleaved hydrogen atoms. Bonds to sp^3 carbons are broken rather than bonds to sp (acetylenic) or sp^2 (aromatic, olefinic) carbons [Moa99]. The macroradicals formed are unstable due to the steric hindrance caused by the methyl groups.

Other side reactions may be coupled to the grafting such as the shear induced and thermal degradation of the polymer or the homopolymerization of the monomer.
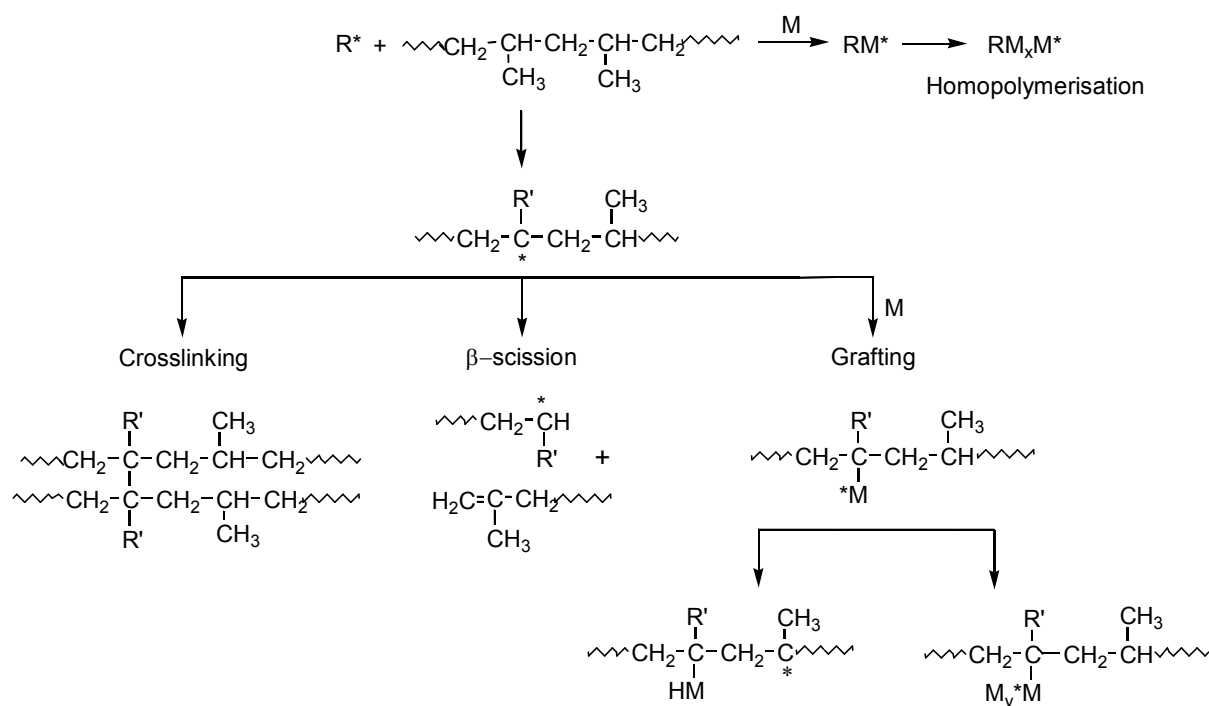

Fig. 2.1.1: General scheme of the grafting reaction [Böl01,Hu96]

It is obvious that the functionalization of polypropylene with monomers is a complex process in which many reactions may simultaneously occur. As mentioned above, grafting is initiated by decomposition of the peroxide. Thus, the initiator plays a major role and must be well chosen in order to achieve an optimal reaction efficiency.

2.1.2 Organic peroxides

For the functionalization of the polypropylene, free radicals can be generated by organic peroxides, ionization of a gas, thermal or mechanical means (hydroperoxides formed under air or oxygen). The decomposition of organic peroxides, due to the lability of the oxygen-oxygen bonds, occurs under the influence of thermal energy.

The choice of the organic peroxide depends on many factors such as its decomposition rate (half-life time), its chemical structure (number of active oxygens), its capacity and efficiency to abstract hydrogen atoms from the polymer backbone, its solubility in the polymer melt, its toxicity and volatility. The extent of cage reaction, i.e. when peroxide primary radicals are trapped in a closed environment made of solvent, monomer or polymer molecules, is also an important factor affecting the initiator grafting efficiency. Other parameters such as the introduction method of the peroxide in the reactor, the polymer type or interfering species in the melt need to be considered [Hu96, Moa99].

The decomposition rate is related to the temperature and, to a lesser extent, to the pressure. A measure of the decomposition rate of the peroxide is its half-life time at a given temperature; that is the time required for the decomposition of 50% of the peroxide. Hence, it should be chosen so that the residence time in the reactor is five to six times its half-life at a defined temperature [Mie94]. On a theoretical point of view, the decomposition is a first order reaction under ideal conditions, i.e. in the gas form or in an inert medium which does not react with the peroxide. The decrease of the peroxide concentration is proportional to the still unreacted peroxide quantity:

$$-\frac{dC}{dt} = kC \qquad\qquad \textbf{Eq. 2.1.1}$$

$$t = \ln\left(\frac{C_0}{C_t}\right)\Big/ k \qquad\qquad \textbf{Eq. 2.1.2}$$

$$t_{1/2} = \frac{\ln(2)}{k} \qquad\qquad \textbf{Eq. 2.1.3}$$

C is the peroxide concentration, t the reaction time and k the intrinsic rate constant. The reaction rate and the intrinsic rate constant depend on temperature. According to Arrhenius their temperature dependence can be written as follows:

$$k = k_{\max} \cdot e^{-E_A/RT} \qquad\qquad \textbf{Eq. 2.1.4}$$

$$t_{1/2} = (\ln 2 / k_{\max}) \cdot e^{E_A/RT} \qquad\qquad \textbf{Eq. 2.1.5}$$

k_{max} is the maximal intrinsic rate constant, E_A the activation energy, R the gas constant and T the absolute temperature. In general, the activation energy of organic peroxides ranges from 100 to 150 kJ/mol [Int]. A low energy means a continuous,

balanced decomposition rate along a large temperature range. A high energy occurs when only a slight temperature raise causes a strong increase of the decomposition rate.

In the practice, the determination of the half-life times depends not only on temperature and pressure but also on the peroxide concentration, the polarity of the solvent or substances that are reactive to the peroxide. This is due to the fact that the peroxide can also decompose under the attack of the radicals formed by the peroxide itself or the solvent (induced decomposition). Under these circumstances, to reduce the influence of the induced decomposition, the determination of the half-lives is conducted in inert solvents such as benzene or cumene in a concentration range of 0.1 – 0.2 mol/l.

Among the peroxides, dialkyl initiators are the most commonly used for melt free-radical grafting. Two organic peroxides of this group were considered in this work: 2,5-dimethyl-2,5-di (tert.butylperoxy) hexane (DHBP) and 1,1-Bis(tert.butylperoxy)-3,3,5-trimethyl cyclohexane (TMCH). They possess a similar effective concentration of active oxygen but differ in their structure. Their half-life times are of 1 min at 190°C for DHBP and 155°C for TMCH. DHBP represents, considering its properties, a good compromise in terms of efficiency, security and handling [Deg]. It is listed under "Food Additives" in the U.S. Code of Federal Regulations and in the Recommendation VII of the German Health Agency at levels restricted to a maximum of 0.1 wt.% and also complies with the requirements of the FDA (Food and Drug Administration) [Fla91,Xan92,Hog96]. DHBP was also found to be the most soluble in PP among the peroxides [Hog96].

On the other side, TMCH is known in the literature [Won97] as initiator for the grafting of glycidyl methacrylate on polypropylene.

The radical generation mechanism is initiated over the initial O-O bond homolysis to create tert-alkoxy radicals (e.g tert-butoxy, cumyloxy). Secondary cleavages may follow to form active alkyl and volatile species [Xan92, Moa99]. DHBP decomposes to give tert-butoxy and, in a secondary step, methyl radicals that both participate to the grafting reaction (Fig. 2.1.2). The radicals formed may also react with the peroxide itself by hydrogen extraction (radical induced decomposition), leading to a decrease of the peroxide performance. Other peroxides may be formed by hydrogen abstraction. Such secondary decomposition reactions are enhanced at higher process temperatures.
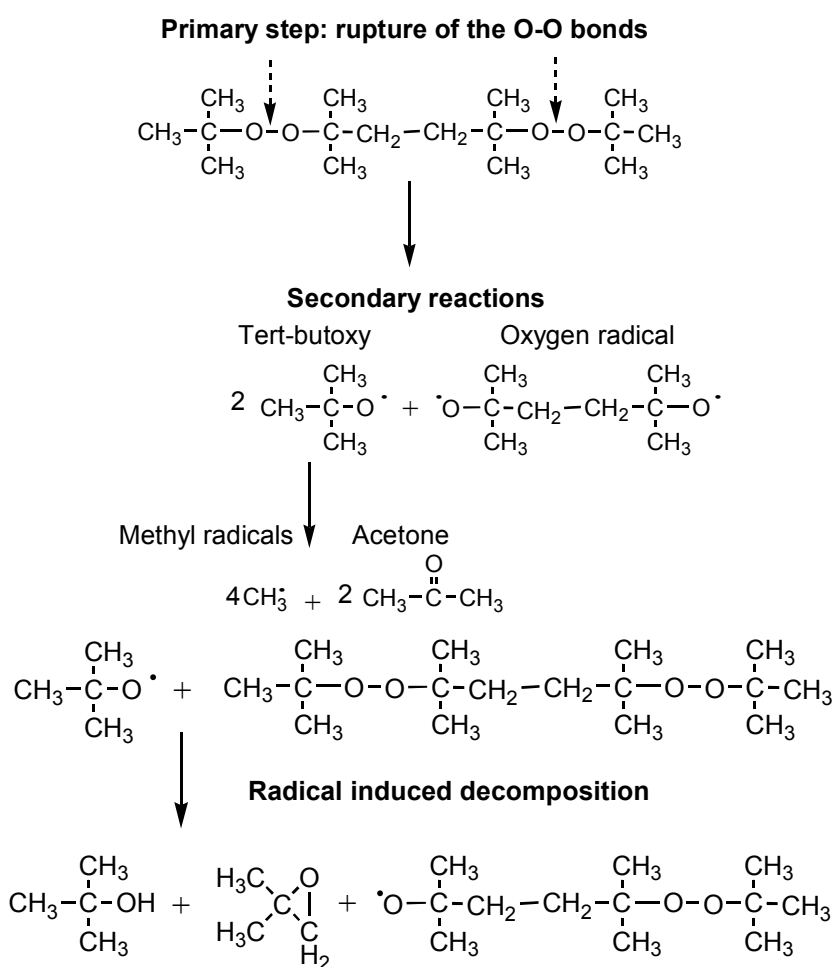
Primary step: rupture of the O-O bonds

Secondary reactions

Tert-butoxy   Oxygen radical

Methyl radicals   Acetone

$4CH_3^{\bullet} + 2\ CH_3\text{-}\overset{O}{\overset{\|}{C}}\text{-}CH_3$

Radical induced decomposition

Fig. 2.1.2: Examples of decomposition mechanisms of DHBP [Hu96, Abe00]

TMCH is a source of tert-butoxy and methyl radicals as shown in Fig. 2.1.3.

Methyl radicals ▼   Acetone

$4CH_3^{\bullet} + 2\ CH_3\text{-}\overset{O}{\overset{\|}{C}}\text{-}CH_3$
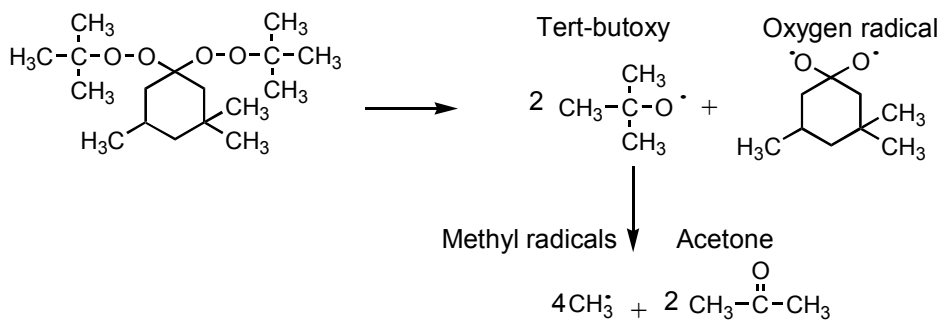
Fig. 2.1.3: Decomposition mechanism of TMCH [Hu96]

Although they decompose in primary tert-butoxy radicals which are known to be the most effective for MAH melt grafting because of their ability to extract hydrogen

atoms from alcanes, DHBP and TMCH may not have the same influence on grafting [Hu96].

The choice of appropriate peroxides for the free-radical grafting reaction is very important since it influences the monomers grafting yields, the molecular structure of the resin and its final properties. Peroxides are chosen based on their decomposition kinetics (half-life time) but also on the type of polymer and monomer (MAH or GMA) involved in the reaction (solubility).

2.1.3 Maleic anhydride grafting onto PP

Maleic anhydride has numerous industrial uses and is of significant commercial interest worldwide. It was first produced by vapour-phase oxidation of benzene, then by using benzene, and later on, butane as reactor feedblock. Its annual world production had grown from 858×10^3 t in 1993 to 1359×10^3 t in 2000, showing the increasing demand for MAH and the diversification of its applications [Hun01]. As a matter of fact, it is a versatile unsaturated carboxylic monomer bearing a double bond and a cyclic anhydride which lend themselves to a variety of chemical reactions. It is functionally reactive to amines, alcohols, thiols, and epoxies in the presence of a catalyst [Hu96]. MAH was chosen in this study as compatibilizer for the polypropylene/polyamide multilayers because of its structure and reactivity potential. It is, for instance, used as a copolymer precursor in polyamide/polyolefin blends, as well as compatibilizer in adhesion, painting or coating applications [Ide74, Sea93, Utr95, Fri96, Ro97/1-3, Moa99, Bas00].

The grafting of MAH on PP has been studied since the end of the fifties and is still an interesting research subject. Basically, the grafting reaction of MAH may follow the path described in section 2.1.1. According to the current mechanism concepts, the PP macroradicals formed after decomposition of the peroxides and hydrogen abstraction may react with MAH-molecules or undergo β-scission. Macroradicals created by the degradation reaction may also contribute to the grafting process (Fig. 2.1.4).
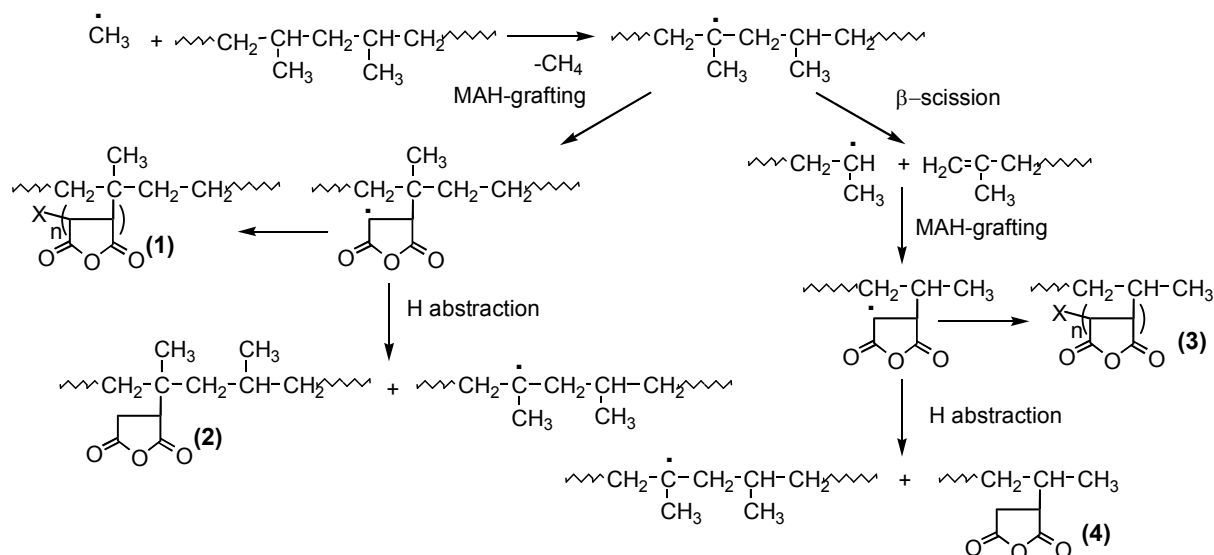
Fig. 2.1.4: Grafting mechanism of PP on MAH [Mie94]

Kinetics studies of the reactions point out the relationship between grafting, degradation and crosslinking. These reactions process simultaneously and depend on the concentration of polymer radicals. Because the β-scission doesn't promote the formation of polymer radicals, the initial concentration of peroxide plays a more important role for the grafting efficiency than the monomer concentration. The latter can lead under homogeneous mixing of the components to an enhancement of the functionalization process. A competition between degradation and grafting is clearly identified and its outcome depends on the addition rate of MAH on the PP backbone. Should the β-scission constant rate be superior to the grafting one, the polymer chain will break, and vice versa [Mie94]. According to other authors [Moa99, Hu96], the importance of degradation and addition of MAH depends also strongly on the local MAH concentration as well as the reaction temperature. Other parameters such as the viscosity of the polymer, the solubility of the monomer and peroxide in the matrix, the homogeneity of the mixture or the processing conditions influence the grafting yields and the structure.

Many studies using IR spectroscopy, ^{1}H and ^{13}C NMR [Ide74, Bet00, Ro95, Ro96, Rus88, Rus95, Hei96] as well as fluorescence method [Duh04] were pursued to determine the grafting level and to understand the grafting mechanism as well as the structure of the grafts. Thus, after grafting of a MAH unit further reactions may occur [Moa99]:

- reactions with MAH to give oligomeric or single succinic anhydride grafts (1 in Fig. 2.1.4),

- radical deactivation processes such as hydrogen transfer from a donor molecule –
for example PP (2 in Fig. 2.1.4), induced decomposition of the initiator and reactions
with radical species by combination (c in Fig. 2.1.5), disproportionation (a, b in Fig.
2.1.5) or electron transfer (d in Fig. 2.5). (R·) represent initiator radicals, PP radicals
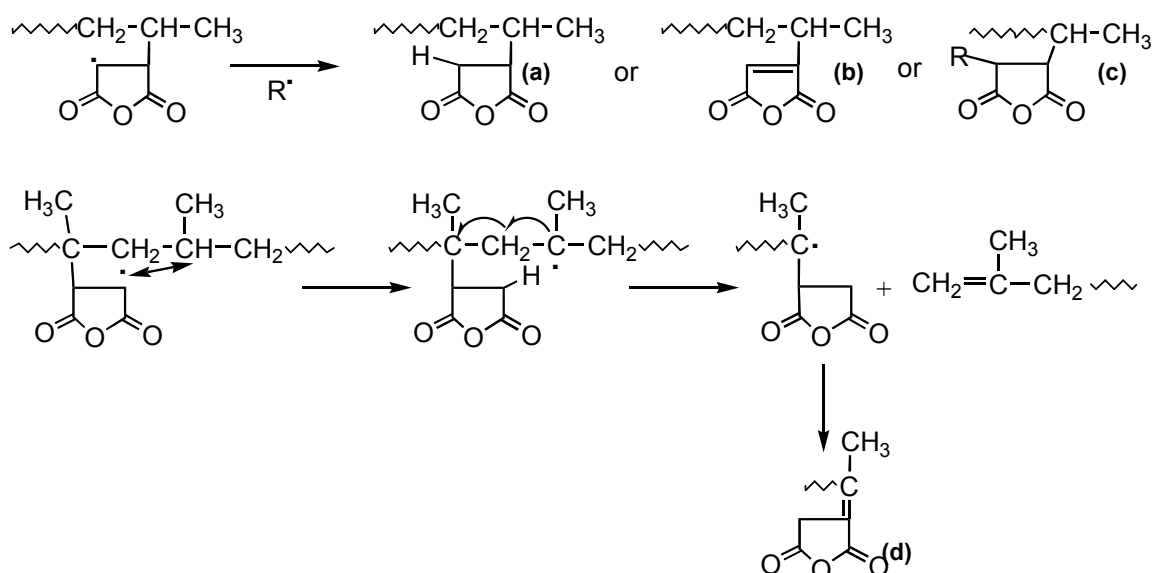or oxygen.

Fig. 2.1.5: Other grafting structures to be found in modified PP [Moa99]

Homopolymerisation of MAH actually appears to be limited during the grafting
process because of the low reactivity of the MAH double bond. MAH
homopolymerizes under drastic conditions for instance in the presence of high
peroxide concentrations [Gay75]. This explains the fact that the grafts formed on the PP
backbone are mostly single anhydride succinic entities.

The main issues encountered by the MAH grafting onto PP are the limited MAH
grafting yields and the degradation of the modified PP. The latter is characterized by
a reduction of the molecular weight of the polymer and leads to the decrease of the
mechanical properties in comparison to the virgin resin.

MAH is known to have a low reactivity toward radicals. It is due to its structural
characteristics which are [Hu96]:

- a strong steric hindrance caused by its carbonyl groups,
- the electron deficiency around its double bond due to the electron-attracting nature
  of the adjacent carbonyl groups,
- the symmetry of its double bond and the corresponding electron cloud.

11

Thus, efforts to improve the MAH low reactivity toward free radical attack have to be made in order to reduce the PP degradation and produce higher grafting yields. One of the solutions consists of using an electron-donating co-monomer which is capable of forming a charge transfer complex (CTC) with MAH. In this case, the double bond of MAH looses its symmetric character with the formation of a radical anion (Fig. 2.1.6). This complex is then expected to have a higher reactivity than MAH itself.
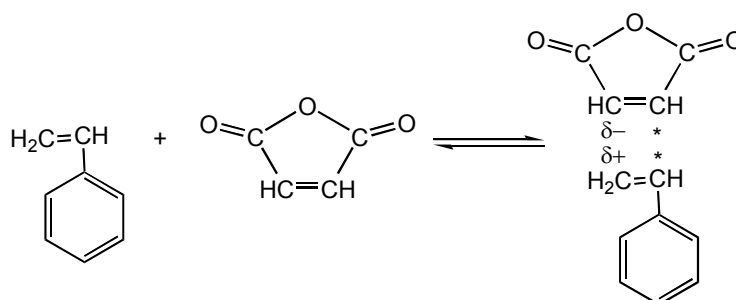

Fig. 2.1.6: Charge transfer complex (CTC) MAH/Styrene

Comonomers are, for instance, styrene, α-methylstyrene, methyl methacrylate, vinyl acetate, N-vinylpyrolidone, butyl 3-(2-furanyl) propenoate, etc… [Gay72, Fla91, Xan92, Hu96, Moa99, Aug04]. The most efficient comonomer is styrene which has been the subject of many studies [Hu93,Whi01,Fri96,Böl01]. It appeared that its presence greatly improved the MAH grafting yield and reduced the PP chain degradation by functionalization in a batch mixer as well as in an extruder. Styrene not only activates the MAH double bond by the formation of a CTC, but it also increases the solubility of MAH in the molten PP. The structure of the grafts could be elucidated using ^{1}H NMR for high concentration levels of MAH and styrene (10 phr and 12.7 phr, respectively). A fraction of MAH and styrene was found to be grafted in the form of CTC as well as free styrene and MAH [Hu96] as illustrated in Fig. 2.1.7. The presence of longer sequences of CTC on the PP backbone cannot be excluded considering the fact that alternation in the copolymerization of maleic anhydride and styrene at high temperatures (>80°C) arises from the reactivities of the monomers as a consequence of spontaneous crosspropagation reactions [Gay73,Ebd86].
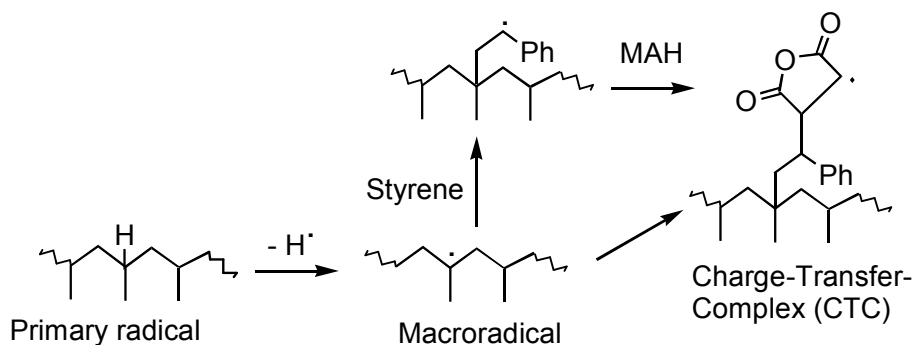
Fig. 2.1.7: Grafting of MAH/Styrene onto PP [Moa99]

The grafting of MAH onto PP without the use of additional monomers has been thoroughly investigated in terms of process, structure and final properties of the material. The system becomes more complex when other monomers come into play and the determination of the structure of such grafted PP still remains challenging.

2.1.4 Glycidyl methacrylate grafting onto PP

Glycidyl Methacrylate (GMA) monomer possesses a dual functionality, containing both epoxy and acrylic groups, providing the design and performance versatility required for coating and resin applications. On the one hand, the acrylic and vinyl functionality (free-radical reactivity) allows copolymerization with a variety of other vinyl monomers in aqueous and nonaqueous systems. The resulting polymers feature a combination of epoxy functionality with an acrylic backbone. On the other hand, the epoxy group (functional reactivity) enables reactions with amines, carboxylic acids, anhydrides and hydroxyl-containing polymers. It allows structural modification of the polymer backbone that can result in differentiated properties and higher performance.

GMA is used in a wide range of applications as coating promoter, comonomer in polymers with tailored properties or compatibilization agent for polymer blending [Liu92,Chi96,Tsa96,Kou97,Zh97/1-2,Zh98/1-2,Pit99,Zou01,Ted02,Sin03,Edm04].

Typical chemical reaction schemes achieved by linking GMA through its methacrylate and epoxide groups provide the polymers with many performance benefits, including [Hu96,Dow].

- excellent weathering resistance (methacrylate reactions only),

- excellent acid resistance (epoxide reactions only),

- improved impact resistance, adhesive strength, water and heat resistance,

<div align="center">13</div>

- improved thermoplastic polymer blend compatibility.

The grafting of glycidyl methacrylate onto polypropylene begins, as for the MAH functionalization, with the decomposition of an organic peroxide followed by extraction of hydrogen atoms on the PP backbone by the peroxide radicals. It is known that the grafting yields of GMA onto PP is very low and achieves only a maximum of 10% [Car98]. As a matter of fact, the double bond of GMA is poorly reactive toward radical attacks because of its bulky size [Cha00]. Several studies considered the use of an additional monomer like styrene to enhance the grafting efficiency of GMA [Sun95/1-2,Won96,Car98]. The comonomer is then expected to form stable styryl radicals with the PP macroradicals which can subsequently react with the GMA molecules in a propagation step (Fig. 2.1.8). This is due to the conjugated effect of the double bond and benzene ring of the styrene molecule on the radical reactivity [Hu94] as well as the proven solubility of PP in styrene [Won96]. No CTC moieties could be detected, leading to the conclusion that the grafting of GMA onto PP in the presence of styrene is statistical.
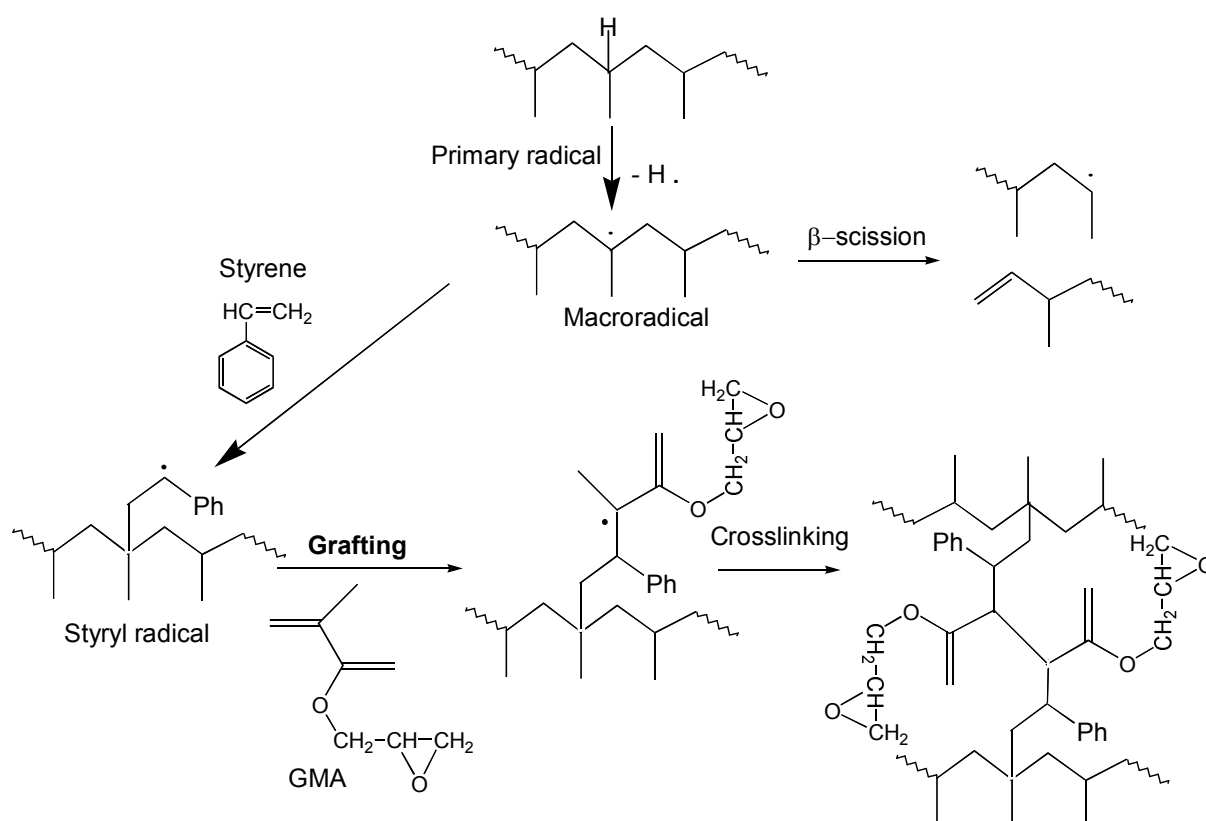

Fig. 2.1.8: Grafting of GMA onto PP [Car98,Won97]

14

This chapter leads to the conclusion that the melt grafting of vinyl monomers such as MAH and GMA onto polymer matrices is a complex but well documented process from a theoretical as well as experimental point of view. The grafting mechanisms described in sections 2.1.3 and 2.1.4 are widely accepted by the majority of the studies related to the subject. As for the process conditions and materials used, they appear to be determining parameters for the grafting yields and the final properties of the functionalized polypropylene.

Considering the information gained from the literature and in order to realize the peroxide initiated melt grafting of polypropylene with MAH and GMA, several grafting experiments are to be performed in a batch mixer or an extruder.

2.2 Materials and process description

2.2.1 Polymers and chemical agents

2.2.1.1 Polypropylene

Polypropylene is a versatile and relatively low cost thermoplastic resin. Its important growth potential is reflected by its annual world production that increased from 30.7×10^6 t in 1998 to 41.6×10^6 t in 2004 [Gle04]. It is available in a wide range of formulations from general purpose homopolymer, random copolymer and impact copolymer grades to highly specialized resins for engineering applications. The wide range of physical properties and relative ease of processing make PP an attractive material capable of competing with more expensive resins in demanding applications. It is highly resistant to many chemical solvents, bases, acids as well as mineral oils, and is water repellent.

Grades of PP are available to meet the needs of various moulding processes such as extrusion, injection moulding, thermoforming, blow moulding, biaxially oriented film (BOPP), fibre spinning, extrusion coating and laminating. It can be manufactured to a high degree of purity, making it useful for the semiconductor industry. It is also resistant to bacterial growth, making it suitable for disposable syringes and other medical equipment. Other applications are piping, filter material and plastic products that require a higher quality than polyethylene [Lie90,Moo96].

Four polypropylene grades from the company Borealis were chosen for the experimental investigations: two isotactic homopolymers HD601CF und HB205TF for the outer layer and two random copolymers RD208CF und RB501BF for the inner layer. The MAH grafted polypropylene Bynel CXA 50E725 from the Company Dupont

was taken as a reference for the coextrusion trials. Their characteristics are given in Tab. 2.2.1.

The resins HD601CF / HB205TF and RD208CF / RB501BF differ in their viscosity levels. HB205TF und RB501BF are high molecular grades specially suited for the film blowing processes. Two PP types (homopolymer and copolymer) were used in order to have a temperature difference between the inner and outer layer of 20 to 30°C. As a matter of fact, the three-layer film may be welded to injection moulded parts in a subsequent step to the functionalization and coextrusion trials. Thus, only the inner layer would melt and adhere to the part.

Polypropy-lene grades	MFI 230°C/2,16kg (g/10min)	M_n (g/mol) M_W (g/mol)	Density (g/cm^3)	Melting temperature (°C)	Tensile strength (MPa)		Elastic modulus (MPa)
					Longitudi-nal	Transver-sal	
Random Copolymer (7,5 mol.% Ethylen) RD208CF	7.1	9.762×10^4 2.858×10^5	0.9 – 0.91	138 – 142	30 – 50	25 – 45	350 – 450
Random Copolymer (3,6 gew.% Ethylen) RB501BF	2.3	1.157×10^5 3.778×10^5	–	142 – 148	20	20	1100 – 1300
Isotactic Homopolymer HD601CF	8.3	7.519×10^4 3.003×10^5	0.9 – 0.91	162 – 166	30 – 50	25 – 45	650 – 750
Isotactic Homopolymer HB501TF	1.4	1.438×10^5 4.477×10^5	0.905	162 – 165	29	27	1100 – 1000

Tab. 2.2.1: Characteristics of the polypropylene films

For the chemical characterization of the grafted polypropylene, an equimolar copolymer of alternating styrene and MAH (P(St-alt-MAH)) was synthesized by radical copolymerization in 1,4-dioxan using azobisisobutyronitrile (AIBN) as initiator. The copolymer was precipitated in polyether and dried in a vacuum oven. 1 wt.% of copolymer was subsequently blended with the polypropylene in a batch mixer.

2.2.1.2 Polyamide

Polyamides, also called nylons, are thermoplastic polymers that comprise polar amide groups. They can be amorphous or semi-crystalline depending on their structure. There are many routes to produce a great variety of polyamides (linear or aromatic) and copolymers containing diacids, diamines or amino acids, making them available for a great number of applications. PAs are used in the production of synthetic fibres and engineering resins (hot-melt adhesives, binders for printing inks, compounds,…). They generally possess a good wear resistance, excellent mechanical and barrier properties as well as a satisfying processability [Zim90].

For this study the gas barrier material is a polyamide chosen among the following grades (Tab. 2.2.2):

-        Polyamide 6 (PA6), Type B 100 ZP (Honeywell),

-        Copolyamide 6-6,6 (PA6-6,6), Type CA 95 ZP (Honeywell),

-        Polyamide 12 (PA12), Type Grilamid L 25 (EMS-Chemie).
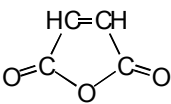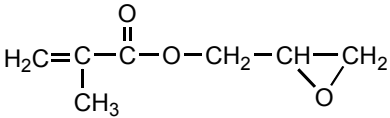

The presented PAs possess middle to high viscosities suitable for cast film or film blowing extrusion. The low melt temperatures of PA6-6,6 und PA 12 allow the use of a reduced process temperature. Besides, PA 12 shows lower water absorption than the other grades. The concentration of amine end groups in the PA is an important criterion for the adhesion with the polypropylene layers as well.

Polyamide grades	MFI $_{235°C/1\ kg}$ (g/10min)	Density (g/cm^3)	Melt temperature (°C)	Gas permeability (cm^3/24h*m^2)			Water absorption at saturation (%)	Equili-brium humidity (%) 23°C/50% r.H.
				O$_2$	N$_2$	CO$_2$		
PA 6 B100ZP	3	1.13	220	2.6	0.9	4.7	9.5	2.5
PA 6/6.6 CA95ZP	3	1.13	196	2.4	0.5	7.3	9	2.5
PA12 Grilamid L25	–	1.01	178	350	–	1500	1.5	0.7

Tab. 2.2.2: Characteristics of the polyamide resins

2.2.1.3 Maleic anhydride and glycidyl methacrylate

Maleic anhydride chemically named 2,5-furan-dione (MAH) and glycidyl methacrylate (GMA) were provided from the company Fluka and used as received. Their characteristics and chemical structure are presented in Tab. 2.1.3.

Chemical structure	HC=CH / O=C−O−C=O	$H_2C=C(CH_3)-C(=O)-O-CH_2-CH-CH_2$ (epoxide O)
Molecular weight (g/mol)	98.06	142.16
Melting point (°C)	52.15	-
Boiling point (°C)	202	189
Density (g/cm^3)	1.43	1.042

Tab. 2.2.3: Characteristics of the monomers

MAH is used in form of a white powder with an acrid odour. It may decompose on exposure to air, moisture or water and is soluble in most current organic solvents and alcohols. It is incompatible to strong oxidizing agents, strong acids or bases, reducing agents, alkali metals.

GMA is a clear, colourless liquid. It may polymerize on exposure to light and is incompatible to strong oxidizing agents, acids and bases. It also may decompose to carbon monoxide and dioxide.

2.2.1.4 Peroxides

2,5-dimethyl-2,5-di (tert.butyl peroxy) hexane (DHBP) is a technically pure bifunctional dialkyl peroxide which is used as initiator in the crosslinking of polymers and for rheology control of polypropylene.

1,1-Bis(tert.butylperoxy)-3,3,5-trimethyl cyclohexane (TMCH) is a technically pure cyclo-aliphatic perketal used for the polymerisation of polymers (styrene), the curing of unsaturated polyester and the crosslinking of polymers.

DHBP and TMCH were provided from the company Fluka. Their characteristics and chemical structure are given in Tab. 2.2.4.

Peroxides	DHBP		TMCH	
Chemical structure	$H_3C-\overset{\overset{CH_3}{\|}}{\underset{\underset{CH_3}{\|}}{C}}-O-O-\overset{\overset{CH_3}{\|}}{\underset{\underset{CH_3}{\|}}{C}}-CH_2-CH_2-\overset{\overset{CH_3}{\|}}{\underset{\underset{CH_3}{\|}}{C}}-O-O-\overset{\overset{CH_3}{\|}}{\underset{\underset{CH_3}{\|}}{C}}-CH_3$		$H_3C-\overset{\overset{CH_3}{\|}}{\underset{\underset{CH_3}{\|}}{C}}-O-O$ ... $O-O-\overset{\overset{CH_3}{\|}}{\underset{\underset{CH_3}{\|}}{C}}-CH_3$ (cyclohexane ring with CH_3, H_3C, CH_3)	
Half life time	1 min at 190°C	27 s at 200°C	1 min at 155°C	1.3 s at 200°C
Active oxygen (wt.%)	10.1		10.37	
Density at 20°C (g/cm³)	0.87		0.91	
Molar mass (g/mol)	290.4		302.4	
Physical form	colourless liquid		colourless liquid	
Miscible in / Immiscible in	alcohol, esters	water	alcohol, styrene	water

Tab. 2.2.4: Characteristics of the organic peroxides

2.2.2 Grafting formulations and process description

MAH and GMA possess the potential through their chemical structure to be used as compatibilizers or bridges between immiscible polymers. The first step, before considering the adhesion problematic with the polyamide, consists of the grafting reaction of the monomer on the polypropylene. This functionalization inevitably modifies the PP structure and as consequence its properties.

Several process conditions are important to obtain optimum grafting yields, control the grafted product and reduce the side reactions. The following parameters are to be considered for the functionalization process.

On a technological basis

- The mechanical mixing of the components is fundamental for the grafting reaction. It is mostly realized in co-rotating twin-screw extruders or batch mixers. Its efficiency depends on the screw speed, the screw design (and the induced shear strains), the temperature and pressure in the extruder as well as on the rheology of the polymers. It influences the grafting yield when the mixture is heterogeneous and the reaction is diffusion-controlled.

- Temperature is a key parameter which conducts the kinetics of all reactions during functionalization. The effects on the grafting yields may be positive in promoting the decomposition of the initiator or the rate of grafting of the

monomer on the polymer, but also negative in activating the other undesirable secondary reactions.

- The mean residence time measures the length of time that material spends in the reactor. It depends on throughput rate, screw speed, screw design, and extruder length to diameter (L/D) ratio. The residence time influences the grafting yield because it should allow the reaction to be completed.

- Devolatilization is a process in which low-molecular-weight components such as unreacted monomer and various reaction by-products are eliminated from the polymer. These volatile substances may be removed to comply with various regulations or to improve the polymer properties.

- The feeding method of the components in the extruder can also affect the grafting reaction because it may promote one or the other reaction such as grafting, β-scission or monomer polymerisation.

On a material point of view

- The polypropylene grade, its molecular weight and molecular weight distribution (related to the rheological properties) greatly influence its flow behaviour in the extruder and its ability to be mixed with the grafting chemicals. The physical state of the polymer can be a mattering factor. If all components are mixed and fed into the extruder, the use of a powdery PP, because of its increased surface, allows a better absorption of the fluid chemicals than PP pellets would do.

- The monomer influences the grafting yield through its concentration level, solubility in the polymer melt, volatility, reactivity towards radicals, homopolymerization tendency.

- The initiator's most important variable is its half-life time which should be within the range of the residence time of the material in the extruder. Other major parameters are its concentration, solubility in the polymer and monomer, reactivity, derived by-products, volatility and toxicity.

- The comonomer, in our case, styrene, is used to improve the grafting yields.

Several extrusion trials were carried out and the chemical agents, monomers, styrene and peroxide as well as the process parameters temperature, screw speed and flow rate were varied (see Appendix 2.1). The purpose of these trials was to

determine the influence of the formulation on the modified polymer physical properties, and subsequently, on adhesion between the grafted PP and the polyamide films.

In terms of proportions, MAH and GMA were added with amounts of $0.1 \leq C_{MAH} \leq 1.0$ phr (part per hundred parts resin) and $1.0 \leq C_{GMA} \leq 7.0$ phr, respectively. It was found from earlier studies at the IKT concerning PP/PA-blends that very low amounts of MAH were sufficient to achieve a satisfactory compatibilization between the species. As for the peroxide, it was added at very low concentrations (0.005 phr) because of its tendency to enhance the degradation reaction of the polymer. For the preparation of the MAH grafted PP (PP-g-MAH) concentrates, amounts of up to 0.2 phr were added in the formulation for a controlled degradation of the PP. The co-monomer was added in molar ratios to the monomer of $0 \leq$ Styrene/monomer ≤ 2 mol/mol.

The production of PP-g-MAH as adhesion concentrates to be added to the pure PP during coextrusion was realized in the same way as the direct grafted PP pellets.

2.2.2.1 Batch kneader process

The batch mixer used for this study is a Haake Rheocord 90 with a maximum capacity of 60 cm^3, torque of 200 Nm and a rotor blades speed range of 5 to 200 min^{-1}. This device allows the use of small amount of material, for instance, for preliminary studies.

Grafting trials with the monomers MAH and GMA were conducted in a batch mixer in order to gain first information about the effects of grafting on the material such as the influence of the formulation on the rheological properties of the PP. After setting the process parameters and calibrating the device, 40 to 50g of PP pellets was introduced in the kneader chamber and the liquid chemicals were subsequently injected with a syringe. The components were homogeneously mixed by the counterotating rotors during 10 min and finally the grafted PP was extracted from the chamber, cooled under nitrogen and analyzed. All experiments were conducted with a rotation speed of 60 min^{-1} under a constant temperature of 200°C and are presented in Appendix 2.2.

The batch mixer was also employed for the preparation of 20/80, 50/50 and 80/20 ratios of PP/PA blend model systems. The blends were used for investigation of the reaction between PP-g-MAH and different polyamides. By all runs, the speed was kept constant at 80 min^{-1} and the kneading time at 5 min. Different temperatures

were used depending on the polyamide types. Detailed PP-g-MAH formulations and blend compositions are given in Appendix 2.3.

2.2.2.2 Extrusion process

Co-rotating close intermeshing twin-screw extruders, ZSK30 (D = 30 mm, L/D = 40) and ZSK40 (D = 40 mm, L/D = 56) from the company Coperion Werner & Pfleiderer were used in the present work for the PP melt grafting reaction.

The process sections of these twin screw extruders were formed of modular components (barrel section, shaft or screw components) that were assembled in a specific configuration to meet the required unit operations. The barrel sections allow upstream or downstream feeding of diverse material forms (pellets, flakes, powders, liquids) as well as a vacuum devolatilization of gases or volatile reaction by-products. As the modular barrel system, the screw components were designed to accomplish specific tasks and can be combined according to the requirement (Fig. 2.2.1). In addition to conveying elements with high pitches, typically for the feed or devolatilization areas, or narrow pitches in areas where compaction of the polymer was needed, we added kneading blocks and toothed mixing elements (ZME "Zahnmischelement") to achieve dispersive and distributive mixing of the materials. Restrictive elements were used to increase the residence time and degree of loading of a mixing section composed of kneading blocks and toothed mixing elements [Tod98].

a) PP powder and chemicals

b) PP pellets **Fluid chemicals injected by a pumping system** **Devolatilization**


Fig. 2.2.1: Screw configuration used for the functionalization processes (ZSK30)

As described in Fig. 2.2.2a and 2.2.2b, two processes were utilized for the fabrication of cast films and pellets for the coextrusion. In a first step, cast films of grafted polypropylene were extruded by using a coat hanger die (width = 250 mm; slit = 0.4 mm) flanged to the extruder. PP powder and the grafting chemicals were tumble-mixed and introduced in the extruder with a gravimetric feeder. The reagents were then molten, mixed, homogenized by a combination of toothed mixing elements and kneading blocks in the screw configuration and finally devolatilized before exiting the

coat hanger die. The molten extrudate was subsequently quenched and cast over the chill roll unit. In order to achieve thin films of 100 and 200 μm, the throughput was kept low at 2 kg/h.

In a second step, the grafted PP pellets of selected formulations were produced in a sufficient amount for the coextrusion trials. The pure PP pellets were introduced into the extruder and mixed with the liquid chemicals (MAH, styrene and the peroxide dissolved in acetone) which were pumped downstream in the second zone of the extruder. Finally, the molten polymer mass exited the strand die, was cooled down in a water cooling bath and pelletized. This process allowed increasing the throughput up to 4 kg/h.
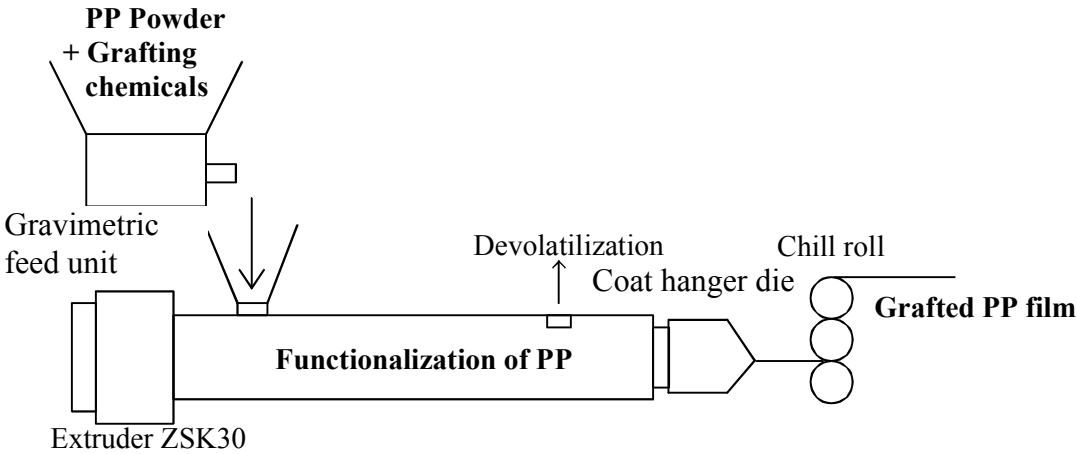
(a) Fabrication of cast films
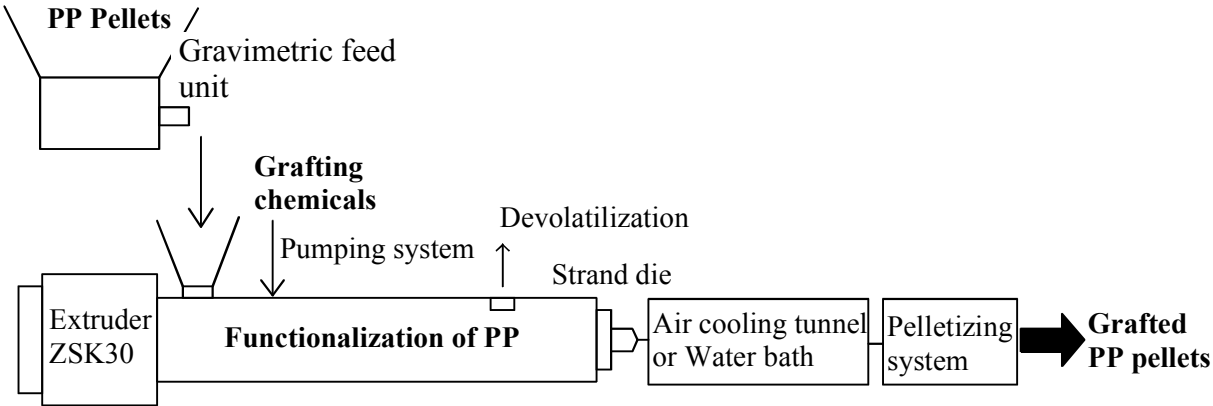
(b) Fabrication of pellets

Fig. 2.2.2: Processes for the production of functionalized PP

The processing conditions during the extrusion experiments were the following:

-      Feed rates: 1 to 4 kg/h,
-      Screw speeds: 50 to 200 rpm,
-      Temperature profiles:

Temp. zones (°C)	1	2	3	4	5	6	7	8	9	10	11	12
Film extrusion	150	200	200	200	200	200	200	200	200	200	200	200
	150	200	220	220	220	220	220	220	220	220	220	220
	150	200	220	240	240	240	240	240	240	240	240	240
Pellet extrusion	70	150	200	200	200	200	200	200	200	200	200	200

Tab. 2.2.5: Temperature profiles for the extrusion of films and pellets

The nip rolls temperature was kept constant at 40°C for the cast film extrusion of the PP copolymers and 80°C for the PP homopolymers.

The influence of the feed rate and screw speed on the residence time was considered as well. For that purpose, measurements of the residence time were conducted using the PP-g-MAH HB-MAH0.5-MD22.2-St1 as a formulation and blue ink as a visual reference. Although this method lacks of accuracy because of the difficulty to determine visually the colour change of the material within the first seconds after exiting the extruder die, a trend could be observed. The results are presented in Fig. 2.2.3a and 2.2.3b which show an exponentially decrease of the residence time against the throughput and the screw speed. In both cases, the polymer is conveyed faster along the screw. The screw speed however affects the residence time only slightly.
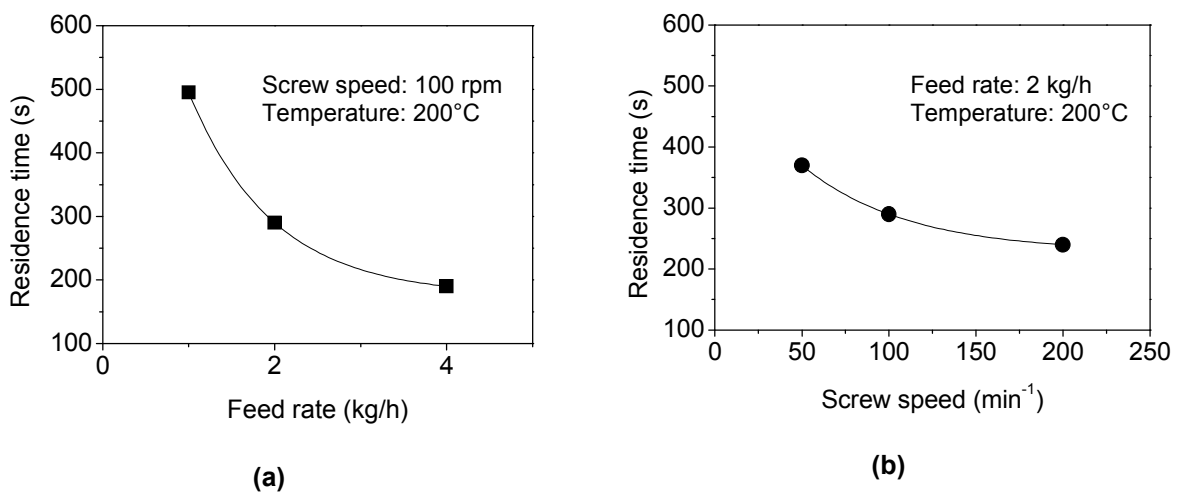

(a)   **(b)**

Fig. 2.2.3: Residence time as function of the material flow rate **(a)** and extruder screw speed **(b)**

Pellets of the PP-g-MAH concentrates to be blended with the pure resin were also produced. In the formulations, the quantity of peroxide (DHBP) was varied to obtain PP-g-MAH of different molecular weights as shown in Appendix 2.4. No styrene was added to the formulation to achieve a certain degree of degradation of the PP. Subsequently, cast films of PP/PP-g-MAH blends with different amounts of PP-g-MAH were extruded using the twin screw extruder and the coat hanger die.

In the same way as MAH, GMA was grafted on the PP matrix and the process parameters for the production of cast films remained as described previously.

Once the functionalization of the polypropylene resins realized, the polymer films were analyzed in terms of chemical, rheological, thermal, mechanical and surface properties in order to evaluate the major changes in the physical properties of the grafted materials. The films generated from different formulations were subsequently tested in terms of adhesion to find optimal formulations for the coextrusion trials.

3 Properties of the functionalized polypropylene films

3.1 Chemical analysis of the functionalized PP

3.1.1 Fourier Transform Infrared Spectroscopy

3.1.1.1 Principles of Fourier Transform Infrared Spectroscopy (FTIR)

Infrared spectroscopy is a well-established technique for the chemical characterization of polymers. Much information can be provided such as the qualitative, quantitative and structural analyses of polymers, the study of chemical composition, modification, degradation and oxidation of polymers, the analysis of the conformation of polymer chains, the determination of the degree of crystallinity and orientation in stretched polymer films or fibres.

Typically, when infrared (IR) radiation passes through a material, specific bands or frequencies of radiation are absorbed. The interaction between the infrared electromagnetic field and the material generates the absorption of given wave lengths of this radiation. The energy corresponding to this absorption is the transition energy between vibration and rotation states of molecules or atom groups. The frequencies which are absorbed are dependent upon the functional groups within the molecule and the symmetry of the molecule. Infrared spectroscopy focuses on electromagnetic radiation in the wavenumber (1/wavelength) range from 400 to 5000cm^{-1}. To generate the infrared spectrum, radiation containing all frequencies in the IR region is passed through the sample. The absorbed frequencies are decreased in the detected signal. This information is displayed as a spectrum of % transmitted radiation plotted against wavenumber. The absorption bands are related to vibration modes (stretching, bending, rocking…) which depend on conformational arrangements (trans, gauche…) or crystalline/amorphous phases.

Basically, a Fourier-Transform spectrometer consists of an optical bench and a data acquisition system (Fig. 3.1.1). The sample is simultaneously exposed to the entire range of IR frequencies. The resulting signal, the interferogram, is converted by a computer to a normal spectrum via a mathematical technique called the Fourier Transformation.

The normal instrumentation comprises the following devices [Col90, Koe99].
- The source emits the infrared radiation in the frequency range of interest.

- The laser produces a unique frequency in the IR spectrum. It follows the same path as the source and is used as a reference in the spectrometer.
- The interferometer produces a unique signal which contains all the infrared frequencies encoded into it. Most interferometers employ a beamsplitter which divides the incoming infrared radiation into two optical beams. One is directed towards a fixed mirror and the other towards a moving mirror. The beams are reflected and recombined at the exit of the interferometer. The moving mirror reflects the beam from different positions and these small motions, called scans, create a constant change in the intensity of the recombined beam.
- The detector is produces an electric signal when receiving the coded radiation. An interferogram is generated by collecting the amount of light reaching the detector per unit of time. This interferogram is called the background when the radiation passes through the optical bench without sample.
- The computer determines the frequency and intensity of each component wave of the interferogram, by performing a Fourier Transform of the data. These frequencies and intensities make up the peaks of an IR spectrum.
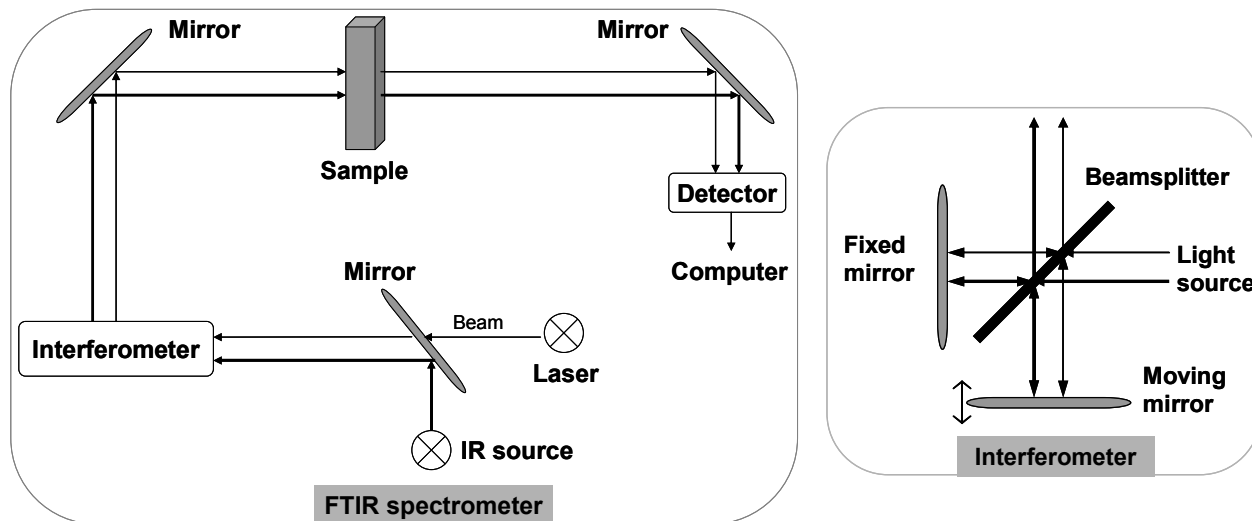

Fig. 3.1.1: Description of a FTIR spectrometer

The absorption spectra can be obtained in reflection or transmission. The commonest IR technique, transmission, allows the measurement of the fraction of radiation absorbed by the sample. Another option is the Attenuated Total Reflectance (ATR) which is used for the analysis of thick or opaque samples (Fig. 3.1.2). It is a contact sampling method which measures the radiation absorbed (evanescent wave) at a few microns by a low refractive sample after several reflections in a highly

reflective crystal. The latter possesses a high refractive index and low IR absorption in the IR region of interest. The depth of penetration d_p which is on the order of the radiation wavelength can be calculated as follows:

$$d_p = \frac{\lambda_0}{2\pi n_1 \left(\sin^2 \theta - n_{21}^2\right)^{1/2}} \qquad \textbf{Eq. 3.1.1}$$

where λ_0 is the wave length of the radiation in air, θ is the angle of incidence, n_1 is the refractive index of the ATR crystal and n_{21} is the ratio of the refractive index of the sample to that of the ATR crystal.
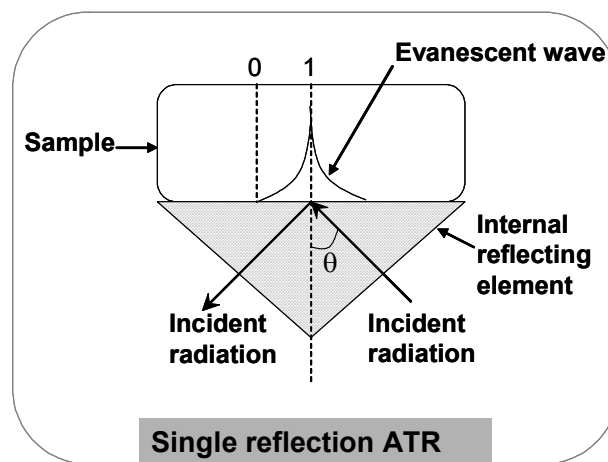
Fig. 3.1.2: Transmission and reflection sampling methods

3.1.1.2 Method

The transparent samples were analyzed in transmission as well as in reflection by using FTIR device from Brucker (IFS 66/S at IAMC and Vector 22 at IKT) which can be equipped with a diamond ATR tool ("Golden Gate") for the measurements in reflection. The spectrometer analyses thin films in a transmission wavenumber range between 3800 and 600 cm^{-1}. The measurements were realized at a resolution of 0.5 cm^{-1} and 32 scans at the IAMC and 4 cm^{-1} 20 scans at the IKT.

Films of 50-100 μm thickness were obtained by compression-molding of 0.1-0.2 g samples between Teflon sheets under approximatively 20 kN at a temperature superior to the PP melting point during 2 min.

The relevant characteristic absorption bands of the polypropylene and the monomer MAH, styrene are detected in the FTIR spectra shown in Fig. 3.1.3. In the spectrum

of PP no significant peak can be identified within the range of 1600 and 2000 cm^{-1}. Among the characteristic bands of the PP one can detect for example bands around 900, 1000, 1100 or 1167 cm^{-1}.

In Fig. 3.1.4a, the IR spectrum of PP-g-MAH presents a strong characteristic band at 1782 cm^{-1} (C=O symmetric stretching band) which indicates the presence of carbonyl groups in PP-g-MAH. A weak absorption band near 1850 cm^{-1} corresponds to the asymmetric C=O stretching band of MAH. The presence of styrene is detected by the ring deformation absorption band near 700 cm^{-1} (Fig. 3.1.4b).
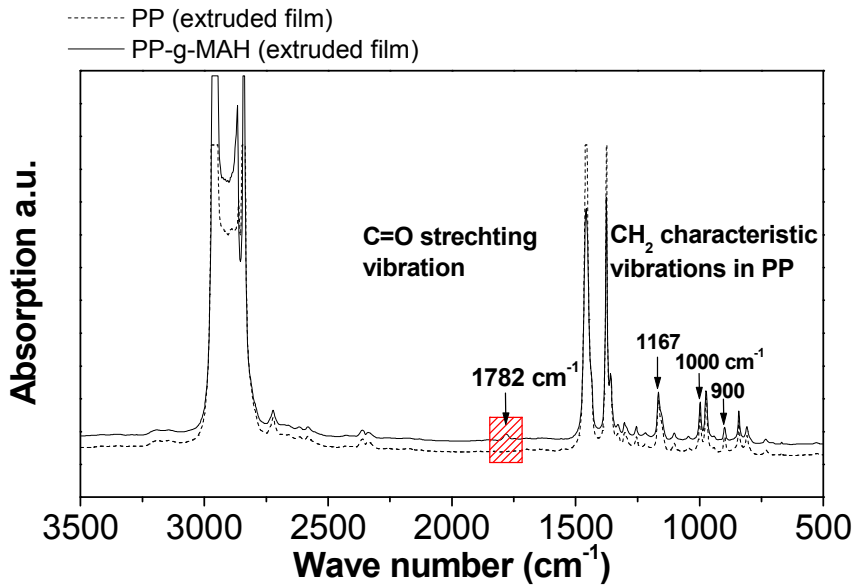
Fig. 3.1.3: FTIR spectra of PP and PP-g-MAH samples measured in transmission
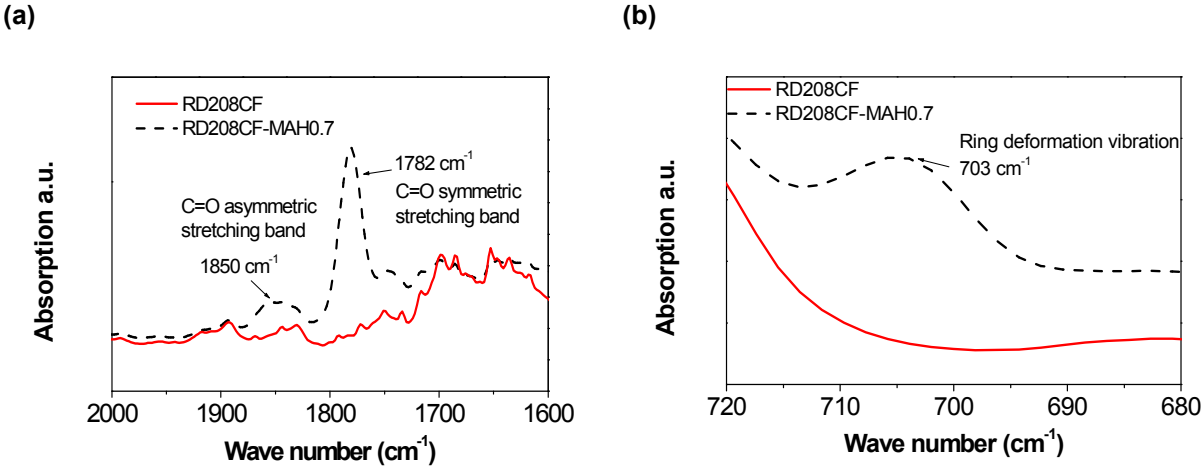
Fig. 3.1.4: Details of the PP-g-MAH FTIR spectra

Furthermore, polypropylene homopolymer and copolymer can be distinguished by the CH_2 rocking vibration around 731 cm^{-1} caused by the ethylene sequences present in the copolymer (Fig. 3.1.5).
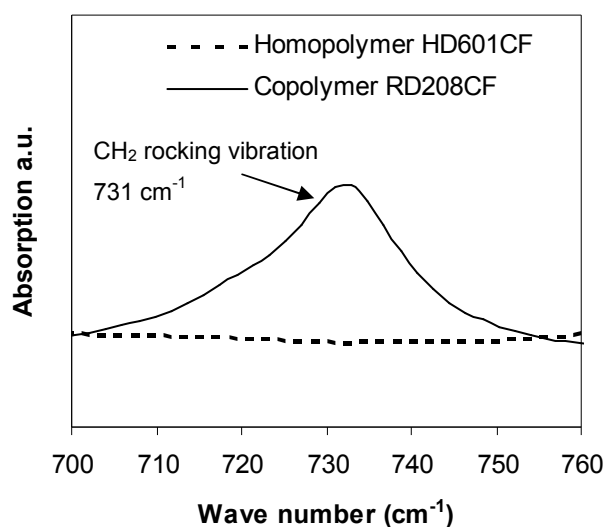

Fig. 3.1.5: Comparison of PP homopolymer and copolymer FTIR spectra

Considering the PP-g-GMA samples, the characteristic band of GMA is situated around 1741 cm^{-1}. The carbonyl absorption band of GMA is shifted from 1741 to 1730 cm^{-1} when styrene is present in the formulation (Fig. 3.1.6). This confirms that the grafting of GMA onto the polypropylene backbone is realized over styrene radicals as discussed in section 2.1.4.
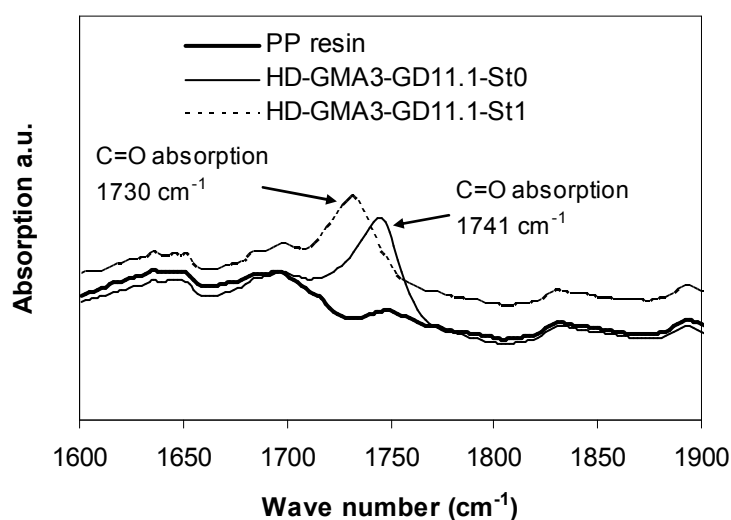

Fig. 3.1.6: FTIR spectra of the pure PP and PP-g-GMA samples
(PP-g-GMA with and without St)

To quantify the relative amount of grafted monomer, the intensity of the monomer transmission band around 1782 cm^{-1} for MAH, 1741 and 1730 cm^{-1} for GMA, 700 cm^{-1} for styrene as well as the intensity of a PP characteristic band – for instance around 1000 cm^{-1} – were measured. All spectra were normalized prior to integration of the monomer specific band.

The monomer relative grafting yield is calculated as follows:

$$R_{Monomer/PP} = \frac{A_{monomer}}{A_{PP}} = \frac{\int_{v}(n_{monomer}cm^{-1})}{\int_{v}(1000cm^{-1})} \qquad \textbf{Eq. 3.1.2}$$

where $A_{monomer}$ is the surface or height of a specific absorption band of the monomer (carbonyl band for MAH, ring deformation band for styrene…) and A_{PP} the surface or height of the absorption band of the PP.

The determination of the effective grafting yield is achieved by using a calibration curve with defined amounts of monomer in the PP. Calibration curves were realized by using blends of PP and alternating styrene/maleic anhydride copolymer (P(St-alt-MAH)), polystyrene, octadecyl succinic anhydride as well as dodecenyl succinide anhydride. The calculation of the effective grafting yields was restricted to the grafted samples RD208CF and HD601CF using the PP/P(St-alt-MAH) and PP/polystyrene blends (Fig. 3.1.7). The reference samples were produced in a batch mixer under defined process conditions (see Appendix 3.1).
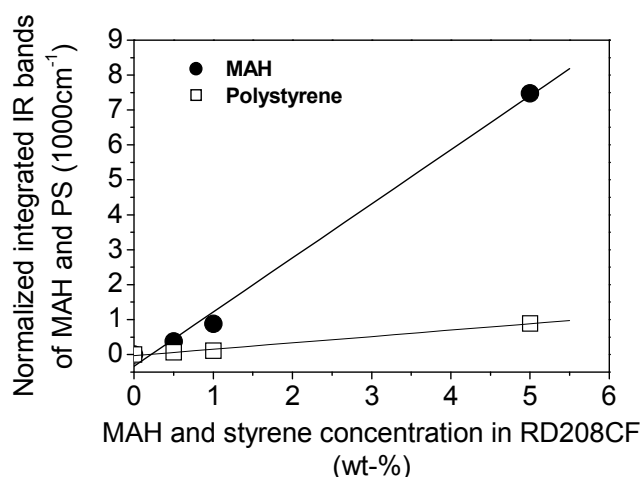

Fig. 3.1.7: Calibration curves of PP/P(St-alt-MAH) and PP/polystyrene blends

For an accurate determination of the monomer content in the PP-g-MAH, the samples were purified to eliminate the unreacted monomers, ungrafted polymerized monomers as well as other low molecular species that were formed during the

functionalization process. The samples were dissolved in boiling xylene at 138°C, then precipitated in acetone and finally dried at 60°C during 24h in a vacuum oven. A comparison of the characteristic band of MAH at 1782 cm^{-1} in purified and raw samples confirms the presence of ungrafted MAH species, as shown in Fig. 3.1.8a. Samples of RD208CF-MD22.2-St1 with MAH initial concentrations of 0.5, 0.7 and 1 phr were taken as an example. For these formulations, about 54 to 87% of the MAH present in the raw samples is actually grafted. Only a few percent of styrene is free in the raw material.
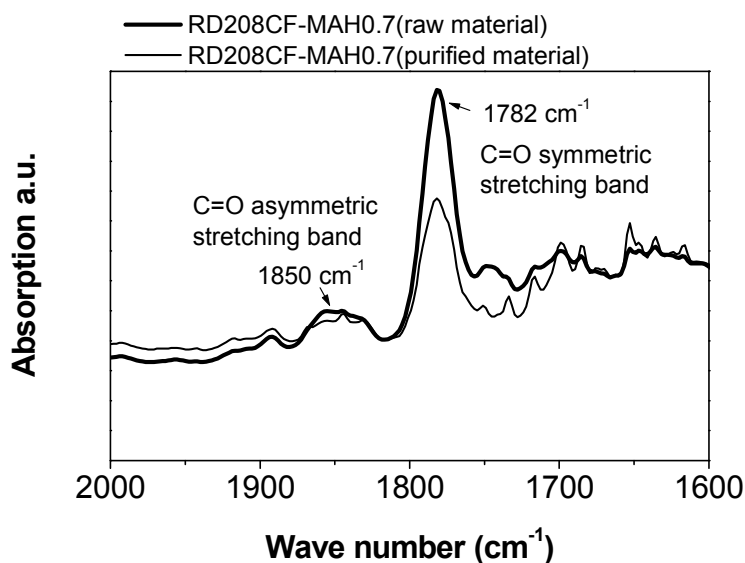
(a) Comparison of the FTIR spectra of raw and purified PP-g-MAH samples
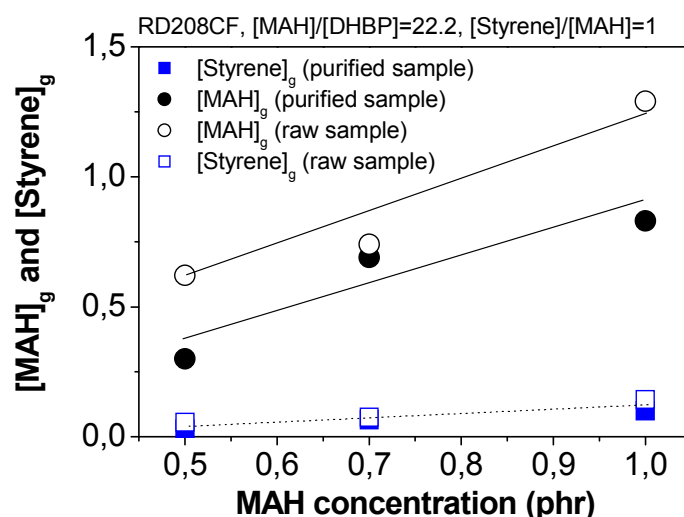
(b) Calculated grafting yields of MAH and styrene

Fig. 3.1.8: Comparison of the grafting yields of purified and non purified PP-g-MAH samples

3.1.2 Analysis of the grafting reaction

3.1.2.1 Influence of the chemical formulation on the monomer grafting yields

a) Grafting of maleic anhydride onto PP

As seen in chapter 2, many factors influence the grafting reaction of MAH onto PP. The concentrations of the different components in the formulation as well as the presence of co-monomers are important parameters for an efficient functionalization. Considering the fact that the comonomer presence plays a fundamental role in the grafting reaction, we started by investigating the grafting of the system MAH/Styrene on PP. For this purpose, a copolymer RD208CF sample with a MAH amount of 0.7 phr and a styrene/MAH molar ration of 1 (RD-MAH0.7-MD11.1-St1) was selected and purified to eliminate the impurities present in the material. Its FTIR spectrum was compared to the spectra of the pure PP resin, blends of the raw PP with an alternating styrene/maleic anhydride copolymer (P(St-alt-MAH)), polystyrene and octadecyl succinic anhydride.

The comparison of the shape of the band at 1782 cm^{-1} with the bands of model systems of PP blended with 1wt-% of the P(St-alt-MAH) and 0.5 wt-% of octadecyl succinic anhydride, at 1777 and 1794 cm^{-1}, respectively, reveals that the grafted copolymer consists of a great amount of alternating styrene/MAH structures (Fig. 3.1.9). As a matter of fact, the absorption bands of poly(maleic anhydride) and n-octadecyl succinic anhydride are situated around 1784 and 1792 cm^{-1}, respectively [Ro95]. The latter is detected as a small deformation in the C=O band at 1782 cm^{-1} of the grafted PP, indicating the presence of a reduced amount of single MAH grafts on the PP backbone. This result shows that the complexion of MAH with styrene eventually occurs and enhances the reactivity of MAH towards the PP macroradicals.
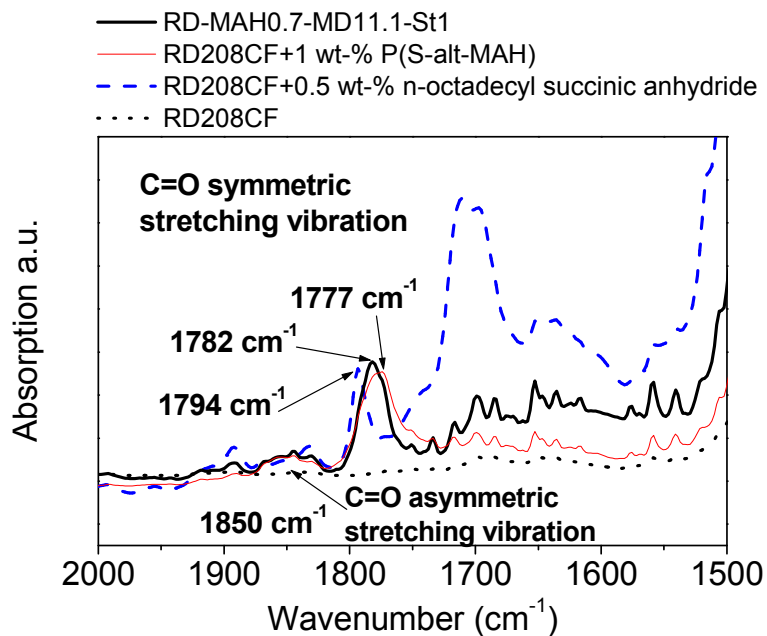
Fig. 3.1.9: FTIR spectra of the PP resin RD208CF, the purified RD-MAH0.7-MD11.1-St1, PP + 1 wt-% P(St-alt-MAH) and PP + 0.5 wt-% of octadecyl succinic anhydride

The ring deformation band of styrene in a blend of PP and polystyrene is located at 699 cm^{-1} (Fig. 3.1.10). This absorption band is shifted to 702 cm^{-1} for the blend containing PP and 1 wt-% P(St-alt-MAH). The considered signal is detected as well at 703 cm^{-1} for the purified RD-MAH0.7-MD11.1-St1 sample, thus confirming the presence of P(St-alt-MAH) in the grafted material.
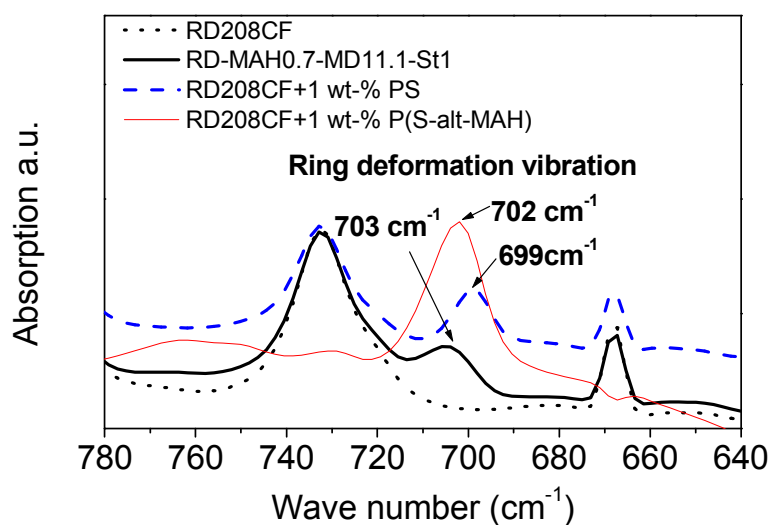

Fig. 3.1.10: FTIR spectra of the pure PP copolymer RD208CF, the purified RD-MAH0.7-MD11.1-St1, PP + 1wt-% P(St-alt-MAH) and PP + 1 wt-% of polystyrene

The concentrations of the components in the formulations were varied and the grafting efficiencies of the materials were determined.

In a first step, the low molecular weight polypropylenes RD208CF (copolymer) and HD601CF (homopolymer) were taken into consideration. It was shown that increasing the amount of added MAH and keeping simultaneously the MAH/DHBP and styrene/MAH proportions constant at 22.2 phr/phr and 1 mol/mol, respectively, enhanced the grafting yield of MAH (Fig. 3.1.11 and Fig. 3.1.12). As a matter of fact, with a raising initial MAH concentration, the probability of grafting is increased. Besides, the simultaneous increase of the styrene amount led to a slightly growth of its grafting yield.
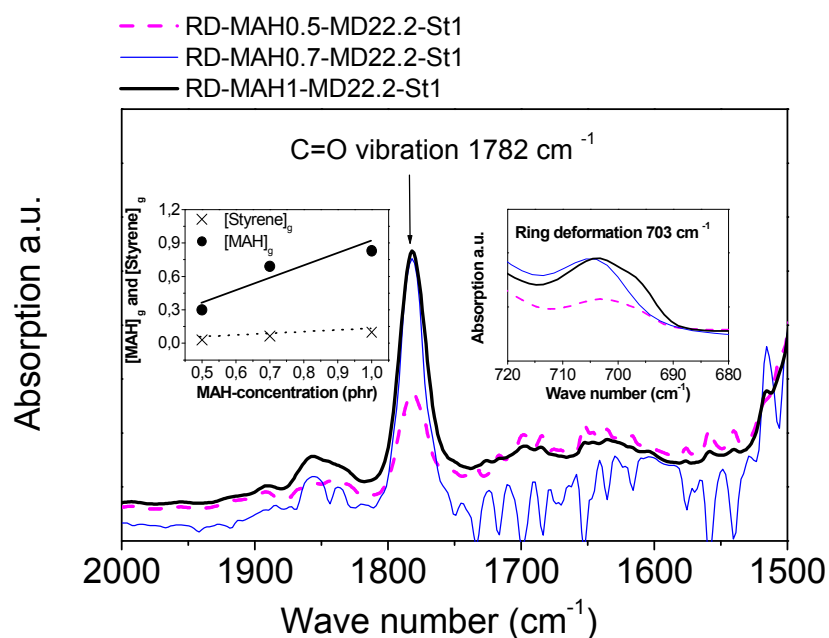

Fig. 3.1.11: Analysis of the MAH and styrene grafting yield as a function of the initial amount of MAH and styrene for the copolymer RD208CF

Fig. 3.1.13 demonstrates that an augmentation of the styrene/MAH molar proportion obviously promoted grafting. As already mentioned, styrene can form with MAH Charge Transfer Complexes that are more reactive to the PP macromolecules. Thus, MAH and styrene are grafted to a greater extent and the β-scission is reduced.
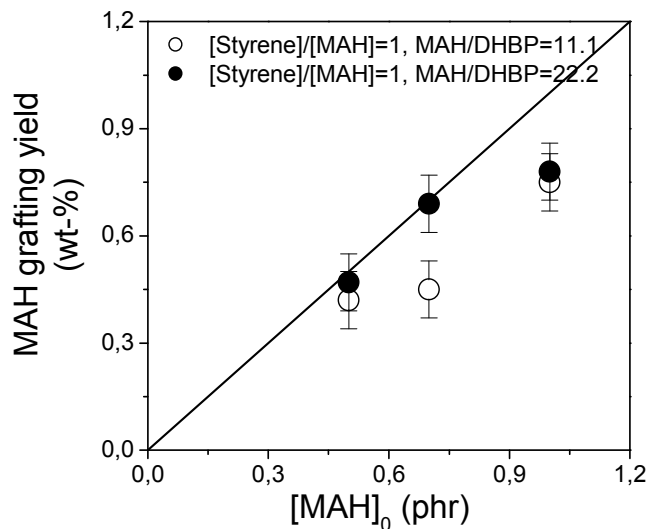
Fig. 3.1.12: MAH grafting yield as a function of the initial amount of MAH and DHBP introduced in the copolymer RD208CF
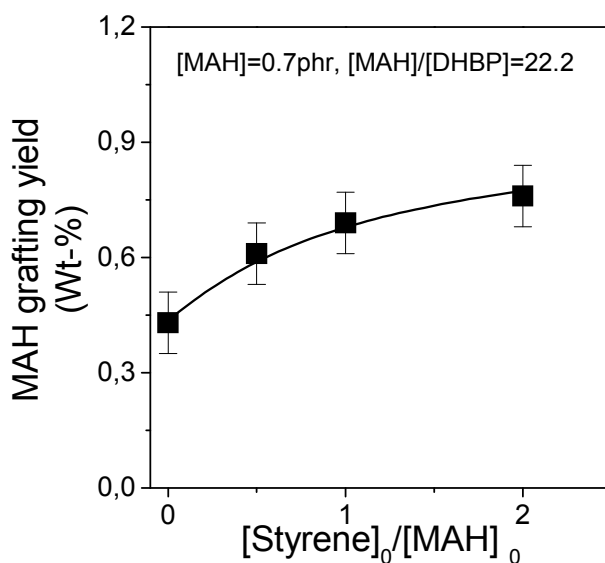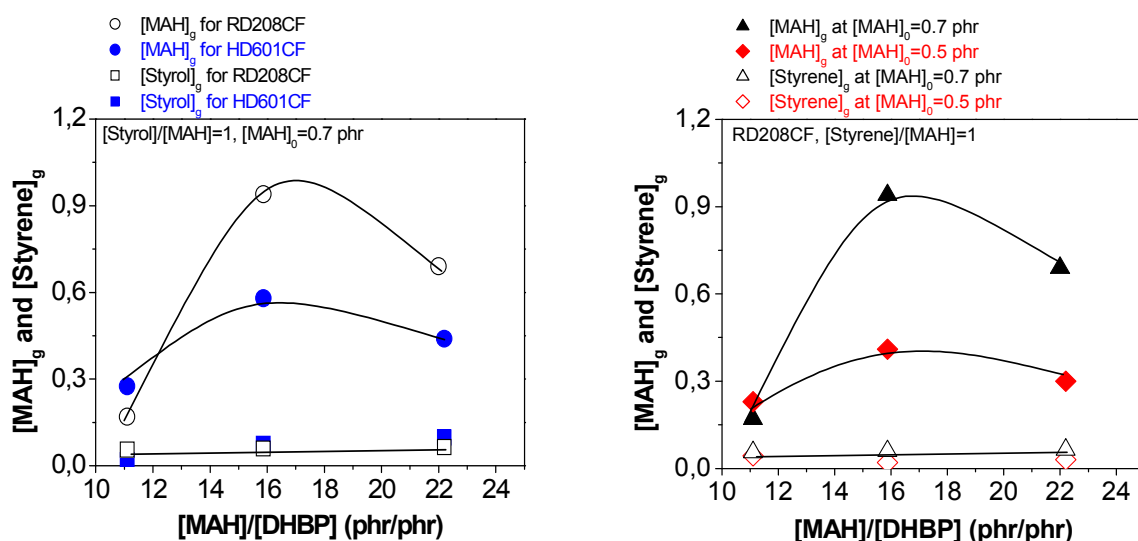

Fig. 3.1.13: MAH grafting yield as a function of the styrene/MAH molar proportion introduced in the copolymer RD208CF

The amount of grafted styrene was found to be independent of the MAH/DHBP proportions as well as of PP types (Fig. 3.1.14a and 3.14b). Increasing the MAH/DHBP ratio led to the same trends for two MAH concentrations (0.5 and 0.7 phr), showing a maximum value at MAH/DHBP=15.87 (Fig. 3.1.14b). A comparison of the grafting efficiencies of the grafted copolymers RD208CF and homopolymers HD601CF indicated better results for the copolymers (Fig. 3.1.14a). Degradation, as

a competing reaction, tends to inhibit grafting to a greater extent for the homopolymers than for the copolymers. This is due to the structure of the homopolymers. Effectively, the tertiary hydrogen atoms of propylene sequences are more sterically hindered than are the secondary ones of ethylene sequences. Steric hindrance also explains the fact that the free-radical reactivity of PP increases with rising ethylene content [Mie94]. Thus, copolymers are more prone to be grafted with MAH or to crosslink.

(a) Comparison of the grafting yields of the copolymer and the homopolymer PP-g-MAH

(b) Grafting yields of the copolymer PP-g-MAH for initial MAH concentrations of 0.7 and 0.5 phr

Fig. 3.1.14: MAH and styrene grafting yields as a function of MAH/DHBP weight proportions introduced in the copolymer RD208CF and the homopolymer HD601CF

In a second step, the grafting of high molecular polypropylenes RB501BF (copolymer) and HB205TF (homopolymer), more suitable for the film blowing process, were investigated in terms of functionalization efficiencies. Relative grafting yields were used as indication for the determination of the influence of the components on the functionalization efficiency. For the present set of measurements, the polypropylene CH_2 band at 1000 cm^{-1} was used for the normalization and integration calculations.

Concerning the grafted copolymers, an increase of the relative grafting yields with rising quantity of introduced MAH and peroxide (TMCH or DHBP) was observed. By adding a greater amount of peroxide in the material, the initial primary radicals as well as the macroradicals are more numerous and the probability for grafting or β-scission to occur is higher. Besides, the presence of styrene enhanced considerably

the grafting yields independently of the peroxide type used in the formulations (Fig. 3.1.15).

As for the grafted homopolymers, the FTIR analyses showed similar results to those obtained for the copolymers: increase of the relative grafting yields with the augmentation of MAH, peroxide or styrene in the formulations (Fig. 3.1.16).
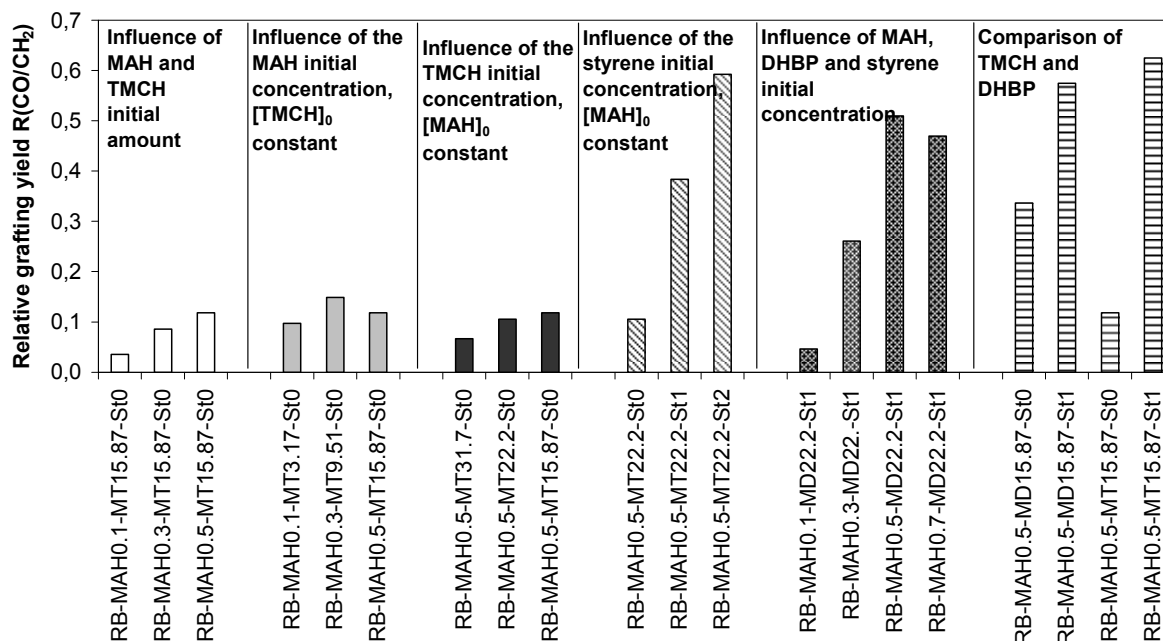

Fig. 3.1.15: Relative grafting yields of the PP-g-MAH copolymers RB501BF as a function of the amount of introduced MAH, peroxide and styrene
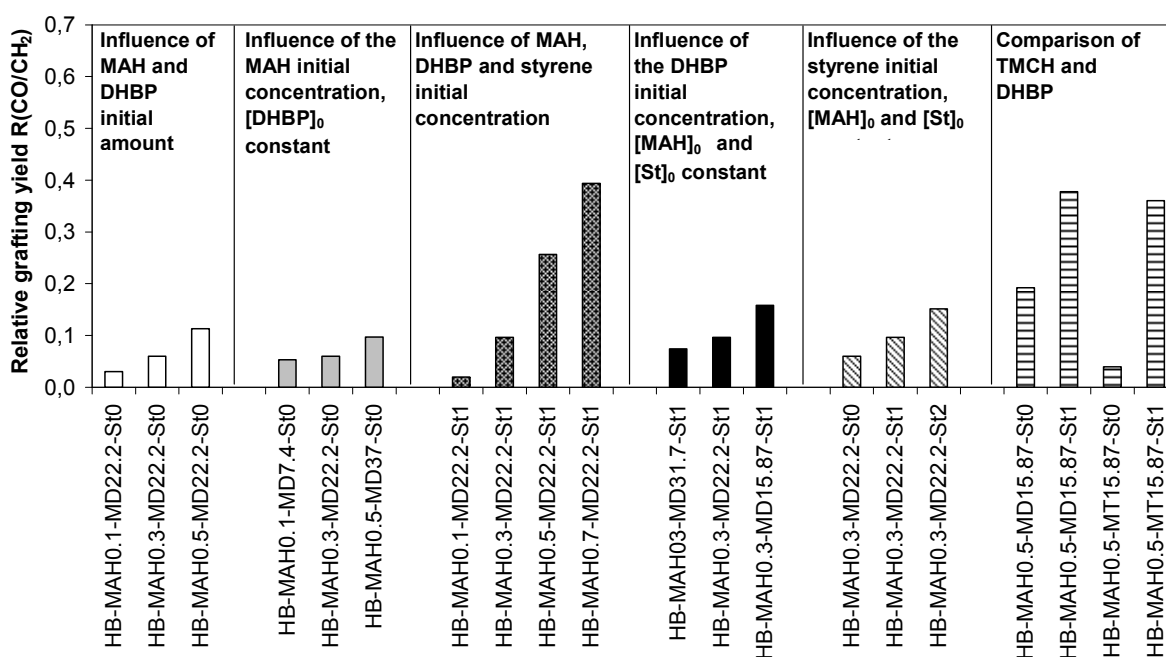

Fig. 3.1.16: Relative grafting yields of the PP-g-MAH homopolymers HB205TF as a function of the amount of introduced MAH, peroxide and styrene

A comparison of the grafting yields of formulations using two different peroxides, DHBP and TMCH, revealed the higher effectiveness of DHBP for both PP types under the same grafting conditions, i.e. without styrene in the formulation. This result may be correlated to their decomposition rates and their solubility in the PP. As seen in Fig. 3.1.17, the chosen peroxides DHBP and TMCH decompose in 0.46 and 0.022 min at 200°C, respectively. In the case of DHBP, the thermal decomposition happened continuously during the grafting process, a period of 2 min being taken as residence or decomposition time. Considering TMCH, its decomposition started even before the PP began to melt, thus reducing the grafting and degradation processes and possibly enhancing secondary reactions such as polymerization of the monomers. However, the presence of styrene in the formulation led to similar grafting yields for both peroxides and polymer types.
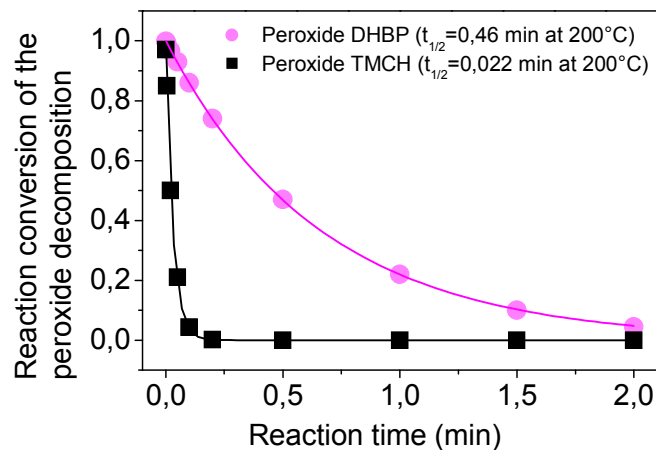

Fig. 3.1.17: Reaction conversion of the peroxide decomposition of DHBP and TMCH as a function of the reaction time at a process temperature of 200°C

As already mentioned for the grafted low molecular polypropylenes, the functionalization is more efficient for the grafted PP copolymers in the case of high molecular PP as well (Fig. 3.1.18).
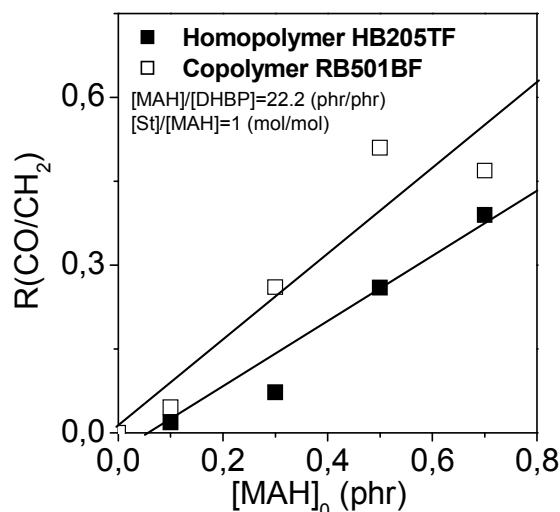
Fig. 3.1.18: Comparison of the relative grafting yields of the PP-g-MAH homopolymers HB205TF and copolymers RB501BF

The PP-g-MAH concentrates to be used as adhesion promoters, with 1 phr of initial MAH, increasing amounts of peroxide DHBP (MAH/DHBP = 5.5, 11.1, 15.87) and without addition of styrene were analyzed in the same way. As expected, they showed growing grafting yields with raising concentration of peroxide (Fig. 3.1.19).

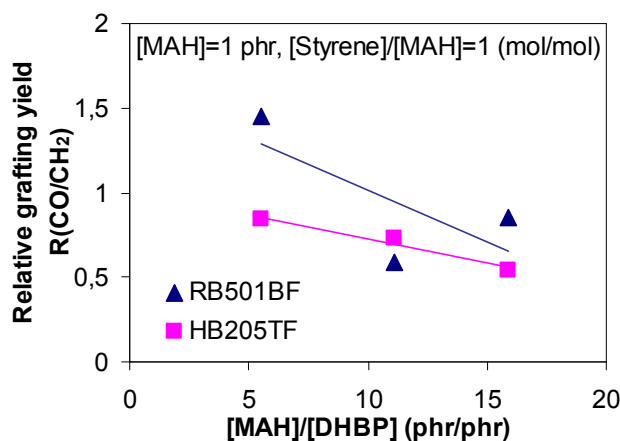**Fig. 3.1.19:** Relative grafting yields of the concentrates PP-g-MAH (homoplymer and copolymer)

b) Grafting of glycidyl methacrylate onto PP

The PP-g-GMA were purified, pressed to 100 µm films and subsequently analyzed using transmission FTIR in the same way as the PP-g-MAH samples. The PP band at 1000 cm^{-1} was chosen for the normalization and the integration of the carbonyl band was realized by using peak heights.

Fig. 3.1.20a the relative grafting yields of the PP-g-GMA copolymer RD208CF, homopolymer HD601CF as function of initial GMA contents are presented. The more GMA introduced in the formulation under the same extrusion conditions, the more GMA was grafted. The functionalization is also more effective for PP copolymers than for homopolymers, thus confirming the results obtained with the PP-g-MAH. The presence of styrene as reactivity promoter during the functionalization process, especially at a molar ration styrene/GMA of 1.5 mol/mol, can be shown in Fig. 3.1.20b. The grafting of GMA onto PP was enhanced to a lesser extent by increasing the peroxide amount.
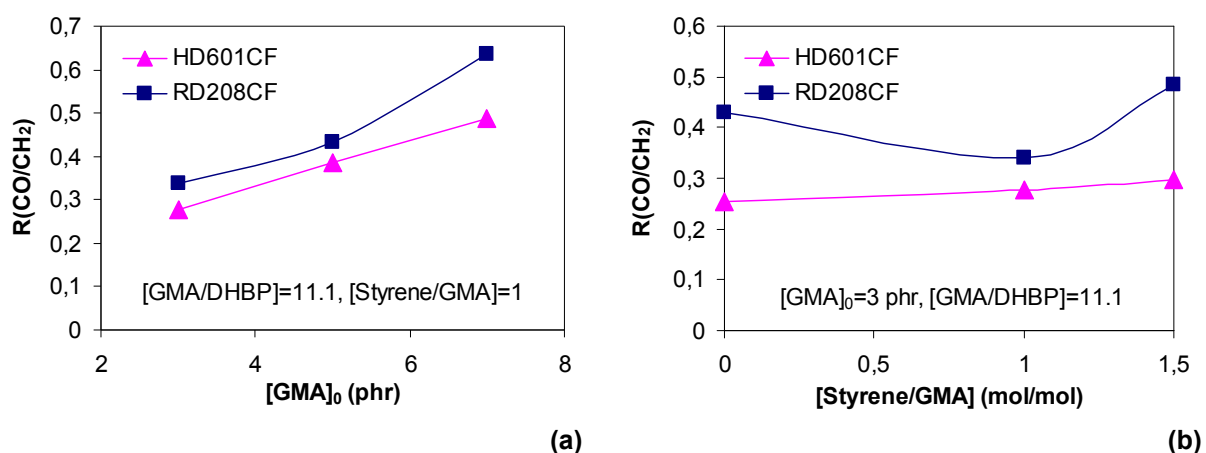

(a)   (b)

Fig. 3.1.20: GMA grafting yield as a function of the GMA initial concentration **(a)** and styrene/GMA molar proportion **(b)** introduced in the copolymer RD208CF

3.1.2.2 Influence of the process conditions on the grafting yields

In order to evaluate the influence of the process parameters on the grafting yields, the sample HB-MAH0.5-MD22.2-St1 was prepared under different compounding conditions. The screw speed was varied from 50 to 200 min^{-1}, the flow rate from 1 to 4 kg/h and the temperature from 200 to 240°C. Fig. 3.1.21 shows the FTIR analyses results of the collected samples. The relative grafting yields were calculated using the polypropylene CH_2 band near 1100 cm^{-1} as well as a height integration of the peaks. Although the grafting rates window between 0.76 and 0.88 is reduced, some trends were able to be observed. On the one hand, with an increasing screw speed, the functionalization efficiency was improved due to the shear induced energy. The augmentation of the throughput led to an amelioration of the grafting because of the higher friction between material and barrel. Both parameters screw speed and flow rate induced a good homogenisation of the components as well. On the other hand, an increasing process temperature resulted in a diminution of the grafting yield. The

temperature possesses a direct impact on the peroxide decomposition and possibly favoured the competing reactions such as β-scission instead of the grafting processes.
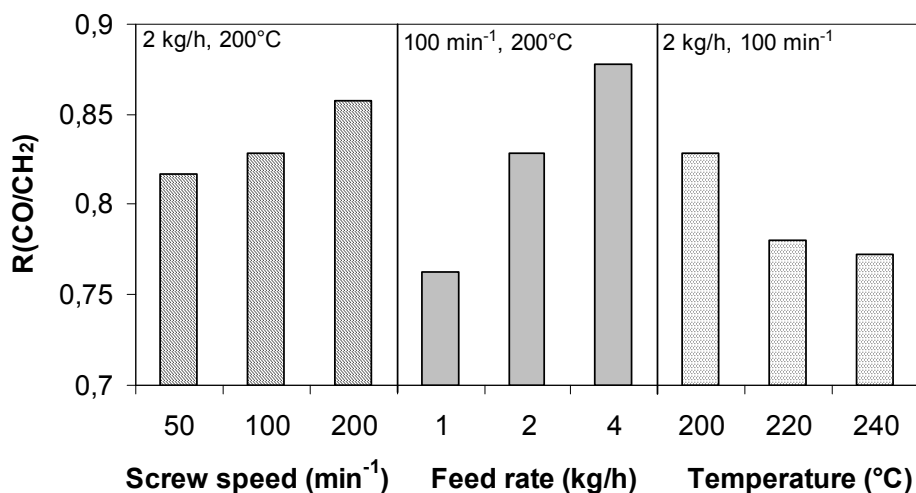

Fig. 3.1.21: Influence of the extrusion parameters on the relative grafting yield

Not only the processing variables but also the process set up implied modification of the functionalization efficiency. A comparison of the grafted PP-g-MAH pellets and films in Fig. 3.1.22 shows that the relative grafting yields of the pellets are drastically higher than the films' ones. The feed rate for the pellets fabrication was fixed at 4kg/h and for the films at 2kg/h. In the case of pellets' production, a more intensive mixture due to the dissipative energy created by the mass augmentation in the barrel enhances the grafting. Besides, the grafting components (PP powder and chemicals) were preliminary tumbled mixed for the preparation of the films whereas, for the pellets production, the fluid chemicals were directly pumped into the first extruder zone and the PP introduced as pellets in the hopper. The differences between the grafting rates of the films and the pellets are more pronounced for the homopolymers than for the copolymers. This may be due to the formulations, i.e. initial amount of styrene or peroxide type must be considered.
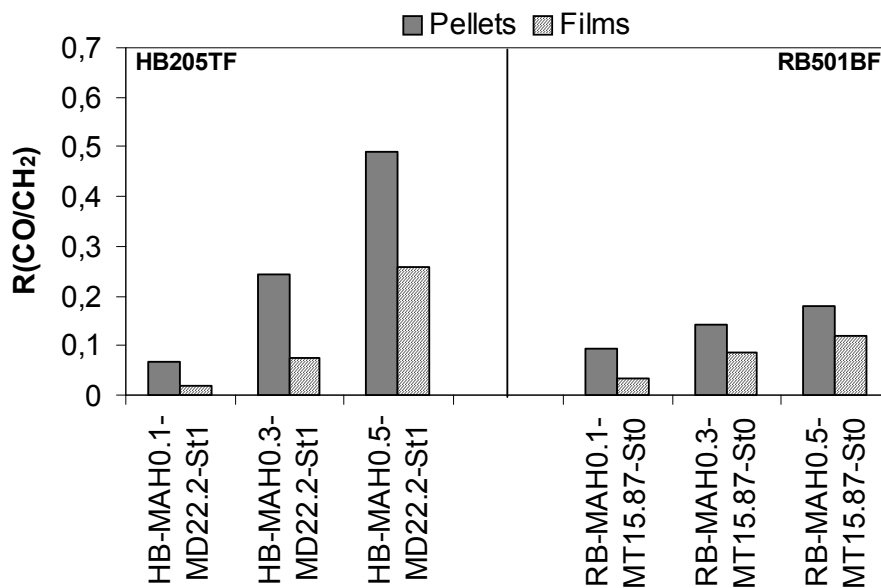
Fig. 3.1.22: Comparison of the grafting yields of purified PP-g-MAH pellets and films

3.2 Rheological characterization of the functionalized PP

Rheology is the study of the flow and deformation of matter in terms of elasticity and viscosity. Molten polymers are rheologically complex materials. They are formed of long chains which build, even in the molten state, entanglements or temporary physical networks depending on their structure and under given conditions. In opposition to Newtonian fluids which deformation rate is proportional to the stress applied, polymer melts possess an elastic component in their response to a mechanical solicitation, showing a viscoelastic behaviour. The rheological properties are sensitive to their molecular structure and play a central role in melt processing. Rheological data from molten polymers can be used to relate the effects of their molecular weight, molecular weight distribution, degree of branching or filler content to processability. Information about the flow properties, structure, morphology, long-term performance can be gained by performing tests under a wide deformation range. The materials are tested under steady or oscillatory/dynamic modes. For these purposes, different instruments are taken into account, delivering, on the one hand, fundamental rheological data and, on the other hand, indicative measurements about the melt flow behaviour. In this work, capillary and rotational rheometry as well as Melt Flow Index measurements were used to characterize the rheological behaviour of the unmodified and functionalized resins.

3.2.1 Instrumentation

3.2.1.1 Principle of a rotational rheometer

Among the different technologies used by rheometers for polymer testing, rotational rheometry permits a great range of analyses (stress, relaxation, oscillation, ramp tests…). Rheological data acquired by rotational rheometers can relate the polymer's morphology and structure to end-use performance.

In principle, measurement occurs by applying a controlled strain or strain rate to the sample and the resulting stress is calculated from the torque or force. A defined stress can also be applied and the resulting strain rate is measured as in the case of the Dynamic Stress Rheometer (DSR). In this study, a DSR from Rheometrics using parallel plate geometry is employed to perform the rheological tests. The parallel geometry is illustrated in Fig. 3.2.1. In this configuration the polymer sample is placed between two parallel circular discs of radius R, one of which rotates with a given angular velocity Ω, the other one being stationary. The gap h between the discs is adjustable. Stress is applied to the upper surface of the sample by the stress head, a rotary actuator attached to a precision air bearing. A position sensor mounted on the stress head outputs the strain, the angular deflection of the stress head. The sample is tested in a closed chamber under nitrogen atmosphere to avoid undesired reactions such as oxidation during measurement.
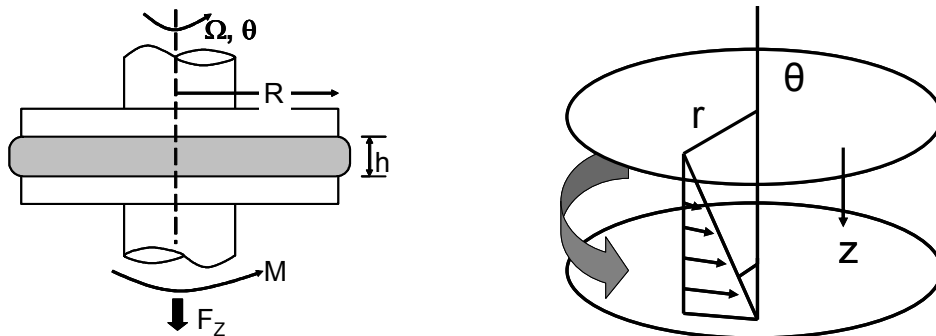
Fig. 3.2.1: Description of the plate geometry of a rotational rheometer

Dynamic rheometers allow determining the viscoelastic properties of polymer melt amongst others under oscillating loading. The moving disc oscillates with a forced frequency ω and the torque amplitude M as well as its phase displacement δ are measured. By considering the flow field and measured values of ω, M, F_Z (normal force), the shear rate, strain and stress are calculated and, derived from them, the loss modulus G", storage modulus G' and complex viscosity η^*. Dynamic measurements are usually realized in the viscoelastic region of the material where G' and G" are functions of the temperature and frequency, the stress being constant.

Different test modes are available among which time sweep, stress sweep and frequency sweep were applied in this work. To determine the linear viscoelastic region of a molten polymer, a stress sweep measurement is performed while temperature and frequency are kept constant. The moduli are registered as functions of the stress. From a critical stress τ_C the polymer's behaviour starts to become non-linear and the moduli decline. The time sweep mode permits to evaluate a material's chemical, thermal or mechanical stability by measuring the moduli or viscosity at a constant frequency, stress and temperature over an extended period of time (15 or 30 min). Fig. 3.2.2 presents, as an example, the time sweep, stress sweep and frequency sweep measurements performed on a PP-g-MAH sample (HB-MAH0.5-MD22.2-St1) to check its thermal stability at 200°C, to determine the linear viscoelastic domain (between 200 und 800 Pa) as well as to register its viscosity and moduli as functions of the frequency.
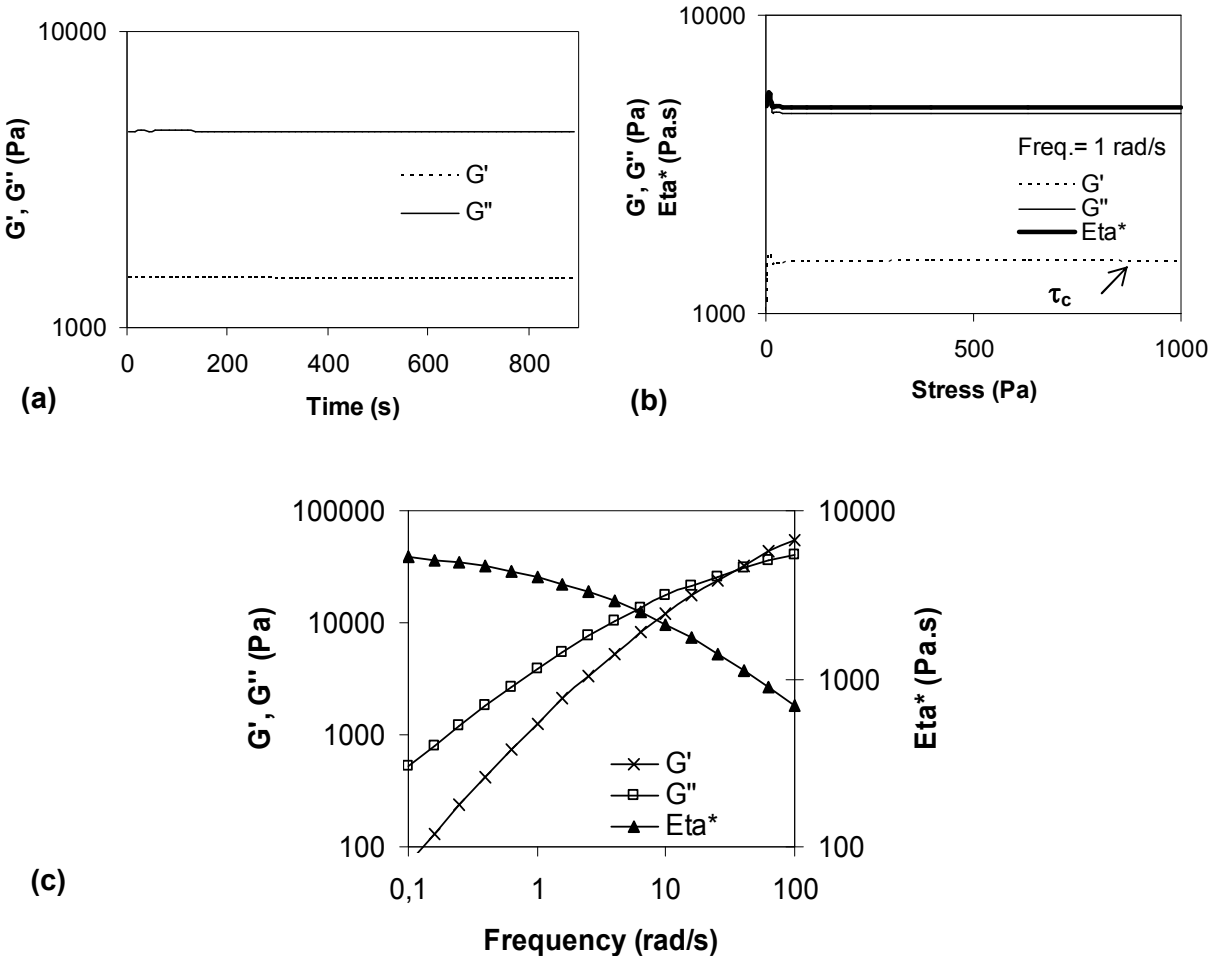

Fig. 3.2.2: Time **(a)**, stress **(b)** and frequency **(c)** sweep measurements performed at 200°C on a PP-g-MAH sample (HB-MAH0.5-MD22.2-St1) using a DSR

45

Samples for the rotational rheometry were prepared from the PP-g-MAH films or pellets. The latter were pressed into discs using a hydraulic press and a special mould. The dimensions of one disc are a diameter of 25 mm and a thickness of 2.5 mm. The samples were moulded at a temperature of 200°C during 2.5 min without pressure and 2.5 min under 50 bar. Finally, they were cooled under pressure during 10 min.

3.2.1.2 Principle of a capillary rheometer

According to the standard specification ASTM D3835, capillary rheometry is an investigation method sensitive to polymer molecular weight and molecular weight distribution, thermal and rheological polymer stability, shear instability, moisture, additives such as plasticizers, lubricants, reinforcements and fillers.

There are different types of capillary rheometers for low viscous materials such as concentrated solutions or for high viscous polymer melts. For the latter, high shear rates from 10^0 up to 10^5 s^{-1} can be achieved. They are comparable to processing shear rates. In principle, the rheometer consists of a heated barrel at a given temperature and a piston that drives the molten polymer through a calibrated die applying a constant speed or shear rate. Pressure transducers record the pressure at the entrance and along the die. Fig. 3.2.3 describes the schematic design of a capillary rheometer.
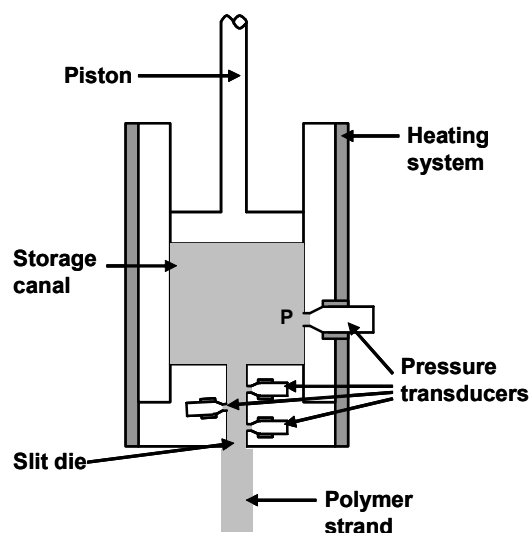

Fig. 3.2.3: Description of a capillary rheometer

To allow a complete development of the melt flow and minimize entrance and exit effects on the flow, the length to diameter ratio of a capillary die must be superior to

10. For the treatment of pressure data some corrections need to be performed such as the Bagley (vortices formation in a ring capillary due to viscoelastic effects), Hagenbach (changes in the flow speed) or Couette corrections (changes in the friction conditions at the wall) [Lau95]. Based on measurements of the piston speed V_{st} and the pressure drop Δp, the viscosity $\eta(\dot{\gamma})$ is derived from the shear stress τ_w and shear rate $\dot{\gamma}_w$ at the wall:

$$\eta = \frac{\tau_w}{\dot{\gamma}_w} \qquad \textbf{Eq. 3.2.1}$$

The shear stress τ_w at the wall is obtained from the pressure drop Δp measured by the transducers along the die length:

$$\tau_w = \frac{h}{2} \cdot \frac{\Delta p}{l} \qquad \textbf{Eq. 3.2.2}$$

h corresponds to the slit height and l the slit length.

The shear rate $\dot{\gamma}_w$ for a Newtonian fluid is calculated as shown in Eq. 3.2.3:

$$\dot{\gamma}_w = 1.5\pi \cdot \frac{D^2}{l.h^2} \cdot V_{st} \qquad \textbf{Eq. 3.2.3}$$

D is the diameter of the storage canal. V_{st} can be derived from the flow rate $\dot{V}$ using the following equation:

$$\dot{V} = \frac{\pi \cdot D^2 \cdot V_{st}}{4} \qquad \textbf{Eq. 3.2.4}$$

The Weissenberg/Rabinowitsch correction is subsequently applied in order to take into account the non-Newtonian behaviour of polymers. The corrected shear rate is calculated using the slope n of the logarithmic plot of the pressure drop against the flow rate:

$$\dot{\gamma}_{korr} = \frac{1}{3} \cdot \gamma_w \left[2 + \frac{1}{n} \right] \qquad \textbf{Eq. 3.2.5}$$

The viscosity functions of the tested polymers were approximated by the Carreau equation as follows:

$$\eta = \frac{a}{\left(1 + b \cdot |\dot{\gamma}|\right)^c} \qquad \textbf{Eq. 3.2.6}$$

η is the viscosity, a the zero shear viscosity, b a material constant und c the slope of the viscosity function at high shear rates (Fig. 3.2.4).
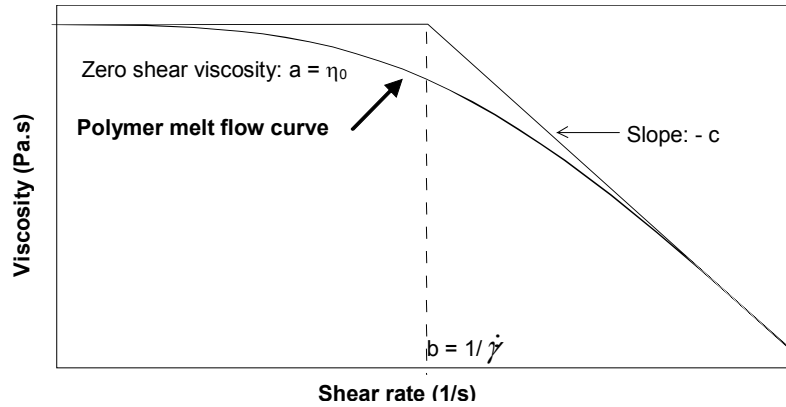
Fig. 3.2.4: Parameters for the Carreau approximation

The capillary rheometer used in this work is a Rheograph 2000 from the company Göttfert Feinwerktechnik GmbH equipped with different slit dies which dimensions are given in Tab. 3.2.1.

Slit die	Die length L (mm)	Slit height h (mm)	Slit width B (mm)	Diameter D of the storage canal (mm)
1	44	0.855	12	20
2	55	1.0	15	20
3	180	0.9	18	20

Tab. 3.2.1: Dimensions of the dies used for the capillary rheometer measurements

3.2.1.3 Principle of Melt Flow Rate measurement

The Melt Flow Rate (MFR) and Melt Volume Rate (MVR) indexers are fast characterization methods of polymer melt flow by a single value. Polymer granules are inserted into a heated barrel and molten for a determined period of time. The MFR measures the amount in g or volume in cm^3 per 10 min of molten polymer contained in the barrel which is extruded through a strand die at a given temperature under a loaded piston. The piston position is detected by distance/time markers and the MFR is calculated considering the density of the polymer melt and barrel geometry. A schematic description of a MFR device is presented in Fig. 3.2.5.

The instrument parts such as die, piston or barrel are standardized as well as the measurement conditions, temperature and weights (Standard specification ISO 1133). For thermoplastic polymers, 190°C or 230°C as well as 1.0 kg, 2.16 kg, 5 kg, 10 kg, 21.6 kg are standard temperatures and loads.
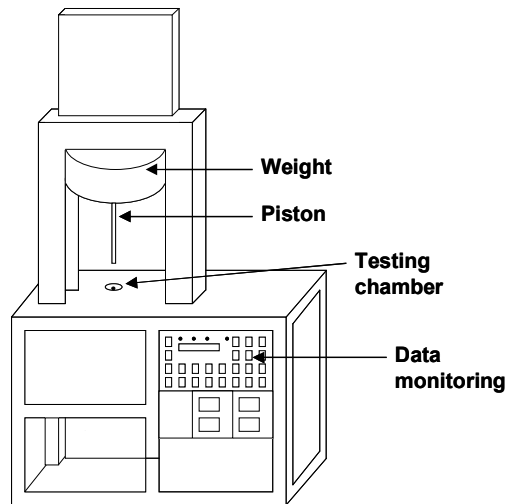
Fig. 3.2.5: Schematic description of a melt flow indexer

The mass and MFR can be related to the strain and stress by simple equations. The flow rates achieved are not a fundamental polymer property. Nevertheless, MFR indexers are useful for the comparison of polymers of the same family and quality control and they represent a relatively inexpensive measurement technique. Some limitations are somehow related to this method. Because the die length to diameter ratio is of about 4, a significant part of the measurement is composed of the entrance pressure loss. Besides, the piston is driven by a weight and its velocity is not constant, creating variations in the volume flow rate during the course of the experiment. Furthermore, the determination of MFR occurs in a small shear rate range (> 50 s^{-1}) far from those reached during most of the polymer processing applications [Böl01, Lau95, Mac94, Dea82].

The tests in this work were performed using an indexer MP-D from the company Göttfert GmbH.

3.2.2 Influence of the formulations on the rheological properties of the grafted PP

3.2.2.1 Grafting of maleic anhydride onto polyproppylene

A preliminary rheological investigation using rotation rheometry mode was realized on PP-g-MAH samples produced at 200°C in a batch mixer. The PP copolymer RD208CF and homopolymer HD601CF were grafted under variation of the peroxide, MAH and styrene amounts. Before performing the frequency sweep measurements, the samples were tested using the stress and time sweep modes in order to determine the linear viscoelastic region and to verify that the sample undergoes no

major degradation during the tests. The complexity of degradation reactions of the PP during extrusion was studied by Mierau [Mie94]. It was found that the degradation due to thermo-mechanical and thermo-oxidative reactions is not as severe as the one caused by the peroxide radicals. For this reason, the degradation caused by processing was neglected in this study.

Fig. 3.2.6 shows that increasing the initial quantity of MAH from 0.5 to 3.0 phr at a constant MAH/peroxide ratio (MAH/DHBP=11.1) and without styrene in the formulation leads to a diminution of the viscosity of the grafted PP. To explain this phenomenon Gaylord et al. [Gayl83] identified different degradation causes of the PP during the grafting reaction:

- β-scission after the hydrogen abstraction by the peroxide.
- The MAH undergo excitation due to the rapid decomposition of the peroxide and the MAH excimers generated abstract the PP hydrogen which in turn can undergo β-scission.
- Graft copolymers can be formed by reaction between PP macroradicals and poly(maleic anhydride). These PP macroradicals may also undergo degradation.

Thus, further addition of MAH enhances degradation of the PP during functionalization.

Augmentation of the peroxide amount in the formulation leads to the formation of more primary radicals and promotes grafting as well as β-scission. As a consequence, the polymer chains of the grafted PP are shortened and the viscosity is reduced. Styrene confirmed its role of reactivity promoter through the formation of CTC because an increase of its concentration induced an augmentation of the viscosity. Similar trends were observed for the grafted homopolymers.
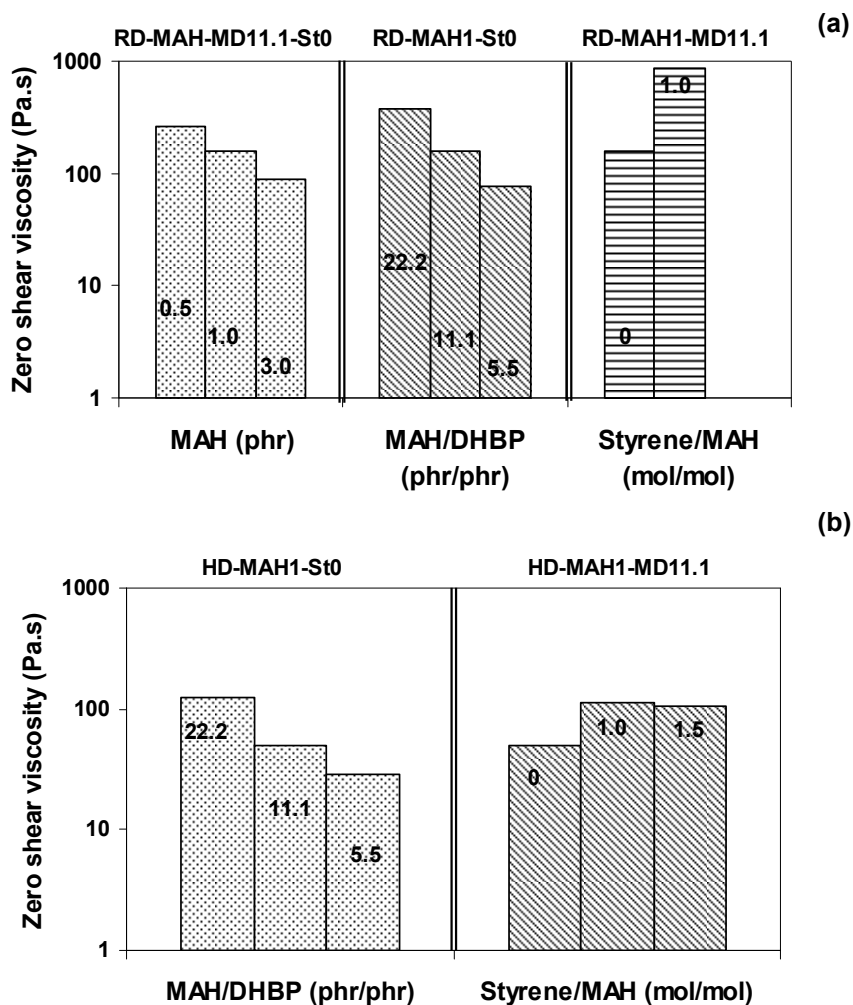
Fig. 3.2.6: Zero shear viscosity obtained from DSR measurements as a function of MAH, peroxide and styrene initial amounts in the PP-g-MAH RD208CF **(a)** and HD601CF **(b)** prepared in the batch mixer

Cast films of different PP-g-MAH formulations were extruded and rheologically analyzed with rotation rheometry. The investigation led to similar conclusions to the rheological analyses with samples prepared in the batch mixer. In that case, all formulations contained styrene. Addition of MAH and/or DHBP resulted in a decrease of the sample viscosity (Fig. 3.3.7). This decrease is an evidence of the PP degradation during the grafting process caused by the initially formed macroradicals which underwent β-scission. The slight increase in the viscosity for the sample RD-MAH1-MD11.1-St1 may be related to the formation of alternating MAH-St copolymer side chains on the PP backbone [Fri96]. This sample was produced again but the same result in terms of rheology was found, eliminating in that way the probability of a production failure.
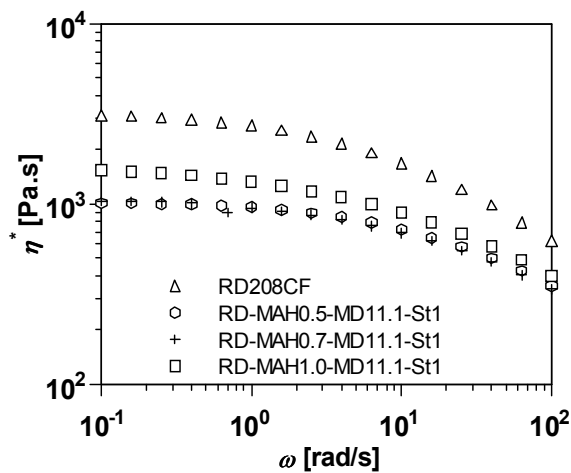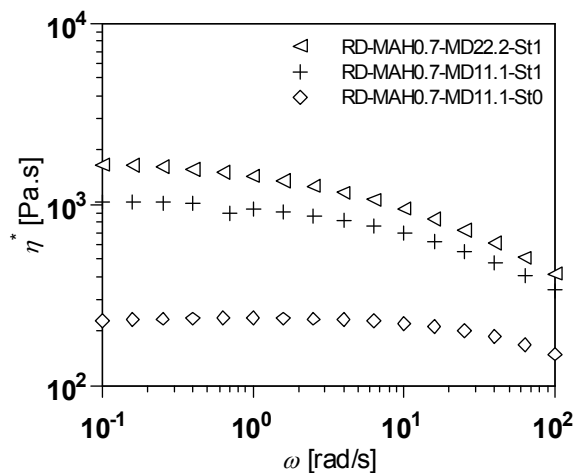
Influence of the MAH initial content   Influence of the styrene initial amount
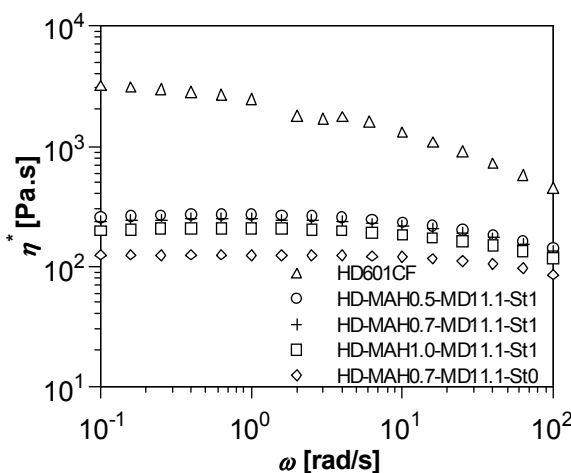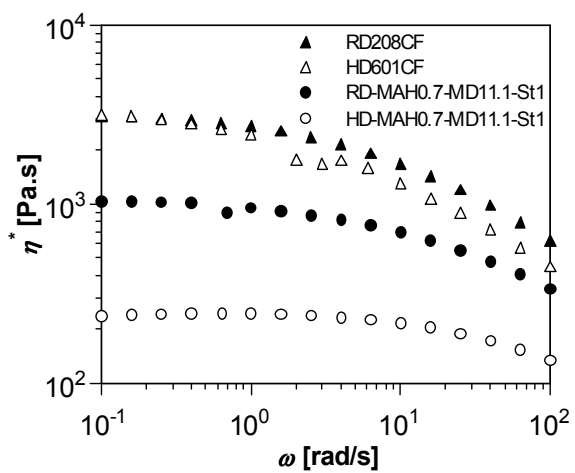
Influence of the MAH initial content   Comparison of the grafted copolymers and homopolymers

Fig. 3.2.7: Viscosity functions obtained from DSR measurements of MAH grafted PP copolymers RD208CF and homopolymers HD601CF prepared in the twin screw extruder

A comparison of the grafted homopoylmers HD601CF and copolymers RD208CF showed that the copolymers are less sensitive to degradation. However the ethylene sequences of the copolymers are not sufficient to eliminate sensitivity to β-scission. Thus, for samples of the same formulation (PP-MAH0.7-MD11.1-St1) prepared under similar extrusion conditions, the viscosity of the grafted homopolymer is around 13 times smaller than the pure resin's one and the copolymer's one only about 3 times. Moreover, it is interesting to note that the copolymer may also undergo branching or crosslinking caused by macroradicals combinations, which enhances the complexity degree of the reactions [Moa99].

The results of the rheological analyses obtained for the high molecular PP-g-MAH films confirmed those of the low molecular ones. They are summarized in Fig. 3.2.8a und 3.2.8b.

A comparison of formulations composed of DHBP and TMCH showed that TMCH induced less degradation than DHBP for both types of PP (HB205TF and RB501BF), although they possess similar active oxygen (approx. 10 wt.%).
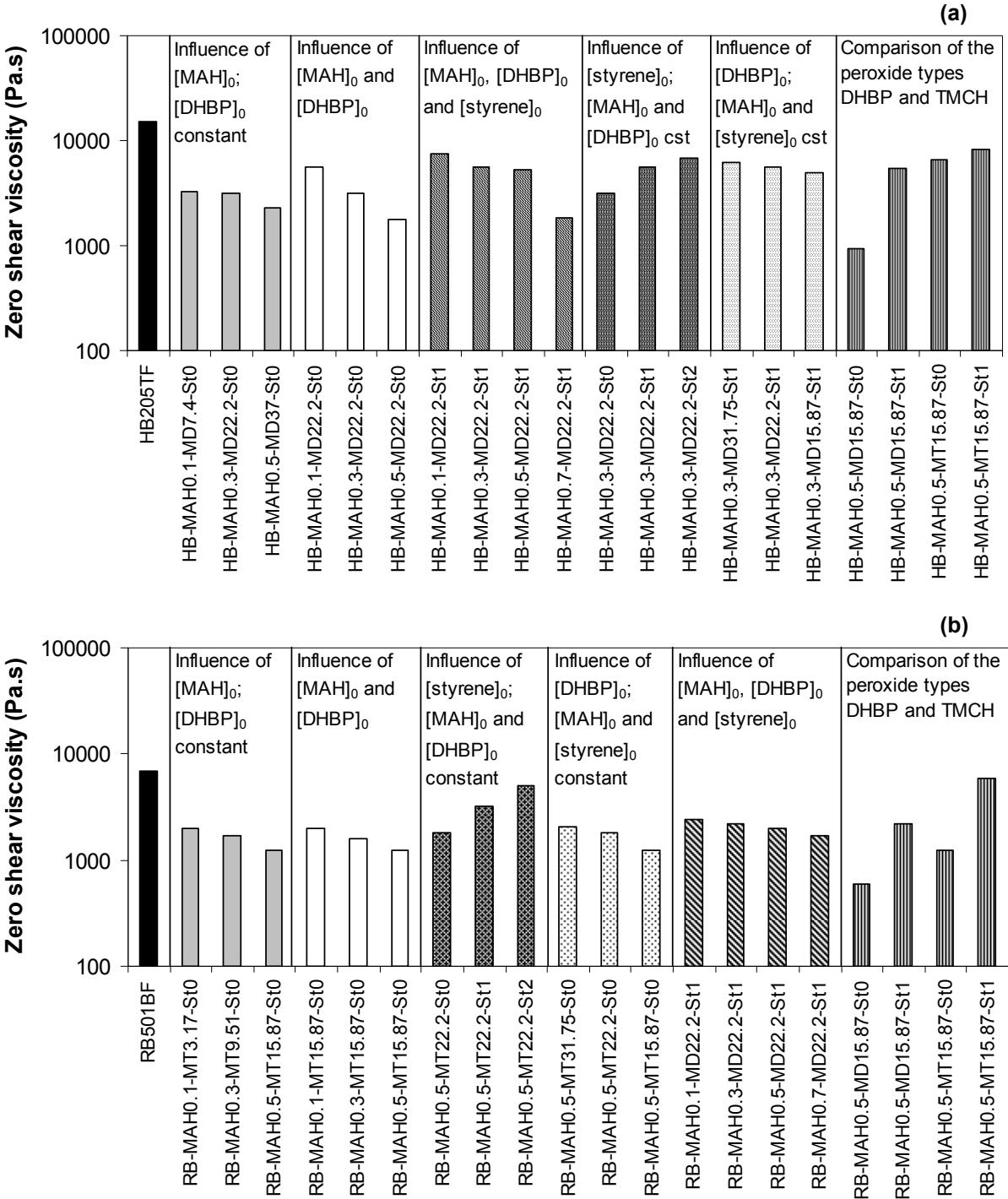
Fig. 3.2.8: Zero shear viscosity obtained from DSR measurements of MAH grafted homopolymers HB205TF **(a)** and copolymers RB501BF **(b)** prepared in the twin screw extruder

The PP-g-MAH concentrates to be used as adhesion promoters and made of 1 phr MAH with different peroxide contents ([MAH]/[DHBP]= 15.87; 11.1; 5.5) exhibited, as expected, a decreasing viscosity with increasing initial amounts of peroxide (Fig. 3.2.9).
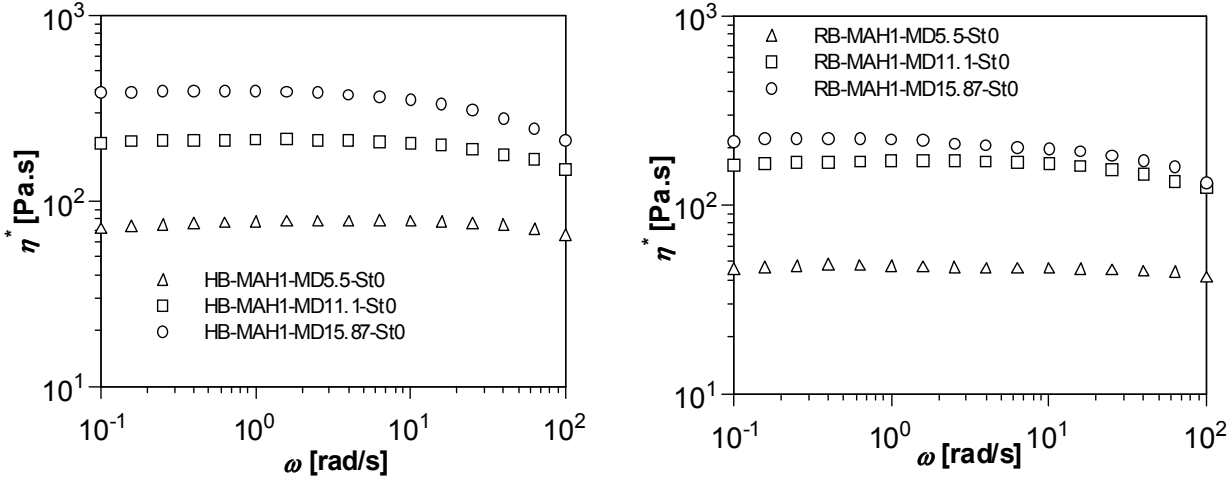
Fig. 3.2.9: Viscosity functions of PP-g-MAH concentrates obtained from DSR measurements

Concentrations of 1 to 10 wt.% of PP-g-MAH concentrates (formulation: PP-MAH1-MD11.1-St0) as well as a concentration of 5 wt.% of the three PP-g-MAH formulations were blended with the pure resins. The shear viscosity values of these blends are shown in Fig. 3.2.10. One can notice that the viscosity values of the blends are lower than those of the pure resins but vary only slightly from one another because of the small concentrate quantities.
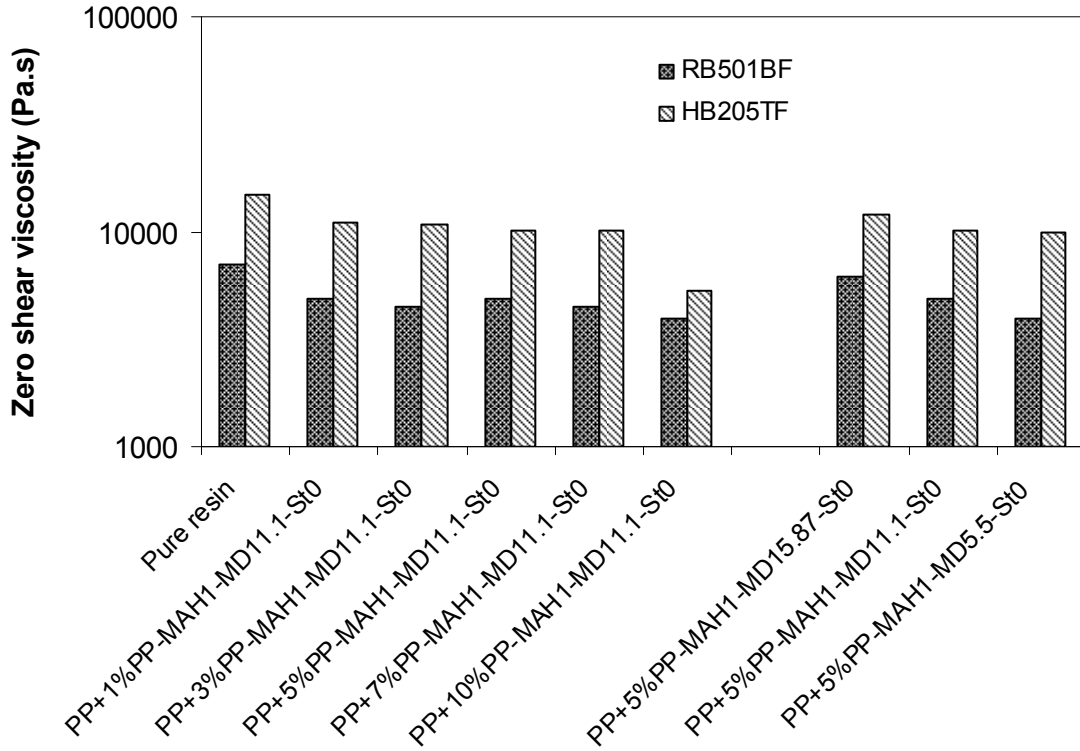
Fig. 3.2.10: Zero shear viscosities of the PP/PP-g-MAH blends obtained from DSR measurements

The effect of the formulations on the viscosity implied, as already mentioned, a modification of the molecular structure. Tab. 3.2.2 presents the results of the Gel Permeation Chromatography (GPC) of the raw PP resins and some PP-g-MAH as well as their corresponding zero shear viscosities. They follow the same trend, confirming the well-known correlation between the weight average molecular weight M_w and the zero shear viscosity η_0 given by the Mark-Houwink-Sakurada equation:

$$\left[\eta_0\right] = K M_w{}^{a_0} \qquad \textbf{Eq. 3.2.7}$$

K and a_0 are constants which depend on the polymer, solvent and temperature. As described in Fig. 3.2.11, they can be determined graphically by measuring the intrinsic viscosity of a number of monodisperse samples (or fractions with a narrow molecular weight distributions) of the polymer and using Eq. 3.2.8. The molecular weight would have been determined previously by an absolute method.

$$\log \eta_0 = \log K + a_0 \log M_w \qquad \textbf{Eq. 3.2.8}$$
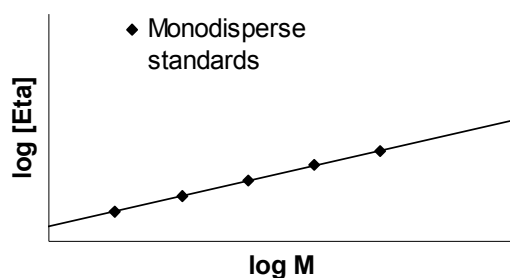
Fig. 3.2.11: Illustration of the determination of the constants K and a [Pai94]

	M_n x 10^4 (g/mol)	M_w x 10^4 (g/mol)	η_0 (Pa.s) at 200°C
RD208CF	9.762	28.58	3097.1
HD601CF	7.519	30.03	3175.8
HB205TF	14.38	44.77	15010
RB501BF	11.57	37.78	6972.4
RB-MAH0.5-MT22.2-St0	10.11	24.13	1819.19
RB-MAH0.5-MT22.2-St2	12.03	27.66	4993.21

Tab. 3.2.2: Results of GPC and DSR measurements of the raw PP and some PP-g-MAH

Moreover, the branching degree of a polymer is usually characterized by the number of CH_3 groups per carbon atom. Another method is to determine the activation energy by using the Arrhenius relation (Eq. 3.2.9). It stipulates that the movement of the macromolecules is realized by overcoming a thermal energy barrier (rotation potential energy of a molecule segment, for instance).

$$\eta_0(T) = \eta_0(T_0) \cdot \exp\left[\frac{E_0}{R}\left(\frac{1}{T} - \frac{1}{T_0}\right)\right] \qquad \textbf{Eq. 3.2.9}$$

η_0 is the zero shear viscosity, E_0 the flow activation energy and R the gas constant. All temperatures are absolute temperatures. E_0 will obviously increase with the level of branching.

Fig. 3.2.12 depicts the activation energy of samples containing a raising concentration of styrene. The grafted homopolymers showed a constant increasing activation energy with addition of styrene from 49 to 56 kJ/mol, the energy of the pure resin being only of about 34 kJ/mol. Because of the functionalization reactions, the PP-g-MAH samples obviously possess a higher degree of branching or long chain branching. Hence, more energy is needed to set their molecules in motion.
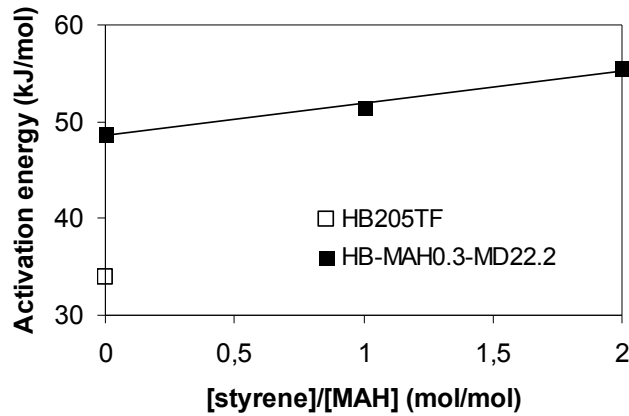
Fig. 3.2.12: Evolution of the activation energy of the grafted homopolymers against the styrene content

Some more information about the molecular structure of the polymers were gained from the data obtained by capillary rheometry.
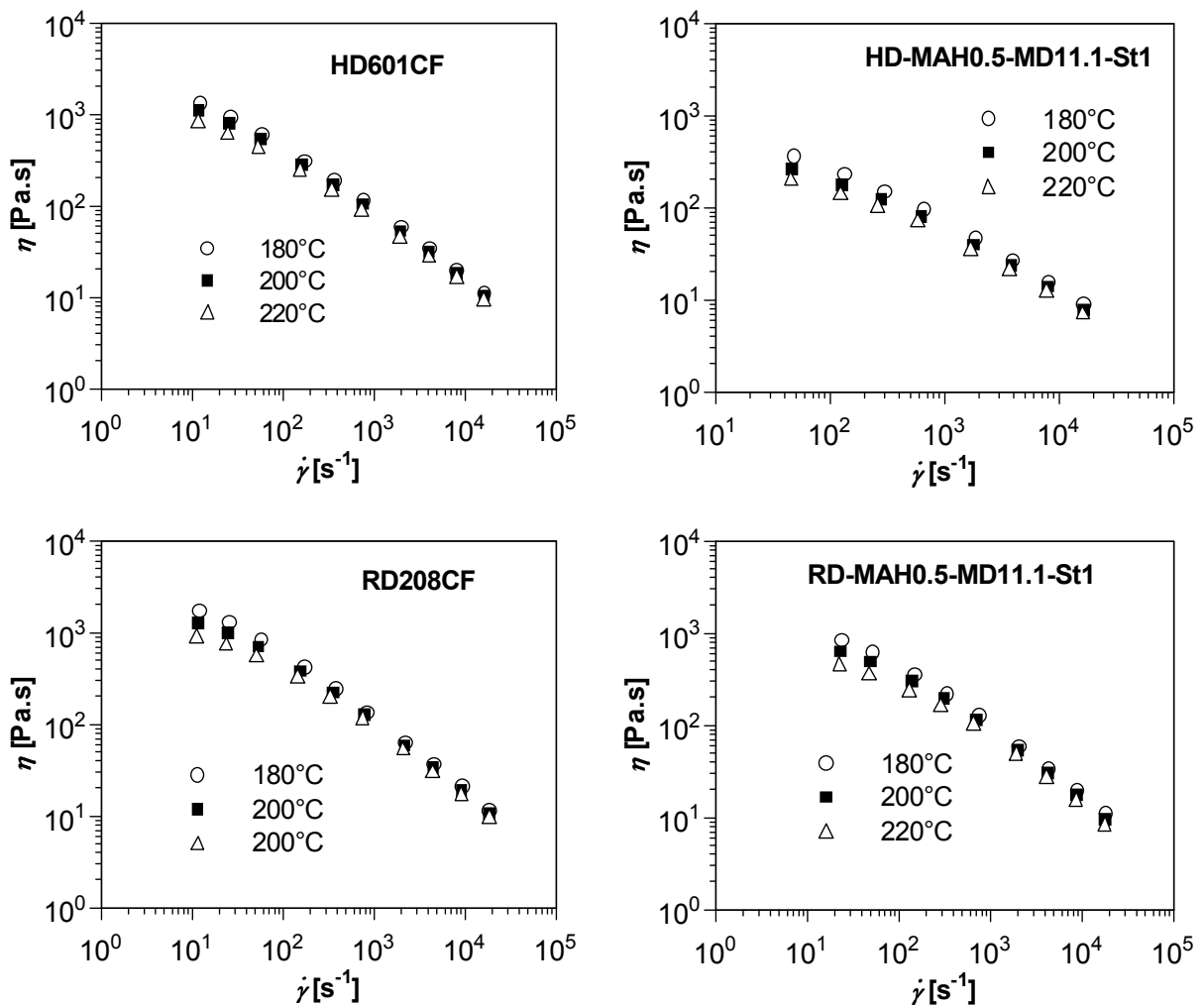
Fig. 3.2.13: Viscosity functions of the pure resins and PP-g-MAH measured by capillary rheometry

In Fig. 3.2.13 a slight temperature dependency of the viscosity can be observed for the pure resins (RD208CF and HD601CF) as well as for the PP-g-MAH. As expected, all materials show a shear thinning behaviour.

The Carreau parameters (a, $1/b$ and c) were plotted as functions of the MAH amount and are presented in Fig. 3.2.14. The parameter $1/b$ can be correlated to the broadness of the molar mass distribution (MMD). $1/b$ in this case increased with raising amounts of MAH in the formulations, indicating a narrowing of the MMD. This phenomenon is more pronounced for the grafted PP homopolymers which strongly degrade with addition of MAH and peroxide. The zero shear viscosity a, as already mentioned, decreased with increasing MAH concentration. c describes the shear thinning behaviour of the material. A marked shear thinning behaviour for the homopolymers can be observed whereas it diminishes for the copolymers. This is an evidence of the complexity of the reactions and resulting products that are created in the copolymer during grafting (crosslinking, branching…).
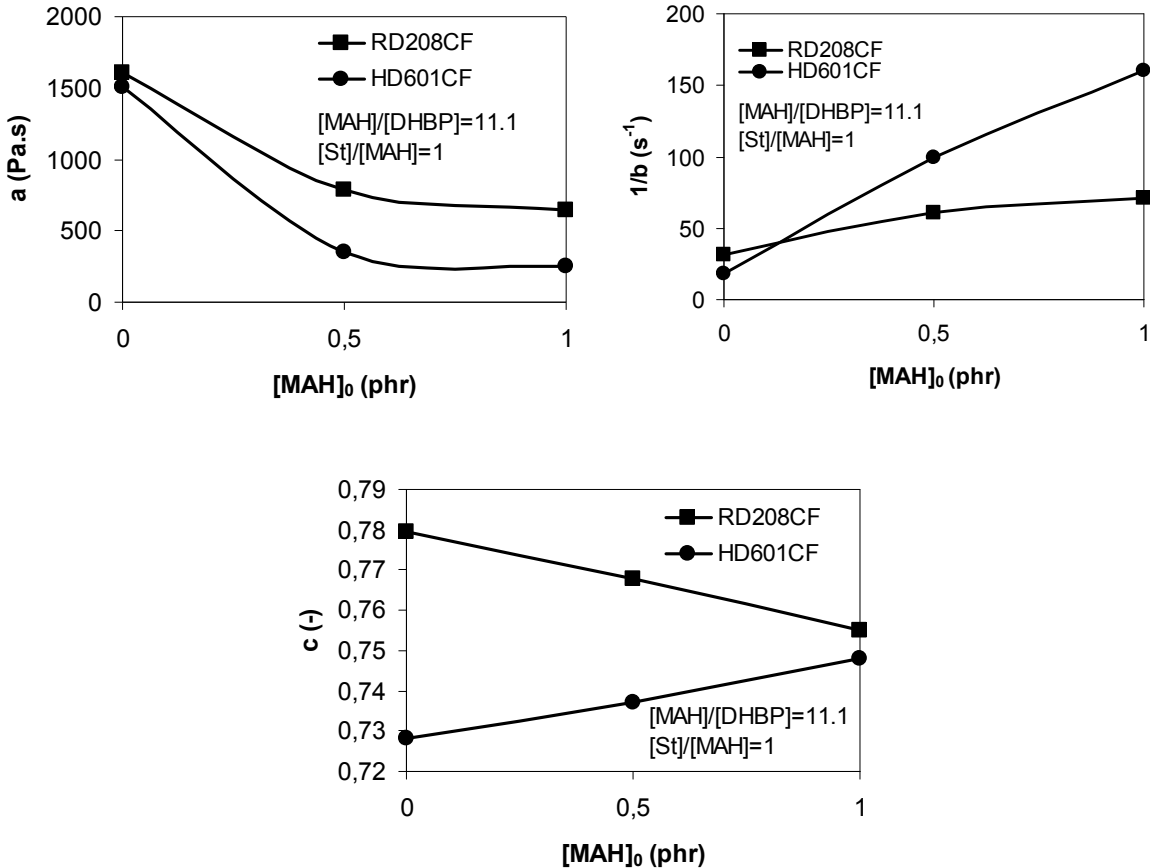
Fig. 3.2.14: Plots of the Carreau parameters a, 1/b and c in function of the amounts of introduced MAH (Formulation: MAH/DHBP=11.1, styrene/MAH=1)

A well-known empirical relation in the rheology of polymer melts is the Cox-Merz rule. It relates the steady shear viscosity η, plotted against the shear rate $\dot{\gamma}$, and the magnitude of the complex viscosity $|\eta*|$, plotted against the angular frequency ω. This method can be use to predict $\eta(\dot{\gamma})$ from oscillatory measurements or $|\eta*(\omega)|$ from steady shear viscosity data in case one or the other operating mode is not available. In our case, Fig. 3.2.15 shows that the rule could be applied considering the pure copolymer resin and one of the formulations (RD-MAH0.5-MD11.1-St1). This implies that for practical reasons the use of rotational rheometry is sufficient and, if needed, an extrapolation of the dynamic data to higher frequencies can be made.
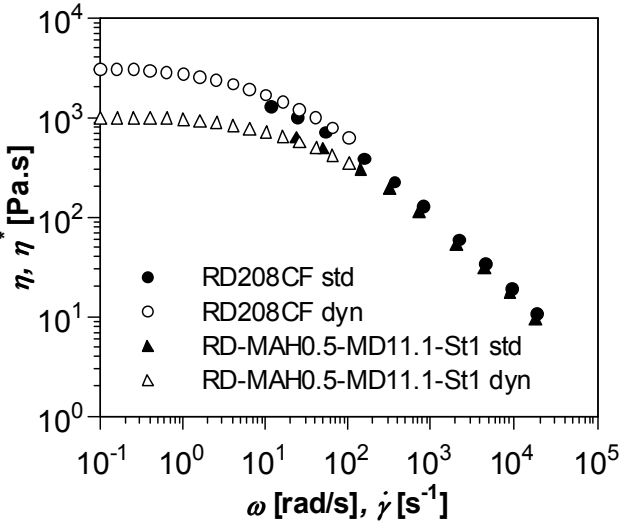
Fig. 3.2.15: Cox-Merz rule applied to the pure resin and RD-MAH0.5-MD11.1-St1

3.2.2.2 Grafting of glycidyl methacrylate onto polyproppylene

Tab. 3.2.3 presents the results of MVR measurements performed on PP-g-GMA prepared in the batch mixer.

GMA (phr)	GMA/DHBP	MVR(cm^3/10min)	
		RD208CF	**HD601CF**
0	0	5.37	6.12
0.5	22.2	14.77	19.98
1	22.2	17.98	13.72
0.5	11.1	18	27.03
1	11.1	16.13	27.47
0.5	5.5	23.42	43.74
0.1	5.5	33.36	57.51

Styrene / GMA (mol/mol)	GMA (phr)	GMA/DHBP	MVR (cm^3/10min)	
			RD208CF	HD601CF
0	1	0	16.13	27.47
0.5	1	11.1	15.4	28.8
1.5	1	11.1	15.8	26.1

Tab. 3.2.3: Results of the MVR measurements for samples prepared in the batch mixer

Fig. 3.2.16a and 3.2.16b show that the addition of peroxide decreases the viscosity of the PP-g-GMA. In opposition to the MAH grafting process, increasing the amount of GMA leads to a higher viscosity. By adding a greater amount of monomer, the probability of β-scission occurring is reduced and the grafting of GMA is higher.

(a)   **(b)**
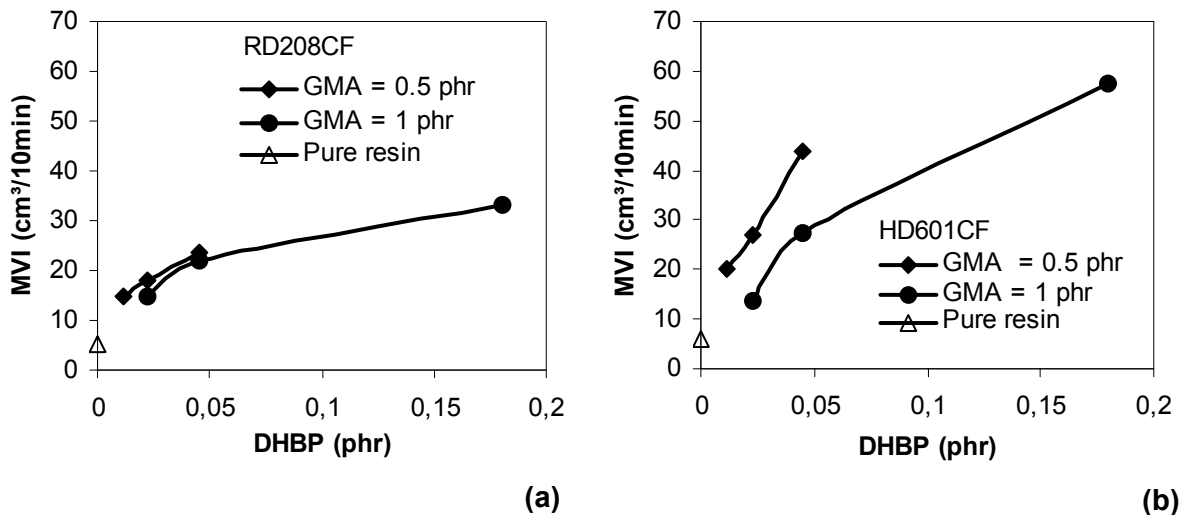
Fig. 3.2.16: Influence of the peroxide and GMA introduced amounts on the MVI of the grafted PP RD208CF **(a)** and HD601CF **(b)**

A slight decrease of the MVR values for batch mixer PP-g-GMA as well as extruded samples can be observed in Fig. 3.2.17. Having a higher reactivity towards PP macroradicals than GMA, styrene minimizes the β-scission reaction by forming stable styryl radicals with them. The MVR values of the extruded grafted homopolymers are lower than those of the batch mixer ones, showing that degradation is more pronounced in the kneader. This is due to the long residence time in the batch mixer (10 min compared to 2 min in the extruder) and to the fact that the system is open. This allows more oxygen to be present in the chamber, leading to oxidative degradation. For a styrene/GMA ratio $C_{GMA} > 1.5$, the MVR values reach a plateau.
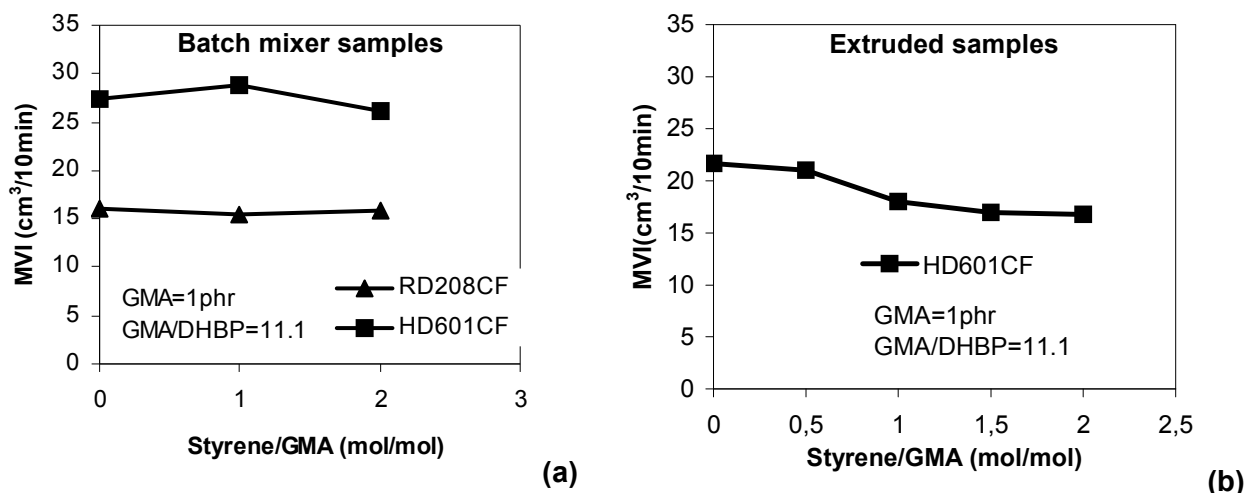
Fig. 3.2.17: Influence of the styrene introduced amount on the MVI of the batch mixer PP-g-GMA **(a)** and extruded samples **(b)**

Viscosity measurements performed by a rotational rheometer (frequency sweep mode) at 200°C confirmed the results of the MVR measurements. In Fig. 3.2.18 a molecular weight reduction expressed by a diminution of the viscosity with raising amounts of peroxide is noticeable. The viscosity of the PP-g-GMA increases again at an initial GMA concentration of 5 phr for the copolymers RD208CF and 7 phr for the homopolymers HD601CF. In the same way, the elastic modulus *G'* at low frequencies grows, indicating an increase of the elastic properties of the PP-g-GMA. However no partial crosslinking could be detected by using boiling xylene extraction of the PP-g-GMA samples. The crosslinking density might be low in order to create an insoluble three-dimensional network and the resulting macromolecular structure may rather be formed of long chain branching. This phenomenon seems more pronounced in the case of the copolymers.
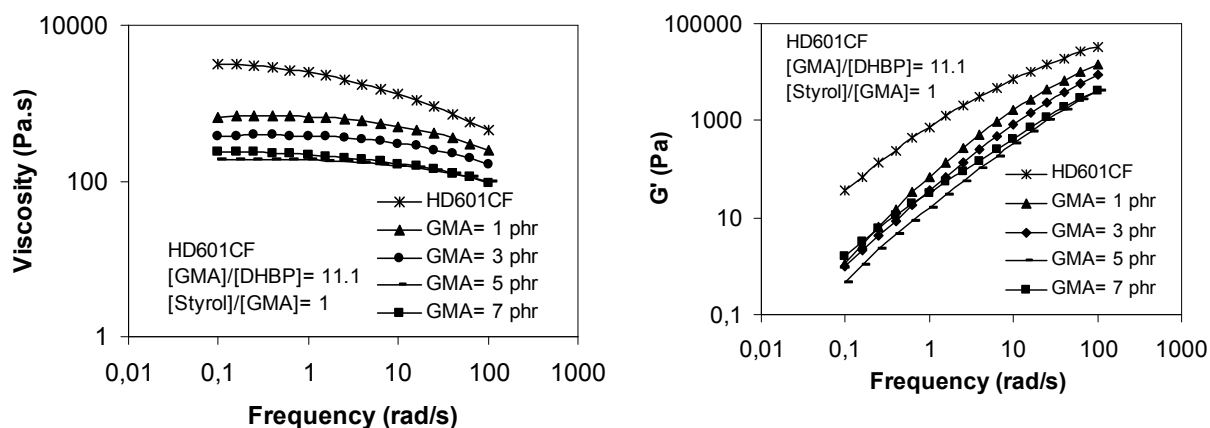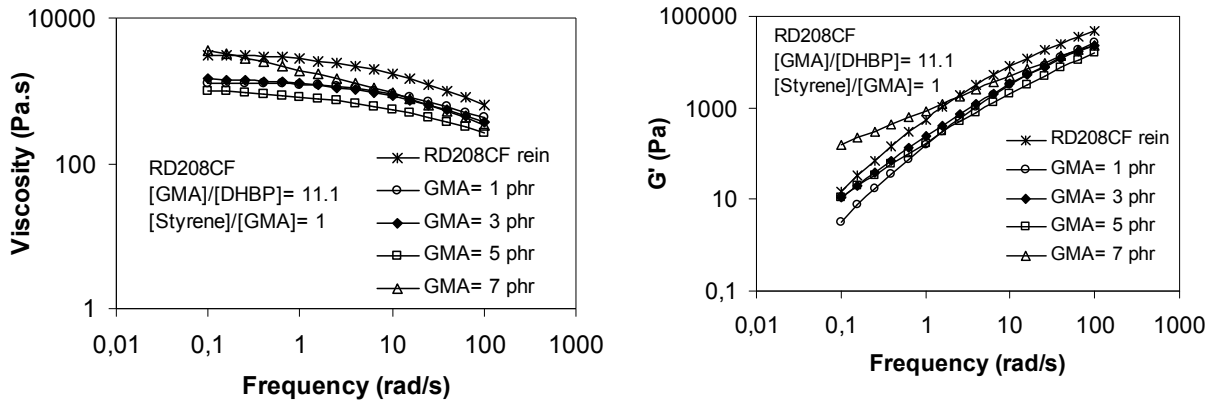
Fig. 3.2.18: Viscosity functions and elastic modules of the pure resins and PP-g-GMA measured by DSR at 200°C

The role of styrene as radical stabilizer is confirmed as well for both grafted homopolymers and copolymers (Fig. 3.2.19).
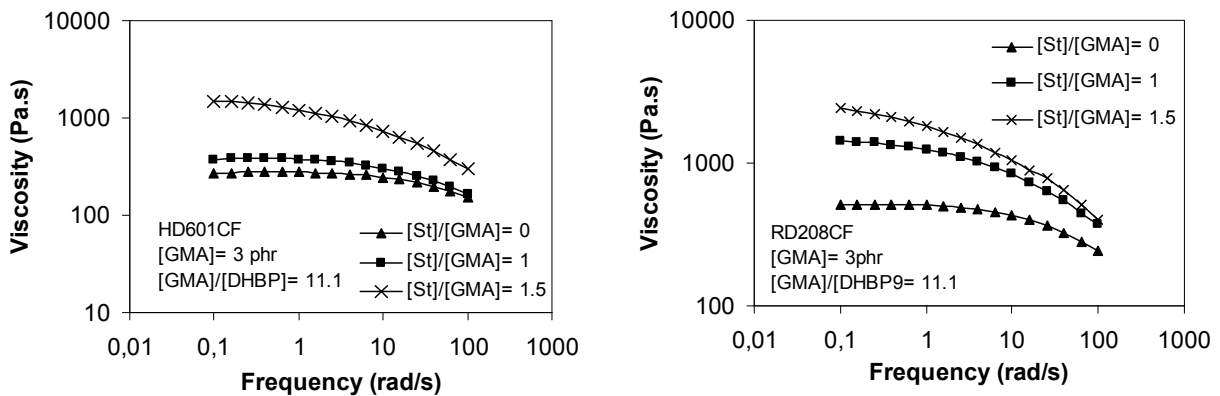
Fig. 3.2.19: Influence of the initial amount of styrene on the viscosity functions of the PP-g-GMA measured by DSR at 200°C

3.2.3 Influence of the process parameters on the rheological properties of the grafted PP

The role of the process parameters is determining for the efficiency of the grafting reaction as well as for the final properties of the grafted material. The variation of the screw rotation speed, the temperature and the throughput induced changes in the molecular structure of the grafted polypropylene and as a consequence on their viscosity. On the one hand, an increase of the temperature from 200 to 220°C led to a drastic viscosity diminution for the sample RD-MAH0.7-MD22.2-St1. The energy input not only accelerated the decomposition of the primary radicals and the grafting of the monomers on the PP backbones but also promoted the β-scission reaction,

resulting in a reduced molecular weight and viscosity. On the other hand, the influence of the screw rotation speed on the zero shear viscosity of sample RD-MAH0.7-MD15.87-St1 appeared to be quite limited between 50 and 200 rpm as shown in Fig. 3.2.20. At 200 rpm, local temperature peaks between the screws occur due to dissipated mechanical energy (local high shear rates up to 1000 s^{-1}) and induce a slight lowering of the viscosity.
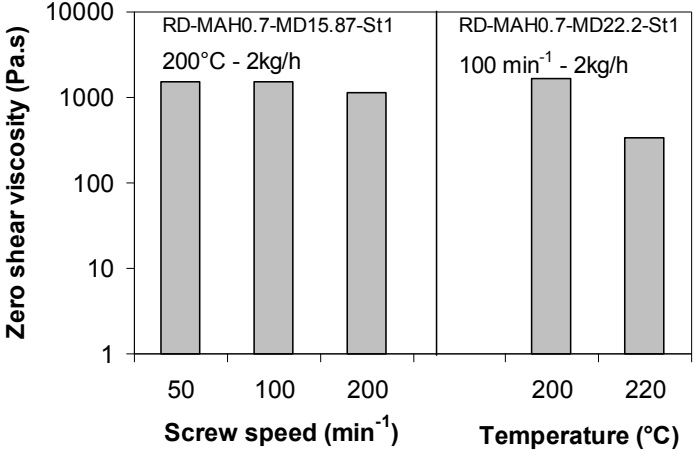
Fig. 3.2.20: Influence of the process parameters on the zero shear viscosity obtained from DSR measurements (Formulation: RD-MAH0.7-MD15.87-St1)

A systematic investigation of the process conditions using HB-MAH0.5-MD22.2-St1 as sample confirmed the first results mentioned above (Fig. 3.2.21).
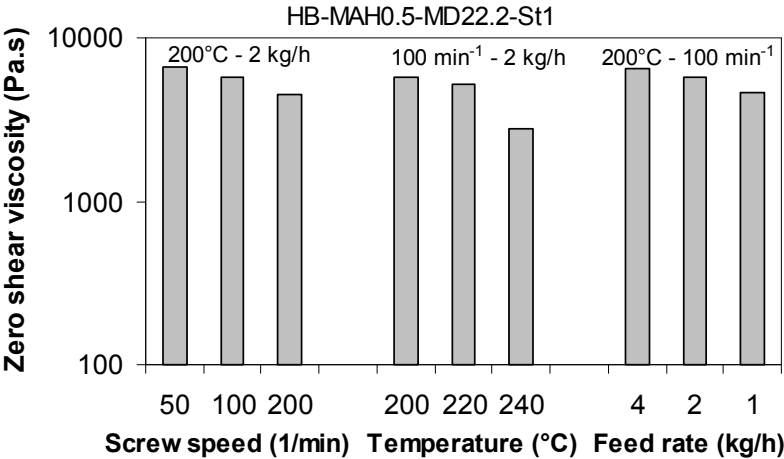
Fig. 3.2.21: Influence of the process parameters on the zero shear viscosity obtained from DSR measurements (Formulation: HB-MAH0.5-MD22.2-St1)

3.3 Thermal properties of the functionalized PP

3.3.1 Differential scanning calorimetry

Differential Scanning Calorimetry (DSC) is a widely used technique in the polymer field for thermal analytical study. A large range of investigations are allowed including the determination of heat capacity, heats of transition or reaction, thermal conductivity and temperature transitions (glass-transition, fusion, crystallisation temperatures). Investigations conducted with the DSC allow the determination of thermodynamic constants as well as the influence of preparation, composition, treatments (annealing), molecular weight distribution (degradation, gelation) on these constants. DSC is employed for the measurement and calculation of kinetics parameters: cure rates, rates of thermal, oxidative and radiation degradation, rates of physical and chemical changes occurring in polymeric systems. Degree of crystallinity of semi-crystalline resins can also be calculated.

Practically, the materials are subjected to a controlled temperature program and the thermal energy difference or the heat flux generated between the sample and reference are registered, allowing a quantitative measurement. In other terms, this method permits the measurement of the absorbed and released energy (endothermic and exothermic transitions) by a sample and a reference under the same thermal conditions. A computer monitors the temperature, regulates the heat flow and plots the heat absorbed by the polymer against temperature [Ehr98, Run90]. A DSC device is schematically described in Fig. 3.3.1.

The DSC device used in this study is a Netzsch 204. Most of the tests were performed with a heating and cooling rate of 10 K/min under nitrogen atmosphere. Before testing the samples were pressed to 300 µm films during 2 min, stamped into 5 mm diameter discs and placed in an aluminium pan. The samples were submitted to a thermal program which consisted of a first heating phase in order to erase their thermal history, cooling and heating phases to obtain information about the crystallisation and melting processes.
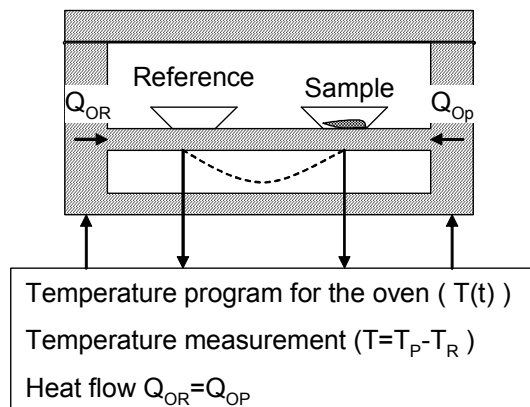
Fig. 3.3.1: Principle of a DSC device

3.3.2 Influence of the formulations on the thermal behaviour of the functionalized PP

Differences in the thermal properties of the coextruded polymers as well as the residual stresses are known to lower the adhesion strength between the layers [Mor96, Ves02]. Considering this, it was necessary to study the effects of the formulations on the thermal behaviour of the PP-g-MAH materials.

The melting temperatures (second heating process) as well as the crystallisation peaks for some low molecular weight PP-g-MAH samples are presented in Fig. 3.3.2.
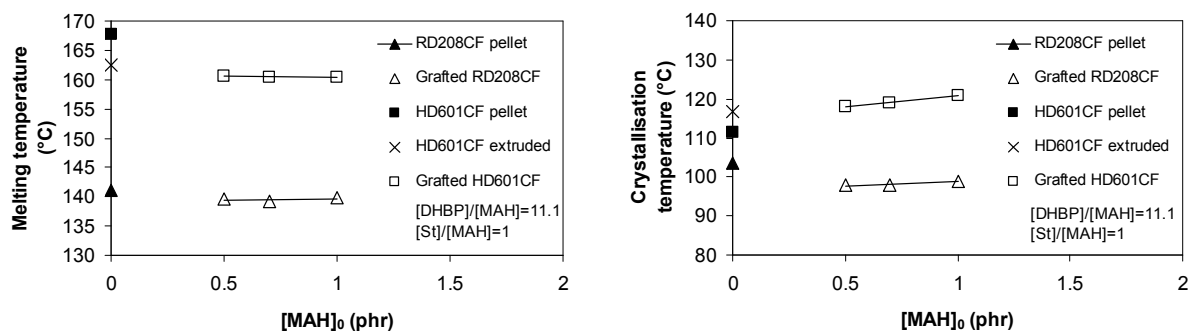
Fig. 3.3.2: Thermal properties of the low molecular weight PP-g-MAH

The grafting of increasing MAH, styrene or DHBP initial content in the formulation of PP-g-MAH raised the crystallisation temperatures from 97.8 to 99°C for the RD208CF resins and from 117.9 to 120.7 °C for the HD601CF ones. Impurities in the melt may act as nucleating agents and allowed the modified PP-g-MAH to crystallize at higher temperatures (heterogeneous nucleation process). This argument is also valid to explain the difference between the temperatures of the raw polymer and extruded PP. Among the grafted samples, no significant influence on the melting temperature can be noticed. In comparison, though, to the pure PP resin the melt

temperatures are lower. It indicates that the crystal growth was slowed and the lamellae thickness of the PP-g-MAH reduced. This, in turn, can be attributed to the diminution of the molecular weight and structure regularity due to the β-scission reactions.

The thermal analyses of the high molecular weight PP gave similar results to those obtained for the low molecular weight PP. There are detailed in Fig. 3.3.3. The grafted copolymers however showed a decreasing crystallisation temperature. This indicates that the changes in the molecular structure as well as the species created during functionalization tend to inhibit crystallisation in that case.
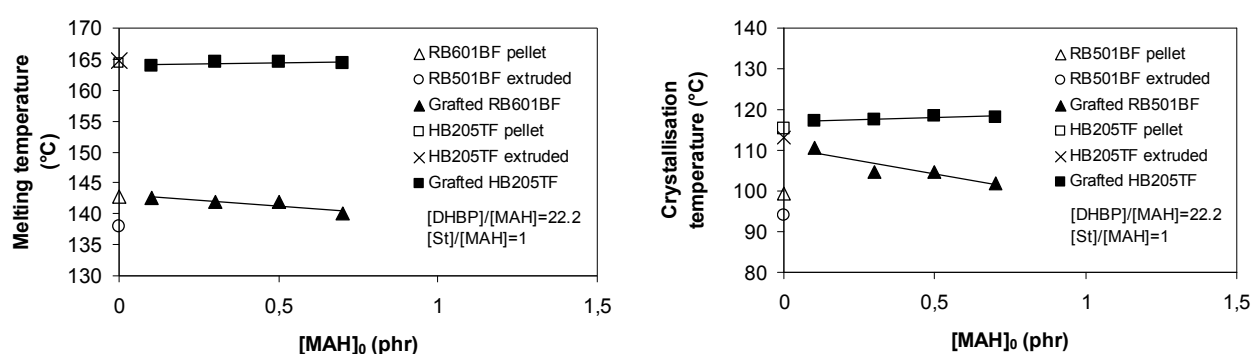
Fig. 3.3.3: Thermal properties of the high molecular weight PP-g-MAH

The complete series of grafted HB205TF was investigated in order to follow the influence of the grafting components on the thermal behaviour of the PP-g-MAH materials. The results are shown in Fig. 3.3.4a and 3.3.4b. The diagrams were divided into five sections as follows:

① The initial concentration of MAH was raised by a constant amount of peroxide DHBP. Styrene was not added in the formulations. No significant change of the crystallisation temperature could be noticed among the grafted samples except for the sample with $[MAH]_0 = 0.5$ phr which demonstrates a slight augmentation of its crystallisation temperature. The melting temperature of this sample is also lower than the others.

② Both MAH and DHBP initial contents were increased without using styrene. The results are similar to those obtained previously.

66

The MAH, DHBP and styrene introduced concentrations were raised simultaneously. The crystallisation temperature was shifted to higher values. The crystallisation and melting temperatures increased to reach a maximum for the sample with MAH concentration of 0.5 phr.

④ The MAH and styrene initial amounts were kept constant while DHBP was increased in the formulations. A slight augmentation of the crystallisation temperature as well as a diminution of the melting temperature was be observed.

⑤ The concentration of styrene was increased and MAH and DHBP initial amount remained constant. Both melting and crystallisation temperatures increased.

(a)

67
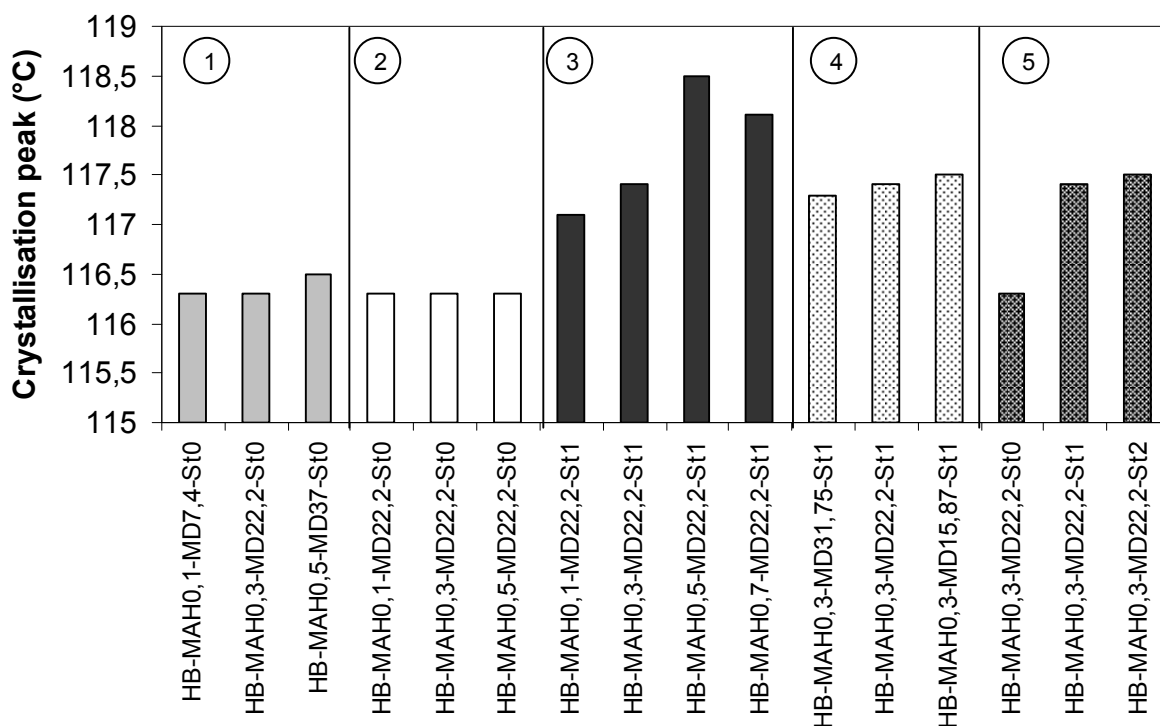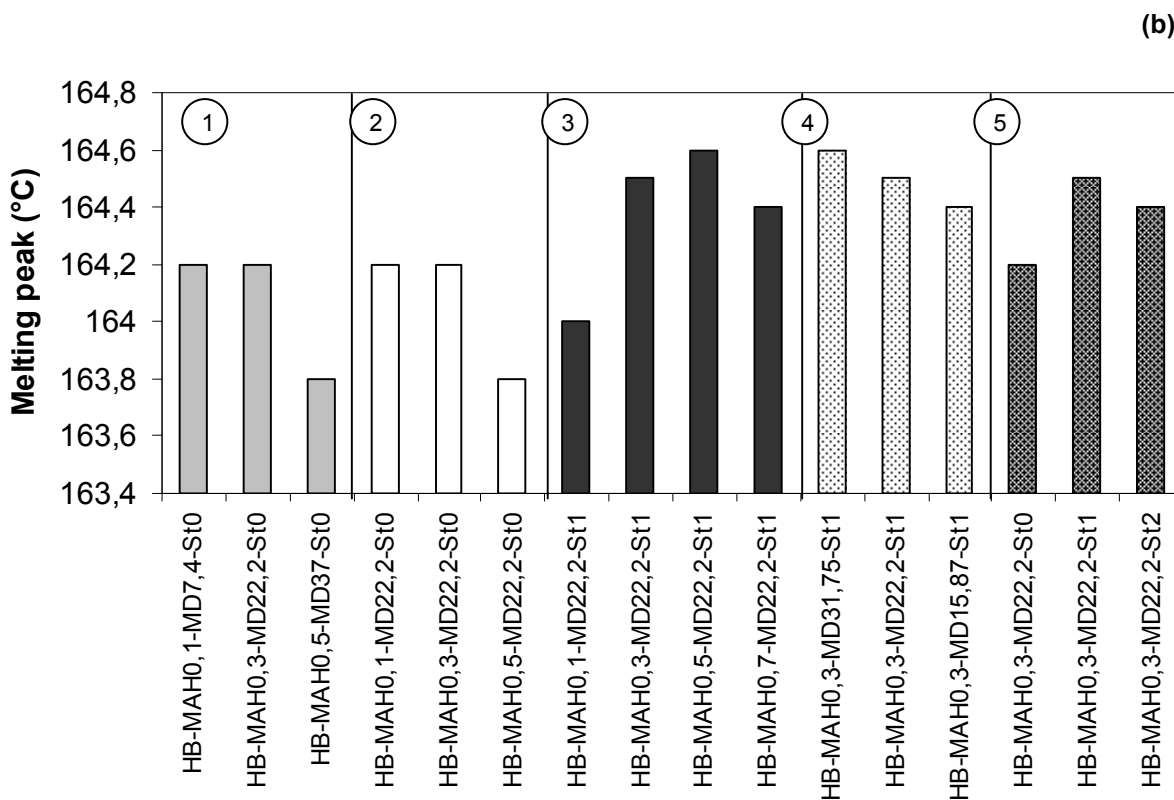
Fig. 3.3.4: Influence of the grafting components on the crystallisation **(a)** and melting **(b)** temperatures

From the previous observations, it can be concluded that the molecular structure induced by the variation of the grafting formulations influences greatly the thermal properties. Styrene was the component which caused most pronounced changes in the melting and crystallisation processes. This is explained by the complexity of the structures which are generated by the presence of styrene in the formulations, especially the formation of low molecular P(St-alt-MAH) copolymers. The presence of these impurities generated higher crystallisation temperatures. DHBP and to a lesser extent MAH reduced the molecular weight of the PP and probably contributed to a diminution of the lamellae thickness, thus, leading to the decrease of the melting point.

Considering the PP-g-GMA samples, the influence of the grafting components on the thermal behaviour of the grafted homopolymers and copolymers is described in Fig. 3.3.5a and 3.3.5b.
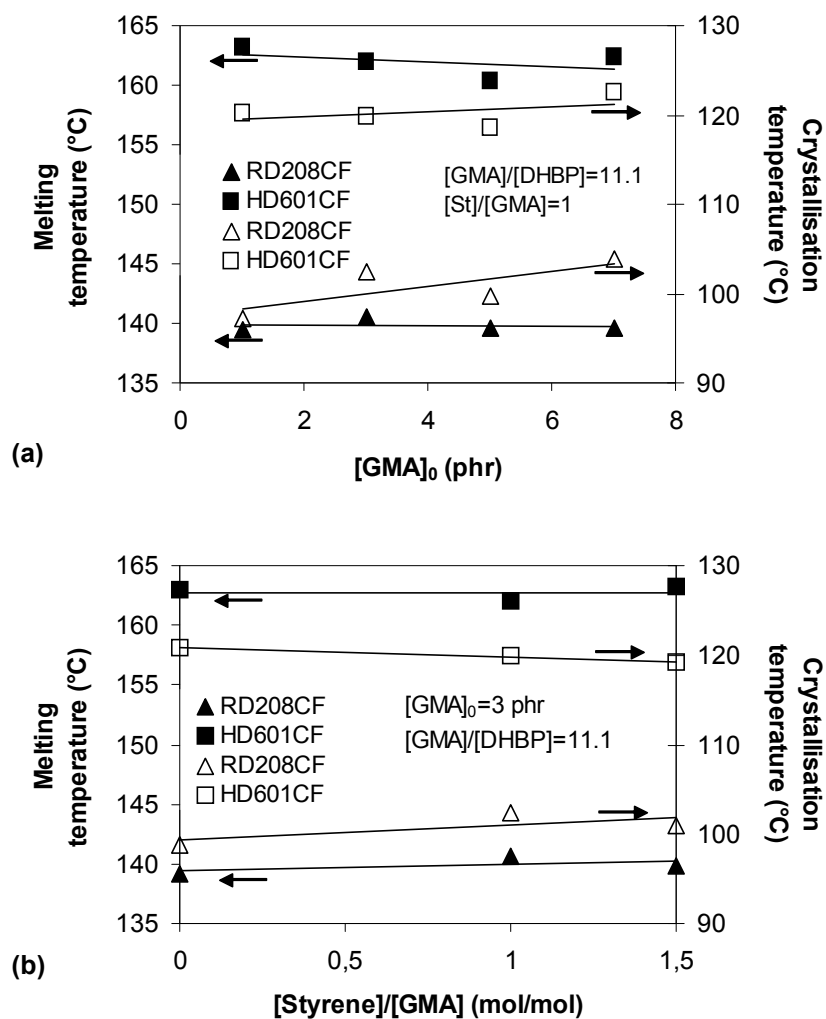
Fig. 3.3.5: Melting and crystallisation temperatures as functions of the initial GMA concentration **(a)** and the styrene/GMA ratio **(b)**

When the initial contents of GMA, DHBP and styrene were increased in the formulations, the crystallisation temperature raised and the melting point decreased slightly for both polymers. The trends were even less significant considering the effect of styrene. However, in comparison to the melting and crystallisation temperatures of the pure resins, the values of the PP-g-GMA appeared to be respectively higher and lower. The tendencies remained relative unclear for the grafted copolymers which underwent during functionalization additional reactions such as crosslinking. This contributed to the formation of more complex molecular structures and, thus, thermal behaviour.

Polypropylenes are semi-crystalline polymers in which the macromolecules are partially ordered. The physical properties of the PP (mechanical, permeation or

optical properties) depend strongly on the degree of crystallinity. Besides, many factors such as the crystallisation temperature, the molecular weight, the number of nuclei and the growth rate of crystalline entities influence the crystallization behaviour of the materials [Ton00, Run90].

It is possible to determine the degree of crystallinity by DSC, using the following equation:

$$K = \frac{\Delta H_m}{\Delta H_m^0} \times 100 \quad [\%] \qquad \textbf{Eq. 3.3.1}$$

where ΔH_m the experimental melting enthalpy of the sample and ΔH^0_m is the equilibrium enthalpy of fusion determined for a 100% crystalline polymer.

ΔH^0_m can be found in the literature (ΔH^0_m= 207 J/g is given by [Ehr98]) or calculated. It characterizes the enthalpy of a perfect infinitely large crystal. This means that the melting temperature of this crystal is equivalent to its crystallisation temperature. The sample is heated, then cooled down at a given crystallisation temperature (isothermal crystallization) and, after the completion of crystallisation, reheated. The last enthalpy of fusion and the corresponding enthalpy of crystallisation are registered. Several temperatures of crystallisation are chosen and the enthalpies are plotted against the corresponding enthalpies of fusion. A linear curve is obtained and extrapolated to the curve of a perfect crystal ($\Delta H_m = \Delta H_C$). The intersection point of the two curves corresponds to the equilibrium enthalpy of fusion ΔH^0_m.

Fig. 3.3.6 and 3.3.7 give an illustration of the method for a PP-g-MAH sample (RD-MAH0.1-MD11.1-St1). The melting curves obtained for the crystallisation temperatures 113, 115, 117, 119, 122°C as well as their isothermal curves are presented in Fig. 3.3.6. The calculation of the equilibrium enthalpy is explained in Fig. 3.3.7. It led to an equilibrium enthalpy value of 87 J/g for the PP-g-MAH as well as for the pure resin RD208CF.

Reheating the sample after cooling at slow rates reveals the existence of a double melting peak for isothermal as well as dynamical crystallisation processes. In the case of the copolymer RD208CF, this confirms the presence of different crystallites (spherulites and sheetlike aggregates) as it can be seen on the optical micrographs.
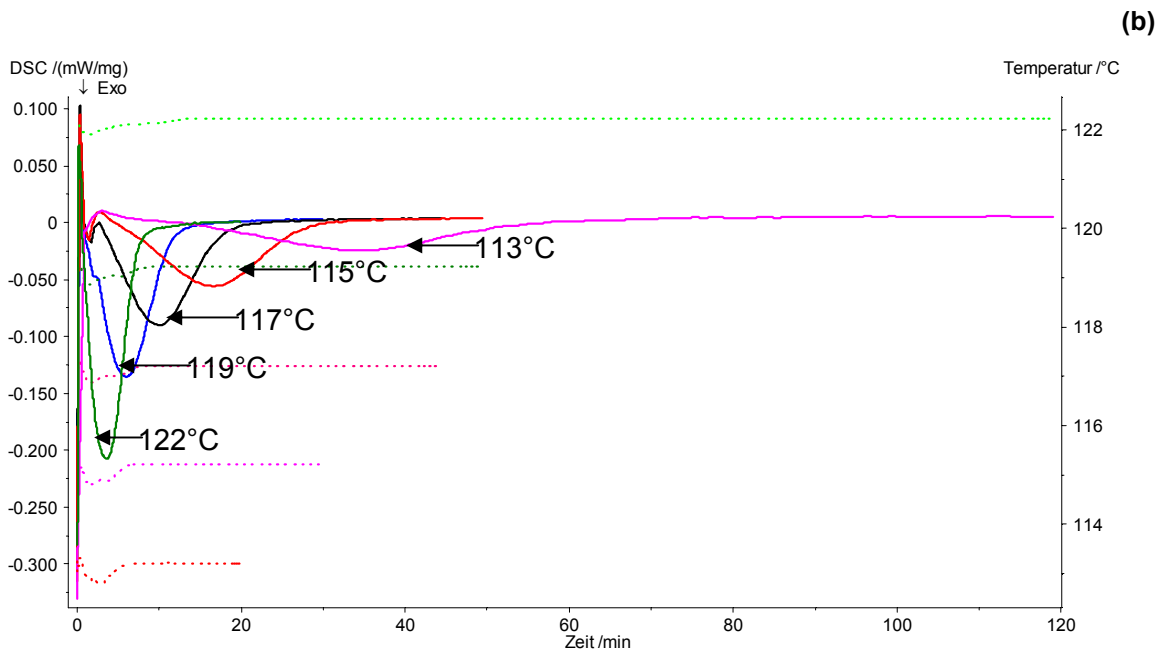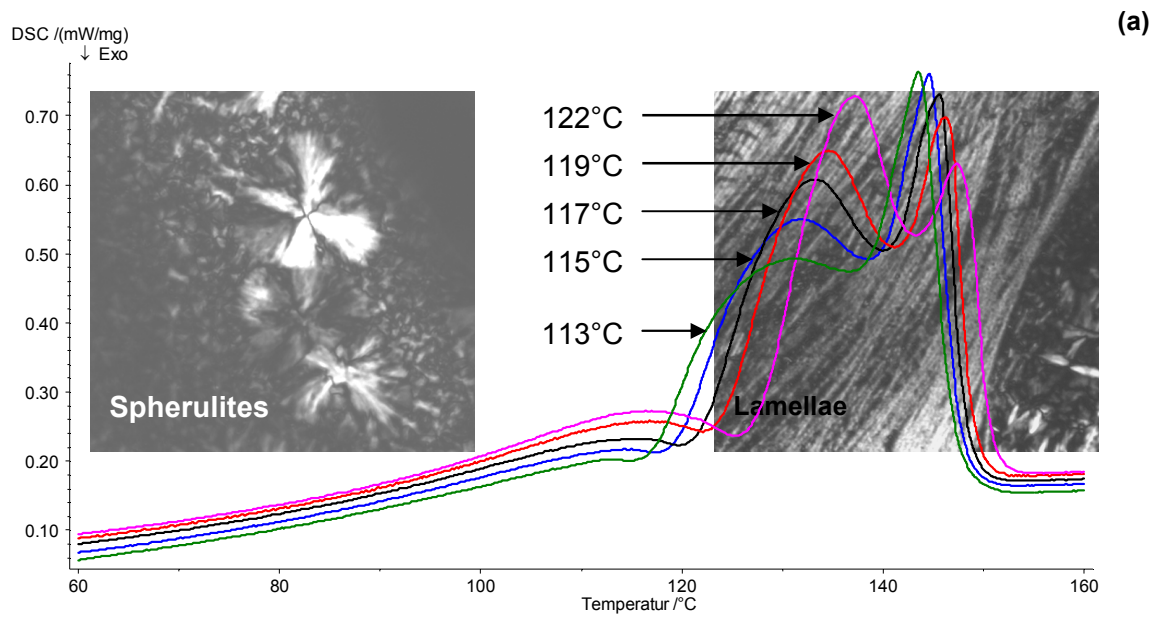
Fig. 3.3.6: Melting temperature **(a)** and isothermal **(b)** curves for a PP-g-MAH sample
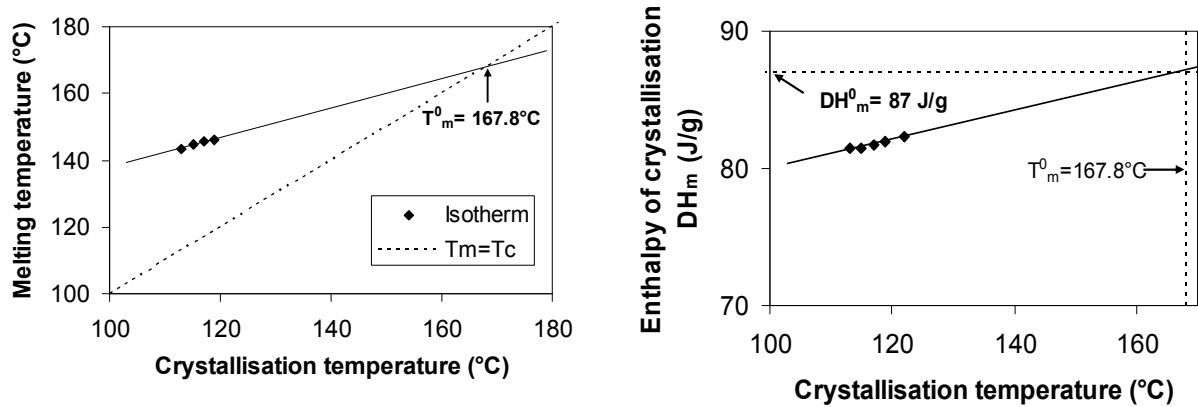
Fig. 3.3.7: Determination of the equilibrium enthalpy of fusion ΔH^0_m for a PP-g-MAH sample

The degrees of crystallinity of the four polypropylenes were calculated from the equilibrium enthalpies of crystallisation used in the literature [Ehr98]. A comparison of the degrees of crystallinity calculated with literature data and the ones determined with the method described previously for the RD208CF samples is given in Tab. 3.3.1. However, the values obtained with the calculated ΔH^0_m seem too high on a realistic point of view.

Material	Degree of crystallisation (%)	
RD208CF (pellet)	68.6*	28.8**
RD-MAH0.5-MD11.1-St1	76.2*	32.0**
RD-MAH0.7-MD11.1-St1	74.7*	31.4**
RD-MAH1.0-MD11.1-St1	84.8*	35.7**
HD601CF (pellet)	52.2	
HD601CF (extruded film)	50.6	
HD-MAH0.5-MD11.1-St1	48.6	
HD-MAH0.7-MD11.1-St1	55.7	
HD-MAH1.0-MD11.1-St1	56.0	

* Calculated ΔH^0_m value
** Literature ΔH^0_m value

Material	Degree of crystallisation (%)
RB501BF (pellet)	31.0
RB-MAH0.1-MD22.2-St1	28.1
RB-MAH0.3-MD22.2-St1	30.7
RB-MAH0.5-MD22.2-St1	29.0
RB-MAH0.7-MD22.2-St1	24.7
HB205BF (pellet)	44.4
HB-MAH0.1-MD22.2-St1	50.4
HB-MAH0.3-MD22.2-St1	49.7
HB-MAH0.5-MD22.2-St1	50
HD-MAH7-MD22.2-St1	48.6

Tab. 3.3.1: Degree of crystallinity of some PP-g-MAH samples

On the one hand, the augmentation of the MAH, styrene or DHBP amounts in the formulations leads to an increase of the degree of crystallinity of the low molecular weight PP-g-MAH. As a matter of fact, monomers or low molecular weight species present in the melt play the role of nucleating agents, increasing the number of nuclei, inducing an earlier crystallisation during cooling and hence, the degree of crystallinity. On the other hand, the high molecular weight PP-g-MAH showed a decreasing degree of crystallinity with the growing amount of the grafting component in the formulation. The differences of crystallinity amont the PP resins are due to their

molecular weight distribution and the types of structures formed during functionalization.

In both cases, the PP copolymers showed lower crystallinity levels than the homopolymers because of the random inclusion of ethylene sequences in the copolymers. They cannot fit into the propylene crystalline lattice and are excluded from the crystalline domains. As a consequence, they reduce and broaden the crystalline melting zone (see Fig. 3.3.6a).

Considering the PP-g-GMA samples (Fig. 3.3.8), the degree of crystallinity decreased from 51.8 % for $[GMA]_0$= 1 phr to 41.4% for $[GMA]_0$= 3 phr and raised up to 56% for $[GMA]_0$= 7 phr. The tendency is a slight decrease in the case of the grafted copolymers. Styrene appeared to have no significant effect on the degree of crystallinity of the PP-g-GMA although the samples containing a high concentration of styrene appeared to be translucent instead of transparent. This may be due to the amount of impurities produced by the different chemical reactions.
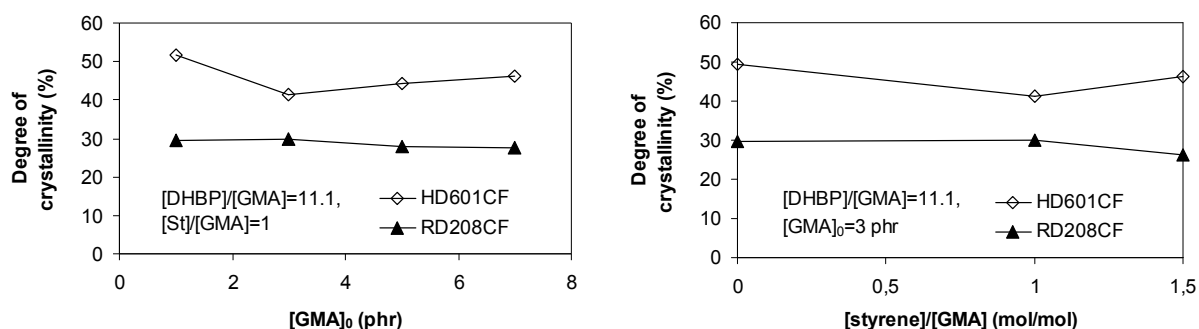
Fig. 3.3.8: Degree of crystallinity as function of the initial GMA concentration and styrene/GMA ratio

Crystallisation conditions play a major role in the characteristics of the material. Crystallisation temperature and cooling rate vary widely during the fabrication process, giving rise to extensive variations in the final properties of the end product. Optical microscopy pictures (Fig. 3.3.9) show two samples of the copolymer RD208CF cooled under nip rolls temperatures of 40 and 80°C. A difference in the structure of the resulting films is observable, with numerous small spherulites at a low nip rolls temperature and larger ones at a higher cooling temperature. Thus, it is clear from Fig. 3.3.10 that the cooling rate greatly affects the crystallisation temperature, increasing cooling rates resulting in lower crystallisation temperatures. As a

consequence, the time available for crystallisation is reduced and the degree of crystallinity decreases.
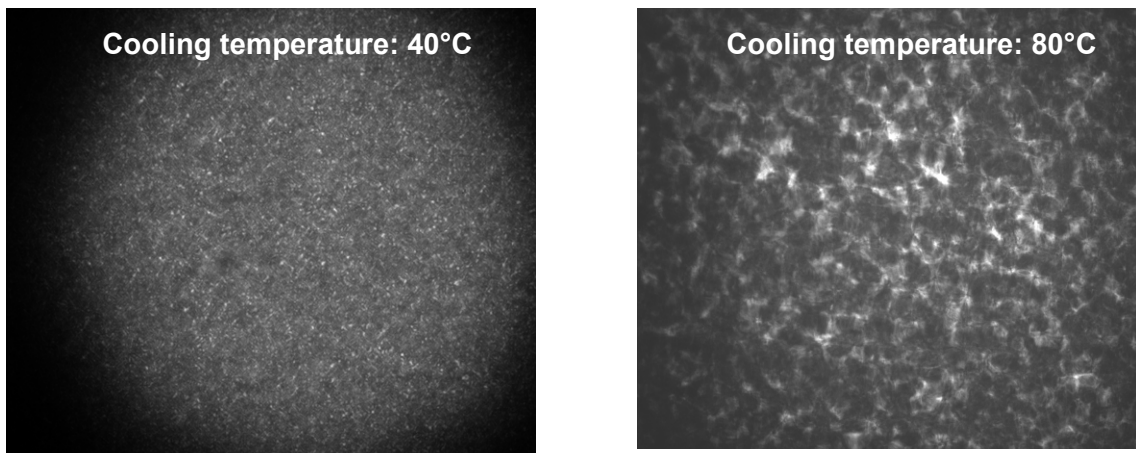
Fig. 3.3.9: Effect of the nip rolls temperature on the film crystallisation and morphology
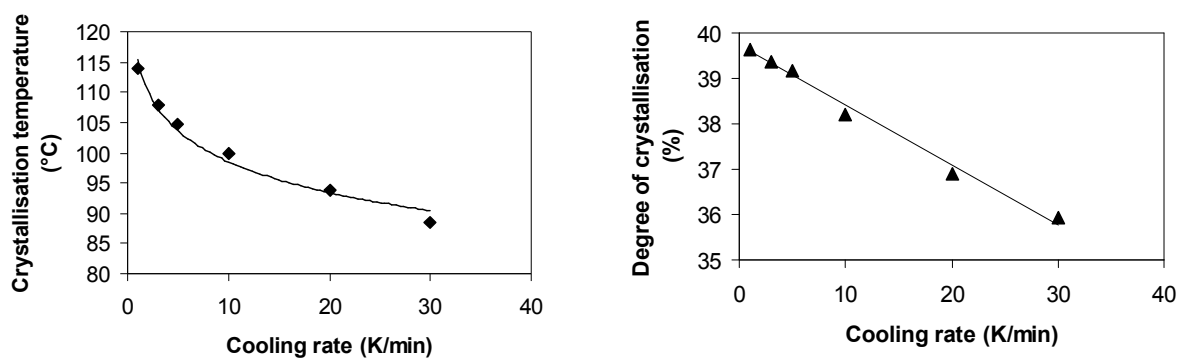
Fig. 3.3.10: Effect of cooling rate on crystallisation temperature and degree of crystallinity of the PP copolymer RD208CF

3.4 Mechanical properties of the functionalized PP

3.4.1 Sample preparation and measuring procedure

The cast films of the grafted polypropylene were studied in terms of mechanical properties in order to evaluate the effects of the functionalization.

Apart from the variation in the formulation which affect directly the molecular structure, many process parameters (temperature, screw design and shear rates, material throughput…) influence the mechanical properties of the final product. The cast film process ends up at the winding station where the material is collected. From the die to this end step, the film will be formed, stretched, calibrated to a given thickness and cooled to room temperature. Thus, the flow patterns resulting from the die design (coat hanger manifold), uniaxial stretching of the film at the exit of the die

which induces a longitudinal orientation of the macromolecules as well as the crystallization process initiated by the nip rolls quenching are decisive factors for the mechanical properties. As a matter of fact, films with a high crystalline phase possess a greater stiffness. The films were tested in the "machine direction". 100 mm thick strips with a width of 15 mm and a length of 50 mm (test length) were cut from each film, along the machine direction. The tensile properties were measured according to the European standard EN ISO 527-3 using a 1455 Zwick machine. The two ends of the strip were placed in the top and the bottom jaws of the tensile testing instrument. The bottom jaw then moved downward at a crosshead speed of 100 mm/min under constant temperature and relative humidity conditions (23°C, 50%) until failure of the material occured. The minimum number of specimens for one test was not less than five. The tensile strength σ_B and the elongation at break ε_B of the film were determined using the software TestXpert.

3.4.2 Tensile properties of the functionalized PP cast films

The tensile properties of the PP-g-MAH low molecular weight samples are presented in Fig. 3.4.1. The overall tendency is a decrease in the mechanical properties due to the PP chemical modification. This effect is caused by the degradation of the polymer during the grafting process. It leads to a reduction of the molecular weight and, as a consequence, to brittleness of the samples (drastic decrease of the elongation at break). It is especially pronounced for the modified homopolymer grades (HD601CF) which elongation at break is more than 32 times lower than the elongation of the pure polymer. The tensile strength at break diminished slightly for the grafted copolymers RD208CF whereas it remained almost unmodified for the homopolymers, these becoming stiffer with addition of MAH, DHBP and styrene.

A lower peroxide DHBP concentration in the formulations had a positive influence on the mechanical properties. For instance, the elongation at break increases from 132 to 842 % when only half of the peroxide content was added to the formulation (samples RD-MAH0.5-MD11.1-St1 and RD-MAH0.5-MD22.2-St1).
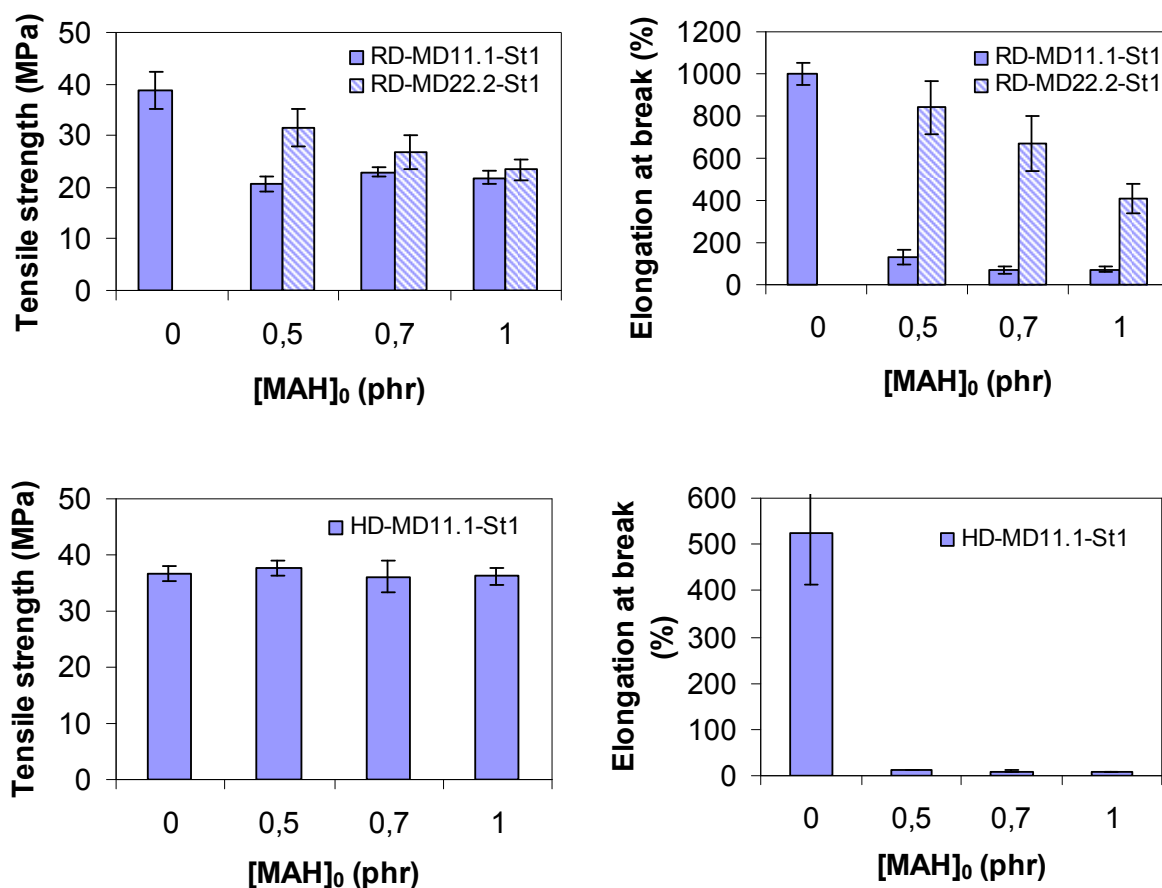
Fig. 3.4.1: Influence of the MAH, DHBP and styrene initial amounts on the tensile properties of the functionalized polypropylenes RD208CF and HD601CF

The previous results were confirmed by the high molecular weight polypropylenes HB205TF and RB501BF: with increasing MAH, DHBP and styrene contents, the tensile strength and elongation at break diminished (Fig. 3.4.2). The grafted homopolymers are more brittle than the copolymers, showing an elongation at break of 180 % for the sample HB-MAH0.7-MD22.2-St1 in comparison to 810 % for the grafted copolymer. While the tensile strength at break decreased in comparison to the value of the pure resin, there were only small variations among the PP-g-MAH with addition of MAH, DHBP and styrene.
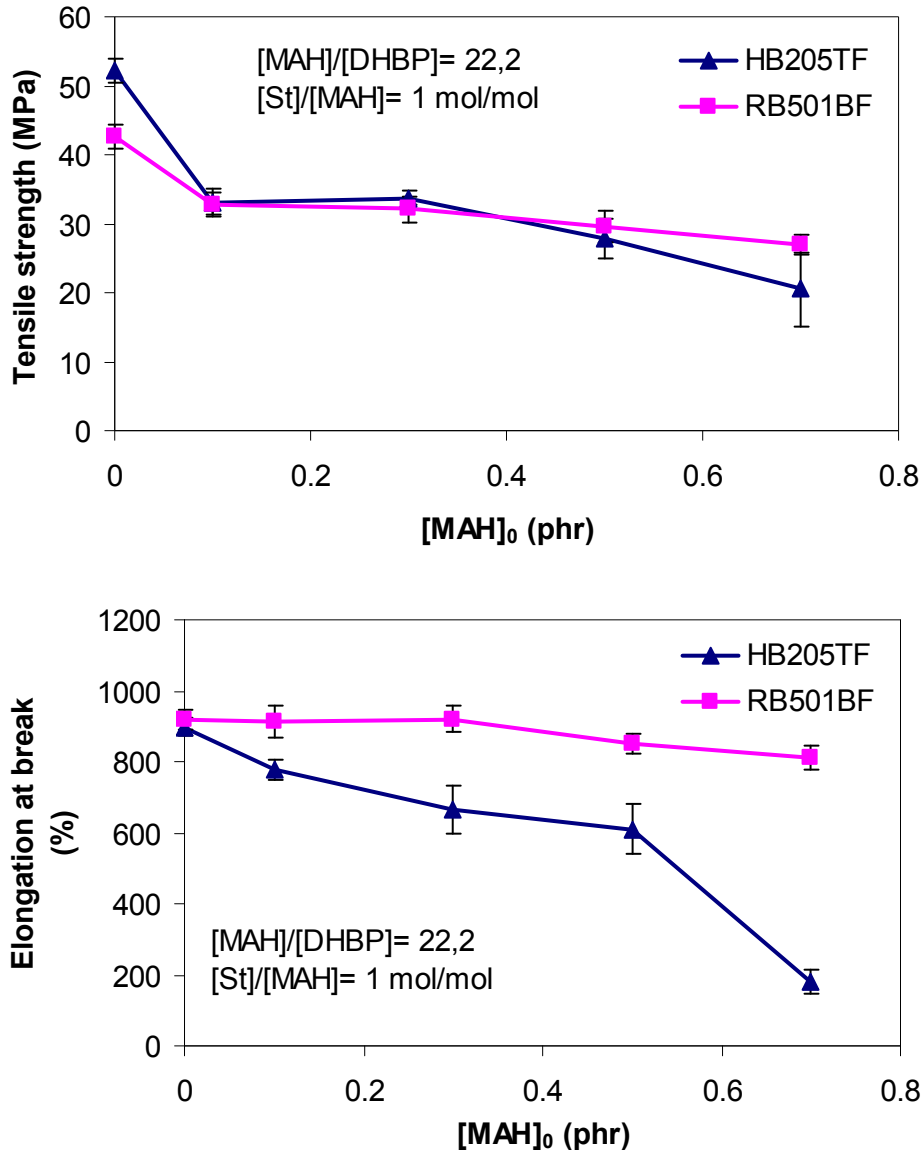
Fig. 3.4.2: Influence of the MAH, DHBP and styrene amounts on the tensile properties of the functionalized polypropylenes RB501BF and HB205TF

The results in terms of tensile properties for the PP-g-GMA are presented in Fig. 3.4.3. The effect of the β-scission during grafting is marked for the homopolymers HD601CF: the strong diminution of the elongation at break from 579 % (pure resin) to 11 % (HD-GMA3-GD11.1-St1) is due to the polymer degradation caused by the high amount of peroxide used in the formulation. However, a reduction of the DHBP content from 0.27 to 0.14 phr was not sufficient to obtain a positive influence on the tensile properties. As for the functionalized copolymers RD208CF, the elongation at break was decreased of about 10 to 15 % and tensile strength of 40% in comparison to the mechanical values of pure resin. A further increase of the initial GMA and DHBP concentrations led to a slight improvement of the tensile strength. The

numerous reactions occurring during grafting of the copolymer with GMA make the interpretation of the results more complex. Grafting, β-scission (to a smaller extent in comparison to the homopolymer), crosslinking, polymerisation of GMA or styrene and other possible reactions are competing and their proportions are not quantitatively defined so that their influence on the mechanical properties is difficult to evaluate.
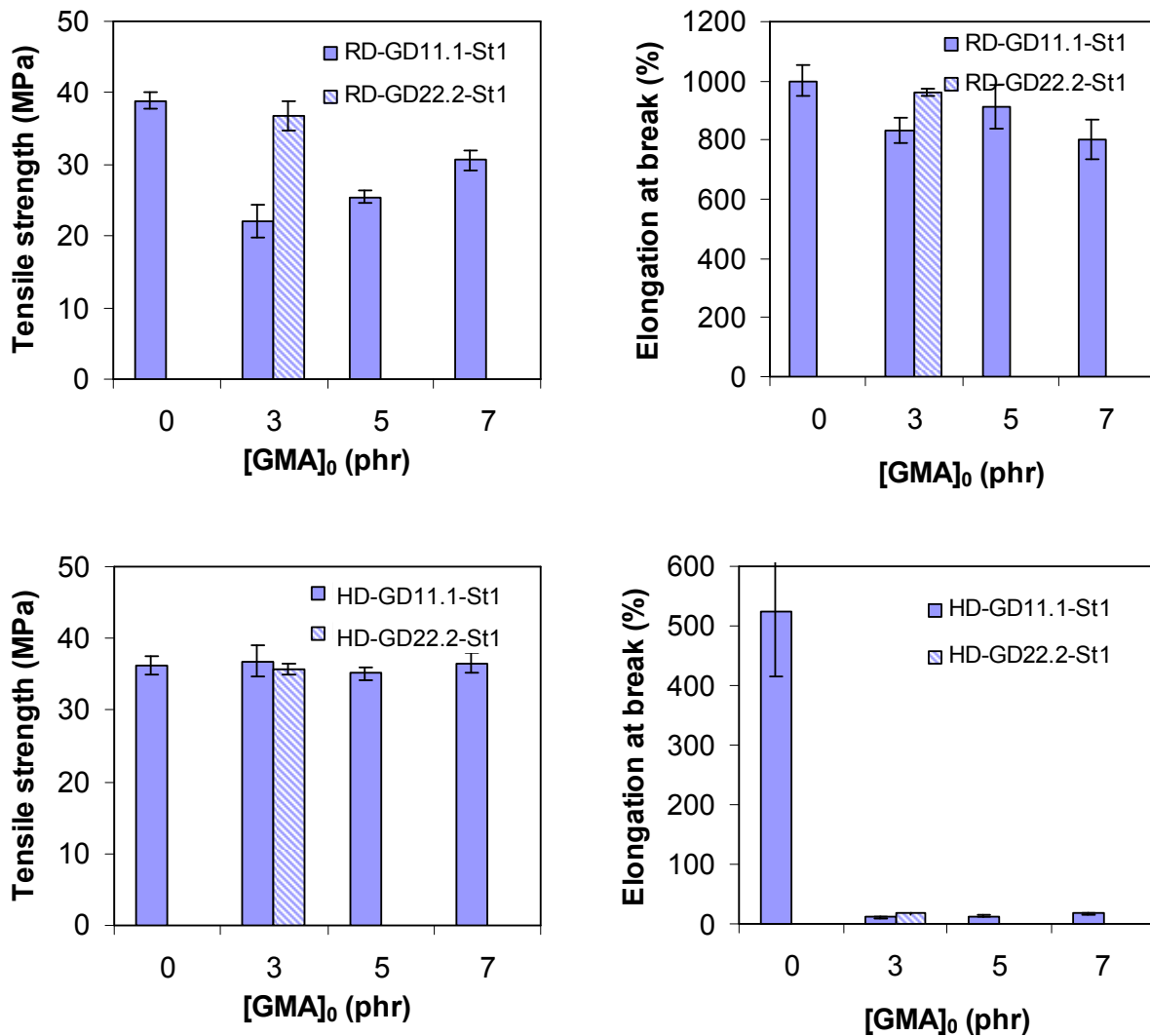
Fig. 3.4.3: Influence of the GMA, DHBP and styrene initial amounts on the tensile properties of the functionalized polypropylenes RD208CF and HD601CF

Styrene was used to reduce the PP degradation but no improvement in the tensile properties of the PP-g-GMA copolymers could be noticed (Fig. 3.4.4). Besides, the elongation at break of a PP-g-GMA homopolymer with a [styrene]/[GMA] mole proportion of 1.5 reached up to 50 times the value of a sample containing no styrene. In this case the minimization of the β-scission led to a reduction of the material brittleness.
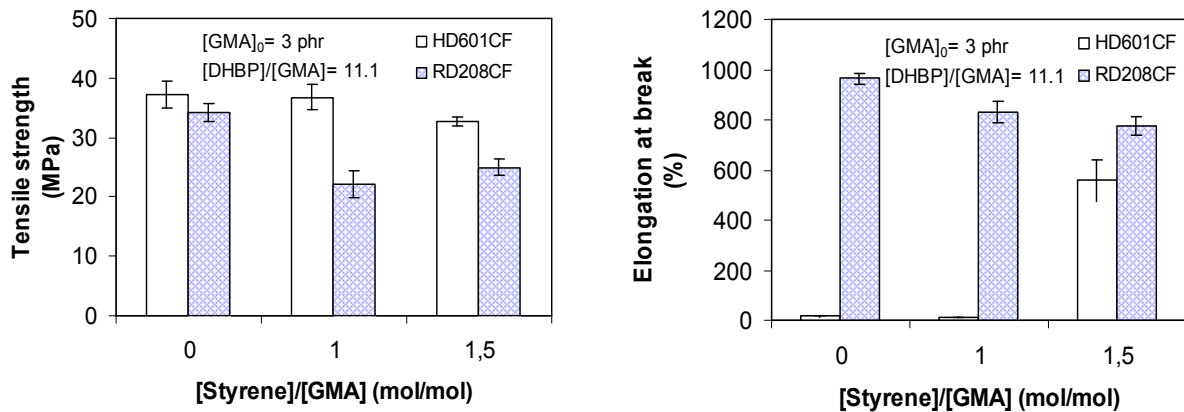
Fig. 3.4.4: Influence of the [styrene]/[GMA] molar proportions on the tensile properties of the functionalized polypropylenes RD208CF and HD601CF

Films of pure PP copolymer were produced using two nip roll temperatures (40 and 80°C). It was shown in section 3.3.2 that a slow crystallisation rate induced the development of large spherulites whereas the structure appeared to be finer at a higher cooling rate. The consequence in our case is a low elongation at break in the direction perpendicular to the machine direction (Fig. 3.4.5). The macromolecules and crystallites are stretched and oriented along the drawing direction. At a lower cooling rate (nip roll temperature of 80°C) the lamellae are thicker in the machine direction (MD) and thinner in the transverse direction (TD). As a consequence, the mechanical properties appeared to be lower in the tranverse direction.
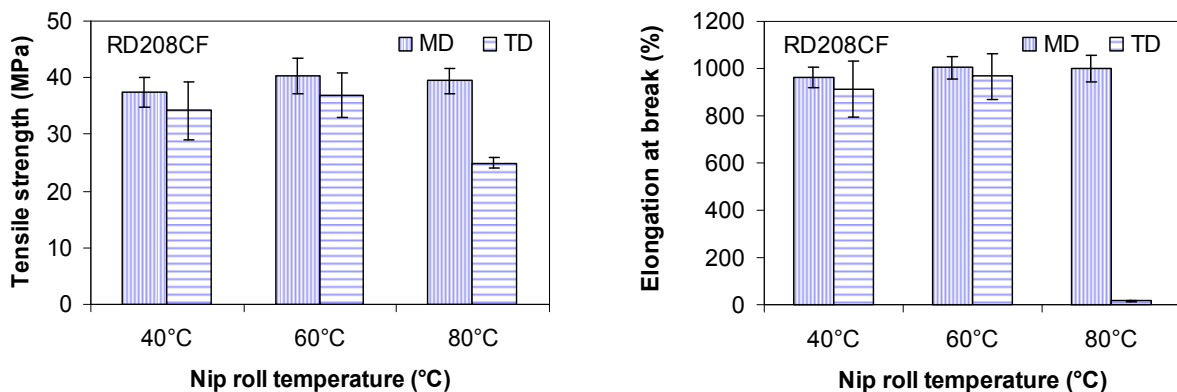
Fig. 3.4.5: Correlation between cooling conditions, structure and mechanical properties

The purpose of this work resided not only in the achievement of the PP functionalization with a minimum reduction of the physical properties of the initial polymer, but also in the realization of adhesion between the immiscible polymers PP and PA. Important, in our case, was the influence of the different formulations on the adhesion properties of films of modified PP and polyamide.

4 Polypropylene and polyamide multilayer films

4.1 Basics of adhesion

4.1.1 Introduction

The phenomenon of adhesion in the polymer field is illustrated by many examples: spreading of latex or bitumen on a substrate, polymer/fibre linkage in composites, polymer/metal adhesion in the automotive field, etc… In that way, adhesion is studied in the scientific fields of rheology, mechanical rupture, surface science, polymer chemistry or physics.

Adhesion between two materials can be described as the bond created by the intermolecular forces at the interface for short contact times as well as the mechanisms that occur at the interface at longer contact times such as interdiffusion, modification of the network parameters and chemical reactions. These phenomena lead to the creation of an "interphase" which possesses specific properties (or gradients of properties) in comparison to the homogeneous bonded materials. Generally, the term adhesion is used to define the mechanisms involved (microscopic interactions) and adhesion strength to characterize the resistance (the adhesive performance) or the fracture of the bond (measurement) at a macroscopic level.

Several approaches or models to describe adhesion were developed in the literature in accordance to the systems studied and the mechanisms involved. These contributions investigated the formation of a bond or the resistance to fracture depending on the state of the surfaces, the nature and the symmetry of the interface (polymer/polymer, polymer/glass, electrical charge at the interface), etc… The main mechanisms of adhesion are the mechanical interlocking, the polarisation theory (de Bruyne), the electrostatic model (Derjagin), the diffusion theory (Vojuckij, Vasenin, de Gennes, Doi&Edwards), the thermodynamic of adsorption or wetting model (Sharpe, Schonhorn, Zisman, Good, Fowkes, Wu), the formation of chemical bonds (Michel, Somorjai, Brockmann) and the theory of weak boundary layers (Birkerman) [Kin87,Jab94,Spä99,Sch99,Hai03]. Some of the models relevant for this work will be described in the following sections.

4.1.2 Theories of adhesion

4.1.2.1 Mechanical interlocking

The mechanical model stipulates that the adhesion strength is principally due to interlocking of the adhesive into the surface irregularities of the substrate (pores, cavities, asperities) [McB25]. This model considered adhesion to wood, unglazed porcelain, pumice and
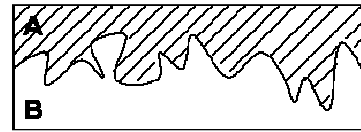
Fig. 4.1.1: Schematic description of the mechanical interlocking

charcoal porous substrates. Most of the work based on this theory was associated to electroless deposition of metals onto plastics (etching of plastics in order to obtain pits on a micrometer scale) or to adhesion of porous and microfibrous surfaces on metals [Wak82,Pak83]. It was considered that strong and durable bonds could be obtained by using highly porous surface oxide, providing that values of viscosity and surface tension of the adhesive allowed its penetration in the pores [Pak83]. To minimize the limitations of the mechanical theory, Wake suggested that the effects of mechanical interlocking and thermodynamic interfacial interactions could be associated to determine the joint strength G [Wak82]:

G = (constant) x *(mechanical interlocking component)* x *(interfacial interactions component)*

The interfacial component appeared to be higher than the mechanical effect in that experiment. In most of the cases, the mechanical bonding is not the major cause of adhesion but it can contribute to increase it. As a matter of fact, the increased area of effective contact leads to an augmentation of the interfacial forces. To achieve the required surface topography, a specific treatment (chemical or mechanical treatments) can be realized. This one alters the surface by removing a weak boundary layer and changing the physico-chemical nature of the surface [Gen90]. It was also suggested that the high surface roughness increases the energy dissipated viscoelastically and plastically around the crack tip and in the bulk of the material during joint rupture [Hin84,Bai71,Wan72].

The mechanical model has been tested and confirmed in a wide range of situations. However, it should be associated to the adsorption theory in order to relate the molecular configuration at the interface to the microscopic properties of the adhesive joint [Pak].

4.1.2.2 Diffusion theory

This theory, supported by Voyutskij [Voy63,Voy57], is based on the statement that after intimate contact between two materials, segments of the polymer chains diffuse across the interface into one another, creating an interphase. The properties of the interphase correspond to a gradient of the characteristics of both polymers. Hence, adhesion strength results from the interdiffusion mechanism. In the case of self-adhesion, the diffusion mechanism is called autohesion. The initial requirement for such a model is chain mobility and a similar solubility parameter. The condition for molecular mixing is given by the following equation:

$$\Delta G_m = \Delta H_m - T\Delta S_m \leq 0 \qquad \textbf{Eq. 4.1.1}$$

ΔG_m is the Gibbs energy of mixing, ΔH_m the enthalpy of mixing and ΔS_m the entropy of mixing. ΔH_m is usually positive (endothermic) in the absence of strong specific interactions. ΔS_m favours mixing but is too small for macromolecules because of limited chain configurations so that ΔG_m tends to be positive, preventing the mixing of entire macromolecules. However, local segmental interdiffusion occurs and is analyzed by the theories of Flory-Huggins and Hildebrand-Scott [Wu82,Bal96].

$$\chi_{12} = \frac{v_r}{RT}(\delta_1 - \delta_2)^2 \qquad \textbf{Eq. 4.1.2}$$

χ_{12} is the interaction parameter, δ_1 δ_2 the parameters of solubility and v_r the molar volume of a repeat unit.

The difference between the solubility parameters of polyamide and polypropylene translates their immiscibility as shown by: δ_{PA6} = 27.8 $[J/m^3]^{1/2}$ and δ_{PP} = 17.19 $[J/m^3]^{1/2}$ [Imm89].

Adhesion strength will depend upon factors such as the contact time, the temperature, the pressure, the nature and molecular weight of the polymers, the viscosity.

According to Vasenin [Vas69], the peeling energy to rupture the interphase region is proportional to the depth of penetration of a diffusing molecule and the density of chains crossing the phase boundary Σ. This diffusion theory was developed from the Fick's first law.

Further work on the diffusion theory has been realized by considering the aspect of dynamics of the polymer chains in the interfacial region [deG80,Doi86,Pra81,Jud81,Kim83].

A resulting scaling law for the fracture energy as function of the healing time t is given by Eq. 4.1.3:

$$G \cong t^{\frac{1}{2}} M^{-\beta} \qquad \textbf{Eq. 4.1.3}$$

where t is the healing time, M the molecular weight and β is given by $-\frac{3}{2} \leq \beta \leq -\frac{1}{2}$ according to the factors that control the healing process (number of bridges across the interface, crossing density of molecular contacts or bridges, centre-of-mass Fickian interdiffusion distance, monomer segment interpenetration distance [Sch99]).

The diffusion phenomenon surely contributes to the adhesion strength in the case of autohesion, healing or welding of identical polymers. However, diffusion becomes unlikely when the conditions of solubility of the materials and mobility of the chains are only partially fulfilled (immiscible materials, crosslinked or highly crystalline polymers, sealing temperature below the glass transition temperature…).

4.1.2.3 Thermodynamic model

The thermodynamic model, also called the adsorption, wetting or acide-base theory, is the most widely used adhesion approach. It states that adhesion (liquid/liquid, liquid/solid, solid/solid) is first due to interatomic and intermolecular forces at the interface when the adhesive and the substrate come to intimate contact. These forces allow a good initial wetting which is a necessary but not sufficient criterion for good adhesion.

The model uses the initial interaction forces (van der Waals, acid-base, electrostatic forces…), interdiffusion mechanisms, chemical reactions across the interface as well as dissipation phenomena during the fracture of the interface.

Wetting equilibrium in a solid-liquid system can be described by Young's equation:

$$\gamma_{SV} = \gamma_{SL} + \gamma_{LV} \cos\theta \qquad \textbf{Eq. 4.1.4}$$

where γ_{SV}, γ_{SL} and γ_{LV} are the surface tensions of the solid-vapour, solid-liquid and liquid-vapour interfaces, respectively.

A wetting criterion can be given in terms of the spreading coefficient S of the liquid on the surface as:

$$S = \gamma_S - \gamma_{SL} - \gamma_{LV} \geq 0 \qquad \textbf{Eq. 4.1.5}$$

In that case, the liquid spreads spontaneously on the surface. γ_S is the surface free energy of the solid in vacuum. It is related to the surface free energy γ_{SV} after equilibrium adsorption of vapour from the liquid by the following relation:

$$\pi = \gamma_S - \gamma_{SV}$$ **Eq. 4.1.6**

π is the spreading pressure which can often be neglected especially for polymeric materials so that γ_S can be used in place of γ_{SV} [Sch99].

According to Dupré and Young, the reversible work of adhesion W_{SL}, required separating a unit area of solid and a liquid, is defined as:

$$W_{SL} = \gamma_{SV} + \gamma_{LV} - \gamma_{SL} = \gamma_{LV}(1 + \cos\theta)$$ **Eq. 4.1.7**

The spreading pressure in the Dupré's relation is neglected.

If viscoelastic materials are bonded, the energy involved to separate the materials (G) or adhesion strength is a function of the molecular bond energy as well as dissipation. The latter corresponds to the energy absorbed in the viscoelastic and plastic deformations. It is a function of the bond separation speed (v), the temperature (T) and the deformation (ε). This model, also called the rheological model, was developed by Schultz-Gent [Gen71, Gen72], Andrews-Kinloch [And73], Maugis [Mau85], de Gennes [deG89]. Hence, the measured adhesion strength or fracture energy is given by:

$$G = W\Phi(v, T, \varepsilon)$$ **Eq. 4.1.8**

where Φ is the mechanical loss function that corresponds to the energy irreversibly dissipated in viscoelastic and plastic deformations and W the thermodynamic work of adhesion. From a general point of view, it is more convenient to use the intrinsic fracture energy G_0 instead of W. G_0 represents the energy required to propagate a crack through a unit area of interface in the absence of viscoelastic energy losses. Thus, G is expressed as:

$$G = G_0\Phi(v, T, \varepsilon)$$ **Eq. 4.1.9**

G_0 can only be equivalent to W if the bond separation implies an interfacial rupture of van der Waals interactions. If the viscoelastic and plastic energy losses are negligible, then $G = G_0$.

4.1.2.4 Chemical bonding theory

The adhesion strength can be enhanced when chemical reactions across the interface are involved. They prevent molecular slippage at a sharp interface during fracture and increase the interfacial attraction. The use of coupling agents with specific functional groups is an example of this field of adhesion research. They are able to react with both the adhesive and the substrate, creating a chemical bridge at the interface as described in Fig. 4.1.1. However, detection of the chemical bonds at the interface is difficult to realize because of the thinness of the interface [Wu82,Sch99].
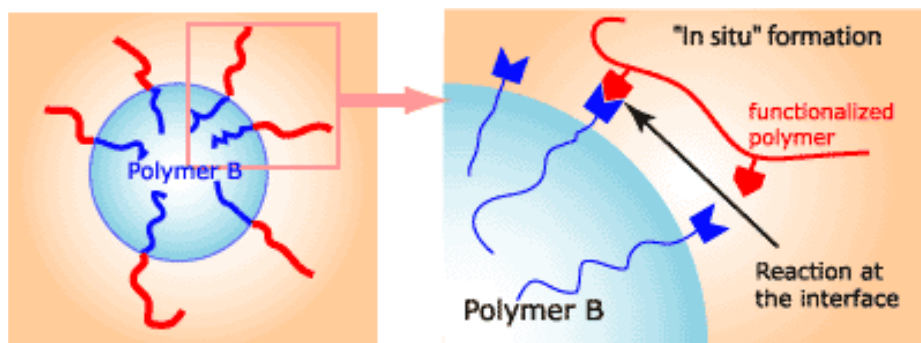
Fig. 4.1.2: Schematic description of the chemical bonding theory [Spchm]

The mechanisms of adhesion are numerous and depend strongly on the type of materials and systems as well as the bonding process and parameters. They may contribute simultaneously to adhesion between two polymeric surfaces. First, the molten polymers are brought into intimate molecular contact by wetting. Then, the molecules move until adsorptive equilibrium is achieved and diffusion across the interface takes place so that chemical reactions can occur. In the case of the PP and PA bonded films, adhesion can only be achieved over addition of functional groups in the PP matrix through grafting of the bulk or addition of lower molecular grafted PP because the polymers are immiscible. In this way, the PP acquires functional groups and chemical reactions between the materials are able to occur.

In the following sections, an analysis of the PP surface properties after chemical modification, fusion bonding of the modified PP and PA films, coextrusion of these materials as well as the determination of their adhesion properties are described.

4.2   Surface properties of the PP-g-MAH films

4.2.1   Contact angle measurement

The surface energy of a polymer surface can be estimated by contact angle measurement by assuming that the surface is perfectly smooth, the liquid is not a solvent of the polymer and the gravitation forces are negligible. The wetting phenomenon has been described by the Young equation (see section 4.1.2.3). A zero contact angle implies an instantaneous wetting of the surface, that's to say a very high surface energy, whereas a contact angle of 180° corresponds to no wetting of the surface by the liquid.

In this work, distilled water was used as wetting liquid. A drop of 4 µl was placed on the surface and the contact angle at the three phase points between the solid, the liquid and the vapour was measured. Considering that the polymer surfaces were not completely homogeneous, several measurements at different locations were conducted and the average contact angle was calculated. The films were analyzed without any preliminary treatment.

The measurements were performed using a Dataphysics OCA20 from the company Krüss and according to the sessile drop method. The measurement device is composed of a sample support, a charge-coupled camera with imaging lens, a light source and a mechanical unit for the precise measurement of the liquid volume and its deposition on the sample through the use of a syringe (Fig. 4.2.1). An appropriate software allows image recording and measurement of the contact angle between the base line of the drop and the tangent at the drop boundary.
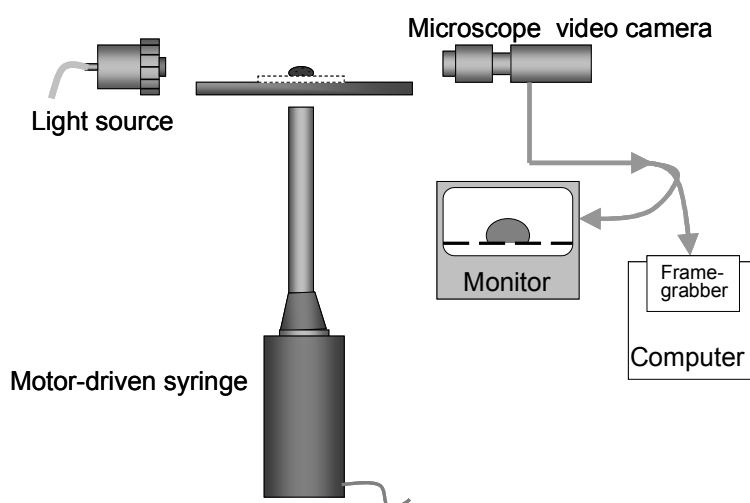
Fig. 4.2.1: Schematic description of a contact angle measurements device

4.2.2 Results of the contact angle measurements

Polypropylene is a non polar polymer so that water will not be able to wet completely its surface. Addition of polar molecules in the PP increases the surface energy, intermolecular interactions occur and the surface is better wetted by the fluid. This is demonstrated for the different PP used in this study. It was observed that MAH as well as GMA functionalization decreased the contact angles of the PP surfaces and favoured their hydrophilic properties [Rst03,Rst05,Nzg03]. The polyamide 6-6,6 and 6 films are polar materials and showed lower contact angles than those of the pure PP. The contact angles for the PA6-6,6 and PA6 are 67° and 95°, respectively.

The contact angles of the RD208CF series are lowered from 96° to 90-91° but there is no clear trend in the values with raising MAH concentration (Fig. 4.2.2).
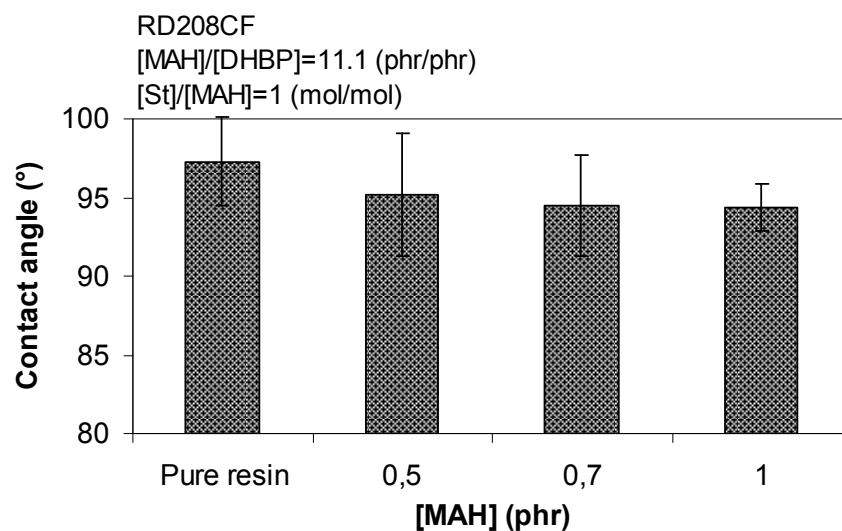
Fig. 4.2.2: Influence of the MAH initial amount on the contact angle of the PP-g-MAH (RD208CF)

For the grafted RB501BF and HB205TF series, a more pronounced trend in the contact angles could be detected (Fig. 4.2.3 and Fig. 4.2.4). This may be due to the absence of styrene in these formulations.
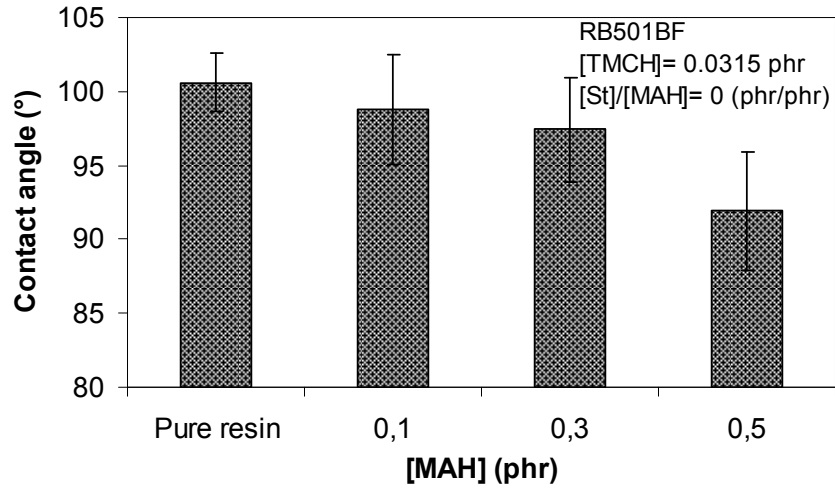
Fig. 4.2.3: Influence of the MAH initial amount on the contact angle of the PP-g-MAH (RB501BF)

The influence of styrene was studied for the grafted homopolymers (Fig. 4.2.4). With addition of styrene, the contact angles increased. In that case, other reactions occured simultaneously during the grafting process, creating many by-products which enhanced the surface heterogeneity of the film. Thus, an augmentation of the local roughness is observed, leading, in turn, to an increase of the contact angle. As a matter of fact, if a surface is rough or heterogeneous, the water drop will not advance when deposited on the surface and it will grow taller without moving its periphery. Wenzel equation shows that roughness may change the apparent advancing contact angle θ_W of a liquid on a rough surface compared to the contact angle θ_S of a liquid on a smooth surface. It is expressed as follows [Wu82,Kin87]:

$$\cos\theta_W = r\cos\theta_S \qquad \textbf{Eq. 4.2.1}$$

r represents the roughness factor or ratio of the true surface area (taking into account the peaks and valleys on the surface) to the apparent surface area.

If for a smooth surface θ_S is greater than 90°, roughening the surface will increase the contact angle θ_W further and therefore diminish the degree of wetting.
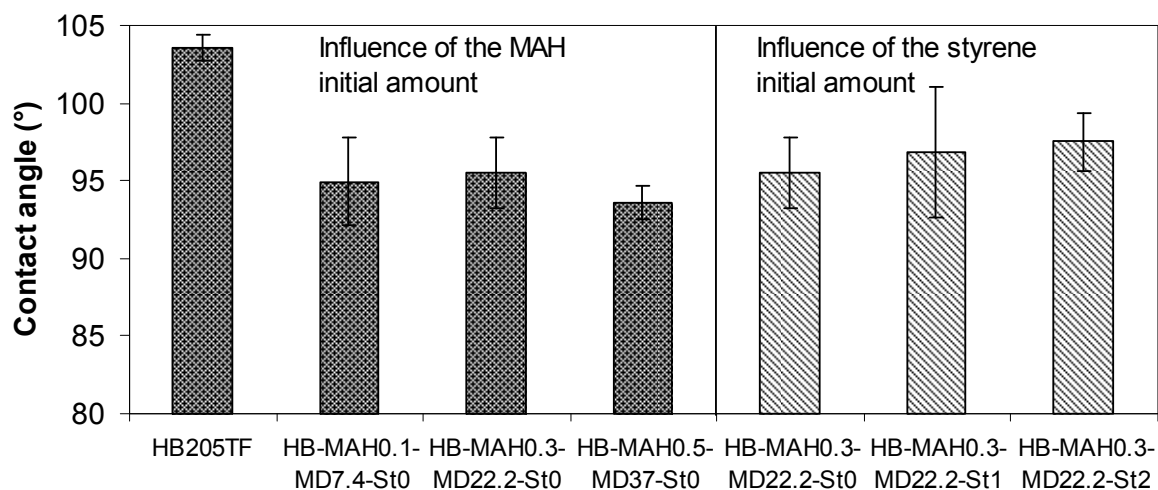
Fig. 4.2.4: Influence of the MAH and styrene initial amounts on the contact angle of the PP-g-MAH (HB205TF)

Considering the PP-g-GMA samples, a diminution of the contact angles with addition of GMA in the formulations is also observed (Fig. 4.2.5). Moreover, the presence of styrene, as already discussed for the PP-g-MAH, creates an augmentation of the contact angle.
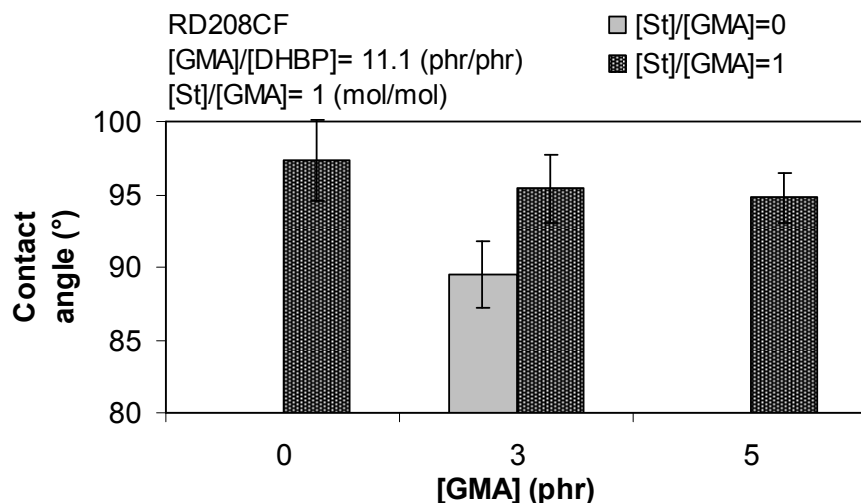
Fig. 4.2.5: Influence of the GMA initial amount on the contact angle of the PP-g-GMA (RD208CF)

The modification of the surface polarity by the presence of functional groups in the grafted films could be demonstrated through contact angle measurements. In this way, the wetting phase between the modified PP and the polar PA films, and eventually adhesion, should be improved during fusion bonding or coextrusion blown film.

4.3 Fusion bonding of functionalized PP and PA films

In order to determine the influence of the functionalization formulations on adhesion between the modified PP and the PA films, cast films of the polymers were bonded with a hydraulic press under defined conditions. The bonded films were subsequently mechanically tested in terms of adhesion using a peeling test. The surface peeled films and the major chemical reaction between the PA and PP-g-MAH were also investigated.

4.3.1 Materials and press procedure

The polymers used for the tests were the polyamides PA6-6.6, PA6, PA12, and the modified polypropylenes PP-g-MAH, PP-g-GMA as well as blends of pure PP and PP-g-MAH films.

To realize the peeling tests, specimens were prepared using a Dr. Collin GmbH hydraulic hot press. Before proceeding to the fusion bonding of the materials, the PA films dried in a vacuum oven during 12 hours to avoid thermal degradation of the PA due to the presence of moisture.

Two procedures were employed to press the films. On the one hand, the PP and PA films were laid in a 160 x 160 mm mould, only separated at one extremity from one another with a 4 mm width Teflon film to serve as a crack initiator for T-peel measurements. The mould was introduced in the press, held at a chosen temperature then pressed under pressure for a given time. The bonding parameters, temperature, pressure and time were varied to study their influence on adhesion between the modified PP and the PA. Once the heating process completed, the cooling phase was initiated still under pressure. The use of a mould permitted to keep material form and quantity during the press procedure. However, in the case of PP-g-GMA/PA6-6,6 bonds, the functionalized PP exhibiting low viscosities tend to flow out of the mould and make the opening of the mould difficult. For this reason, a maximum pressure of 12 bar was used to avoid this situation.

On the other hand, the cast films of PP and PA were laid on one another between two PTFE sheets. The above described procedure was then pursued in order to bond the samples. This method allows shorter press times which are more comparable to the contact times achieved during the film blowing process. The fusion bonding process between two Teflon sheets was realized with the high viscous PP under a low hydraulic pressure of 3 bar so that the bonded films kept their form.

The parameters time, temperature, pressure employed for the different press trials as well as a press program example are presented in Tab. 4.3.1 and 4.3.2.

Parameter / Sample	Heating time (min)	Cooling time (min)	Temperature (°C)	Hydraulic pressure (bar)
PP-g-MAH/PA6-6,6; PA6; PA12 RD208CF, HD601CF (Mould)	5	15	210	5
	7	15	230	10
	8	15	250	15
PP-g-GMA/PA6-6,6 RD208CF, HD601CF (Mould)	5	15	190	5
	8	15	210	10
	12	15	230	12
PP-g-MAH/PA12 RB501BF, HB205TF (Mould)	4	15	200	3
PP-g-MAH/PA12 RB501BF, HB205TF PP/PP-g-MAH blends (Teflon sheets)	1	10	200	3

Tab. 4.3.1: Press parameters used for PP/PA fusion bonding

Press phases / Parameters	1: Heating phase	2: Pressure application	3: Cooling phase
Time (min)	3	1	15
Temperature (°C)	200	200	200 → 25
Hydraulic pressure (bar)	0	3	3

Tab. 4.3.2: Example of a press program

The fusion bonded films were cut into 15 mm x 140 mm strips (with a peeling length of 100 mm) in order to perform the mechanical adhesion tests. The strips were conditioned in a climatic chamber for at least 48 h under the norm conditions of 23°C and 50% of relative humidity. Chemical, thermal as well as surface characterization tests were also conducted on the bonded samples.

4.3.2 Characterization of adhesion

4.3.2.1 Mechanical peel test

Adhesion strength results from different adhesion mechanisms which can occur simultaneously. Hence, adhesion can be characterized by fracture mechanics which was proven to be efficient in testing the toughness of adhesive bonds and estimating

the mechanisms of failure. Many test methods such as the floating roller, the climbing drum, the T-peel, the 90° (L-peel) or the 180° (T-peel) tests, cantilever beam, blister or cone tests, are used depending on the adhesive bond form and type. In this study, the T-peel test was used (Fig. 4.3.1).
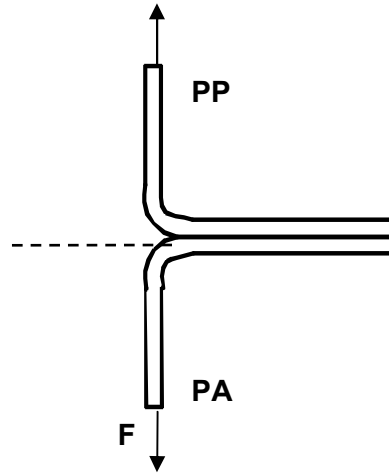
Fig. 4.3.1: Mechanical adhesion T-peel test

Fracture energy in peel tests consists of several components which are difficult to separate from one another. It has been reported that the measured fracture energy, according to the energy balance approach, corresponds to the summation of the different energies involved during a steady peel test: adhesion energy related to the work of adhesion, energy expended in separating an interfacial area, energy expended in deforming the sample (plastic, elastic bending and straightening energy) [Spä99]. The analysis of the fracture energy in peel test reported by Wu was chosen in this work [Wu82]. Considering that the test is processed at a constant peel force speed F and assuming that the peel angle θ is constant during peeling, the work of peel W is expressed by:

$$W = F(\lambda - \cos\theta) \times c_p \qquad \textbf{Eq. 4.3.1}$$

where c_p is the peeled distance and λ the extension ratio.

The energy Γ expended in separating an interfacial area $b_p c_p$ is given by:

$$\Gamma = b_p c_p G \qquad \textbf{Eq. 4.3.2}$$

where G is the fracture energy per unit interfacial area.

The energy V is also expended in deforming the peeling strip in the straight region. It contains a stored elastic energy component and a plastically dissipated energy component, that is:

$$V = S_a b_p c_p d_a + S b_p c_p d \qquad \textbf{Eq. 4.3.3}$$

where V corresponds to deformation energy for peeling an interfacial area $b_p c_p$, S_a the deformation energy per unit volume of the adhesive and S that of the flexible adherend. d and d_a are the thicknesses of the adherend and the adhesive. Conservation of energy requires W-Γ-V=0 and using Eq. 4.3.1 to 4.3.3, it gives:

$$\frac{F}{b_p} = \frac{G + S_a d_a + S d}{\lambda - \cos\theta} \qquad \textbf{Eq. 4.3.4}$$

Considering that the adherent is flexible and inextensible λ = 1 and S_a = S = 0, Eq. 4.3.4 simplifies to

$$\frac{F}{b_p} = \frac{G}{1 - \cos\theta} \qquad \textbf{Eq. 4.3.5}$$

In this study, the adhesion fracture energy G per unit interfacial area in a T-peel configuration (θ = 180°) is given by:

$$G = [1 - \cos(180°)]P = 2P \qquad \textbf{Eq. 4.3.6}$$

where P is the peel force (in N) per unit width (in m).

The peel tests were carried out under constant temperature and relative humidity conditions (23°C, 50%) and according to the norm DIN 53530. The tensile test machine was a Zwick 1455 used with a crosshead speed of 100 mm/min. At the beginning of the test, the distance between the testing machine jaws was 50 mm. Five to ten specimens were tested for each sample and the mean value of the peel force over the width was calculated using the software TestXpert.

Fig. 4.3.2 depicts the evolution of the peel force for a peel distance of 100 mm. The curves represent mean value curves for the sample RD-MAH0.7-MD11.1-St1/PA6-6,6 pressed at 210°C and under a pressure of 5 bar during 8 min. The curve is relatively smooth and the values of the force are high, indicating a good adhesion of the films. However, the random fluctuations of the peel force are mainly due to random imperfections in the films (local variation of thickness, concentration of functional groups or impurities…) which in turn cause variations of the adhesion level.
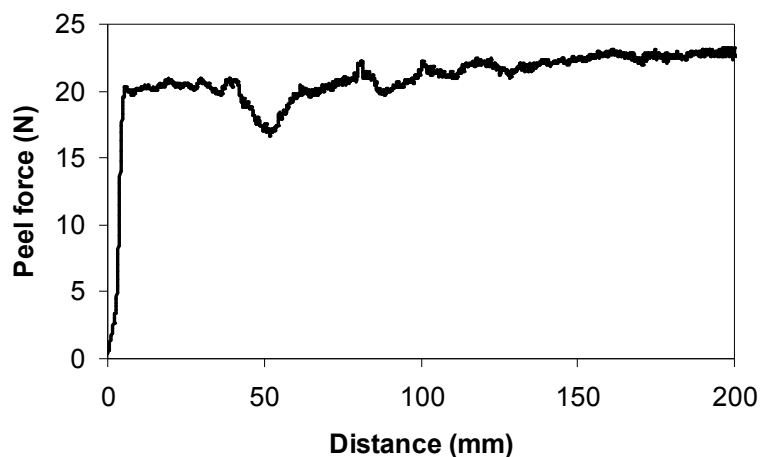
Fig. 4.3.2: Peel force as a function of the distance

These peel test results were taken as indication for the comparison of the bond strengths of the different functionalized PP/PA laminates. They should not be considered as absolute values of adhesion strengths. Several factors such as film thickness, surface roughness or process parameters influence the measurement. The concentration of the grafting reagents in the films and the press parameters (time, temperature, pressure, cooling…) were varied in order to evaluate their impact on the fracture energy. The results of peel tests for PP-g-MAH/PA and PP-g-GMA/PA two-layer bonds are presented in the following sections as preliminary work to the coextrusion trials.

a) PP-g-MAH / PA bonds

In a first step, pure PP and PA films were pressed. The immediate delamination of the bond after extraction from the mould confirmed the immiscibility of the materials. In a second step, different formulations of the low molecular weight PP-g-MAH RD208CF and HD601CF were pressed with PA films.

Fig. 4.3.3 and 4.3.4 show the fracture energies as a function of the introduced MAH amount and the styrene/MAH molar ratio for both PP types, respectively. It was found that the fracture energies of bonded films of PP-g-MAH with raising MAH content decrease from 2380 to 1100 J/m^2 at a low MAH/peroxide ratio of 11.1 – that is a high peroxide concentration [Rst03]. Several explanations to this phenomenon can be considered. First, it was found that a molecular weight reduction due to the β-scission occurs with increasing MAH, DHBP and styrene concentration (see section 2.1.3).

The resulting polymer chains possess a better mobility in the molten state, which is an important condition for the diffusion process, but they may become too short to create entanglements on both sides of the interface [San98]. These entanglements are important for the formation of a copolymer between the reactive groups of the polyamide and the MAH. It plays the role of a connector between the immiscible polymer phases.

Second, this adhesion weakening may also be related to the lowered mechanical strength of the grafted PP, this being a consequence of its molecular weight diminution. According to micromechanical studies of fracture performed on PP/PA assemblies using an asymmetric double cantilever beam, because the yield stress of the PP is smaller than that of PA, dissipation occurs in the PP by formation of a large plastic zone at the crack tip. This deformation is principally induced by the creation of crazelike fibrils. The joint fails by scission of the PP side of the copolymer chains at the interface. As a consequence, the mechanical properties of the PP are the most relevant during fracture and the PA plays the role of a rigid surface, being only involved in the interfacial linking [Bou94,Bou96].
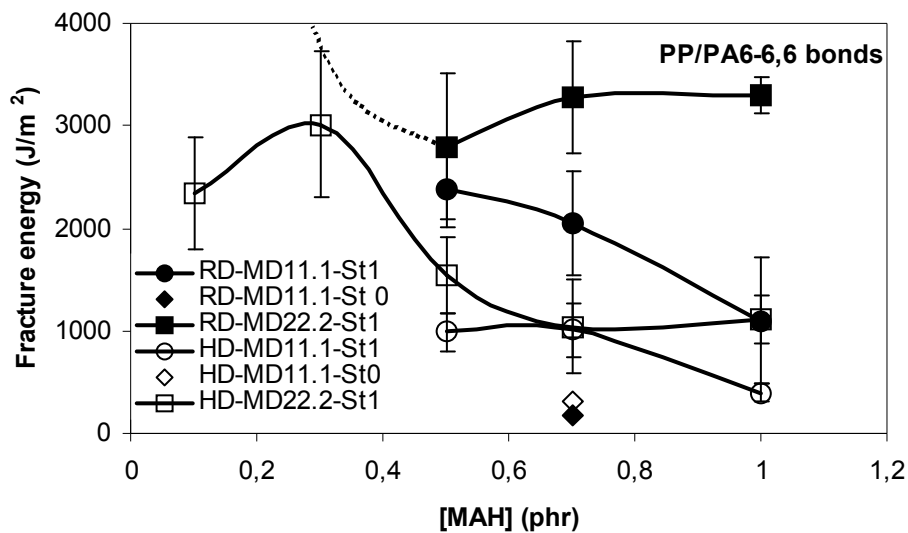
Fig. 4.3.3: Influence of the MAH, DHBP and styrene initial concentrations on the adhesion energy of PP-g-MAH/PA6-6,6 bonds
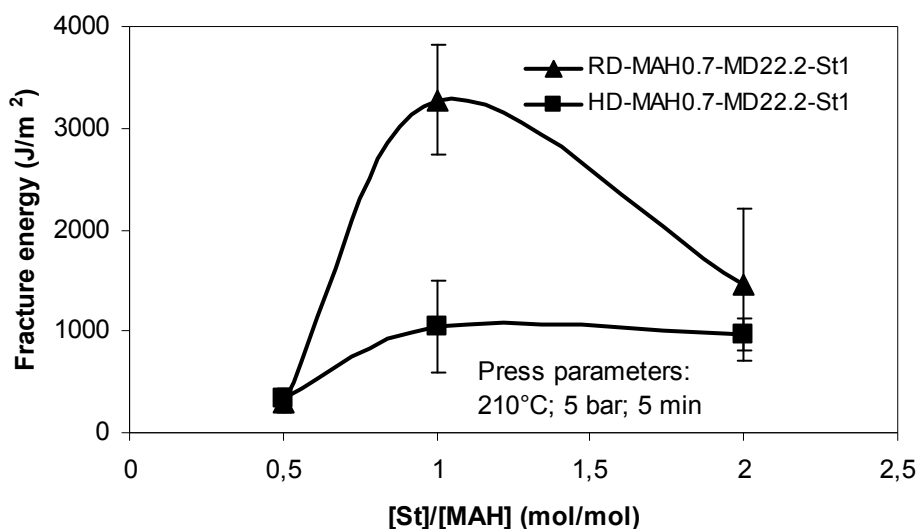
Fig. 4.3.4: Influence of the styrene initial concentration on the adhesion energy of PP-g-MAH/PA6-6,6 bonds

Third, by increasing simultaneously the MAH, peroxide and styrene contents in the grafting formulation many reaction by-products are created in the film. Hence, it can be assumed that these by-products, including non grafted MAH, saturate the interface and disturb the connections between the grafted reactive groups across the interface.

The decrease of the fracture energy with growing MAH, styrene and DHBP concentrations becomes less pronounced for a MAH/peroxide ratio of 22.2. In this case, the trend is a diminution of the fracture energy with increasing reagents to reach a plateau around MAH = 0.5 phr. The dashed line in Fig. 4.3.3 corresponds to the high adhesion energies reached by the joints PA6-6,6/RD-MAH0.1-MD22.2-St1 and PA6-6,6/RD-MAH0.3-MD22.2-St1 which could not be separated and tested.

It is noticeable that the values of adhesion energies are much lower for the PA/homopolymer than for PA/copolymer bonds. This result may be related to the molecular weight of the PP-g-MAH. Before functionalization, the two pure PP resins exhibit comparable molecular weights. However, during the grafting process, the homopolymer is more prone to degrade than the copolymer and its molecular weight significantly decreases (see section 3.2.2.1). As a consequence, the grafted homopolymer chains are shorter than those of the copolymer which can more effectively build entanglements across the interface. For instance, a laminate made of the grafted PP copolymer RD-MAH0.7-MD11.1-St1 demonstrates a fracture energy of 2044 J/m^2 in comparison to 1012 J/m^2 for the corresponding homopolymer

one pressed under the same bonding conditions. The influence of the PP-g-MAH molecular weight on the joint adhesion is confirmed by the low fracture energies of 169 J/m^2 and 314 J/m^2 measured for PA/copolymer and PA/homopolymer bonds, respectively. The formulation of these PP-g-MAH (PP-MAH0.7-MD11.1-St0) contains no styrene so that the materials are strongly degraded. Their viscosities were found to be of about 5 and 2 times lower than those of samples produced with styrene, for the copolymer and homopolymer, respectively. Furthermore, Fig. 4.3.4 demonstrates the positive influence of styrene on the bond adhesion. A first increase of the fracture energy with addition of styrene is observed – that is St/MAH molar ratios of 0.5 and 1. This effect is however limited for St/MAH ratios equal to 2. As a matter of fact, styrene not only minimizes the polymer degradation reaction, but its excess also strongly modifies the molecular structure of the PP-g-MAH. Long St/MAH copolymer side chains are created on the PP backbone and seem to impair the adhesion mechanisms.

Because the process parameters during functionalization of the PP have an influence on the grafted PP properties, it is interesting to study how they indirectly affect the PP/PA joint adhesion. For this reason, PP-g-MAH films of RD-MAH0.7-MD15.87-St1 and RD-MAH0.7-MD22.2-St1 extruded under different conditions were fusion bonded with the PA6-6,6. Different extrusion screw speeds (50, 100 and 200 rpm) and temperatures (200 and 220°C) were used.

Fig. 4.3.5 shows that the fracture toughness of the bonds grows with increasing extrusion screw rates but decreases with higher process temperatures. As mentioned in section 3.2.3, a high functionalization temperature implied a diminution of the PP-g-MAH viscosity or molecular weight, which in turn implies a weak bond to polyamide. An increasing screw rate intensifies the mixing effect of the components and therefore should ameliorate the grafting yield of the PP-g-MAH samples. To make a correlation between the film extrusion parameters and the adhesion properties, it is relevant to study the chemical modifications of the extruded film surface by using IR spectroscopy in reflection (with an ATR unit) without any sample purification. Fig. 4.3.6 shows the normalized IR spectra of the PP-g-MAH films extruded at screw rates of 50, 100 and 200 rpm. The intensity of the carbonyl band around 1782 cm^{-1} clearly appears to increase with raising screw speed. This implies that more MAH groups are present at the film surface. As a matter of fact, more

grafted PP chains diffused from the bulk to the surface because of the higher shear rates created in the extruder and the die. As a consequence, the chemical reactions between the species as well as the joint adhesion were promoted.
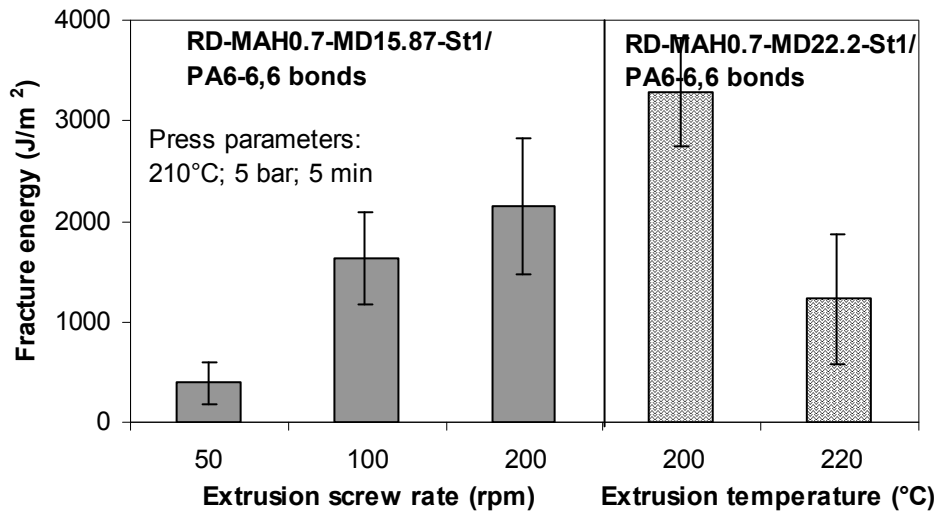
Fig. 4.3.5: Influence of the extrusion parameters during PP functionalization with MAH on the adhesion energy of PP-g-MAH/PA6-6,6 bonds
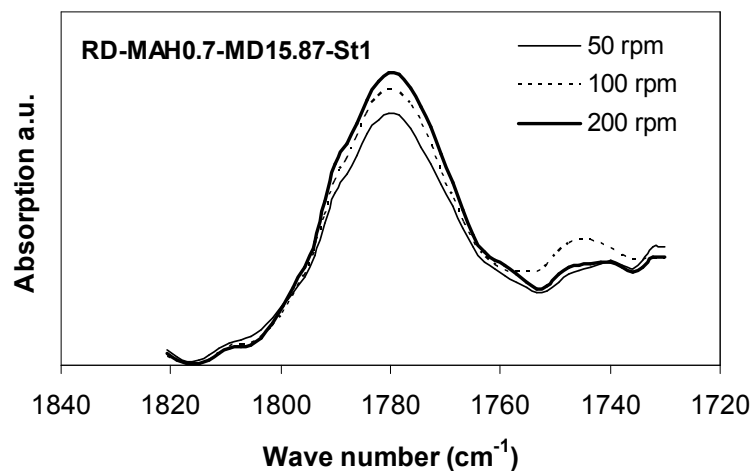
Fig. 4.3.6: Evolution of the carbonyl band measured by IR spectroscopy in reflection as a function of the screw speed during PP functionalization with MAH

The type of polyamide should also be a determining factor for the improvement of the joint adhesion because of their different polarities (see section 4.2.2). However, no significant differences is observed between the peel energies of laminates composed of the PA types PA6, PA6-6,6 and PA12 with RD-MAH0.7-MD11.1-St1 as PP-g-MAH films (Fig. 4.3.7). The press temperatures of these trials were chosen about 10°C above the melt temperature of the polyamides.
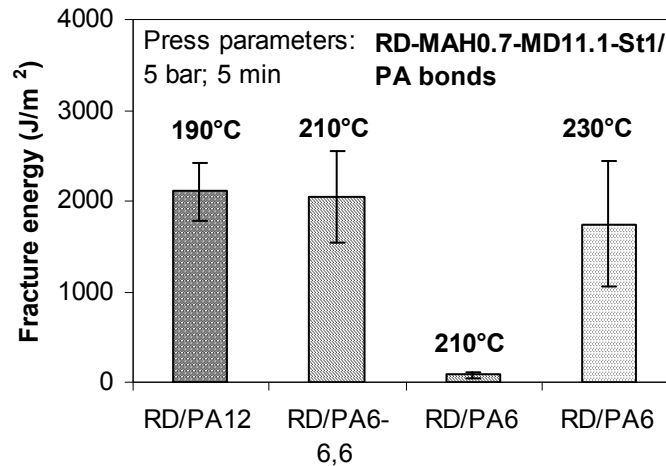
Fig. 4.3.7: Influence of the press temperature and polyamide type on the adhesion energy of PP-g-MAH/PA6-6,6 bonds

Furthermore, it can be noticed that the bonding temperature plays an important role in the adhesion efficiency: the fracture energy of the PP/PA6 bond grows from 32 to 1700 J/m^2 when the press temperature is raised from 210 to 230°C. This represents a great increase of the fracture energy and may be explained by the fact that a temperature superior to the melt temperature of the PA favours the diffusion of the polymers as well as the chemical reactions at the interface. To understand this phenomenon, Boucher and al. [Bou97] studied the adhesion of laminates made of PA6 and PP/PP-g-MAH blends – which contained high molecular weight PP-g-MAH – prepared at process temperatures lower and higher than the PA melt temperature. They concluded that the large difference between the fracture energies is rather due to the efficiency of the in situ formed copolymer at producing larger plastic deformation zones (changes in the dissipation process within the PP) than to an increase of its surface density. Furthermore, the modification of the dissipation mechanism could be caused by the presence of PP β-form at the interface. However, this hypothesis was invalidated by studies of the microstructure near the interface [Plu98]. Another study of assemblies made of PA6 and PP/PP-g-MAH blends pressed at temperature superior to the PA6 melt temperature was conducted by Kalb and al. [Kal97]. The importance of the temperature as well as the PP chain length suggested that co-crystallisation phenomena could be responsible for the increased adhesion. It was also concluded that the interfacial reinforcement was independent of the PA molecular structure.

Fig. 4.3.8 shows that increasing bonding pressure and time strongly enhances adhesion. As a matter of fact, the contact time dependence of the fracture energy is attributed to the segmental interdiffusion of the two materials. The rate of interfacial contact which conforms to first-order kinetics is given by Plisko and al. [Wu82] as:

$$\phi + \ln(1 - \phi) = -\frac{Pt}{\eta}$$ **Eq. 4.3.7**

where ϕ is the fractional interfacial contact area, p the applied pressure, t_0 the time and η the viscosity of the adhesive, being the PP-g-MAH film in our case.

Hence, not only the factor time but also pressure influences the rate of interfacial contact. Because of the intimate contact achieved for a sample pressed under a higher hydraulic pressure (15 bar), it is understandable that the bonded films reached a good adhesion strength and could not be separated.
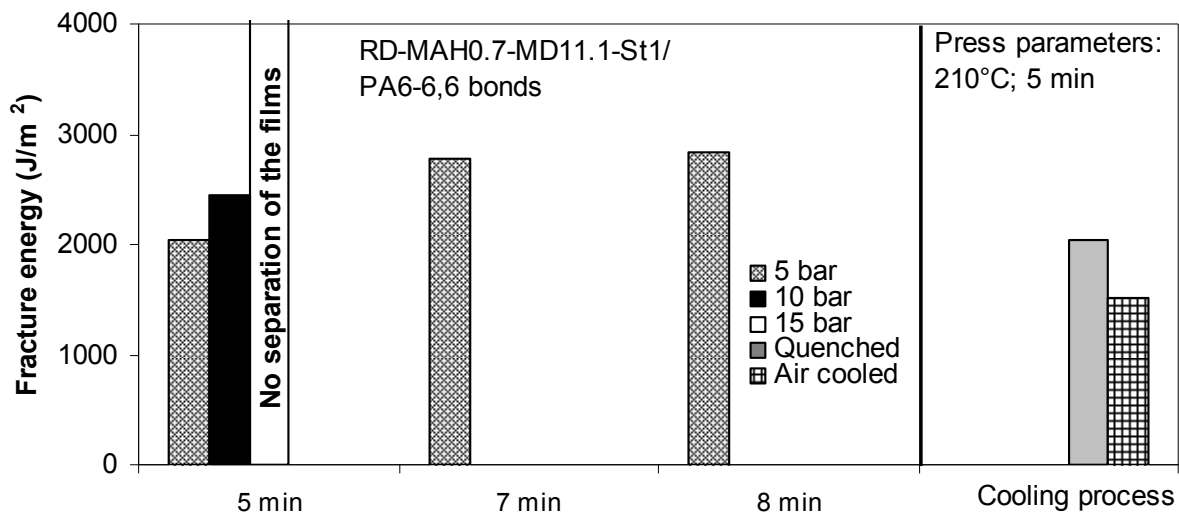
Fig. 4.3.8: Influence of the press time, pressure and cooling process on the adhesion energy of PP-g-MAH/PA6-6,6 bonds

Another factor of influence on the adhesion performance is the cooling process. In Fig. 4.3.8, at cooling rate of about 12.3 K/min the fracture energy of the laminate was higher than that of slower cooling rate – that is when the mould was cooled in the air over several hours. Polymer phase separation or crystallisation phenomena could be at the origin of this result. The effect of crystallinity on adhesion had been studied for assemblies composed of PA6 and blends of PP and high molecular weight PP-g-MAH (M_w= 44.7 kg/mol) [Lar01,Lar02,Lar04/1,Lar04/2]. Effectively, a correlation could be made between the interfacial reinforcement reached for a bonding temperature above the melt temperature of the PA6 and the epitaxial crystallisation of the PP on the PA6 surface. This crystalline orientation appeared to increase with raising cooling rates,

annealing temperatures or times (to a lesser extent) and to depend also on the copolymer formed at the interface. The authors argued that under these conditions the PP lamellae were oriented parallel to the interface. Because of their increased number in this area, they were close enough to be linked to one another by small chains. The PP-g-MAH chains were bridged to several lamellae and the copolymer formed in situ as well. Hence, it was capable of propagating the stress over a greater distance, leading to a higher resistance of the interface.

In a third step, the functionalized high molecular weight PP cast films HB205TF and RB501BF were bonded to PA12 films under conditions described in Tab. 4.3.1. Two series of measurements were realized using a mould [Zan04] and Teflon sheets.
The results of the fracture energies for joints of PA12 and different formulations of grafted homopolymers (HB205TF) are presented in Fig. 4.3.9.

Fig. 4.3.9: Influence of the MAH, DHBP and styrene initial concentrations on the adhesion energy of grafted homopolymer/PA12 bonds pressed in a mould

The simultaneous augmentation of MAH, DHBP and styrene concentrations in the formulations for bonds pressed in a mould led to a degradation of the joint adhesion [Rst05]. This may be due to the degradation of the grafted PP materials as well as their mechanical properties. The presence of styrene seems to have a positive influence on the joint adhesion. For the moulded samples a saturation of the interface seems to be reached at a St/MAH molar ratio of 2. This result can be correlated to the

increase of styrene/MAH copolymers branches on the PP backbone which may disturb the adhesion mechanisms at a certain concentration. When the peroxide content increases – other components being kept constant – the trend is an improvement of the fracture energy. The mobility acquired by the chains shortened through β-scission upon addition of peroxide promotes diffusion, and thus adhesion. Moreover, the more peroxide in the formulation, the more efficient the grafting and the less free MAH monomers are present in the film. As a matter of fact, non grafted MAH species can also be a factor for adhesion weakness since they may react with the amine end groups in the place of the grafted ones. This explanation is also valid for the influence of MAH addition in the copolymer RB501BF on the joint adhesion performance of moulded samples (Fig. 4.3.10). In this case, one can observe a decrease of the fracture toughness. Considering that the peroxide amount increases simultanously, the diminution of the PP-g-MAH molecular weight may also be a cause for this result.
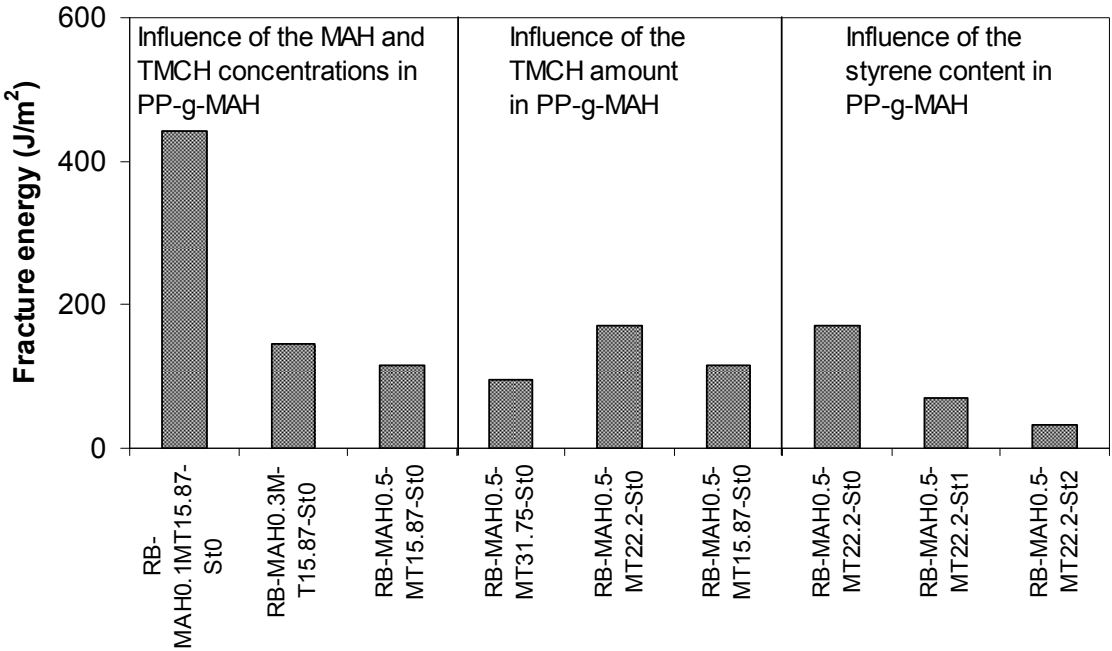
Fig. 4.3.10: Influence of the MAH, TMCH and styrene initial concentrations on the adhesion energy of grafted copolymer/PA12 bonds pressed in a mould

The variation of the peroxide at a constant MAH concentration shows no determining influence on adhesion. A maximum value is achieved for the laminate PA12/RB-MAH0.5-MT22.2-St0. When styrene is added the fracture energy diminishes. This implies that the presence of styrene, styrene/MAH copolymers branches or other reaction species in the PP-g-MAH inhibits adhesion. The MAH molecules bonded in

these long chain branches may not participate to the adhesion mechanisms because of steric hindrances or slow diffusion processes.

At this stage of the discussion, a question arises: why is the adhesion behaviour of the PA/homopolymer and PA/copolymer bonds so different with regards to the influence of the grafting formulation? Answering this question implies comparing the two types of PA/grafted PP bonds. This would not be correct, since neither the molecular weight of the polypropylenes nor the PP-g-MAH recipes are identical. However, a comparison of the fracture toughness of PA/copolymer and PA/homopolymer laminates, with PP-g-MAH having the same functionalization formulations, shows that the PA/homopolymer bonds demonstrate a better interface resistance (Fig. 4.3.11). For increasing contents of MAH, peroxide (DHBP) and styrene in the PP-g-MAH recipe, as already mentioned, the joint fracture energy diminishes slightly for the PA/copolymer and drastically for the PA/homopolymer. It seems that the high molecular weights of the grafted homopolymers favour a good interfacial toughness. Effectively, if one compares the zero viscosities of the samples PP-g-MAH, they are higher for the grafted homopolymers than for the copolymers (see section 3.2.2.1).
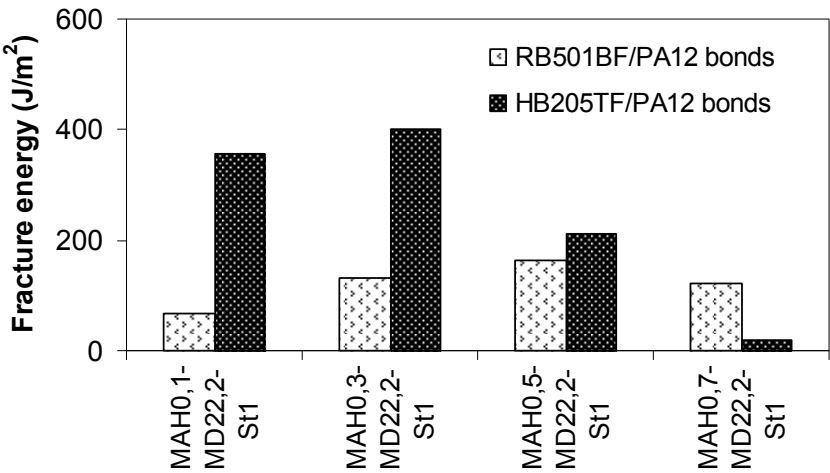
Fig. 4.3.11: Comparison of the adhesion energies of bonded PA12/grafted homopolymer and PA12/grafted copolymer films using the same PP-g-MAH formulations and pressed in a mould

The results of the Teflon pressed PA/homopolymer bonds are presented in Fig. 4.3.12. It can be seen that addition of MAH and peroxide (DHBP) without the presence of styrene promotes the bond adhesion of Teflon pressed PA/homopolymer joints. Logically, the more functional groups grafted on the PP, the more chemical

links are created and the higher the surface density of copolymer at the interface. The slight decrease of the viscosity observed for these high molecular weight PP-g-MAH samples (see section 3.2.2.1) is also favourable to a better interdiffusion of the polymers chains during bond formation. In the same way, when the MAH concentration alone is raised, the DHBP content being kept constant, the bond fracture energy increases. The simultaneous rise of MAH, DHBP and styrene concentrations leads successively to an augmentation of the fracture energy up to 1908.4 J/m^2 for a PP-g-MAH sample with MAH= 0.5 phr and to a drastic diminution down to 92.45 J/m^2 for a sample with MAH= 0.7 phr. Addition of styrene leads to a neat amelioration of the bond adhesion without any saturation such as in the case of the moulded samples. The results of the peroxide influence on the fracture energy are similar to those of the moulded samples – that is the promotion of adhesion.

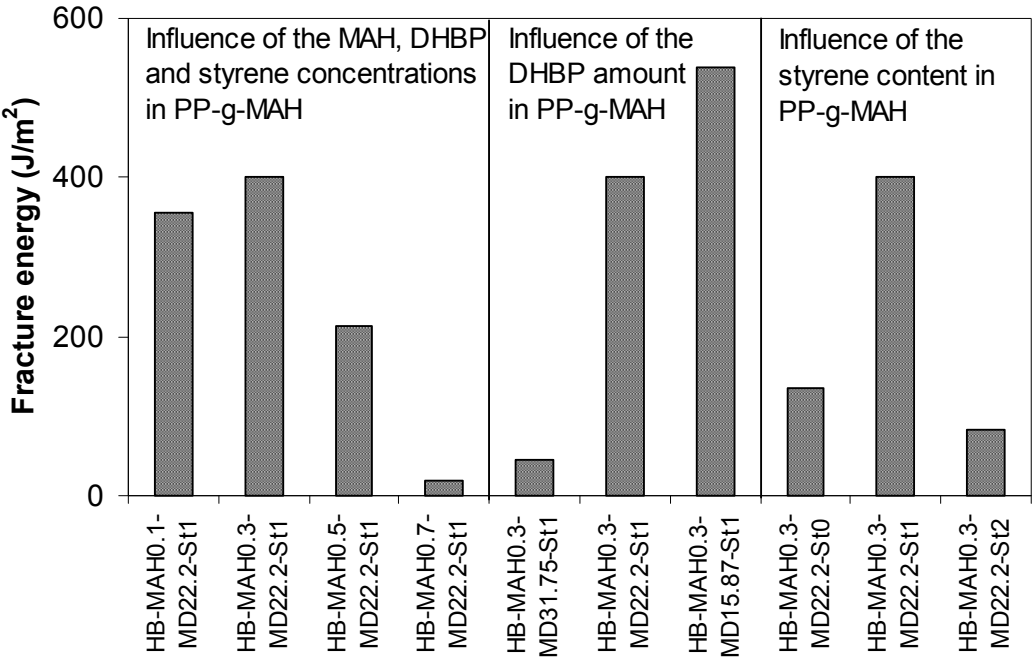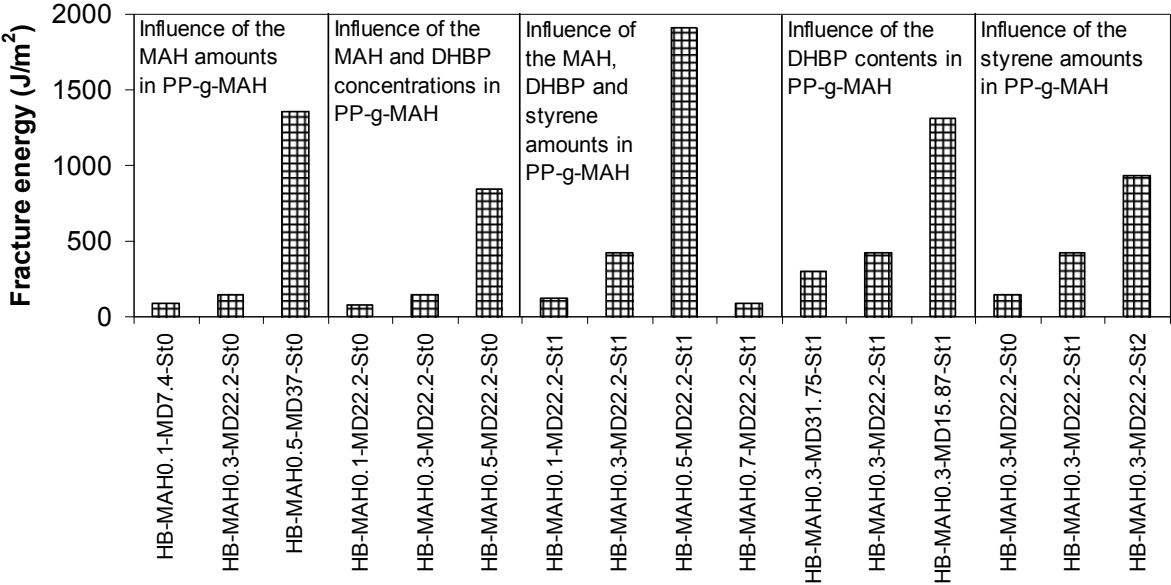**Fig. 4.3.12:** Influence of the MAH, DHBP and styrene initial concentrations on the adhesion energy of grafted homopolymer/PA12 bonds pressed between Teflon sheets

The results of the two preparation methods exhibit some differences. The heat exchanges during the heating and cooling processes are faster within the thin Teflon sheets than within the metallic mould. Hence, the energy needed to give mobility to the polymer chains and activate the interdiffusion processes at the interface is rapidly reached. As a consequence, the fracture energies are much higher for Teflon pressed samples, although the time imparted to the press phase is shorter for this method than for the moulding one. Besides, the cooling rate is increased, leading to

changes in the crystallisation behaviour in the immediate vicinity of the interface, and this in turn has an influence on the adhesion performance.

b) PP/PP-g-MAH-blends/PA bonds

Another option for the adhesion promotion of PP and PA joints is the addition of small amount of PP-g-MAH as compatibilizer in the PP matrix. The PP-g-MAH is able to diffuse to the interface and react with the polyamide. The reaction product at the interface is a copolymer which amount is influenced by the reaction rate between the species as well as the diffusion kinetics of the polymers. Studies demonstrated that its formation is rather controlled by the rate of diffusion of the PP-g-MAH in the PP bulk [Bou96]. An additional important factor for the grafted polymer and the pure resin is its miscibility with the PP matrix in order to avoid phase separation during crystallisation. The PP-g-MAH chains should also be long enough to create entanglements on both sides of the PP/PA joint interface and prevent failure by chain pull out. The mechanism of fracture is not well understood for assemblies of crystalline polymers whereas it has been studied in details for amorphous polymers [Cre01]. For the latter, it was found to depend strongly on the molecular weights of the copolymer blocks added to one of the polymers and on the area density of chains at the interface. In the case of PP/PA6 crystalline assemblies, for a specific molecular weight of the PP-g-MAH, it was shown that the results were similar to those obtained for glassy polymers in which several deformation regimes could occur in the fracture of the interface.

In Fig. 4.3.13 and 4.3.14, the results of the T-peel tests are presented for Teflon pressed bonds of PP/PP-g-MAH blends and PA12 films. The formulations of the PP/PP-g-MAH blends were prepared in the same way for the homopolymer HB205TF and copolymer RB501BF. At a constant MAH concentration of 1 phr, the amount of peroxide was varied in the PP-g-MAH concentrates with MAH/DHBP ratios of 5.5, 11.1 and 15.87. Addition of DHBP in the concentrate formulation leads to a diminution of the molecular weight or viscosity of the PP-g-MAH due to the increase effect of the β-scission reaction (see section 3.2.2.1). On the one hand, 5 wt% of the compatibilizer with different MAH/DHBP ratios were blended with the pure resin. On the other hand, for the formulation PP-MAH1-MD11.1-St0, the quantity of concentrate was increased from 1 to 10 wt.%.
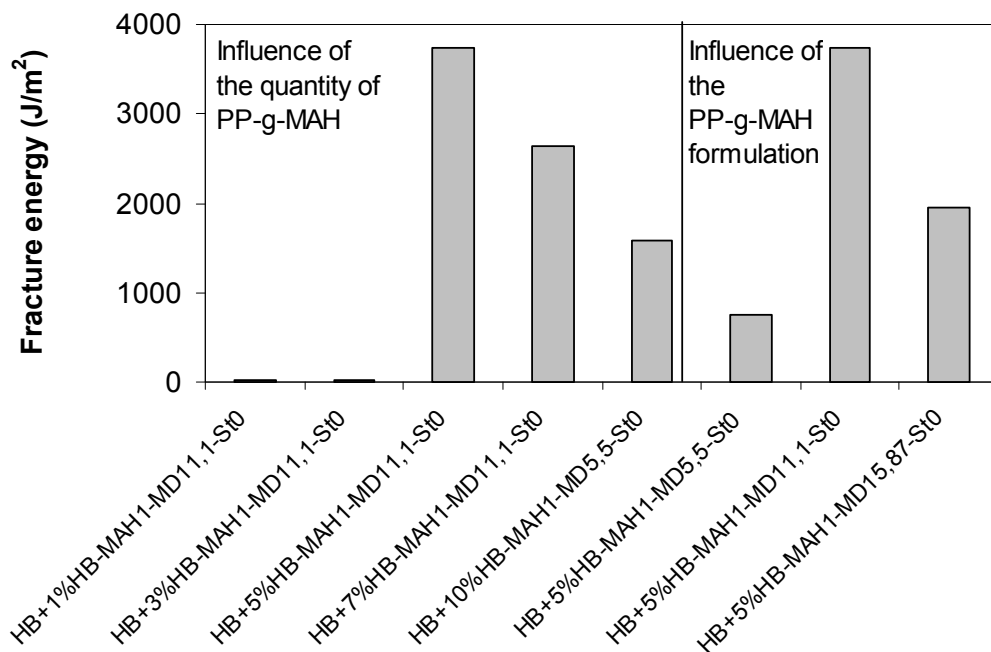
Fig. 4.3.13: Influence of the quantity of homopolymer concentrates on the adhesion energy of bonded films of PP/PP-g-MAH blends and PA12 pressed between Teflon sheets

The analysis of the adhesion tests reveals that increasing the amount of the compatibilizer up to 5 wt.% leads to adhesion enhancement of the bonds for the PA/copolymer as well as the PA/homopolymer bonds. More than 5 wt.% concentrate in the PP blend seems to saturate the joint interface and even have a detrimental influence on the bond strength. The diminution of joint strength can be related to the weakening the cohesive strength of the PP matrix. The competition between the diffusion rate and the reaction rate may also be taken as an explanation of this phenomenon. When the quantity of reactive groups is high, the reaction rate is much faster than the diffusion rate so that many reactive sites on a PP-g-MAH chain can be grafted to the interface. Such molecular structures do not generally allow good entanglements with the matrix and the interface is mechanically weak [Lee94,Lee98].
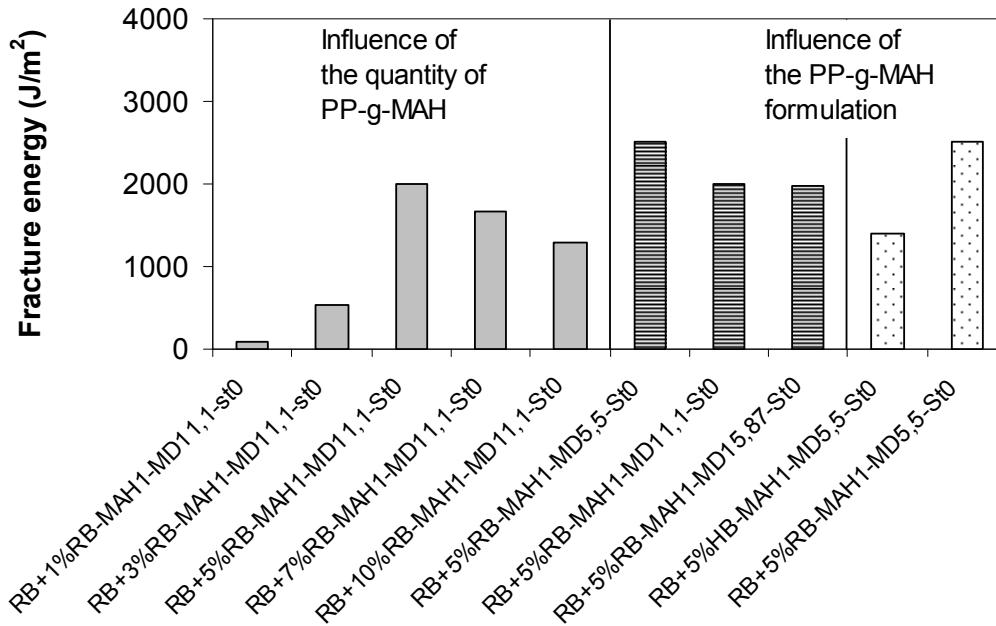
Fig. 4.3.14: Influence of the quantity of copolymer concentrates on the adhesion energy of bonded films of PP/PP-g-MAH blends and PA12 pressed between Teflon sheets

The comparison of the fracture energies of the PA/copolymer bonds shows that with a growing MAH/DHBP ratio (or diminishing DHBP concentration) in the PP-g-MAH formulation, adhesion decreases (Fig. 4.3.14). A PP-g-MAH having a high MAH/DHBP ratio possesses a higher molecular weight than a PP with a low MAH/DHBP ratio. Hence, the mobility of its chains as well as their diffusion to the interface will be less efficient. For the PA/homopolymer bonds, a maximum fracture energy value (3727.5 J/m^2) is found for laminates made of PA12 and HB+5%HB-MAH1-MD11.1-St0 (Fig. 4.3.13). The adhesion performance seems also to be controlled by the molecular weight. Too short PP-g-MAH chains may not be able to create entanglements on both sides of the interface. Too long chains may not be able to diffuse fast enough and the in situ copolymer formed at the interface is not sufficient to achieve a reinforcement effect. When the amount of a given concentrate formulation (PP-MAH1-MD11.1-St0) is raised, the fracture energy increases. Above a PP-g-MAH concentration of 5 wt.% in the PP blend, the joint strength for both PA/copolymer and PA/homopolymer laminates decreases. Furthermore, a comparison of the PA/copolymer and PA/homopolymer bonds reveals that the highest adhesion strengths are obtained for the PA/homopolymer laminates. The zero shear viscosities of both PP-g-MAH materials are quite close (η_0= 207 Pa.s for HB-MAH1-MD11.1-St0 and η_0= 162 Pa.s for the corresponding copolymer). Only

those of the related blends present significant differences, depending on the viscosities of the pure resins. For instance, the zero shear viscosity of the blend RB+5%RB-MAH1-MD11.1-St0 is about 4881.5 Pa.s whereas it reaches 10168.2 Pa.s for HB+5%HB-MAH1-MD11.1-St0. Thus, one can argue that the molecular weight and structure of the polypropylenes is responsible for these differences. The presence of ethylene sequences in the copolymer may also be a factor limiting diffusion of the PP-g-MAH in the matrix. This result is however in accordance with the one found for the bulk grafted PP/PA bonds. No improvement in adhesion was achieved by blending the copolymer with 5 wt.% of HB-MAH1-MD5.5-St0 as shown in Fig. 4.3.14. In that case, a phase separation between the types of PP during crystallisation can be awaited.

c) PP-g-GMA/PA bonds

Grafting of the monomer GMA on the PP backbone was taken as an alternative option to the MAH system [Nzu03]. This study was conducted using the polypropylene types RD208Cf and HD601CF. The PP-g-GMA and PA6-6,6 films were fusion bonded in a mould under different conditions and the formulations of the PP-g-GMA were varied. The bond strengths of the PP-g-GMA/PA6-6,6 laminates were tested under the conditions described in Tab. 4.3.1.

It can be seen in Fig. 4.3.15a that the fracture energy increases with raising temperature. As it was already observed for the PA/PP-g-MAH joints, if the press temperature is above the melt temperature of the sample RD-GMA5-MD11.1-St1 (139.6°C) and under the melt temperature of the PA6-6,6 (196°C), the fracture energy remains low at about 18.1 J/m^2. A temperature increase of 40°C causes a fracture energy increase of about 5 times (up to 88 J/m^2). Through the energy input, the reactions at the interface are intensified and the amount of copolymer contributes stronger to the interface reinforcement. As shown in Fig. 4.3.15b a longer press time has also a positive influence on the adhesion performance. As a matter of fact a greater amount of grafted GMA can diffuse to the interface, the reaction time between the species is longer and the copolymer density higher. With increasing pressure, however, the fracture energy varies only slightly (Fig. 4.3.15a). This can be explained by the fact that, under higher pressure, the relative low viscous PP-g-GMA flowed out of the mould, decreasing the thickness of the bonded films.

(a)

(b)
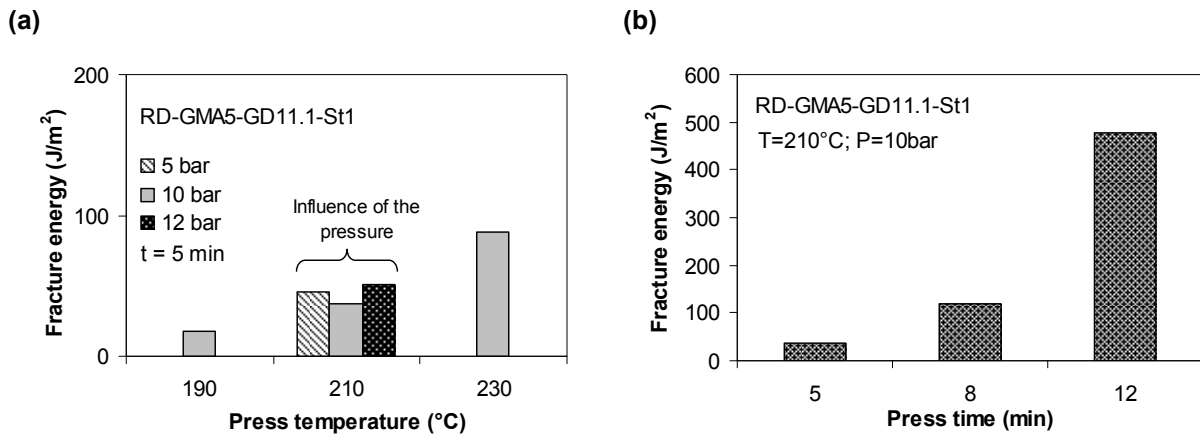
Fig. 4.3.15: Influence of the press parameters temperature, pressure and time on the adhesion energy of PA6-6,6/PP-g-GMA bonds pressed in a mould

The PP-g-GMA formulation was varied and, with the increasing GMA amount from 3 to 5 phr (GMA/DHBP= 11.1; St/GMA= 1), the bond fracture energy diminishes from 140 to 77.3 J/m^2. A GMA concentration of 1 phr in the grafted copolymer seems to be too low to achieve any adhesion reinforcement of the interface. This result is similar to the one obtained for the PA/PP-g-MAH bonds. The saturation of the interface by the grafting by-products (ungrafted GMA molecules, polyglycidylmethacrylat, polystyrene, polyglycidylmethacrylat-co-styrene, crosslinked sequences...), the lowering of the PP-g-GMA molecular weight with increasing peroxide in the formulation and the corresponding weakening of the film tensile strength may be responsible for the adhesion diminution. Considering the PA/homopolymer bonds, the brittleness of the grafted PP did not allow T-peel measurements for samples with more than 3 phr GMA in the formulation. The adhesion level is lower for the PA/homopolymer laminate than for the PA/copolymer one because of the marked molecular weight reduction of the grafted homopolymer.
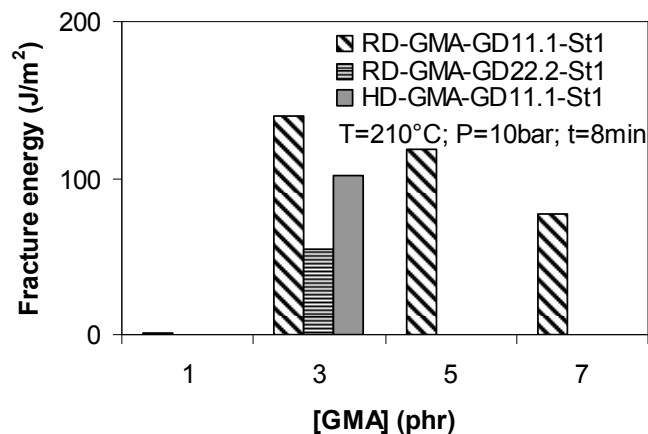
Fig. 4.3.16: Influence of the GMA and DHBP initial concentrations on the adhesion energy of PP-g-GMA/PA6-6,6 bonds pressed in a mould

In Fig. 4.3.17 and 4.3.18, it can be seen that increasing the GMA/styrene molar ratio from 0 to 1.5 in the PP-g-GMA formulation has a positive influence on the joint adhesion of the PA/copolymer as well as PA/homopolymer bonds. This can be related, once again, to the molecular weight which is less reduced during functionalization in presence of styrene. In this case, the PP-g-GMA chains are long enough to play the role of tie molecules at the interface. Besides, the mechanical properties are positively influenced so that during fracture the stress can be transferred over a greater distance and the deformation is higher. However, this result seems in contradiction to the contact angle measurements which indicate an increase of the contact angle with addition of styrene, implying a less good wetting of the film.
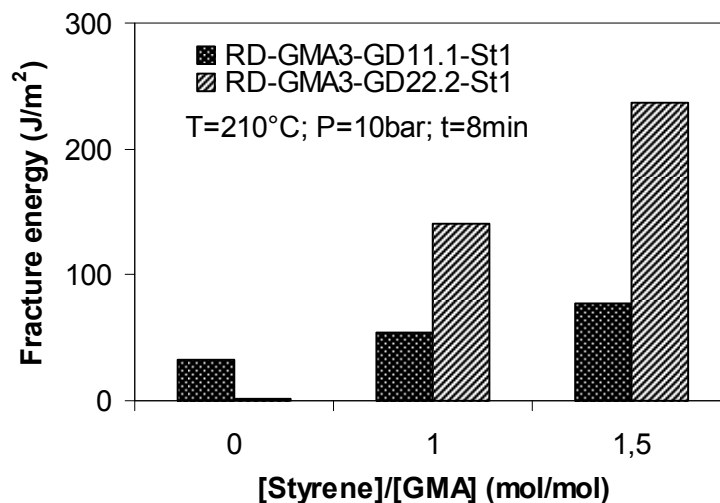
Fig. 4.3.17: Influence of the styrene and DHBP initial concentrations on the adhesion energy of grafted copolymer/PA6-6,6 bonds pressed in a mould
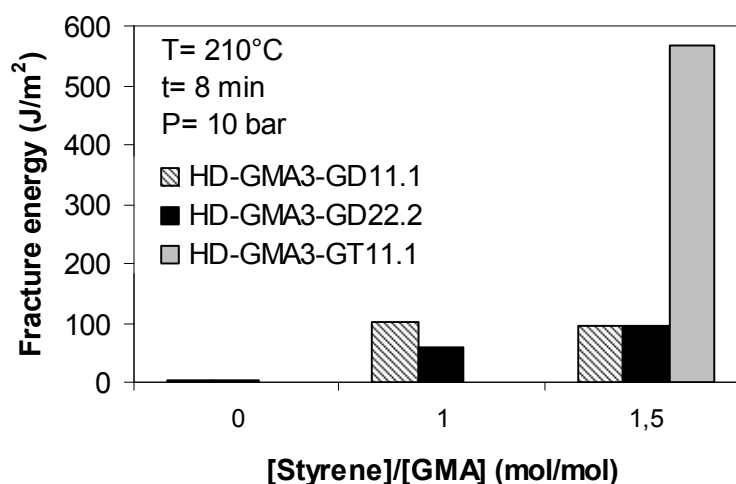
Fig. 4.3.18: Influence of the GMA, DHBP initial concentrations and peroxide type on the adhesion energy of grafted homopolymer/PA6-6,6 bonds pressed in a mould

The diminution of the peroxide amount in the PP-g-GMA formulation decreases the fracture energy of the bonds in both cases (Fig. 4.3.17 and 4.3.18), and this phenomenon is more pronounced for the PA/copolymer laminates (Fig. 4.3.17). However, one would have awaited an increase of the adhesion properties in accordance with the molecular weight theory. The fracture energy diminishes from 101.3 J/m^2 for the sample PA6-6,6/RD-GMA3-MD11.1-St1 to 54.7 J/m^2 for the sample RD-GMA3-MD22.2-St1. Obviously, another factor plays a predominant role. Considering that the grafting of GMA is less efficient with a low concentration of peroxide, it is possible that the free bulky GMA molecules in the films become disturbing for the interfacial adhesion (reaction between free GMA and the PA). Simultaneously, there might be a lower quantity of grafted GMA molecules available for the chemical reactions at the interface.

The differences between the fracture energies in function of the formulation are less pronounced for the PA/homopolymer than for the PA/copolymer bonds. However, a fusion bonding trial with the sample HD-GMA3-GT11.1-St1.5 led to a fracture energy of 568 J/m^2 (Fig. 4.3.18). The use of TMCH as peroxide in the PP-g-GMA formulation in combination with a high amount of styrene conducted to this enhanced adhesion result.

4.3.2.2 Chemical characterization and film surface analysis

The possible reactions at the PP-g-MAH/PA and PP-g-GMA/PA interfaces are described in Fig. 4.3.19 and 4.3.20. The coupling reactions are supposed to be predominantly realized over end functional groups. As a matter of fact, they appeared to be faster than with mid functional groups because of the steric hindrance by the polymer chain shielding the functional groups [Jeo04].

Considering the reaction between PA and PP-g-GMA, the chemical reactions, and therefore the formation of an in situ copolymer, take place between the GMA epoxy groups and the PA amine as well as carboxyl end groups.

As for the PP-g-MAH and polyamide, it is known that PA possesses two functional groups (amines and amides) which may react with the anhydride groups of MAH, leading to many possible coupling reactions [Dui97]. At temperatures superior to 200°C, the amine groups may react with anhydrides by forming imide groups, followed by amidation-hydrolysis. PA chain scission occurs and new amine and carboxylic acid end groups are formed. In that way, the amide groups do not react directly with the

anhydrides but via amine end groups. It was found that the main reaction, which is also the faster (see Tab. 4.3.3), is the one involving the anhydride groups and the amine end groups [Ro97/1,Xan92,Moa99].

Components		Temperature of the melt (°C)	Kinetic constant k (kg/mol.s)	Half-life time $T_{1/2}$
(2-decene-1-yl)-succinic anhydride	dodecylamine	170	k_1 (instantaneous reaction)	—
		170	$k_2 = 2.10^{-3}$	~ 8.3 min
	n-dodecyl octadecanamide	160	$k_3 = 4.4.10^{-7}$	~ 630 h
		160	$k_4 \sim k_3$	—

Tab. 4.3.3: Kinetics constants and half-life times for amine/anhydride and amide/anydride model systems [Ro97/1]

Experiments were conducted by reacting terminally functional small molecules of polystyrene and poly(methyl methacrylate) at 180°C [Orr01]. They showed that the conversion data at 2 min of the functional pairs were ordered as follows: aliphatic amine/anhydride (99%) > acid/epoxy (9%) > aliphatic amine/epoxy (1.8%) > hydroxyl/(anhydride or acid) (0%) > acid/amine (0%). By comparing the conversions at 170 and 160°C, it is evident that the imide formation (k_2) is predominant in comparison to the other reactions.

Reaction of amino end groups with the anhydride groups
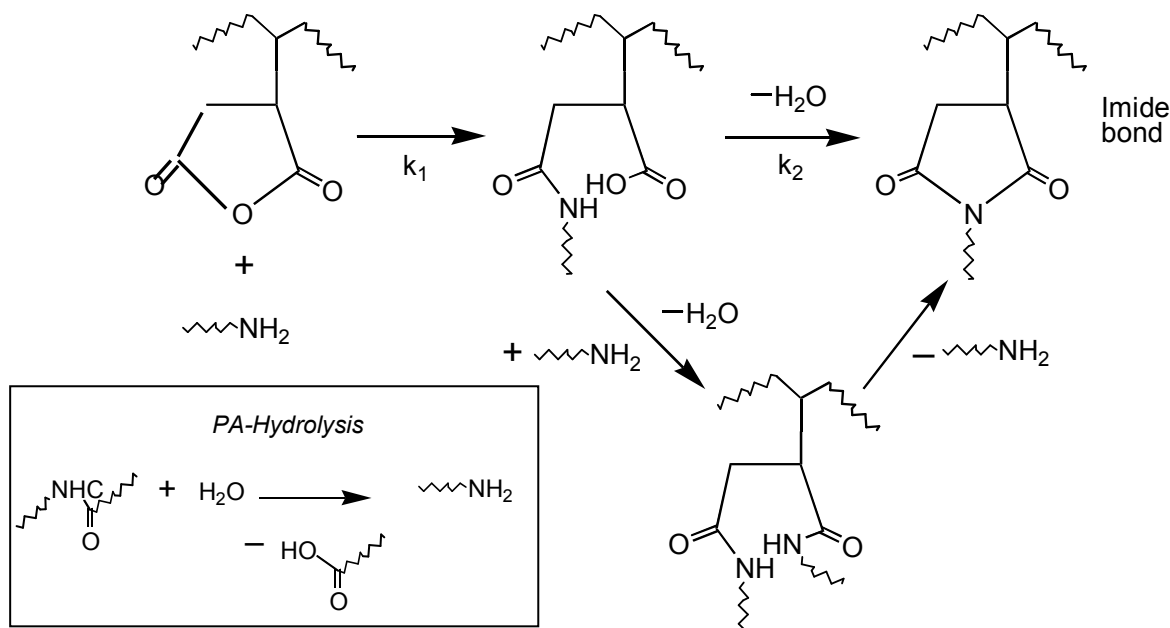
Reaction of in-chain amide with the anhydride groups
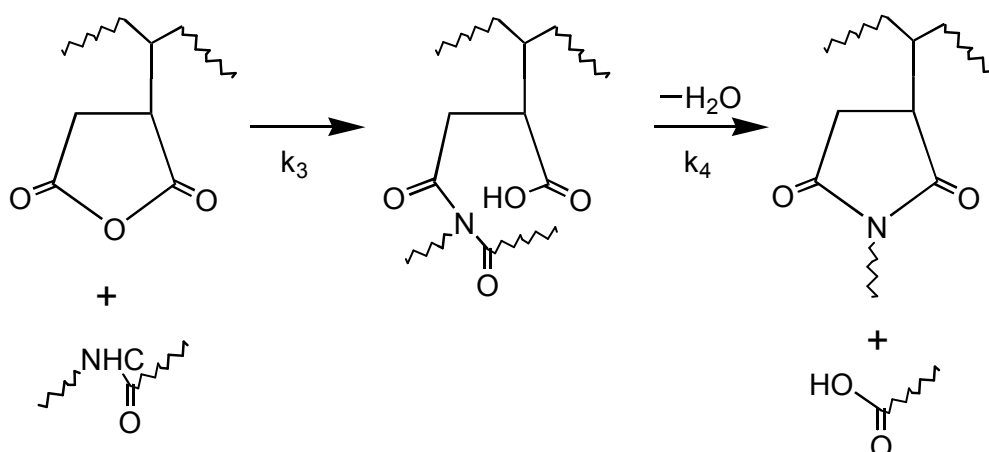
Fig. 4.3.19: Chemical reactions between the PP-g-MAH and the PA6
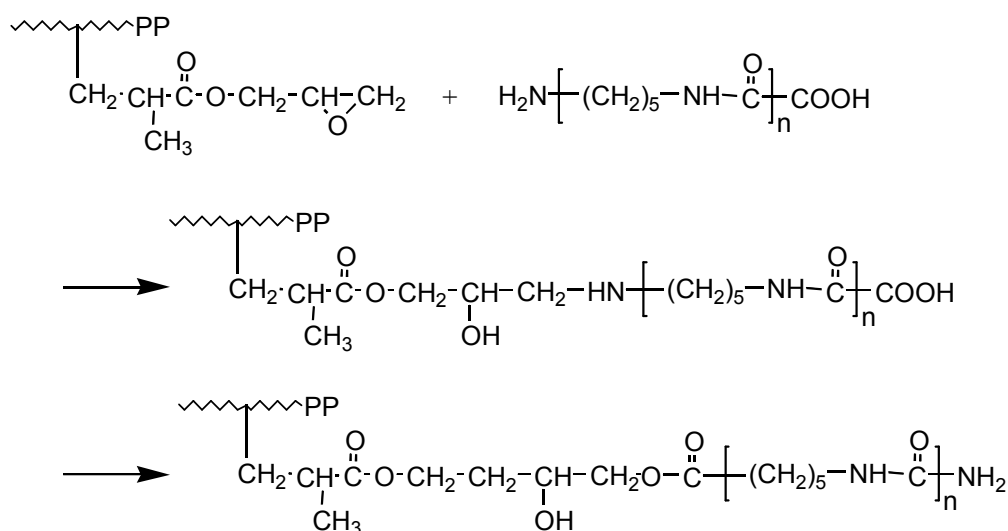
Fig. 4.3.20: Chemical reactions between PP-g-GMA and PA6

The quantity of copolymer formed between the anhydride and the amine groups at the interface will depend on the reactive groups' number of each species. The detection of this reaction can be realized by infrared spectroscopy or, among others, forward recoil spectroscopy, size exclusion chromatography, X-ray spectroscopy to determine the area density of chains crossing the interface [Schz01,Bou96].

Another more common test which is used for the qualitative reaction detection in polymer blends is the Molau test [Mol70]. In this method, the sample to be investigated is immersed in a formic acid solution in order to dissolve the PA. If the solution remains clear, it means that there is no block copolymer formed between the reactive groups. A stable, white, colloidal solution, on the other side, confirms the presence of

an insoluble reaction product in the sample (PA-g-PP). For that purpose, the laminate RD-MAH0.7-MD22.2-St1/PA6-6,6 which shows a high peel energy (no delamination of the films) as well as blends of PP-g-MAH and PA6-6,6 (20/80, 30/80, 40/60, 50/50, 80/20 weight percents) were put in a formic acid bath. As it can be seen from the milky colour of the solution on Fig. 4.3.21, the Molau test is positive only for the 20/80 and 30/70 PP-g-MAH/PA-blends. To form enough copolymer to be detected by this method the amine end groups must be quantitatively sufficient, that is by adding an excess of PA in the blend. According to this result, the detectable quantity of copolymer formed between the reactive species is too low for the 50/50, 80/20 PP-g-MAH/PA-blends as well as for the laminate. In the latter, only a few NH_2 groups react at the interface with the PP-g-MAH. Thus, it is interesting to consider the anhydride/amine molar ratio by the reaction analysis. If it is below 1.0, the reaction between the PP-g-MAH and the PA will occur via the amine end groups and generate quickly the in situ copolymer. If it is higher than 1.0, chemical reactions involving amide groups may occur (slower process) and may also result in reactions such as PA chain scission [Dui97].
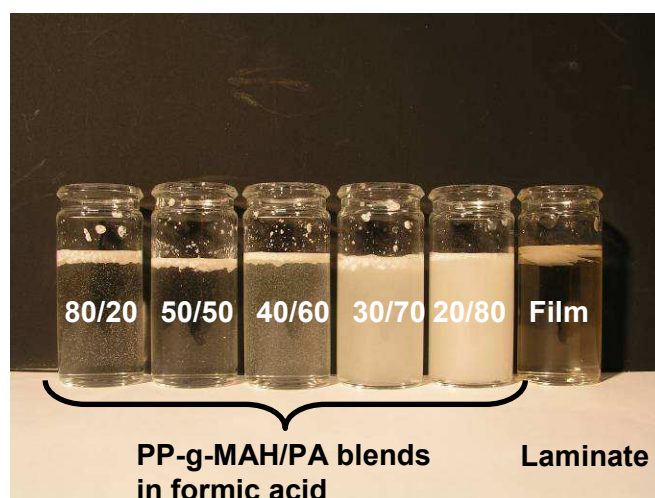
Fig. 4.3.21: Result of the Molau test for a PP-g-MAH/PA6-6,6 laminate and different PP-g-MAH/PA6-6,6 blends (20/80, 30/70, 40/60, 50/50, 80/20)

The trend of the Molau test results is confirmed for the concentrate RB-MAH1-MD5.5-St0 as well (Tab. 4.3.4). This is only valid for the blends containing PA6-6,6 and PA6. PA12 probably possesses in comparision to PA6-6,6 and PA6 less NH_2 end-groups which can react with the MAH.

Functionalized PP	PA type	PP/PA	Molau-Test
RB-MAH1-MD5.5-St0	PA6-6,6	80/20	Negative
		50/50	Negative
		20/80	*Positive*
RB-MAH1-MD5.5-St0	PA6	80/20	Negative
		50/50	Negative
		20/80	*Positive*
RB-MAH1-MD5.5-St0	PA12	80/20	Negative
		50/50	Negative
		20/80	Negative

Tab. 4.3.4: Results of the Molau test for blends of a PP-g-MAH concentrate and different PA types

In order to demonstrate the reaction between the PP-g-MAH and PA, films of PA6-6,6 and RD-MAH0.7-MD22.2-St1 were bonded under different press temperatures (210°C and 230°C) and times (0, 5, 8, 12, 30, 60, 180, 300 min). The laminates were immersed in a solution of formic acid (3 baths) in order to dissolve the PA. The observation of the carbonyl band at 1782 cm^{-1} revealed a diminution of its intensity with increasing press time (Fig. 4.3.22). This implied a growing conversion of the grafted MAH to copolymer at the interface. An elevation of the temperature also increased the reaction conversion at the interface.
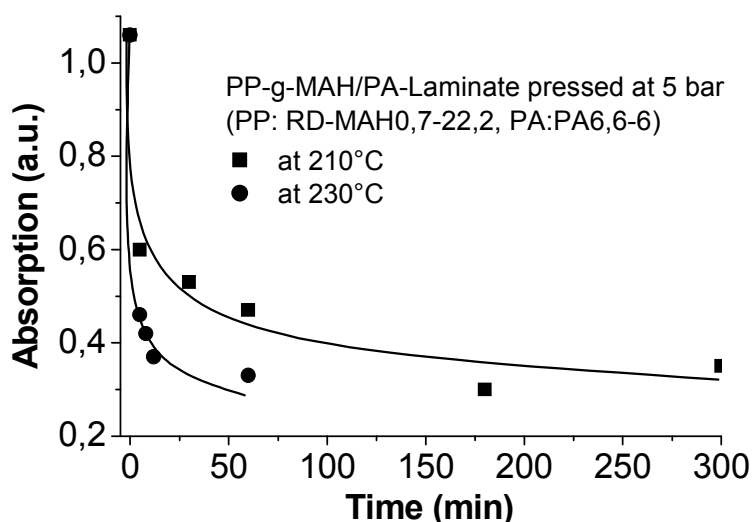
Fig. 4.3.22: Evolution of the MAH conversion as a function of the press time and temperature

Moreover, the analysis of a peeled RD-MAH0.7-MD22.2-St1/PA6-6,6 joint using infrared spectroscopy in reflection (ATR unit) and presented in Fig. 4.3.23 confirmed

the presence at 1700 cm^{-1} of imide bonds on the PP film surface [Rst04]. The IR analysis in transmission of this film and a virgin PP-g-MAH sample also showed a diminution of the peak intensity at 1782 cm^{-1} (Fig. 4.3.24).
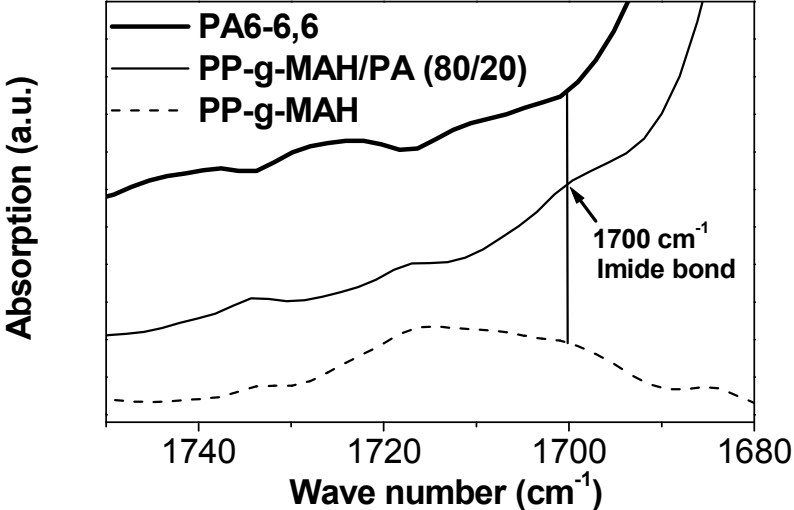
Fig. 4.3.23: IR spectra in reflection of a peeled PP-g-MAH film, a PP-g-MAH/PA6-6,6 blend (80/20) and a PA6-6,6 film
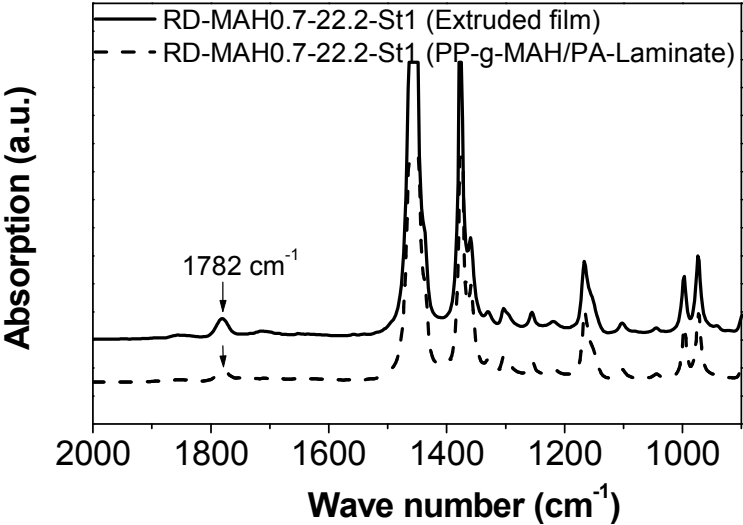
Fig. 4.3.24: IR spectra in transmission of a peeled PP-g-MAH film

The surface of peeled PP-g-MAH samples (RD-MAH0.7-MD11.1-St1) were observed under Scanning Electron Microscopy (Fig. 4.3.25) and showed that with decreasing MAH-concentration – that is an increasing peel strength – the surface became rougher [Rst03]. These fibrillar structures on the surface were due to the crack development within the interface or on the surface during the peel test. The SEM

images of a PP-g-MAH/PA laminate cross-section allow distinguishing the two materials but conclusion could be made considering the adhesion performance between the films, even for magnifications greater than 1000.

PP surfaces of peeled PP-g-MAH/PA laminates   **Cross-section of a laminate**
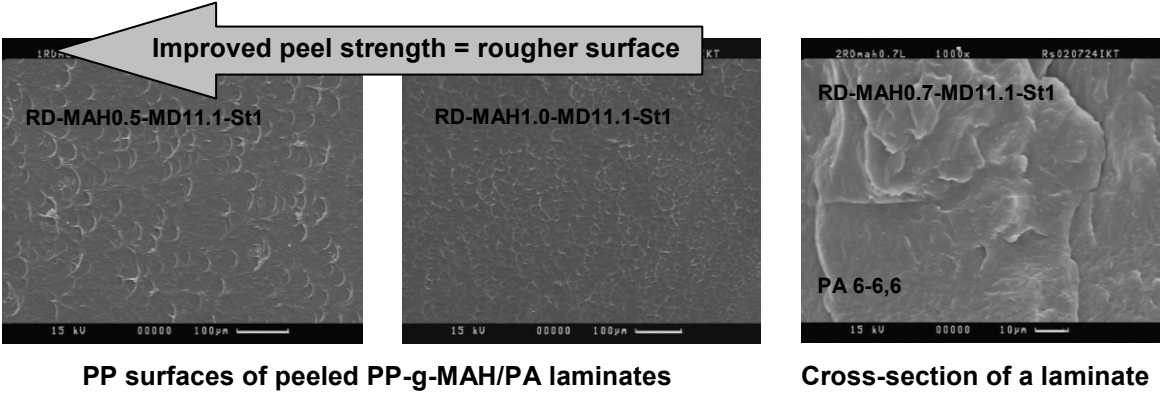
Fig. 4.3.25: SEM pictures of PP-g-MAH peeled surfaces and
PP-g-MAH/PA laminate cross-section

4.4 Coextrusion of three-layer PP/PA/PP films

4.4.1 Process description

Film blowing is an important processing technique broadly used to produce plastic films. The molten polymer is extruded at a constant flow rate through an annular die. Air enters through the die to fill the extruded tube and inflate a bubble to a controlled size. The larger the diameter of the bubble to the diameter of the die (called blow-up ratio), the thinner the film becomes. An air ring situated above the die initiate the cooling process of the polymer film. This crystallisation start can be visualized by the frost line height, change from a transparent to a translucent film appearance. The take-off system (tower) which collapses the bubble after an adequate cooling time is composed of a collapsing frame and water cooled nip rolls that stretch the film with a constant speed. The faster the nip rolls − the higher the take-off speed − is, the thinner the film.

Coextrusion allows the fabrication in one step of polymer multilayer films. For that purpose, special tubular blown film dies are used such as stakable plate dies. In this type of dies, the number of layers can be adjusted by changing the number of plates. They are designed to achieve a uniform concentric flow which controls the thickness and regularity of the layers. The polymers extruded on coextrusion lines are generally non-newtonian fluids and possess high viscosities. Hence, the resulting Reynolds-numbers are inferior to 1 and the steady flows developed in the dies are laminar. In this way, a mixing of the different layers is avoided.

For our experiments, a Dr. Collin film blowing line was adapted for the coextrusion of three-layer films. The trials were carried out using three single screw extruders with the following specifications:

- Inner layer (PP random copolymer): diameter D = 30mm, length/diameter L/D = 25 from the company Dr. Collin,
- Middle layer (Polyamide): D = 30 mm, L/D = 25 from the company Extrudex,
- Outer layer (PP homopolymer): D = 20 mm, L/D = 25, constructed at IKT.

Fig. 4.4.1 presents a description of the coextrusion line.

A coextrusion stacked-type spiral die (diameter D = 60 mm and gap exit S = 0.8 mm) from the Dr.Collin company, named version A, was used. It was designed with

thermal isolation plates between the spiral distributor plates in order to be able to run materials at different process temperatures. A first elaboration of coextruded films (series 1) revealed the need to increase material residence time and pressure build-up after convergence of the material flows in the die to obtain satisfactory results in terms of polymer adhesion. A second die, constructed at the IKT [Cre03] (diameter D = 50 mm and gap S = 0.9 mm) and named version B, was adapted to achieve these requirements. The material residence time and pressure build-up was realized using a modified die exit system as shown in Fig. 4.4.2 (b).
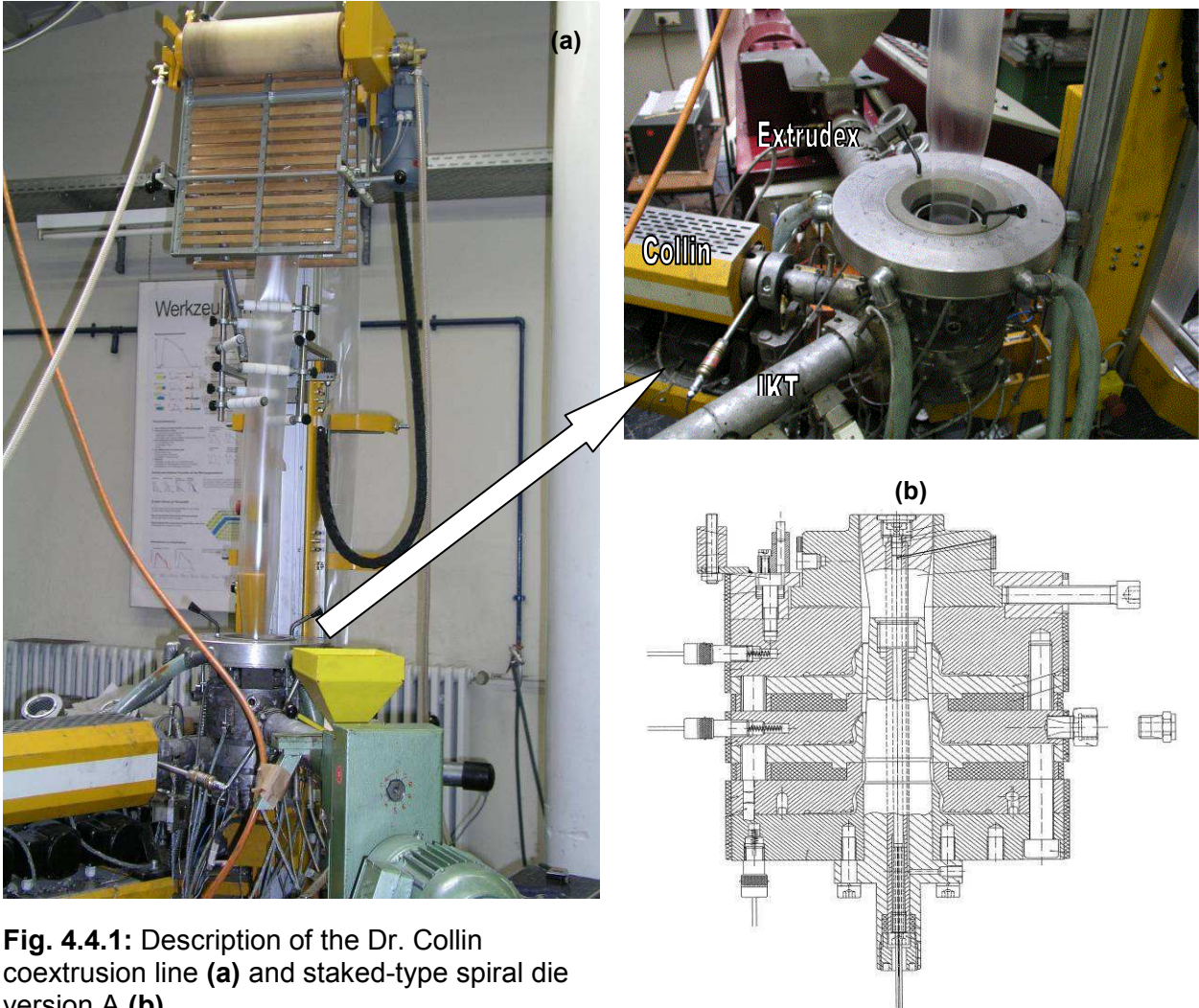
Fig. 4.4.1: Description of the Dr. Collin coextrusion line **(a)** and staked-type spiral die version A **(b)**

Conventional die exit (a) **Modified die exit (b)**
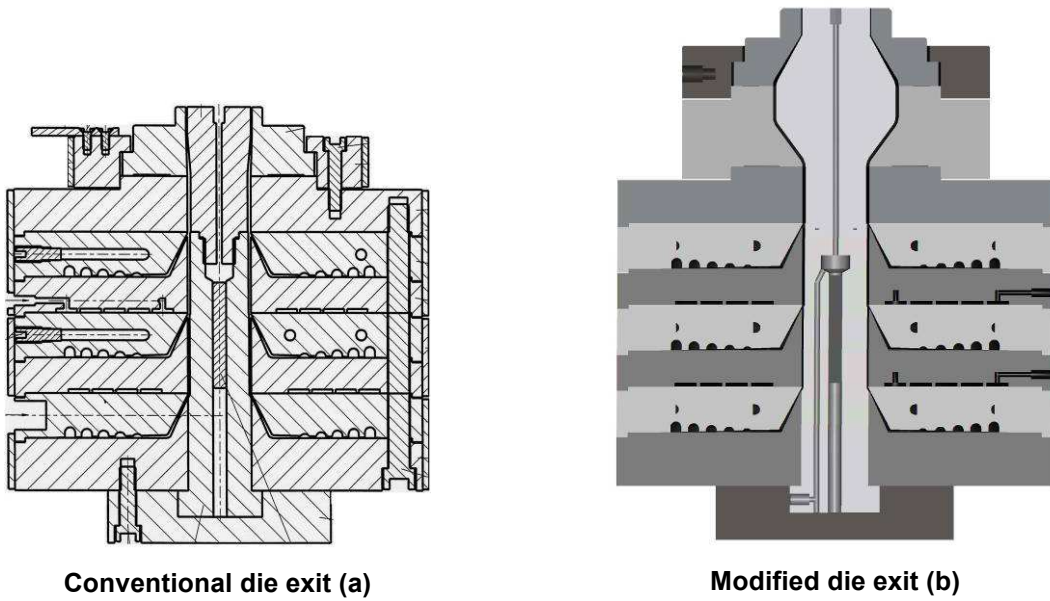
Fig. 4.4.2: Description of the staked-type spiral coextrusion die version B

Simulation trials realized with the program Simflow®, a software package developed at the IKT, demonstrated that the residence time was extended from 37s with the conventional die exit to 60s with the modified one.

The coextrusion experiments were run at total flow rates of 4 kg/h with the die version B and 6 kg/h for the die version A, the central extruder being the one producing half of the total output. Fig. 4.4.3 presents an example of calibration curve (flow rate versus screw speed) for the die version B. The extrusion temperature was kept at 230°C for all runs. One can notice that the outer extruder possesses a limited output and must be run at a maximum speed of about 50 rpm. The inner and middle extruder, on the other side, must be run at very slow screw speeds.
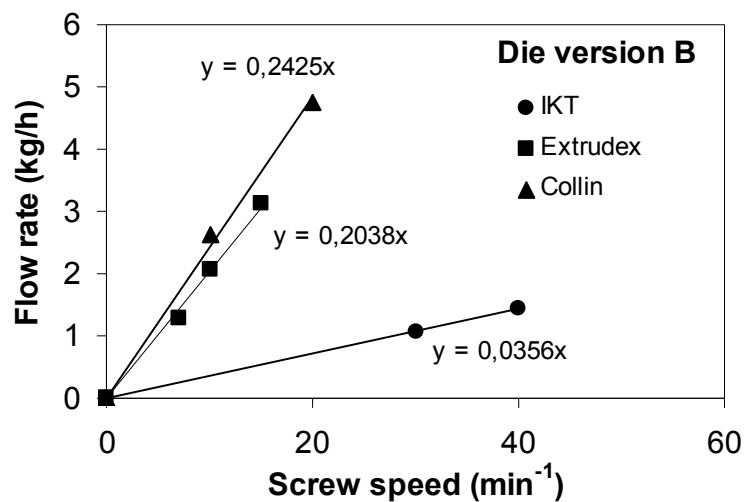
Fig. 4.4.3: Calibration curves of the extruders and the die version B

Materials and process parameters such as the temperature or take-off speed were varied and the mechanical as well as the adhesion properties were subsequently determined.

4.4.2 Materials used for the coextrusion trials

The materials tested for the production of three-layer films are presented in Tab. 4.4.1. The modified PP type RB601BF was used as inner layer and the functionalized HB205TF as outer layer for all experiments. PA6-6,6, PA6 and PA12 were employed as central layer polymers. The commercial PP-g-MAH Bynel was taken for the outer and inner layers as reference because a high adhesion level between the layers was obtained with this material. However, the melt temperature of 140°C was too low for the outer layer and the film lacked of transparency.

First trials using PP-g-MAH were conducted with the die version A in order to observe the materials' behaviour during film blowing and to test adhesion of the multilayers. A qualitative adhesion test of the films (series 1) showed an immediate delamination of the layers. For the second series, elimination of styrene in the grafted copolymers' formulation and diminution of the MAH concentration led to a slight improvement of adhesion. Because no spontaneous delamination was observed for the films of series 3 to 6, quantitative adhesion measurements (T-peel tests) could be performed. These series included coextrudates of PA and PP/PP-g-MAH blends as well as the directly grafted PP. Series 5 and 6 represent multilayers produced with the die version B. The formulations as well as the process parameters are detailed in Appendix 4.

Die version A				
Series	Sample Nr.	Innner layer	Midlayer	Outer layer
1	1	RB-MAH0.7-MD22.2-St1	PA6-6,6	HB-MAH0.7-MD22.2-St1
	2	RB-MAH0.7-MD15.87-St1	"	HB-MAH0.7-MD15.87-St1
	3	RB-MAH1-MD22.2-St1	"	HB-MAH1-MD22.2-St1
2	1	RB-MAH0.1-MT15.87-St0	PA6	HB-MAH0.5-MD15.87-St1
	2	RB-MAH0.1-MT15.87-St0		HB-MAH0.1-MT15.87-St0
	3	RB-MAH0.5-MT15.87-St0		HB-MAH0.5-MT15.87-St0
3	1	RB + 1%RB-MAH1- MD11.1-St0	PA6	HB + 5%HB-MAH1-MD5.5-St0
	2	RB + 3%RB-MAH1- MD11.1-St0	"	HB + 5%HB-MAH1-MD5.5-St0
	3	RB + 3%RB-MAH1- MD11.1-St0	"	HB + 3%HB-MAH1-MD11.1-St0
	4	RB + 3%RB-MAH1- MD11.1-St0	"	HB + 5%HB-MAH1-MD11.1-St0
	5	RB + 5%RB-MAH1- MD11.1-St0	"	HB + 5%HB-MAH1-MD11.1-St0
	6	RB + 5%RB-MAH1- MD11.1-St0	"	HB + 7%HB-MAH1-MD11.1-St0
4	1	Bynel (commercial PP-g-MAH)	PA12	Bynel (commercial PP-g-MAH)
	2	RB + 5%RB-MAH1-MD5.5-St0	"	HB + 5%HB-MAH1-MD5.5-St0
	3	RB + 5%RB-MAH1-MD11.1-St0	"	HB + 5%HB-MAH1-MD11.1-St0
	4	RB + 5%RB-MAH1-MD15.87-St0	"	HB+5%HB-MAH1-MD15.87-St0
	5	RB + 1%RB-MAH1-MD5.5-St0	"	HB + 1%HB-MAH1-MD5.5-St0

	6	RB + 3%RB-MAH1-MD5.5-St0	"	HB + 3%HB-MAH1-MD5.5-St0
	7	RB + 7%RB-MAH1-MD5.5-St0	"	HB + 7%HB-MAH1-MD5.5-St0
	8	RB + 10%RB-MAH1-MD5.5-St0	"	HB + 10%HB-MAH1-MD5.5-St0
Die version B				
5	1	RB-MAH0.1-MT15.87-St0	PA12	HB-MAH0.1-MD22.2-St1
	2	RB-MAH0.1-MT15.87-St0	PA12 / PA6 / PA6-6,6	HB-MAH0.3-MD22.2-St1
	3	RB-MAH0.1-MT15.87-St0	PA12	HB-MAH0.5-MD22.2-St1
	4	RB-MAH0.3-MT15.87-St0	"	HB-MAH0.3-MD22.2-St1
	5	RB-MAH0.5-MT15.87-St0	"	HB-MAH0.3-MD22.2-St1
6	1	RB + 5%RB-MAH1-MD5.5-St0	PA12	HB + 5%HB-MAH1-MD5.5-St0
	2	RB + 5%RB-MAH1-MD11.1-St0	"	HB + 5%HB-MAH1-MD11.1-St0
	3	RB + 5%RB-MAH1-MD15.87-St0	"	HB + 5%HB-MAH1-MD15.87-St0

Tab. 4.4.1: Main materials and configurations of the layers for the coextrusions trials

MVR measurements were performed before coextrusion in order to check the degradation state of the modified polymers because a too low molecular weight grafted PP (MVR > 10 cm^3/10 min) can hardly be blown. Phenomena such as bubble instabilities as well as "fish skin"– slippage of the low viscous polymer on the high viscous one – tend to appear with such materials. Thus, the final properties of the film which also depend on the process conditions can be negatively affected.

Formulations	MVR (cm^3/10 min)	Formulations	MVR (cm^3/10 min)
HB-MAH0.5-MD15.87-St1	2.2	HB-MAH0.1-MD22.2-St1	2.5
HB-MAH0.1-MT15.87-St0	2.4	HB-MAH0.3-MD22.2-St1	3.5
HB-MAH0.5-MT15.87-St0	2.7	HB-MAH0.5-MD22.2-St1	4.1
HB-MAH0.7-MD22.2-St1	4.6	–	–
HB-MAH0.7-MD15.87-St1	5.3	–	–
HB-MAH1-MD22.2-St1	5.6	–	–
RB-MAH0.1-MT15.87-St0	4.7	RB-MAH0.1-MT15.87-St0	5.1
RB-MAH0.5-MT15.87-St0	6.7	RB-MAH0.3-MT15.87-St0	7.0
RB-MAH0.7MD22,2-St1	7.9	RB-MAH0.5-MT15.87-St0	7.7
RB-MAH1-MD22.2-St1	9.6	Bynel 50E725	5.4
RB-MAH0.7MD15.87-St1	12.6	–	–

Tab. 4.4.2: Results of the MVR measurements for PP-g-MAH samples

4.4.3 Tensile properties of the multilayer films

Through the bubble inflation and the take-off process, the film is deformed in two directions and this induces molecular orientation of its molecules. This influences in turn the mechanical properties of the film in the longitudinal and transversal directions. Hence, the tensile strength σ_B and the elongation ε_B at break of the single-layer as well as multilayer films were determined. Considering the fact that the take-off speed was varied and the blow-up ratio kept constant, only the results in the longitudinal direction were taken into account.

4.4.3.1 Multilayer films produced with the die version A

The influence of the take-off speed on the mechanical properties of a homopolymer single layer is demonstrated in Fig. 4.4.4. Increasing the take-off speed reduces the thickness of the film from 90 to 50 µm. The alignment of the molecules induces an increase of the tensile strength and elongation at break in the machine direction.
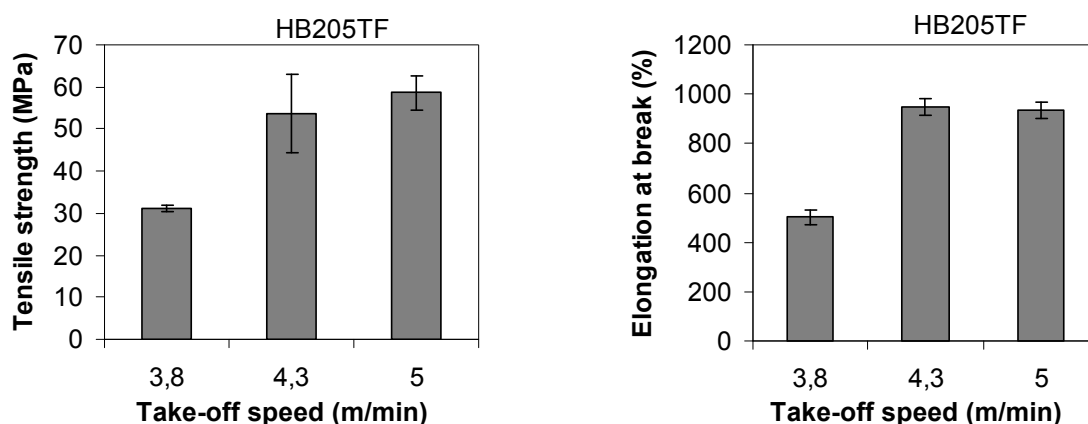
Fig. 4.4.4: Influence of the take-off speed on the tensile properties for a raw homopolymer single layer

A comparison of single films of grafted homopolymer and copolymer (formulation: PP-MAH0.7-MD22.2-St1) with films of their virgin resins confirmed the results obtained in section 3.4.4: a degradation of the tensile properties due to the functionalization process, more pronounced for the homopolymer than for the copolymer (Fig. 4.4.5). One can also observe that addition of PP-g-MAH concentrates in the PP matrix affects the tensile strength and elongation at break to a lesser extent.
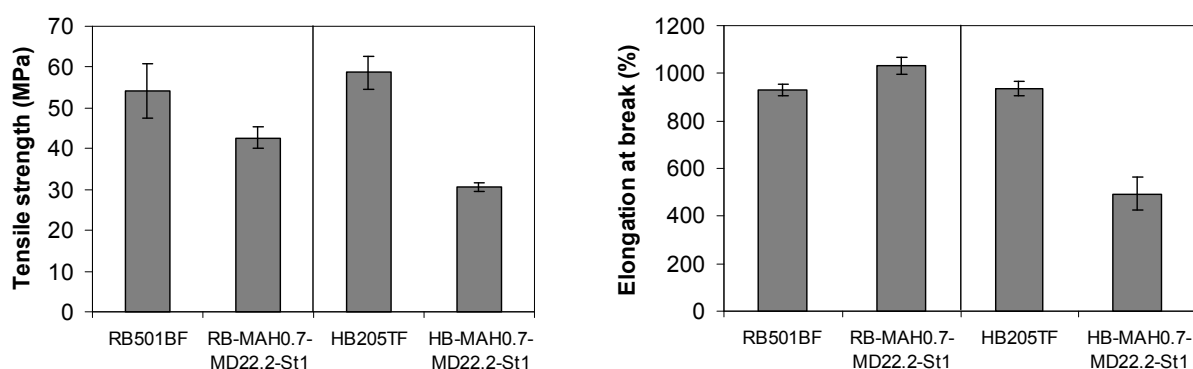
Fig. 4.4.5: Influence of the functionalization on the tensile properties for PP-g-MAH single films (PP-MAH0.7-MD22.2-St1)

Furthermore, a three-layer film composed of PA6 and PP/PP-g-MAH blends (formulations: RB+3%RB-MAH1-MD11.1-St0 and HB+5%HB-MAH1-MD11.1-St0) as well as its single layers were tested (Fig. 4.4.6). It is noticeable that the tensile properties of the three-layer film are situated between those of its single polymeric components. This is especially visible for the elongation at break.
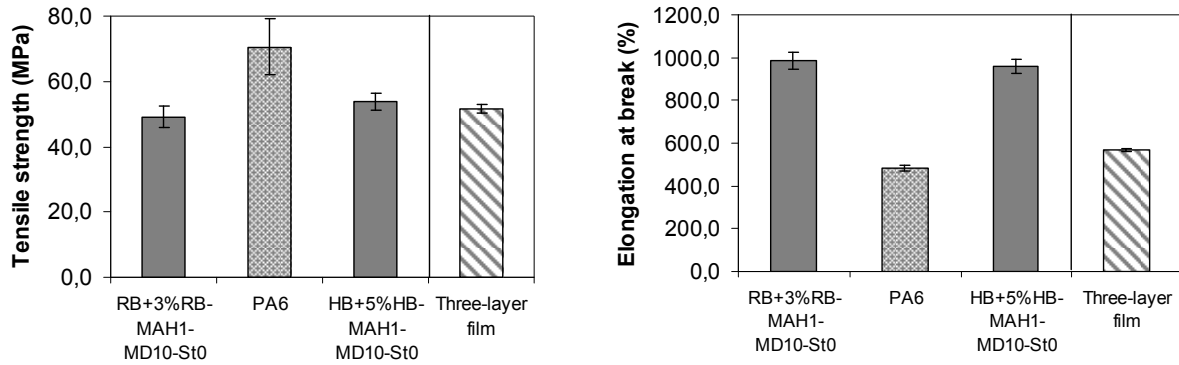
Fig. 4.4.6: Comparison of a three-layer film with single films of the corresponding polymers

The results of the tensile tests for the third series are presented in Fig. 4.4.7 and annotated in Tab. 4.4.3.
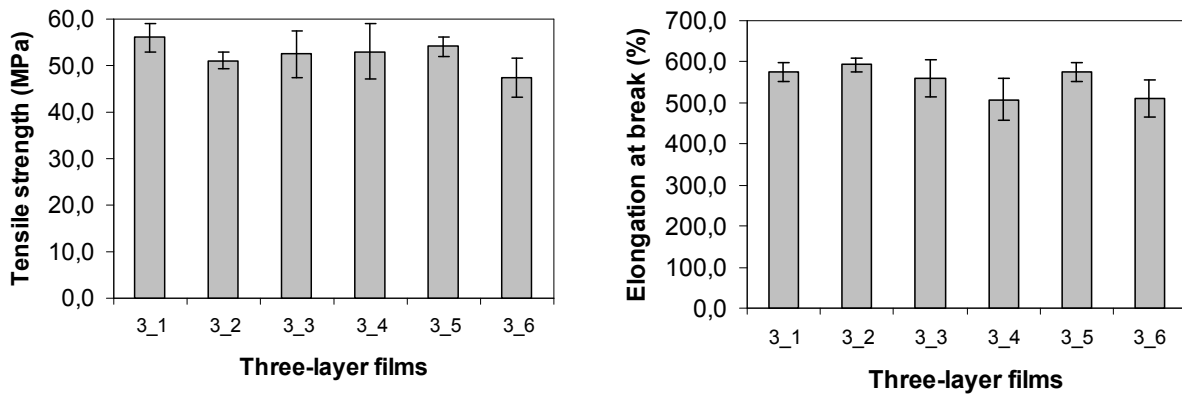
Fig. 4.4.7: Tensile properties of the multilayer films (series 3)

Comparable pairs of PP/PA6/PP multilayers	Modification	Observations

- RB + 3%RB-MAH1-MD11.1-St0 (3_3)
  HB + 3%HB-MAH1-MD11.1-St0
- RB + 3%RB-MAH1-MD11.1-St0 (3_4)
  HB + 5%HB-MAH1-MD11.1-St0
	Increase of the PP-g-MAH amount in the outer layer	σ_B *remains constant and* ε_B *decreases clearly*

- RB + 3%RB-MAH1-MD11.1-St0 (3_4)
  HB + 5%HB-MAH1-MD11.1-St0
- RB + 5%RB-MAH1-MD11.1-St0 (3_5)
  HB + 5%HB-MAH1-MD11.1-St0
	Increase of the PP-g-MAH amount in the inner layer	σ_B increases slightly and ε_B clearly

- RB + 3%RB-MAH1-MD11.1-St0 (3_3)
  HB + 3%HB-MAH1-MD11.1-St0
- RB + 5%RB-MAH1-MD11.1-St0 (3_5)
  HB + 5%HB-MAH1-MD11.1-St0
	Increase of the PP-g-MAH amount in both the inner and the outer layers	σ_B and ε_B increase slightly

- RB + 5%RB-MAH1-MD11.1-St0 (3_5)
  HB + 5%HB-MAH1-MD11.1-St0
- RB + 5%RB-MAH1-MD11.1-St0 (3_6)
  HB + 7%HB-MAH1-MD11.1-St0
	Increase of the PP-g-MAH amount in the outer layer	σ_B *and* ε_B *decrease clearly*

- RB + 1%RB-MAH1-MD11.1-St0 (3_1)
  HB + 5%HB-MAH1-MD5.5-St0
- RB + 3%RB-MAH1-MD11.1-St0 (3_2)
  HB + 5%HB-MAH1-MD5.5-St0
	Increase of the PP-g-MAH amount in the inner layer
	Low MAH/peroxide ratio in the PP-g-MAH formulation for the outer layer
		σ_B decreases clearly and ε_B increases slightly

- RB + 3%RB-MAH1-MD11.1-St0 ((3_4)
  HB + 5%HB-MAH1-MD11.1-St0
- RB + 3%RB-MAH1-MD11.1-St0 (3_2)
  HB + 5%HB-MAH1-MD5.5-St0
	Decrease of the MAH/peroxide ratio in the PP-g-MAH formulation for the outer layer	σ_B decreases slightly and ε_B increases clearly

Tab. 4.4.3: Results of the MVR measurements for PP-g-MAH samples

When the formulations of the blends are varied, only slight differences in the tensile properties of the multilayers can be observed. On the one hand, the elongation at break follows defined trends: it diminishes with increasing concentrations of PP-g-MAH in the outer layer and grows with higher amounts of PP-g-MAH in the inner layer. On the other hand, the tensile strength shows no clear trend and seems to be more sensible to other factors.

Series 4 presents coextrudates of PA12 and PP/PP-g-MAH blends produced at a process temperature of 230°C. The formulations of the PP-g-MAH concentrates and the amount of PP-g-MAH in the blends were successively varied. A study of the influence of the PP-g-MAH formulations on the coextrudates' tensile properties was carried out and the results are shown in Fig. 4.4.8 and 4.4.9. The tensile strength and the elongation at break of these samples increased with a decreasing MAH/peroxide ratio in the PP-g-MAH formulation. This means an augmentation of the peroxide and as a consequence a diminution of the molecular weight of the PP-g-MAH. When the amount of PP-g-MAH increased from 1 to 10 wt.% of PP-g-MAH compatibilizer in the blend, the mechanical properties of the multilayers were improved for a PP-g-MAH content up to 7 wt.% and decreased again with 10 wt.% PP-g-MAH in the blend. Although the single PP layers are mechanically weaker due to the presence of a low molecular weight concentrate in their matrix, the PP/PA/PP multilayers presented improved properties. This is related to the adhesion performance of the layers, which will be treated in section 4.4.5.
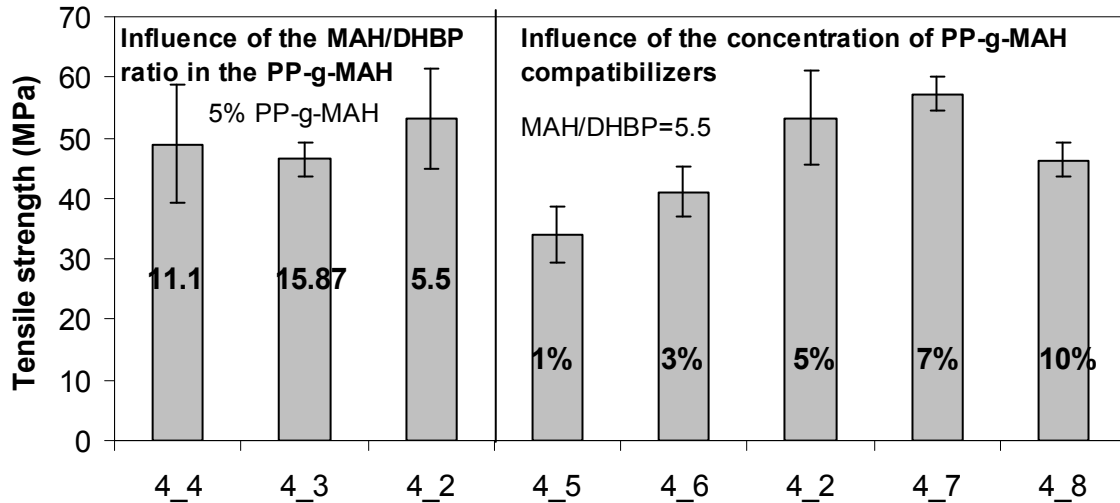
Fig. 4.4.8: Tensile strength of the multilayer films (series 4)
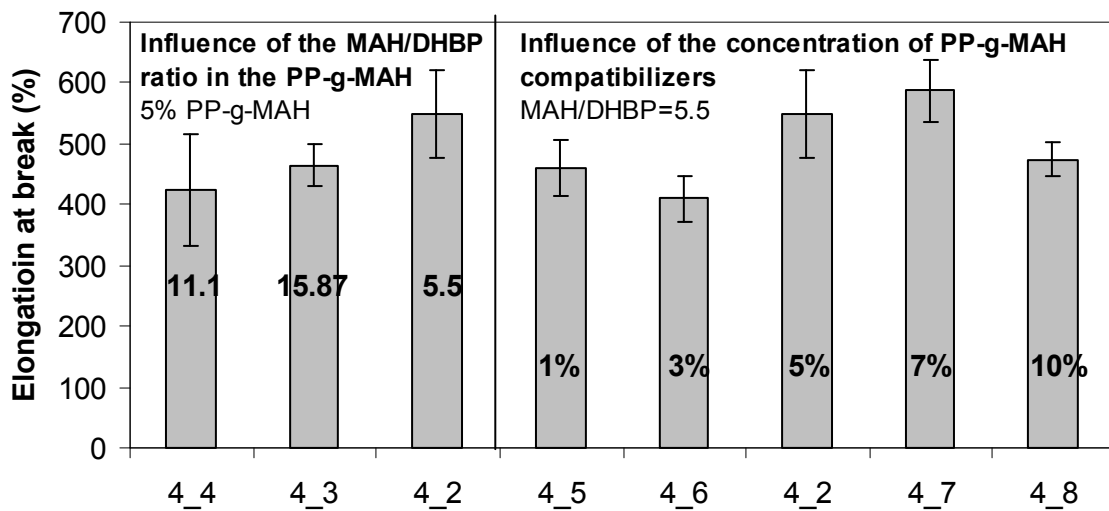
Fig. 4.4.9: Elongation at break of the multilayer films (series 4)

4.4.3.2 Multilayer films produced with the die version B

In a first step, the formulation of the direct grafted PP inner layer was kept constant and the outer layer PP formulation varied at a constant process temperature of 230°C. In a second step, the inverse procedure was performed. Fig. 4.4.10 shows that the tensile properties of the multilayers decreased with addition of MAH, peroxide and styrene in the PP-g-MAH outer layer formulation. When the inner layer formulation was varied, the tensile strength decreased slightly and the elongation at break remained at the same level. This result followed the trend observed for single layers of the grafted homopolymers and copolymers. The influence of adhesion seems quite limited in that case.
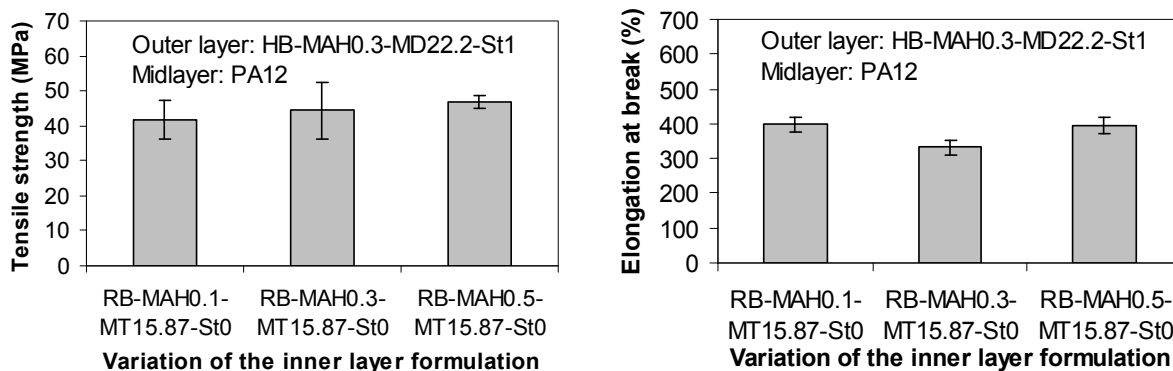
Fig. 4.4.10: Tensile properties of the multilayer films (series 5)

Multilayers composed of RB-MAH0.1-MT15.87-St0 as inner layer, HB-MAH0.3-MD22.2-St1 as outer layer and PA6-6,6, PA6 or PA12 as central layers are compared in Fig. 4.4.11. During their production, the process temperature was kept constant at 250°C. The coextrudate containing PA6-6,6 appeared to possess the higher mechanical properties.
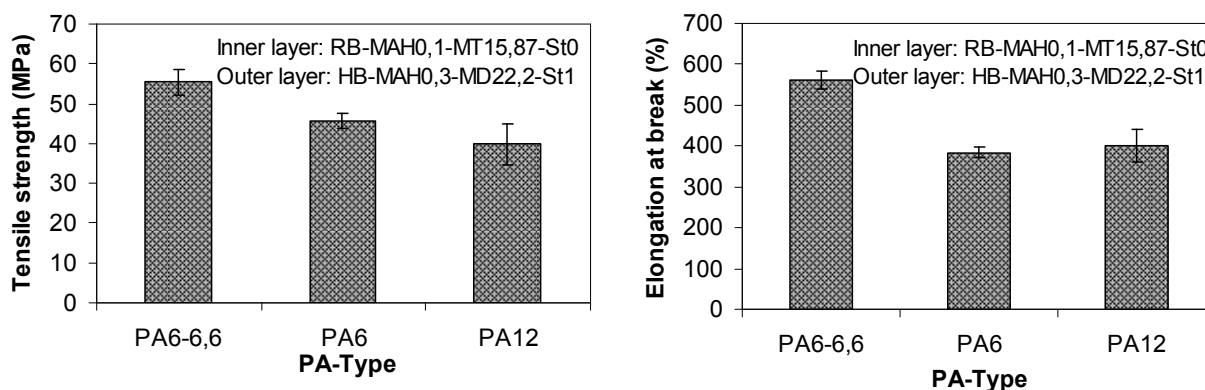
Fig. 4.4.11: Tensile properties of the multilayer films – Comparison of PA types

In series 6, the formulations of the PP-g-MAH concentrates in the blends were varied and the mechanical properties of the (PP blend)/PA/(PP blend) films studied (Fig. 4.4.12). As it has already been mentioned for the same multilayers produced with the die version A at an extrusion temperature of 230°C, the trend is an augmentation of the tensile properties when decreasing the MAH/peroxide ratio of the concentrates.
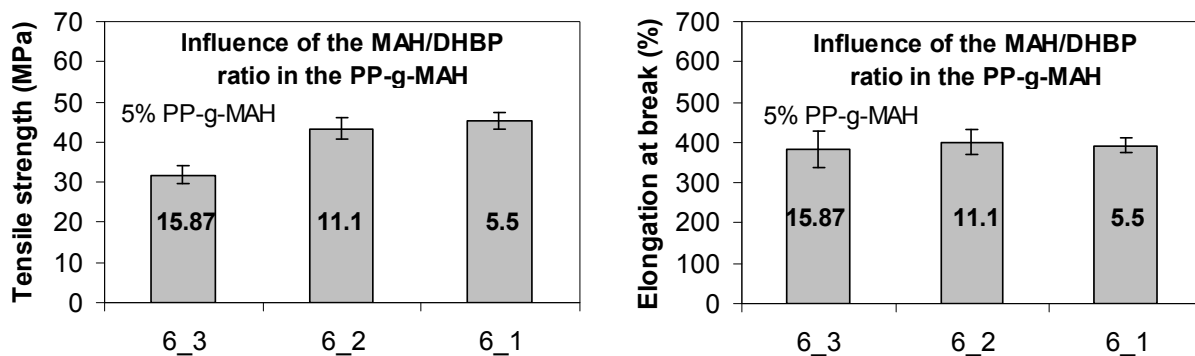
Fig. 4.4.12: Tensile properties of the multilayer films (series 6)

4.4.4 Characterization of adhesion

The investigations concerned the adhesion performance between the layers of the coextruded films. The outer and inner layers' formulations, the polyamide central layer as well as the process parameters take-off speed and temperature were varied during the experiments. The multilayer films were tested in terms of adhesion using T-peel tests. Strips of the coextrudate were cut out of the centre of each tubular film in the longitudinal direction. Because the films were composed of three layers, the tests were conducted by successively separating one layer (inner or outer layer) from the other two layers (outer or inner layer + PA) as shown in Fig. 4.4.13. The calculation of the fracture energy was realized as described in section 4.3.2.1. The adhesion performance of the multilayers was compared for films produced under the same process conditions.
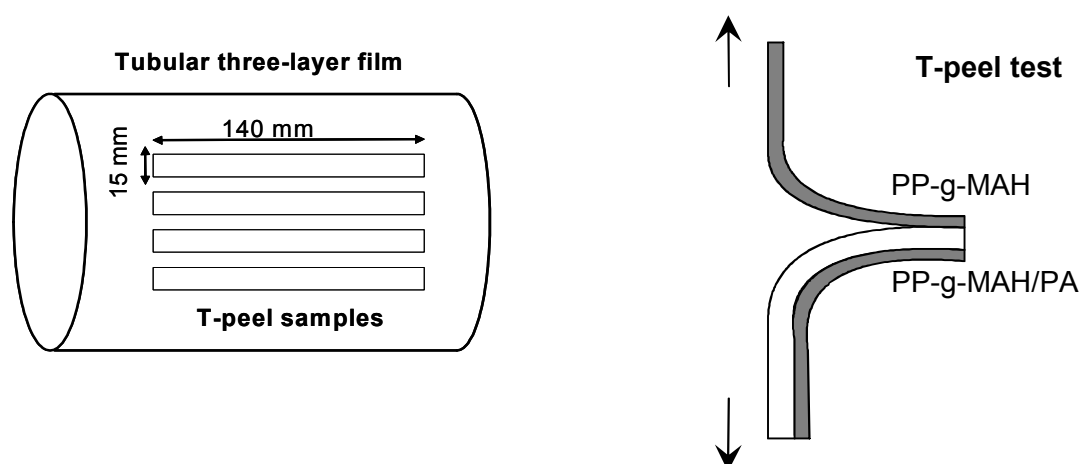
Fig. 4.4.13: Description of the sample preparation for T-peel test

4.4.4.1 Multilayer films produced with die version A

As already mentioned, the samples of series 1 and 2 showed spontaneous delamination of the PP and PA layers. In the series 3, the influence of the PP-g-MAH formulations and the take-off speed on adhesion between the layers was studied (Fig. 4.4.14).
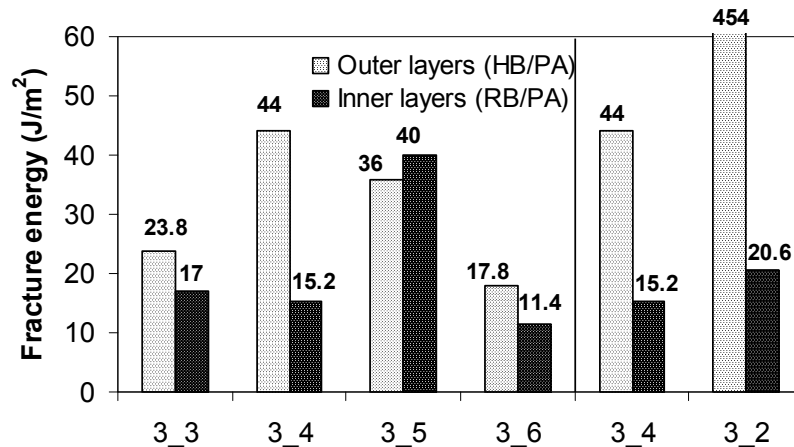
Fig. 4.4.14: Adhesion performance of multilayers produced under the same conditions (series 3)

One could observe that the fracture energies were quite low for these multilayers: between 11.4 and 454 J/m^2. The adhesion fracture energy between the outer and PA6/inner layers increased with the outer layer formulation as follows: HB+5%HB-MAH1-MD11.1-St0 > HB+3%HB-MAH1-MD11.1-St0 > HB+7%HB-MAH1-MD11.1-St0. There were some small differences in the adhesion level of the homopolymer layer depending on the associated PA6/copolymer layer. For instance, the fracture energy values for HB+5%HB-MAH1-MD11.1-St0 with PA6/RB+3%RB-MAH1-MD11.1-St0 or PA6/RB+5%RB-MAH1-MD11.1-St0 were 44 and 36 J/m^2, respectively. As for the inner and PA6/outer layers, the adhesion level raised from about 15 J/m^2 for RB+3%RB-MAH1-MD11.1-St0/PA6/HB+5%HB-MAH1-MD11.1-St0 to 40 J/m^2 for RB+5%RB-MAH1-MD11.1-St0/PA6/HB+5%HB-MAH1-MD11.1-St0. When RB+5%RB-MAH1-MD11.1-St0 was associated with PA6/HB+7%HB-MAH1-MD11.1-St0, the fracture adhesion reached only 11.4 J/m^2. This value is very low in comparison to the previous 40 J/m^2 and may be due to the decreased mechanical strength of the homopolymer layer. Diminution of the MAH/peroxide ratio from 11.1 to 5.5 in the PP-g-MAH of the outer layer led to a ten times higher energy of separation between the homopolymer and PA6/RB+3%RB-MAH1-MD11.1-St0 layers.

Fig. 4.4.15 demonstrates the influence of the take-off speed on the bond adhesion of the coextrudates RB+3%RB-MAH1-MD11.1-St0/PA6/HB+5%HB-MAH1-MD11.1-St0 and RB+5%RB-MAH1-MD11.1-St0/PA6/HB+5%HB-MAH1-MD11.1-St0. By increasing the take-off speed, the contact time between the layers at the die exit – before crystallisation of the materials – diminished so that the time for chemical reactions between the layers was shorter. Further more, the thickness of the films decreased from about 200 to 60 μm with increasing take-off speed. It appeared that the thickness of the films influenced the level of adhesion.
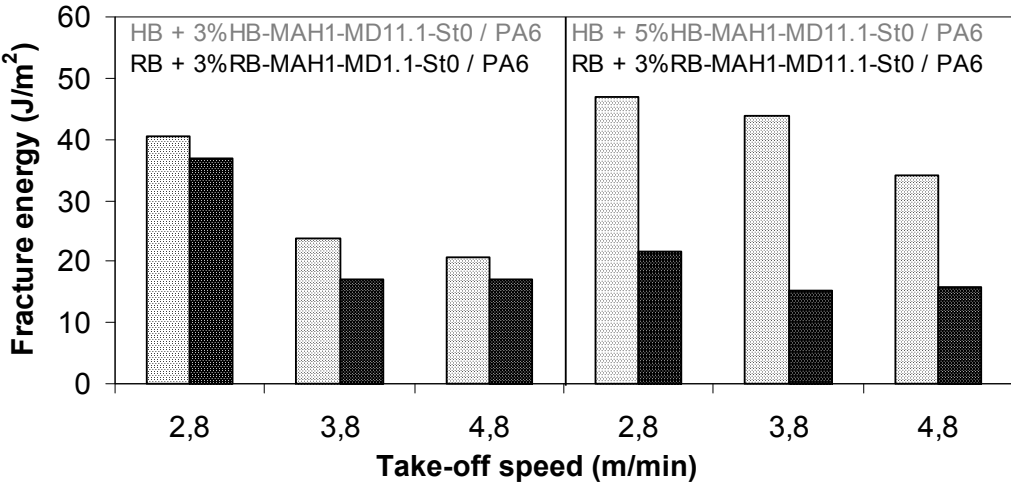
Fig. 4.4.15: Influence of the take-off speed on the adhesion performance of the multilayers (series 3)

Gent and al. [Gen77] demontrated that thin films tended to yield during peeling and the total energy dissipated was lower because of the reduced thickness. As a consequence, the contribution of plastic yielding to the peeling force dimished. Increasing the thickness led to more energy dissipation and the peeling force raised. However, it was found that at a certain thickness no plastic yielding could occur anymore and the peeling force decreased again.

The results of the T-peel tests for the series 4 are summarized in Fig. 4.4.16. Two types of formulation variations for the inner and outer layers were investigated: increase of the MAH/peroxide ratio in the PP-g-MAH concentrates (5.5, 11.1 and 15.87) and augmentation of the PP-g-MAH content in the blends. For the multilayers RB+5%PP-g-MAH/PA12/HB+5%PP-g-MAH, it was found that the fracture energy decreased with addition of PP-g-MAH having increasing MAH/peroxide ratio and as

consequence increasing molecular weight. The diffusion of longer chains within the matrix to reach the interface was more difficult. The homopolymer and PA12/copolymer layers presented higher levels of fracture energy than the inner and PA12/outer layers.

Considering the multilayers made of PA12 and PP/PP-MAH1-MD5.5-St0 blends, it was shown that a raising amount of PP-g-MAH from 1 to 10 wt.% in the blend improved adhesion between the layers. However the positive effect was observed only for PP-g-MAH concentrations up to 5 wt.% in the case of the outer and PA12/inner layers. On the other side, the inner and PA12/outer layers demonstrated a constant growth of their peeling energy from 12 to 222.7 J/m^2.
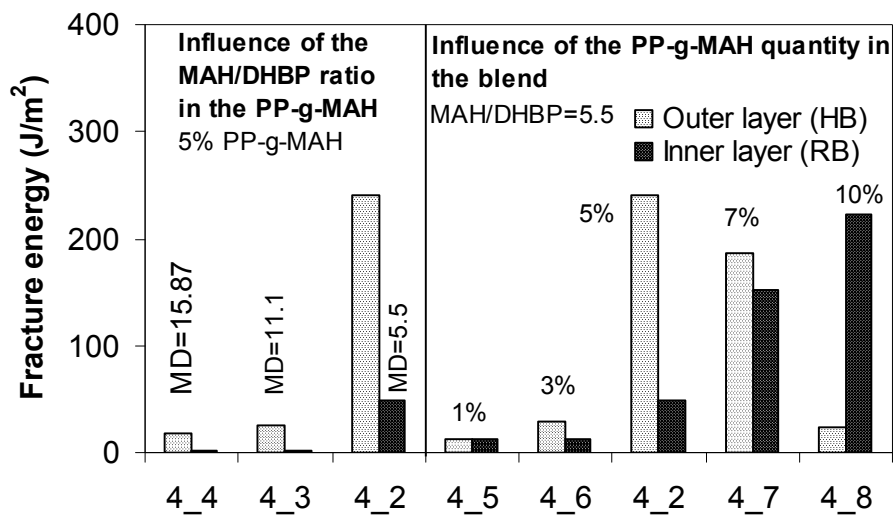
Fig. 4.4.16: Influence of the compatibilizer formulation and concentration on the adhesion performance of the multilayers (series 4)

4.4.4.2 Multilayer films produced with die version B

The die version B was constructed in order to achieve a longer residence time of the materials in the die and therefore intensify the reactions between the species. These coextrusion trials were conducted with PA12 and different PP formulations for the direct grafted PP and the PP/PP-g-MAH blends. Besides, the types of PA and the process temperature were investigated.

Series 5 concerns the direct grafted PP. The formulations of the copolymer layer were successively changed, the formulation of the homopolymer layer being kept constant and vice versa. Fig. 4.4.17 presents the results of the T-peel tests performed on these multilayer films. By increasing the MAH, peroxide and styrene

concentrations in the outer layer, the fracture energy between the outer and PA12/inner layers grew from 5.5 to 11.6 J/m^2. Although the formulation of the inner layer remained constant (RB-MAH0.1-MT15.87-St0), the adhesion strength between the copolymer and PA12/homopolymer layers increased. When the formulations of the inner layer were varied by raising MAH and peroxide contents, the fracture energy also increased from 1.1 to 5.7 J/m^2. The energy value between the outer and PA12/inner layers remained on the same level (about 7 J/m^2) whatever the associated copolymer layer formulation was.
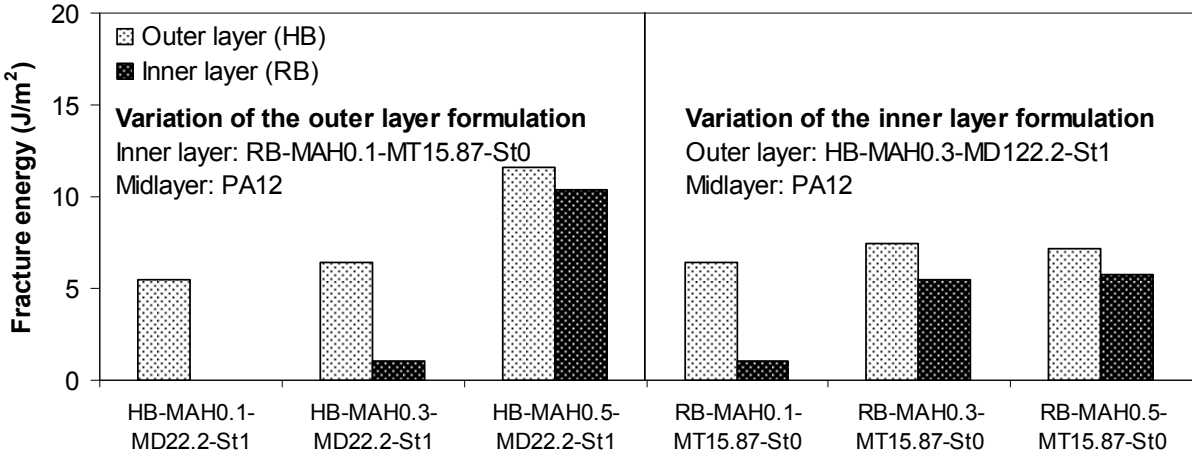
Fig. 4.4.17: Influence of the PP-g-MAH formulation on the adhesion performance of the multilayers (series 5)

The effect of temperature on adhesion can be visualized in Fig. 4.4.18 for the multilayer RB-MAH0.1-MT15.87-St0/PA12/HB-MAH0.3-MD22.2-St1. A change in the process temperature from of 230 to 250°C induced a 6 times higher fracture energy for the outer and PA12/inner layers, and up to no separation of the inner and PA12/outer layers. Thus, the thermal energy increase seems to have a greater impact on the copolymer/PA interactions than on the homopolymer/PA ones.
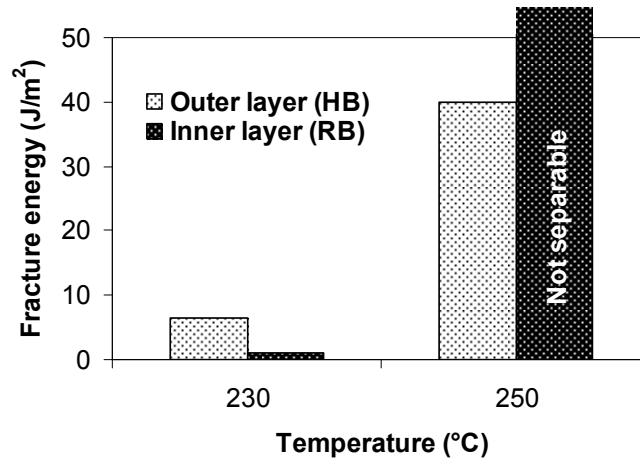
Fig. 4.4.18: Influence of the process temperature on the adhesion performance of the multilayers (series 5)

The influence of the PA types was investigated at a process temperature of 250°C (Fig. 4.4.19b). A coextrudate showing no delamination of the layers was obtained with PA6-6,6 as shown by the light microscope picture in Fig. 4.4.19a. The inner and PA12 or PA6/outer layers could not be separated as well. The fracture energies between the outer and PA12 or PA6/inner layers reached 40 and 29 J/m^2.

Outer layer: HB-MAH0.3-MD122.2-St1
Inner layer: RB-MAH0.1-MT15.87-St0
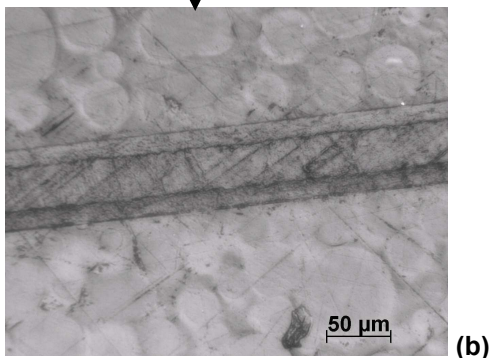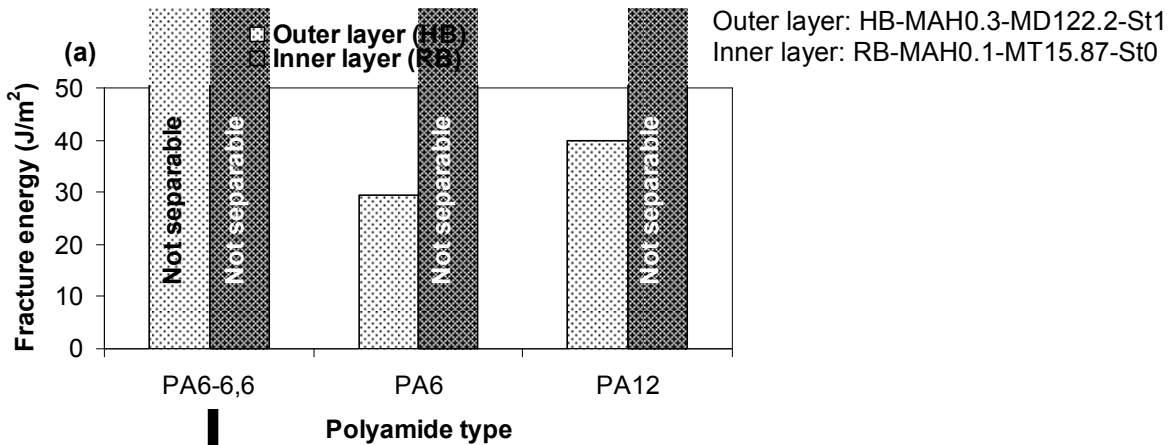
Fig. 4.4.19(a): Influence of the PP-g-MAH formulation on the adhesion performance of the multilayers (series 5)

Fig. 4.4.19(b): Light microscope picture of three-layer film HB-MAH0.3-MD122.2-St1/PA6-6,6/ RB-MAH0.1-MT15.87-St0

The adhesion test results of the PA12 and PP/PP-g-MAH blends multilayers (series 6) are shown in Fig. 4.4.20. The formulation of the PP-g-MAH was varied by increasing the MAH/peroxide ratio, as in series 4. A high level of adhesion (no layers' separation) was obtained between the outer and PA12/inner layers with MAH/peroxide ratios of 5.5 and 11.1 in the PP-g-MAH. As for the inner and PA12/outer layers, the optimal adhesion performance is obtained for a ratio of 5.5.
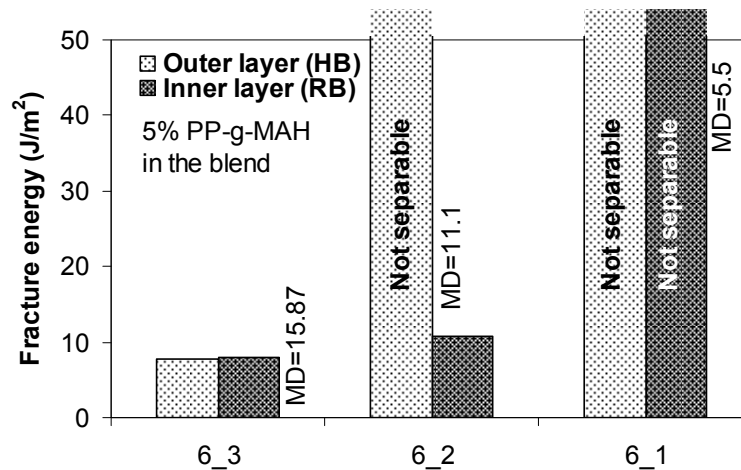
Fig. 4.4.20: Influence of the PP-g-MAH formulation in the blend on the adhesion performance of the multilayers (series 6)

In almost all trials, the homopolymer and PA/inner layers showed greater fracture strengths than the copolymer and PA/outer layers although the copolymer interfaces had the longest contact times in the multilayer die. In that case, reaction time is not the dominating parameter of influence. As it has been seen with the pressed samples, the molecular weight and, as a consequence, the viscosity of the polymers is responsible for that behaviour.

No real comparison of the results obtained with the press moulding and the film blowing can be made with regard to the trends of the fracture energy as function of the formulation variables. In the press, the pressure is applied perpendicularly to the surface of the film and the process is static whereas the film blowing implies non-equilibrium states – mainly due to shear – for the interfaces between the layers. Besides, polymer – polymer slip phenomena at the interfaces also cause a decrease of adhesion between the layers [Zhao02, Zha05]. This is caused by the shear stress which disentangles the polymer chains at the interface, reducing the probability of the reactive groups to meet and chemically react.

5   Conclusion

The aim of the present work was the realization of a polypropylene/polyamide three-layer film by using film blowing coextrusion. The initial purpose was to eliminate the thin adhesion promotor tie-layers which are commonly used to achieve adhesion between the immiscible polymers. One method of compatibilization was the functionalization of the polypropylene inner and outer layers using monomers which possess reactive groups and are able to form covalent bonds with the polyamide. In this study, the polypropylenes were grafted with maleic anhydride and glycidyl methacrylate by reactive extrusion. The second strategy to realize adhesion between the layers was to add grafted PP compatibilizers in the PP matrix.

In the first part, chemical modification of the PP was conducted using a twin screw extruder. The extrusion parameters temperature, screw speed and throughput were varied. Pellets and cast films were extruded using a strand die and a coat hanger die, respectively. The grafted materials were subsequently characterized in terms of grafting yields using Fourier Transform Infrared Spectroscopy, rheological, mechanical and thermal properties. The variation of the initial amounts of grafting components in the formulations influenced greatly the physical properties of the materials. Thus, the choice of an adequate formulation would depend on the resulting material properties. In general, the grafting yields increased accordingly to raising amounts of introduced peroxide (monomer/peroxide ratios of 11.1, 15.87 and 22.2), monomer (from 0.1 to 7.0 phr) or styrene (styrene/monomer ratios between 0 and 2). However, a raising peroxide concentration not only led to the enhancement of grafting but to degradation of the material by β-scission. As a consequence, the molecular weight of the functionalized PP was reduced and the mechanical properties, among others, decreased. A compromise in the formulation had to be found in order to minimize the decrease of the tensile values. In our case, the amount of peroxide was diminished and a monomer/peroxide ratio of 22.2 was chosen. Styrene, used as comonomer, promoted the grafting reactions and at the same time contributed to the minimization of degradation in both functionalization cases with MAH and GMA. Differences in the material behaviour in front of functionalization were found depending on the type of polypropylene (copolymer or homopolymer) as well as their molecular weight. The grafted PP homopolymers appeared to be more

sensitive to β-scission than the copolymers because of their structure made of tertiary carbon atoms. Their molecular weight and zero shear viscosity decreased drastically with addition of peroxide and MAH. The grafted copolymers, on the other side, showed better grafting efficiencies and less degradation because of the presence of ethylene sequences randomly dispersed in the polypropylene chains. They also demonstrated higher elongation at break and were not as brittle as the grafted homopolymers with increasing monomer, peroxide and styrene amounts in the formulations. For low molecular weight PP-g-MAH copolymers the elongations at break were situated between 400 and 800%, and for their homopolymer counterparts around 20%. The high molecular weight PP demonstrate a similar mechanical behaviour to the latter. The initial amounts of the GMA reached 7 phr, and as a consequence, the quantities of peroxide and styrene were higher than in the case of the PP-g-MAH samples. However, the degree of degradation remained moderate, except in the case of the homopolymers. As expected, a GMA/DHBP ratio of 22.2 instead of 11.1 (diminution of the peroxide content) brought an improvement in the mechanical resistance. The influence of styrene was positive on the properties of the PP-g-GMA homopolymers and slightly negative on the copolymers' ones.

Thermal analyses of the grafted polypropylenes showed that the crystallisation process was a significant factor because it affected the physical properties of the film. Crystallisation rate and temperature had a great influence on the mechanical properties, inducing different lamellae thicknesses depending on the samples. Although the same process conditions were used for the production of the films, differences in the crystallisation of the films were due to happen, depending on the PP types, the formulations, the reactions occurring during functionalization as well as the by-products created. The more impurities in the material the faster crystallisation was achieved in the case of the low molecular weight PP-g-MAH (RD208CF and HD601CF). With growing amounts of grafting components, the degree of crystallinity for these samples increased whereas it diminished in the case of the high molecular weight PP. The grafted copolymers showed degree of crystallinity of about 30% and the homopolymers around 50%.

Considering the process conditions, temperature appeared to be the most influencing factor on the grafting efficiency, the melt grafting being a thermal initiated reaction. On the other side, a too high energy input conducted to a more pronounced degradation of the grafted polypropylenes.

In the second part, the adhesion between the modified polypropylenes and polyamide films was investigated. The parameters influencing the fracture energy of the PP/PA fusion bonded films were found to be the PP type, the formulations of the functionalized PP, the grafting conditions – which directly affected the grafted PP films – and the press parameters such as temperature and time. The PA type did not play a major role in the improvement of adhesion. The general statement that can be drawn out of this study is that the molecular weight and structure of the grafted polypropylene are determining factors for the adhesion performance of the PP/PA bonds. They were modified by the grafting formulations and conditions.

In the case of PP/PA laminates with direct grafted PP films, it was found that increasing simultaneously the monomer, peroxide and styrene in the grafting formulation negatively influenced the fracture energy. This is mainly due to the weakening of the cohesive strength of the grafted PP, degraded by β-scission. According to the micromechanical theories of fracture, because PA possesses a higher yield stress than PP, it plays the role of a solid substrate and the mechanical properties of the PP are determining for the adhesion performance. SEM analyses of the PP and PA peeled surfaces confirmed this fracture type, showing fibrils only on the PP side of the laminate. Moreover, grafting reaction by-products in the grafted PP film such as ungrafted MAH, MAH/styrene or polystyrene copolymers, polymerized monomers can represent disturbance factors for the PP/PA adhesion mechanisms. The fracture energy appeared to be improved by a low content of monomer in the grafted PP formulation, a limited concentration of peroxide for low molecular weight PP and a higher one for high molecular weight PP. Adding styrene in the grafting formulation for the low molecular weight PP showed a positive influence on the fracture energy of the laminates. For the high molecular weight PP, it demonstrated a positive effect on the PA/homopolymer adhesion whereas it reduced the PA/copolymer's one. It appeared that GMA showed a far less effective impact on the layers' adhesion than MAH and it was not further used for the coextrusion trials.

Compatibilization using PP/PP-g-MAH blends was also realized. The peroxide amount in the PP-g-MAH as well as the quantity of concentrate in the blend were varied. The best results for the PP/PA adhesion was achieved with 5 wt.% of the formulations HB-MAH1-MD11.1-St0 and RB-MAH1-MD5.5-St0. Once again, the major role of the molecular weight of the PP-g-MAH concentrates was demonstrated. In general, blending the polypropylene matrix with PP-g-MAH concentrates allowed

to achieve higher levels of fracture energies in the PP/PA bonds than with the direct grafted PP (comparison of the samples pressed between Teflon sheets).

As for the chemical reaction between polyamide and MAH, the presence of a copolymer formed in situ between the anhydride and the amine end groups in the bonded films could be indirectly detected by infrared spectroscopy.

Coextrusion film blowing trials were subsequently conducted using the information gained from the experiments with laminated PP/PA films. Two stacked-type spiral dies (version A and B) were used to produce the films. A modified exit die for version B was constructed at the IKT in order to achieve adhesion between the direct grafted PP and PA layers.

The physical properties of the films were fundamental not only for the final performance of the coextruded films but also for the adhesion properties of the bonded films.

The mechanical properties as well as the adhesion properties of the coextruded structures were determined. The tensile properties of the material depend on the processing conditions and the formulations of the PP-g-MAH used directly as compatibilizers or concentrates. Increasing the take-off speed was found to improve the mechanical properties of monolayers in the stretching direction because of an alignment of the molecules in the materials. However, it leads to a decrease of the adhesion performance between the coextrudates' layers due to the diminution of the residence time at the die exit. A reinforcement effect in terms of tensile properties is observed when the adhesion strength between the layers increases. At a low level of fracture energy ($\leq$ 10 J/m^2), stretching of the multilayer film induces a successive delamination of the layers and the tensile values correspond to those of the single PP or PA layers. No or less delamination occurs during strain-stress tests for coextrudates of high adhesion strength ($\geq$ 200 J/m^2) and their mechanical properties are improved. They are situated between the values of the monolayers.

In general, the fracture strengths obtained for the PP/PP-g-MAH blends and PA multilayers are higher than those of the direct grafted PP/PA ones. The low molecular weight chains, especially the PP-g-MAH with MAH/peroxide=5.5, present in the PP matrix show a better mobility than MAH grafted on long PP molecules. Besides, the blends are less degraded than the grafted PP so that their mechanical contribution to adhesion is higher. Moreover, steric hindrance due to the anhydride molecules

attached to the polymer backbone may be another cause for this phenomenon. By using the die version B under a process temperature of 250°C, the residence time of the materials as well as the reactions at the interfaces were increased. The grafted PP/PA and the PP blends/PA films reached a degree of adhesion which impaired the layers separation.

One can notice that time and especially temperature were the main process parameters promoting adhesion as they enhanced the diffusion processes and the chemical reactions between the species at the interface.

In the present thesis, functionalization and coextrusion were performed seperately. In order to simplify the production of the three-layer films, it would be interesting to transform this two-step in a one-step process that would allow functionalization in the coextrusion line. This new concept would afford a modification of the single-screw extruders with new screw designs (addition of mixing zones for example) as well as the introduction devolatilization zones in the barrels.

6 References

Functionalization of polypropylene

[Abe00]: M. Abendschein, *Optimierung der mechanischen Eigenschaften eines langfaserverstärkten Verbunwerkstoffes auf Basis von Flachsfasern und einer Polypropylenmatrix*, unveröffentliche experimentelle Diplomarbeit, (2000)

[Aug04]: E. Passaglia, S. Coiai, F. Ciardelli, J.-L. Pradel, S. Augier, J.-J. Flat, *Functionalization of Propylene polymers: Modulation of maleic anhydride and chain structure conservation*, IUPAC 40th International Symposium on Macromolecules, pp. 58, (2004)

[Bas00]: M. Bastian, *Plastifizierung und Morphologie von inkompatiblen Polymerblends bei der Herstellung mit Gleichdrall-Doppelschneckenextrudern,* PhD Thesis, University of Paderborn, (2000)

[Bet00]: S.H.P. Bettini, J.A.M. Agnelli, *Evaluation of methods used for analysing maleic anhydride grafted onto polypropylene by reactive extrusion*, Polym. Testing, *19, pp.3-15, (2000)*

[Bez99]: T. Bezigian, *Extrusion coating extrusion manual*, Tappi Press, Atlanta, (1999)

[Böl01]: U. Bölz, *Schmelzemodifizierte Polypropylene - Herstellung, Eigenschaften und Anwendungsbeispiele*, PhD Thesis, University of Stuttgart, (2001)

[Car98]: H. Cartier, G.-H. Hu, *Styrene-assisted melt free radical grafting of glycidyl methacrylate onto polypropylene,* J. Polym. Sci. A. Polym. Chem., 36(7), pp. 1053-1063, (1998)

[Cha00]: P. Chandranupap, S.N. Bhattacharya, *Reactive processing of polyolefins with MAH and GMA in the presence of various additives*, J. Appl. Polym. Sci., 78, pp. 2405-2415, (2000)

[Chi96]: C.-R. Chiang, F.-C. Chang, *Polymer blends of polyamide-6 and poly(phenylene oxide) compatibilized by styrene-co-glycidyl methacrylate*, J. Appl. Polym. Sci., 61, pp. 2411-2421, (1996)

[Deg]: Technische Information von Berstoff / Degussa, Degussa *Abbau von Polypropylen mit organischen Peroxiden*

[Dow]: information provided on the website from Dow Chemicals, http://www.dow.com/acrylic/products/gma.html

[Duh04]: M. Zhang, J. Duhamel, M. van Duin, P. Meessen, *Characterization of fluorescence of the distribution of maleic anhydride grafted onto ethylene-propylene copolymers*, Macromol., 37, pp. 1877-1890, (2004)

[Dui03]: M. van Duin, *Grafting of polyolefins with maleic anhydride: Alchemy or technology ?* Macromol. Symp., 202, pp. 1-10, (2003)

[Ebd86]: J.R. Ebdon, C.R. Towns, K. Dodgson, *On the role of monomer-monomer complexes in alternating free-radical copolymerizations: the case of styrene and maleic anhydride*, JMS-Rev. Macromol. Chem. Phys., C26(4), pp. 523-550, (1986)

[Edm04]: S. Edmondson, W.T.S. Huck, *Controlled growth and subsequent chemical modification of poly(glycidyl methacrylate) brushes on silicon wafers*, J. Mater. Chem., 14, pp. 730-734, (2004)

[Fla91]: J.-J. Flat, *Nouveaux développements dans le greffage radicalaire sur polypropylene à l'état fondu*, PhD Thesis, University of Strasbourg, (1991)

[Fri96]: H.-G. Fritz, Q. Cai, U. Bölz, *Struktur/Eigenschaftsbeziehungen von PP/PA6.6-Legierungen*, Kautschuk Gummi Kunststoff, 49, 2, pp. 89-97, (1996)

[Gay72]*: N.G. Gaylord, A. Takahashi, S. Kukichi, R.A. Guzzi, J. Polym. Sci., B10, 95, (1972)

[Gay73]: N.G. Gaylord, *Donor-acceptor complexes in copolymerization*, Adv. Chem. Ser., 129, pp. 209-228, (1973)

[Gay75]*: N.G. Gaylord, J. Macromol. Sci. Rev. Macromol. Chem., C13(2), 235, (1975)

[Gle04]: W. Glenz, *Polypropylen (PP)*, Kunststoffe, 10, pp. 70-71, (2004)

[Hei96]: W. Heinen, C.H. Rosenmöller, C.B. Wenzel, H.J.M. de Groot, J. Lugtenburg, ^{13}C *NMR Study of the Grafting of Maleic Anhydride onto Polyethene, Polyethylene, and Ethene-Propene Copolymers*, Macromol., 29, pp 1151-1157, (1996)

[Hog88]: A.H. Hogt, *Modification of polypropylene with maleic anhydride*, Proceedings of SPE ANTEC, pp. 1478-1480 (1988)

[Hog96]: A.H. Hogt, J. Meijer, J. Jelenič, in *Reactive Modifiers for Polymers*, edited by S. Al-Malaika, Chapman & Hall, London, pp. 86-132, (1996)

[Hu93]: G.-H. Hu, J.-J. Flat, M. Lambla, Makromol. Chem., Makromol. Symp., 75, pp. 137-157, (1993)

[Hu94]: G.-H. Hu, J.-J. Flat, M. Lambla, *Free grafting of chemically activated maleic anhydride onto polypropylene by reactive extrusion*, Proceedings of SPE ANTEC, pp. 2775-2778 (1994)

[Hu96]: G.-H. Hu, J.-J. Flat, M. Lambla, in *Reactive Modifiers for Polymers*, edited by S. Al-Malaika,Chapman & Hall, London, pp. 1-82, (1996)

[Hun01]: T.R. Felthouse, J.C. Burnett, B. Horrell, M.J. Mummey, Y.-J. Kuo, *Maleic anhydride, maleic acid and furamic acid*, Huntsman Petrochemical Corporation report, www.huntsman.com/petrochemicals/Media/KOMaleic.pdf, pp. 15-27, (2001)

[Ide74]: F. Ide, A. Hasegawa, *Studies on polymer blend of nylon 6 and polypropylene or nylon 6 and polystyrene using the reaction of polymer*, J. Appl. Polym. Sci., 18 (4), pp. 963-974, (1974)

[Int]: *General product information on organic peroxides*, Peroxid-Chemie GmbH

[Kar95]: J. Karger-Kocsis, Polypropylene – Structure, blends and composites – Volume 3 Composites, Chapman & Hall, (1995)

[Kou97]: E.G. Koulouri, A.X. Georgaki, J.K. Kallitsis, *Reactive compatibilization of aliphatic polyamides with functionalized polyethylenes*, Polym., 38(16), pp. 4185-4192, (1997)

[Lie90]: R.B. Lieberman, P.C. Barbe, in *Concise encyclopedia of polymer science and engineering* , edited by J.I. Kroschwitz, J. Wiley & Sons, New York Chichester Brisbane Toronto, Singapore, pp. 914-920, (1990)

[Liu92]: N.C. Liu, H.Q. Xie, W.E. Baker, *Comparison of the effectiveness of different basic functional groups for the reactive compatibilization of polymer blends*, Polym., 34(22), pp. 4680-4687, (1992)

[Mie94]: U. Mierau, *Untersuchungen zum Mechanismus der radikalischen Reaktionen am Polypropylen während der Modifizierung mit Maleinsäureanhydrid*, PhD Thesis, Techn. Univ. Dresden, (1994)

[Moa99]: G. Moad, *The synthesis of polyolefin graft copolymers by reactive extrusion*, Prog. Polym. Sci., 24, pp. 81-142, (1999)

[Moo96]: E.P. Moore Jr., in *Polypropylene handbook*, edited by E.P. Moore Jr., Carl Hanser Verlag, Munich Vienna New York Barcelona, pp. 303-348, (1996)

[Pit99]: C. Pitois, S. Vukmirovic, A. Hult, D. Wiesmann, M. Robertsson, *Low-loss passive Optical waveguides based on photosensitive poly(pentafluorostyrene-co-glycidyl methacrylate)*, Macromol., pp 2903-2909, (1999)

[Ro95]: B. de Roover, M. Sclavons, V. Carlier, J. Devaux, R. Legras, A. Momtaz, *Molecular characterization of maleic anhydride-functionalized polypropylene*, J. Polym. Sci. A. Polym. Chem., 33, pp. 829-842, (1995)

[Ro96]: M. Sclavons, V. Carlier, B. de Roover, P. Franquinet, J. Devaux, R. Legras, *The anhydride content of some commercial PP-g-MA : FTIR and titration*, J. Appl. Polym. Sci., 62, pp. 1205-1210, (1996)

[Ro97/1]: B. de Roover, J. Devaux, R. Legras, *PAmXD,6/PP-g-MA blends. I. Compatibilization*, J. Polym. Sci. A. Polym. Chem., 35 (5), pp. 901-915, (1997)

[Ro97/2]: B. de Roover, J. Devaux, R. Legras, *PAmXD,6/PP-g-MA blends. II. Rheology and phase inversion location,* J. Polym. Sci. A. Polym. Chem., 35 (5), pp. 917-925, (1997)

[Ro97/3]: B. de Roover, J. Devaux, R. Legras, *PAmXD,6/PP-g-MA blends. III. Microstructure, blend melt viscosity, and copolymer concentration relationship,* J. Polym. Sci. A. Polym. Chem., 35 (7), pp. 1313-1327, (1997)

[Rus88]: K.E. Russell, *Grafting of maleic anhydride to n-Eicosane*, J. Polym. Sci. A. Polym. Chem., 26, pp. 2273-2280, (1988)

[Rus95]: K.E. Russell, *Grafting of maleic anhydride to hydrocarbons below the ceiling temperature*, J. Polym. Sci. A. Polym. Chem., 33, pp. 555-561, (1995)

[Sea93]: M. Seadan, D. Graebling, M. Lambla, *Polyolefin polyamide blends by reactive extrusion*, Polym. Net. Blends, 3(3), pp. 115-124, (1993)

[Sin03]: N.K. Singha, T. Hunnekens, J. Eversdijk, C. Chlon, F. Vercauteren, B. de Ruiter, *Photoinitiated and thermal crosslinking of epoxides using oxime-blocked2-isocyanato-ethyl-methacrylate*, http://www.pcimag.com/CDA/ArticleInformation/ features/BNP__Features__ Item/0,1846,105013,00.html, Paint & Coatings Industry, (2003)

[Su95/1]: Y.-J. Sun, G.-H. Hu, M. Lambla, *Free radical grafting of glycidyl methacrylate onto polypropylene in a co-rotating twin screw extruder*, J. Appl. Polym. Sci., 57(9), pp. 1043-1054, (1995)

[Su95/2]: Y.-J. Sun, G.-H. Hu, M. Lambla, *Melt free-radical grafting of glycidyl methacrylate onto polypropylene*, Angew. Makromol. Chem., 229, pp. 1-13, (1995)

[Ted02]: A. Tedesco, P.F. Krey, R.V. Barbosa, R.S. Mauler, *Effect of the type of nylon chain-end on the compatibilization of PP/PP-GMA/nylon 6 blends*, Polym. Int., 51(2), pp. 105-110, (2002)

[Tod98]: P.G. Andersen, edited by D. Todd, *Plastics compounding – Equipement and processing*, Hanser Publishers, Munich, pp. 71, (1998)

[Tsa96]: C.-H. Tsai, F.-C. Chang, *Polymer blends of PBT and PP compatibilized by ethylene-co-glycidyl methacrylate copolymers*, J. Appl. Polym. Sci., 61, pp. 321-332, (1996)

[Utr95]: L.A. Utraki, *History of commercial polymer alloys and blends (from a perspective of patent literature)*, Polym. Eng. Sci., 35 (1), pp. 2-17, (1995)

[Whi01]: C. Jaehyug, J.L. White, *Styrene grafting onto a polyolefin in an internal mixer and a twin-screw extruder: experiment and kinetic model*, Polym. Eng. Sci., 41 (7), pp. 1238-1250, (2001)

[Won96]: B. Wong, W.E. Baker, *Polypropylene graft modified with glycidyl methacrylate and syterene*, Proceedings of SPE ANTEC, pp. 283-287 (1996)

[Won97]: B. Wong and W.E. Baker, *Melt rheology of graft modified polypropylene*, Polymer, 38, pp. 2781-2789, (1997)

[Zh97/1]: X. Zhang, X.L. Li, D. Wang, Z. Yin, J. Yin, *Morphology, thermal behavior and mechanical properties of PA1010/PP and PA1010/PP-g-GMA blends*, J. Appl. Polym. Sci., 64(8), pp. 1489-1498, (1997)

[Zh97/2]: X. Zhang, Z. Yin, N. Tainhai, J. Yin, *Morphology, mechanical properties and interfacial behaviour of PA1010/PP/PP-g-GMA ternary blends*, Polym., 38(24), pp. 5905-5912, (1997)

[Zh98/1]: X. Zhang, G. Li, D. Wang, Z. Yin, J. Yin, J. Li, *Morphological studies of PA1010/PP blends*, Polym., 39(1), pp. 15-22, (1998)

[Zh98/2]: X. Zhang, J. Yin, *The characterization of the interfacial reaction in PA1010/PP-g-GMA blends*, Macromol. Chem. Phys., 199, pp. 2631-2634, (1998)

[Zim90]: J. Zimmerman, in *Concise encyclopedia of polymer science and engineering* , edited by J.I. Kroschwitz, J. Wiley & Sons, New York Chichester Brisbane Toronto, Singapore, pp. 748-753, (1990)

[Zou01]: X.P. Zou, E.T. Kang, K.G. Neoh, *Adhesion enhancement of evaporated copper on HDPE surface modified by plasma polymerization of glycidyl methacrylate*, Polym. Eng. Sci., 41(10), pp. 1752-1761, (2001)

[Xan92]: M. Xanthos, *Reactive extrusion – Principles and practice*, edited by M. Xanthos, Carl Hanser Verlag, Munich Vienna New York Barcelona, pp. 34-44, (1992)

Properties of the functionalized polypropylene films

[Col90]: M.M. Coleman, P.C. Painter, in *Concise encyclopedia of polymer science and engineering* , edited by J.I. Kroschwitz, J. Wiley & Sons, New York, pp. 467-469, (1990)

[Run90]: J.P. Runt, in *Concise encyclopedia of polymer science and engineering* , edited by J.I. Kroschwitz, J. Wiley & Sons, New York, pp. 229-235, (1990)

[Koe99]: J.L. Koenig, *Spectroscopy of Polymers*, Elsevier Science, New York, (1999)

[Scl00]: M. Sclavons, P. Franquinet, V. Carlier, G. Verfaillie, I. Fallais, R. Legras, M. Laurent, F.C. Thyrion, *Quantification of maleic anhydride grafted onto polypropylene by chemical and viscosimetric titrations and FTIR spectroscopy*, Polym., 41, pp. 1989-1999, (2000)

[Lau95]: M. Pahl, W. Gleißle, H.-M. Laun, *Praktische Rheologie der Kunststoffe und Elastomere*, VDI-Verlag, Düsseldorf, (1995)

[Dea82]: J. M. Dealy, *Rheometers for molten plastics – A practical guide to testing and property measurement*, Van Nostrand Reinhold Company, New York, (1982)

[Mac94]: C. W. Macosko, *Rheology – Principles, measurements and applications*, VCH Publishers, New York, (1994)

[Gay83]: Gaylord N.G., M.K. Mishra, *Nondegaradtive reaction of maleic anhydride and molten polypropylene in the presence of peroxides*, J. Polym. Sci. Polym. Lett. Rev., 21, pp. 23-30, (1983)

[Ehr98]: G.W. Ehrenstein, G. Riedel, P. Trawiel, *Praxis der thermischen Analyse von Kunststoffen*, Carl Hanser Verlag, München, (1998)

[Ton00]: M.-T. Ton-That, K.C. Cole, J. Denault, *Characterization of grafted polypropylene: crystallisation and permeation behaviour*, 32nd International SAMPE Technical Conference, (2000)

[Mor96]: B.A. Morris, *The effect of processing variables on peel strength performance in coextrusion blown film*, Proceedings of SPE ANTEC, pp. 116-120 (1996)

[Ves02]: R.A. Veselovsky, V.N. Kestelman, *Adhesion of polymers*, McGraw-Hill, New York, pp. 227-262, (2002)

[Pai94]: P.C. Painter, M.M. Coleman, *Fundamentals of polymer science – An introductory text*, Technomic Publishing Company Inc., Switzerland, (1994)

Polypropylene and polyamide multilayer films

[And73]*: E.H. Andrews, A.J. Kinloch, Proc. R. Soc. Lond., A332:385, 401, 1973

[Bai71]*: H.E. Bair, S. Matsuoka, R.G. Vadimsky, T.T. Wang, J. Adhesion, 3, pp.89, (1971)

[Bal96]: N.P. Balsara, in *Physical properties of polymers handbook*, edited by J.E. Mark, AIP Press, pp. 257-268, (1996)

[Bou94]: E. Boucher, J.P. Folker, H. Hervet, L. Léger, *Adhesion between semi-crystalline polymers*, Proceedings of Euradh'94, pp. 442-445, (1994)

[Bou96]: E. Boucher, J.P. Folkers, H. Hubert, L. Léger, C. Creton, *Effects of the formation of copolymer on the interfacial adhesion between semi-crystalline polymers*, Macromol., 29, pp. 774-782, (1996)

[Bou97]: E. Boucher, J.P. Folkers, C. Creton, H. Hubert, L. Léger, *Enhanced adhesion between polypropylene and polyamide-6: role of interfacial nucleation of the β-crystalline form of polypropylene*, Macromol., 30, pp. 2102-2109, (1997)

[Cre01]: C. Creton, E.J. Kramer, H.R. Brown, C.-Y. Hui, *Adhesion and fracture of interfaces between immiscible polymers: from the molecular to the continuum scale*, Adv. Polym. Sci., 156, pp. 53-136, (2001)

[deG80]*: P.G. de Gennes, C.R. Acad. Sci. Paris Ser. B 291 :219, (1980) ; ibid. 292 :1505, (1981)

[deG89]*: P.G. de Gennes, J. Phys. Paris, 50, pp. 2551, (1989)

[Der69]*: B.V. Deryaguin, V.P. Smilga, *Adhesion - Fundamentals and practice*, McLaren, London, pp. 152, (1969)

[Doi78]*: M. Doi, S.F. Edwards, J. Chem. Phys. Faraday Trans., 74:1789, 1802, 1818, (1978)

[Dui97]: M. Van Duin, R.J.M. Borggreve in *Reactive Modifiers for Polymers*, edited by S. Al-Malaika, Sectionman & Hall, London, pp. 132-162, (1997)

[Gen71]*: A.N. Gent, J. Schultz, Proceedings Symposium on recent advances in adhesion, 162nd ACS Meeting, Vol. 31, No. 2, pp. 113, (1972)

[Gen72]*: A.N. Gent, J. Schultz, J. Adhesion, 3, pp. 281, (1972)

[Gen77]: A.N. Gent, G.R. Hamed, *Peel mechanics for an elastic-plastic adherend*, J. Appl. Polym. Sci., 21, pp. 2817-2831, (1977)

[Gen90]: A.N. Gent, G.R. Hamed, in *Concise encyclopedia of polymer science and engineering* , edited by J.I. Kroschwitz, J. Wiley & Sons, New York, pp. 31-34, (1990)

[Hai03]: H. Haidara, *Mécanismes fondamentaux du mouillage et de l'adhésion*, Workshop book of Jadh'2003 – 12èmes journées d'Etude sur l'Adhésion, (2003)

[Hin84]*: P.J. Hine, S. El Muddarris, D.E. Pakham, J. Adhesion, 17, pp. 207, (1984)

[Imm89]: Immergut E.H., *Polymer handbook*, Wiley Interscience, New York, (1989)

[Jab94]: E. Jabbari, N. Peppas, *Polymer-polymer interdiffusion and adhesion*, J.M.S.-Rev. Macromol. Chem. Phys. C34(2), pp. 205-241, (1994)

[Jeo04]: H.K. Jeon, C.W. Macosko, B. Moon, T.R. Hoye, Z. Yin, *Coupling reactions of end- vs mid-functional polymers*, Macromol., 37, pp. 2563-2571, (2004)

[Jud81]*: K. Jud, H.H. Kausch, J.G. Williams, J. Mater. Sci., 16, pp. 204, (1981)

[Kal97]: F. Kalb, H. Hervet, L. Léger, C. Creton, C. Plummer, *Adhésion entre polymères semi-cristallins*, pp. 133-135, Jadh'1997 – 9èmes journées d'Etude sur l'Adhésion, (1997)

[Kim83]*: Y.M. Kim, R.P. Wool, Macromol., 16, pp. 1115, (1983)

[Kin87]: A.J. Kinloch, *Adhesion and adhesives – Science and technology*, Sectionman and Hall, New York, (1987)

[Lar01]: C. Laurens, R. Ober, C. Creton, L. Léger, *Role of the interfacial orientation in adhesion between semicrystalline polymers*, Macromol., 34, pp. 2932-2036, (2001)

[Lar02]: C. Laurens, R. Ober, C. Creton, L. Léger, *Adhesion and crystallinity at polypropy-lene/polyamide 6 interfaces*, Proceedings of the 2nd World Congress and Related Phenomena, pp. 490-492, (2002)

[Lar04/1]: C. Laurens, R. Ober, C. Creton, L. Léger, *Crystalline orientation and adhesion at polypropylene/polyamide 6 interfaces compatibilized with syndiotactic polypropylene-polyamide 6 diblock copolymers*, Macromol., 37, pp. 6806-6813, (2004)

[Lar04/2]: C. Laurens, C. Creton, L. Léger, *Adhesion promotion mechanisms at isotactic polypropylene/polyamide 6 interfaces: role of the copolymer architecture*, Macromol., 37, pp. 6814-6822, (2004)

[Lee94]: Y. Lee, K. Char, *Enhancement of interfacial adhesion between amorphous polyamide and polystyrene by in-situ copolymer formation at the interface*, Macromol., 27, pp. 2603-2606, (1994)

[Lee98]: Y. Lee, K. Char, *Effect of styrene-maleic anhydride copolymers on adhesion between amorphous polyamide and polystyrene*, Macromol., 31, pp. 7091-7094, (1998)

[Mau85]*: D. Maugis, J. Mater. Sci., 20, pp. 3040, (1985)

[McB25]: J.W. McBain, D.G. Hoptkins, *On adhesives and adhesive action*, J. Phys. Chem., 29, pp. 188, (1925)

[Mol70]*: G.E. Molau, Kolloid Z. und Z. Polym., 30, pp. 2457, (1970)

[Nzu03]: P. Nzugang, *Funktionalisierung von Polypropylen mit Glycidylmetacrylat und Erzeugung eines PP/PA-Verbunds*, Studienarbeit, (2003)

[Pak]: D.E. Packam, *The mechanical theory of adhesion – a seventy year and its current status*, http://staff.bath.ac.uk/mssdep/dep70yrs.htm

[Pak83]*: D.E. Pakham, in Adhesion aspects of polymeric coatings, edited by K.L. Mittal, Plenum, New York, pp. 19, (1983)

[Plu98]: J.G. Plummer, H.-H. Kausch, F. Kalb, C. Creton, L. *Léger, Structure and microstructure of (iPP/iPP-g-MA)-PA6 reaction bonded interfaces*, Macromol., 31, pp. 6164-6176, (1998)

[Poc97]: A.V. Pocius, *Adhesion and Adhesives Technology- An introduction*; Hanser Publishers, Munich, Vienna, New York; Cincinnati: Hanser/Gardner Publications, Inc., (1997)

[Pra81]*: S. Prager, M. Tirrell, J. Chem. Phys., 75, pp. 5194, (1981)

[Rst03]: C. Rustal, H.-G. Fritz, Y. Zou, I. Özen, K. Dirnberger, C.D. Eisenbach, *Herstellung von Mehrschichtfolien ohne konventionelle Haftvermittler*, Proceedings of the 18. Stuttgarter Kunststoff-Kolloquium, pp. 2.V3, (2003)

[Rst04]: C. Rustal, H.-G. Fritz, Y. Zou, I. Özen, K. Dirnberger, C.D. Eisenbach, *Adhesion between functionalized polypropylene and polyamide films using maleic anhydride as compatibilizer*, Proceedings of the 40th International Symposium on Macromolecules (World Polymer Congress IUPAC), (2004)

[Rst05]: C. Rustal, H.-G. Fritz, Y. Zou, I. Özen, K. Dirnberger, C.D. Eisenbach, *Kostenoptimierte Herstellung von PP/PA-Mehrschichtfolien mittels Coextrusionsverfahren*, Proceedings of the 19. Stuttgarter Kunststoff-Kolloquium, pp. 3.V7, (2005)

[San98]: S. Sanchez-Valdes, I. Yanes-Flores, L.F. Ramos De Valle, O.S. Rodriguez-Fernandez, F. Orona-Villarreal, M. Lopez-Quintanilla, *Fusion bonding of maleated polyethylene blends to polyamide 6*, Polym. Eng. Sci., 38, pp.127-133 (1998)

[Sch99]: J. Schultz, M. Nardin, in *Adhesion Promotion techniques- Technological applications*, edited by K.L. Mittal and A. Pizzi, Marcel Dekker Inc.; New York, Basel, (1999)

[Spä99]: T. Späth, *Grenzflächenmorphologie und Adhäsionsverhalten von Verbunden aus Polyethylen und Polypropylen*, PhD. Thesis, University of Dortmund, (1999)

[Spchm]:http://www.specialchem4polymers.com/tc/Adhesion-Promoters/ index.aspx?id=3305

[UniP]: General Chemistry Help Homepage of Perdue University – College of science (Indiana, USA)

http://chemed.chem.purdue.edu/genchem/topicreview/bp/ch8/valenceframe.html

[Val03]: M.F. Vallat, *Tests d'adhérence et pertinence des mesures*, Workshop book of Jadh'2003 – 12èmes journées d'Etude sur l'Adhésion, (2003)

[Vas69]*: R.M Vasenin, *Adhesion - Fondamentals and practice*, McLaren and Son, London, pp. 29, (1969)

[Voy57]*: S.S. Vojuckij, A.I. Sapovalova, A.P. Pisarenko, Kolloid. Z., 19 (3), pp. 274, (1957)

[Voy63]*: S.S. Vojuckij, *Autohesion and adhesion of high polymers*, Interscience Publications, New York, London, Sydney, (1963)

[Wak82]*: W.C. Wake, *Adhesion and formulation of adhesive*s, Applied Science, London, (1982)

[Wan72]*: T.T. Wang, H.N. Vasirani, J. Adhesion, 4, pp.353, (1972)

[Wu92]: S. Wu, *Polymer Interface and Adhesion*, Marcel Dekker Inc.; New York, Basel, (1992)

[Zan04]: M. Zannouti, *Formulation and characterization of functionalized polypropylene and polyamide multilayer films*, Diplomarbeit, (2004)

[Zhan05]: J. Zhang, T. P. Lodge, C.W. Macosko, *Interface slip reduces polymer – polymer adhesion during coextrusion*, J. Rheol., 50 (1), pp. 41-57, (2006)

[Zhao02]: R. Zhao, C.W. Macosko, *Slip at the polymer – polymer interfaces: Rheological measurements on coextruded multilayers*, J. Rheol., 46 (1), pp. 145-167, (2002)

* Quoted in other references

7 Appendices

Appendix 2.1 (Extrusion trials)

1. Produced cast films (relevant formulations and process conditions)

1.1 Functionalization of PP with MAH

Low molecular weight PP

PP grade	MAH (phr)	MAH / DHBP (mol/mol)	Styrene / MAH (phr/phr)	Temperature (°C)	Screw speed (min^{-1})	Throughput (kg/h)
RD208CF	0.5	11.1	1	200	100	2
RD208CF	0.5	15.87	1	200	100	2
RD208CF	0.5	22.2	1	200	100	2
RD208CF	0.7	11.1	0	200	100	2
RD208CF	0.7	11.1	1	200	100	2
RD208CF	0.7	15.87	1	200	50 / 100 / 200	2
RD208CF	0.7	22.2	1	200 / 220	100	2
RD208CF	0.7	22.2	0.5	200	100	2
RD208CF	0.7	22.2	2	200	100	2
RD208CF	1.0	11.1	1	200	100	2
RD208CF	1.0	22.2	1	200	100	2
RD208CF	1.0	31.75	1	200	100	2
HD601CF	0.5	11.1	1	200	100	2
HD601CF	0.5	15.87	1	200	100	2
HD601CF	0.5	22.2	1	200	100	2
HD601CF	0.7	11.1	0	200	100	2
HD601CF	0.7	11.1	1	200	100	2
HD601CF	0.7	15.87	1	200	100	2
HD601CF	0.7	22.2	1	200	100	2
HD601CF	0.7	22.2	0.5	200	100	2
HD601CF	0.7	22.2	2	200	100	2
HD601CF	1.0	11.1	1	200	100	2
HD601CF	1.0	22.2	1	200	100	2
HD601CF	1.0	31.75	1	200	100	2

High molecular weight PP

PP grade	MAH (phr)	MAH / DHBP (phr/phr)	Styrene / MAH (mol/mol)	Temperature (°C)	Screw speed (min⁻¹)	Throughput (kg/h)
HB205TF	0.1	22.2	1	200	100	2
HB205TF	0.3	22.2	1	200	100	2
HB205TF	0.5	22.2	1	200 / 220 / 240	50 / 100 / 200	1 / 2 / 4
HB205TF	0.7	22.2	1	200	100	2
HB205TF	0.3	15.87	1	200	100	2
HB205TF	0.3	31.75	1	200	100	2
HB205TF	0.3	22.2	0	200	100	2
HB205TF	0.3	22.2	2	200	100	2
HB205TF	0.1	22.2	0	200	100	2
HB205TF	0.5	22.2	0	200	100	2
HB205TF	0.1	7.4	0	200	100	2
HB205TF	0.5	37.0	0	200	100	2
HB205TF	0.5	15.87	0	200	100	2
HB205TF	0.5	15.87	1	200	100	2

PP grade	MAH (phr)	MAH / TMCH (phr/phr)	Styrene / MAH (mol/mol)	Temperature (°C)	Screw speed (min⁻¹)	Throughput (kg/h)
HB205TF	0.5	15.87	0	200	100	2
HB205TF	0.5	15.87	1	200	100	2
RB501BF	0.1	15.87	0	200	100	2
RB501BF	0.3	15.87	0	200	100	2
RB501BF	0.5	15.87	0	200	100	2
RB501BF	0.5	22.2	0	200	100	2
RB501BF	0.5	31.75	0	200	100	2
RB501BF	0.5	22.2	1	200	100	2
RB501BF	0.5	22.2	2	200	100	2
RB501BF	0.1	3.17	0	200	100	2
RB501BF	0.3	9.52	0	200	100	2
RB501BF	0.5	15.87	1	200	100	2
RB501BF	0.1	6.4	0	200	100	2
RB501BF	0.3	19.11	0	200	100	2
RB501BF	0.1	4.44	0	200	100	2
RB501BF	0.3	13.33	0	200	100	2
RB501BF	0.1	3.17	0	200	100	2

PP grade	MAH (phr)	MAH / DHBP (phr/phr)	Styrene / MAH (mol/mol)	Temperature (°C)	Screw speed (min⁻¹)	Throughput (kg/h)
RB501BF	0.3	9.52	0	200	100	2
PP grade	MAH (phr)	MAH / DHBP (phr/phr)	Styrene / MAH (mol/mol)	Temperature (°C)	Screw speed (min⁻¹)	Throughput (kg/h)
RB501BF	0.1	22.2	1	200	100	2
RB501BF	0.3	22.2	1	200	100	2
RB501BF	0.5	22.2	1	200	100	2
RB501BF	0.7	22.2	1	200	100	2
RB501BF	0.5	15.87	0	200	100	2
RB501BF	0.5	15.87	1	200	100	2

All trials were conducted using the twin-screw extruder ZSK 30 equipped with a coat hanger die (slit width=0.4 mm). The chill roll temperature was set at 40°C and 80°C for the PP copolymers and homopolymers, respectively.

1.2 Functionalization of PP with GMA

PP grade	GMA (phr)	GMA / DHBP (phr/phr)	Styrene / MAH (mol/mol)	Temperature (°C)	Screw speed (min⁻¹)	Throughput (kg/h)
RD208CF	0.5	11.1	1	200	100	2
RD208CF	0.7	11.1	1	200	100	2
RD208CF	1	11.1	1	200	100	2
RD208CF	3	11.1	0	200	100	2
RD208CF	3	11.1	1	200	100	2
RD208CF	3	11.1	1.5	200	100	2
RD208CF	3	22.2	0	200	100	2
RD208CF	3	22.2	1	200	100	2
RD208CF	3	22.2	1.5	200	100	2
RD208CF	5	11.1	1	200	100	2
RD208CF	7	11.1	1	200	100	2
HD601CF	0.5	11.1	1	200	100	2
HD601CF	0.7	11.1	1	200	100	2
HD601CF	1	11.1	1	200	100	2
HD601CF	2	11.1	1.5	200	100	2
HD601CF	3	11.1	0	200	100	2
HD601CF	3	11.1	1	200	100	2
HD601CF	3	11.1	1.5	200	100	2
HD601CF	3	(TMCH) 11.1	1.5	200	100	2
HD601CF	3	22.2	0	200	100	2

HD601CF	3	22.2	1	200	100	2
HD601CF	3	22.2	1.5	200	100	2
HD601CF	5	11.1	1	200	100	2
HD601CF	7	11.1	1	200	100	2

2. Produced pellets (relevant formulations and process conditions)

2.1 Functionalization of PP with MAH

PP grade	MAH (phr)	MAH / DHBP (phr/phr)	Styrene / MAH (mol/mol)	Temperature (°C)	Screw speed (min^{-1})	Throughput (kg/h)
HB205TF	0.1	22.2	1	200	100	4
HB205TF	0.3	22.2	1	200	100	4
HB205TF	0.5	22.2	1	200	100	4
HB205TF	0.3	15.87	1	200	100	4
PP grade	**MAH (phr)**	**MAH / TMCH (phr/phr)**	**Styrene / MAH (mol/mol)**	**Temperature (°C)**	**Screw speed (min^{-1})**	**Throughput (kg/h)**
RB501BF	0.1	15.87	0	200	100	4
RB501BF	0.3	15.87	0	200	100	4
RB501BF	0.5	15.75	0	200	100	4

These trials were realized using ZSK 30 and a pumping system to introduce the liquid agents in the extruder.

2.2 Functionalization of PP with GMA

PP grade	GMA (phr)	GMA / Peroxide (phr/phr)	Styrene / GMA (mol/mol)	Temperature (°C)	Screw speed (min^{-1})	Throughput (kg/h)
HD601CF	1	5 (DHBP)	0	200	200	2
HD601CF	1	10	0	200	200	2
HD601CF	1	20	0	200	200	2
HD601CF	1	10 (DCUP)	0	200	200	2
HD601CF	1	10 (DB)	0	200	200	2
HD601CF	1	10 (DHBP)	0.5	200	200	2
HD601CF	1	10	1	200	200	2
HD601CF	1	10	1.5	200	200	2
HD601CF	1	10	2	200	200	2

These trials were realized using PP powder coated with the fluid reactants.

Appendix 2.2 (Batch mixer trials)

1. Produced PP-g-MAH

Process conditions:
-   Batch mixer Haake
-   Temperature: 200°C
-   Rotor speed: 60 min^{-1}
-   Residence time: 10 min

PP grade	MAH (g)	MAH/DHBP	Styrene /MAH
RD208CF	0.5	11.1	0
RD208CF	1.0	11.1	0
RD208CF	3.0	11.1	0
RD208CF	1.0	11.1	1
RD208CF	1.0	5.5	0
RD208CF	1.0	22.2	0
HD601CF	1.0	5.5	0
HD601CF	1.0	11.1	0
HD601CF	1.0	22.2	0
HD601CF	1.0	11.1	1
HD601CF	1.0	11.1	1.5

2. Produced PP-g-GMA

Process conditions:
-   Batch mixer Haake
-   Temperature: 200°C
-   Rotor speed: 60 min^{-1}
-   Residence time: 10 min

PP grades	GMA (phr)	GMA/DHBP (mol/mol)	Styrol / GMA (phr/phr)
RD208CF / HD601CF	0,5	22,2	0
RD208CF / HD601CF	1	22,2	0
RD208CF / HD601CF	0,5	11,1	0
RD208CF / HD601CF	1	11,1	0
RD208CF / HD601CF	1	11,1	0,7
RD208CF / HD601CF	1	11,1	1,5
RD208CF / HD601CF	0,5	5,5	0
RD208CF / HD601CF	1	5,5	0

Appendix 2.3 (Batch mixer trials)

Process conditions for the production of PP-g-MAH/PA blends:
- Batch mixer Haake
- Rotor speed: 80 min^{-1}
- Residence time: 5 min

Blends				Temperature (°C)
PP-g-MAH		PA		
20%	RD-MAH0.7-MAD22.2-St1	80%	PA6-6,6	210
30%	RD-MAH0.7-MAD22.2-St1	70%	PA6-6,6	210
40%	RD-MAH0.7-MAD22.2-St1	60%	PA6-6,6	210
50%	RD-MAH0.7-MAD22.2-St1	50%	PA6-6,6	210
20%	RD-MAH0.7-MAD22.2-St1	80%	PA6	230
50%	RD-MAH0.7-MAD22.2-St1	50%	PA6	230
80%	RD-MAH0.7-MAD22.2-St1	20%	PA6	230
20%	RB-MAH1-MD5.5-St0	80%	PA6-6,6 / PA6 / PA12	210
50%	RB-MAH1-MD5.5-St0	50%	PA6-6,6 / PA6 / PA12	210
80%	RB-MAH1-MD5.5-St0	20%	PA6-6,6 / PA6 / PA12	210

Appendix 2.4 (Extrusion trials)

1. Produced PP-g-MAH concentrates (relevant formulations and process conditions)

PP grade	MAH (phr)	MAH / DHBP (phr/phr)	Styrene / MAH (mol/mol)	Temperature (°C)	Screw speed (min^{-1})	Throughput (kg/h)
HB205TF	1	5.5	0	200	100	4
HB205TF	1	11.1	0	200	100	4
HB205TF	1	15.87	0	200	100	4
RB501BF	1	5.5	0	200	100	4
RB501BF	1	11.1	0	200	100	4
RB501BF	1	15.87	0	200	100	4

2.   Produced PP/PP-g-MAH blends (cast films)

Blends	Temperature (°C)	Screw speed (min⁻¹)	Throughput (kg/h)
HB205TF + **1 / 3 / 5 / 7 / 10%** HB-MAH1-MD11.1-St0	200	100	2
HB205TF + **5 %** HB-MAH1-MD5.5-St0	200	100	2
HB205TF + **5%** HB-MAH1-MD15.87-St0	200	100	2
RB501BF + **1 / 3 / 5 / 7 / 10%** RB-MAH1-MD11.1-St0	200	100	2
RB501BF + **5%** RB-MAH1-MD5.5-St0	200	100	2
RB501BF + **5%** RB-MAH1-MD15.87-St0	200	100	2
RB501BF + **5%** HB-MAH1-MD5.5-St0	200	100	2

Appendix 3.1 (Batch mixer trials)

1.   Produced PP/P(St-alt-MAH) blends
Process conditions:
-       Batch mixer Haake
-       Temperature: 260°C
-       Rotor speed: 60 min-1
-       Residence time: 10 min
Initial concentrations of P(St-alt-MAH): 0.5, 1, 5 wt-%

2.   Produced PP/polystyrene and PP/ octadecyl succinic anhydride blends
Process conditions:
-       Batch mixer Haake
-       Temperature: 200°C
-       Rotor speed: 60 min-1
-       Residence time: 10 min
Initial concentrations of polystyrene: 0.5, 1, 5, 10 wt-%

Appendix 4

Series 1					
Nr.	Layers composition	Take-off speed (m/min)	Speed (min^{-1})	Temperature (°C)	Die version
1	HB-MAH0.7-MD22.2-St1 PA6-6,6 RB-MAH0.7-MD22.2-St1	3	HB→20 PA→25 RB→10	HB→220 PA→280 RB→220	A
2	HB-MAH1-MD22.2-St1 PA6-6,6 RB-MAH0.7-MD22.2-St1	3	HB→20 PA→25 RB→10	HB→220 PA→280 RB→220	A
3	HB pure	3.8	HB→20	HB→220	A
4	HB pure	4.3	HB→20	HB→220	A
5	HB pure	5	HB→20	HB→220	A
Series 2					
1	HB-MAH0.5-MD15.87-St0 PA6 RB-MAH0.1-MT15.87-St0	3.8	HB→48 PA→20 RB→10	HB→230 PA→260 RB→190	A
2	HB-MAH0.1-MT15.87-St0 PA6 RB-MAH0.1-MT15.87-St0	3.8	HB→48 PA→20 RB→10	HB→230 PA→260 RB→190	A
3	HB-MAH0.5-MT15.87-St0 PA6 RB-MAH0.5-MT15.87-St0	3.8	HB→48 PA→20 RB→10	HB→230 PA→260 RB→190	A
Series 3					
1	HB+5% HB-MAH1-MD5.5-St0 PA6 RB+1% RB-MAH1-MD11.1-St0	3.8	HB→48 PA→20 RB→10	HB→230 PA→260 RB→190	A
2	HB+5% HB-MAH1-MD5.5-St0 PA6 RB+3% RB-MAH1-MD11.1-St0	3.8	HB→48 PA→20 RB→10	HB→230 PA→260 RB→190	A
3	HB+3% HB-MAH1-MD11.1-St0 PA6 RB+3% RB-MAH1-MD11.1-St0	3.8	HB→48 PA→20 RB→10	HB→230 PA→260 RB→190	A
4	HB+5% HB-MAH1-MD11.1-St0 PA6 RB+3% RB-MAH1-MD11.1-St0	3.8	HB→48 PA→20 RB→10	HB→230 PA→260 RB→190	A
5	HB+5% HB-MAH1-MD11.1-St0 PA6 RB+5% RB-MAH1-MD11.1-St0	3.8	HB→48 PA→20 RB→10	HB→230 PA→260 RB→190	A
6	HB+7% HB-MAH1-MD11.1-St0 PA6 RB+5% RB-MAH1-MD11.1-St0	3.8	HB→48 PA→20 RB→10	HB→230 PA→260 RB→190	A
7	HB+5% HB-MAH1-MD11.1-St0	3.4	48	230	A
8	PA6	2.6	20	260	A
9	RB+3% RB-MAH1-MD11.1-St0	3.5	10	190	A
Series 4					
1	Bynel 50E725 PA12 Bynel 50E725	3.5	HB→48 PA→26 RB→10	HB→230 PA→230 RB→230	A
2	HB+5% HB-MAH1-MD5.5-St0 PA12 RB+5% RB-MAH1-MD5.5-St0	3.5	HB→48 PA→26 RB→10	HB→230 PA→230 RB→230	A

3	HB+5% HB-MAH1-MD11.1-St0 PA12 RB+5% RB-MAH1-MD11.1-St0	3.5	HB→48 PA→26 RB→10	HB→230 PA→230 RB→230	A
4	HB+5% HB-MAH1-MD15.87-St0 PA12 RB+5% RB-MAH1-MD15.87-St0	3.5	HB→48 PA→26 RB→10	HB→230 PA→230 RB→230	A
5	HB+1% HB-MAH1-MD5.5-St0 PA12 RB+1% RB-MAH1-MD5.5-St0	3.5	HB→48 PA→26 RB→10	HB→230 PA→230 RB→230	A
6	HB+3% HB-MAH1-MD5.5-St0 PA12 RB+3% RB-MAH1-MD5.5-St0	3.5	HB→48 PA→26 RB→10	HB→230 PA→230 RB→230	A
7	HB+7% HB-MAH1-MD5.5-St0 PA12 RB+7% RB-MAH1-MD5.5-St0	3.5	HB→48 PA→26 RB→10	HB→230 PA→230 RB→230	A
8	HB+10% HB-MAH1-MD5.5-St0 PA12 RB+10% RB-MAH1-MD5.5-St0	3.5	HB→48 PA→26 RB→10	HB→230 PA→230 RB→230	A
Series 5					
1	HB-MAH0.1-MD22.2-St1 PA12 RB-MAH0.1-MT15.87-St0	3.6	HB→26 PA→17 RB→5	HB→230 PA→230 RB→230	B
2	HB-MAH0.3-MD22.2-St1 PA12 RB-MAH0.1-MT15.87-St0	3.6	HB→26 PA→17 RB→5	HB→230 PA→230 RB→230	B
3	HB-MAH0.5-MD22.2-St1 PA12 RB-MAH0.1-MT15.87-St0	3.6	HB→26 PA→17 RB→5	HB→230 PA→230 RB→230	B
4	HB-MAH0.3-MD22.2-St1 PA12 RB-MAH0.3-MT15.87-St0	3.6	HB→26 PA→17 RB→5	HB→230 PA→230 RB→230	B
5	HB-MAH0.3-MD22.2-St1 PA12 RB-MAH0.5-MT15.87-St0	3.6	HB→26 PA→17 RB→5	HB→230 PA→230 RB→230	B
6	HB-MAH0.3-MD22.2-St1 PA12 RB-MAH0.1-MT15.87-St0	3.6	HB→26 PA→17 RB→5	HB→250 PA→250 RB→250	B
7	HB-MAH0.3-MD22.2-St1 PA6-6,6 RB-MAH0.1-MT15.87-St0	3.6	HB→26 PA→17 RB→5	HB→250 PA→250 RB→250	B
8	HB-MAH0.3-MD22.2-St1 PA6 RB-MAH0.1-MT15.87-St0	3.6	HB→26 PA→17 RB→5	HB→250 PA→250 RB→250	B
Series 6					
1	HB+5% HB-MAH1-MD5.5-St0 PA12 RB+5% RB-MAH1-MD5.5-St0	2.9	HB→26 PA→17 RB→5	HB→250 PA→250 RB→250	B
2	HB+5% HB-MAH1-MD11.1-St0 PA12 RB+5% RB-MAH1-MD11.1-St0	2.9	HB→26 PA→17 RB→5	HB→250 PA→250 RB→250	B
3	HB+5% HB-MAH1-MD15.87-St0 PA12 RB+5% RB-MAH1-MD15.87-St0	2.9	HB→26 PA→17 RB→5	HB→250 PA→250 RB→250	B